

# Thames Water

---

REAL TIME FORECASTING AND CONTROL

---

1985/017

MODELS FOR OPERATIONAL CONTROL  
1. RAINFALL-RUNOFF MODELS FOR  
SUBCATCHMENTS

INSTITUTE OF HYDROLOGY  
WALLINGFORD  
OXON.

February 1985

## CONTENTS

|  | Page |
|--|------|
| INTRODUCTION AND OVERVIEW                                  | 1    |
| 1.1 Introduction   |      |
| 1.2 Overview   | 2    |
| 1.3 Summary of Results                                     | 3    |
| CATCHMENTS AND DATA SETS FOR MODEL EVALUATION              |      |
| 2.1 Introduction   | 6    |
| 2.2 Catchments used for model evaluation                   | 6    |
| 2.3 Flow data and model calibration and evaluation periods | 7    |
| 2.4 Rainfall data  | 8    |
| 2.5 Potential evaporation data                             | 8    |
| MODEL DESCRIPTIONS   |      |
| 3.1 National Weather Service Model                         | 13   |
| 3.2 Thames Water Model                                     | 21   |
| 3.3 Probability-distributed Model                          | 30   |
| 3.4 Institute of Hydrology Conceptual Model                | 45   |
| 3.5 Recession Model  | 52   |
| 3.6 Constrained Linear System Models                       | 62   |
| EVALUATION PROCEDURES AND RESULTS                          | 78   |
| 4.1 Model Evaluation                                       | 78   |
| 4.2 Results of evaluation                                  | 80   |
| 4.3 Qualitative comparison of models                       | 84   |
| 4.4 Conclusions  | 85   |
| REFERENCES   | 103  |

## INTRODUCTION AND OVERVIEW

### 1.1 Introduction

Thames Water Authority has undertaken a research programme into real-time operational control. As part of this programme, the Institute of Hydrology is developing procedures for flow forecasting. Flow forecasting is central to all aspects of operational control: the strategic management model, the river operation model, flood control, and for weir operation and control.

For the operational control of the River Thames the forecasts will be used in the following ways:

1. In strategic management, using the forecasts over one to three months. The model will be "updated" on soil-moisture or river flows prior to the management period and the possible range of future flows will be used to look at water supply reliability, sewage treatment plant effluent loadings and water quality parameters. For this management model, the most important characteristic needed in the rainfall-runoff flow model is an accurate representation of soil moisture.
2. In operational management, using forecasts of inflows to better manage water abstraction and sewage treatment plant effluent loadings. For water abstraction, the rainfall-runoff models for subcatchments will forecast tributary inflows. These inflow forecasts in conjunction with a River Thames flow model and weir control model will assist in the scheduling of abstraction throughout a 1-3 day period.

Since accuracy will be most important in the dry summer-autumn period, it is important that good flow forecasts are made under depleted soil-moisture conditions. For sewage treatment plant control, it will be the wetter periods that will allow processes to be by-passed to utilize the self-cleansing ability of the river. For this application, forecasts of 1-5 days in advance are needed.

It is clear that a strong link exists between Thames Water having the capability for managing its system and a flow forecasting system. A flow forecasting model that is responsive to the needs of operational and strategic control must accurately account for soil moisture, depletion of which can significantly affect the direct runoff and baseflow due to precipitation. In the Thames basin, where the potential soil moisture storage is large, this is especially true.

A variety of rainfall-runoff models have been developed by IH and other researchers. For strategic management, one probably desires a model that conceptually rather than physically represents the various components of the water balance. Even within the category of conceptual rainfall-runoff models, a wide variety of models exist from rather simple, lumped representations to complex, non-linear models with thresholds. Simple models work well for daily real-time forecasting. As the forecast period increases, as it will when risk and reliability analyses are carried out, simple models may produce unacceptably large errors. To some extent, the growth of the errors with forecast length (i.e. the time before parameter or state updating) depends upon the complexity and non-linearity of the catchments response to rainfall.

Within the Thames basin, various subcatchments display a diversity of geological conditions. The research described in this report was carried out to assess the performance of models of different complexity in this range of conditions.

## 1.2 Overview

To evaluate the required conceptual model complexity for accurate runoff forecasts, a variety of conceptual rainfall-runoff models were compared on three diverse subcatchments of the River Thames. The models, which are described in Chapter 3, fall into two broad groups.

Group 1, consisting of the US National Weather Service model, the Thames Water Model and IH Conceptual model, represents a complex conceptualization where the water balance fluxes are represented in greater detail through elements such as percolation, shallow groundwater, unsaturated soil moisture and parameter response functions that contain thresholds and other non-linear behaviour.

Group 2, comprises CLS (a linear impulse response model) with a variety of soil moisture accounting preprocessors, a probability-distributed storage model and an empirical recession model.

The models were applied to three subcatchments of the Thames; the Cherwell at Enslow Mill, the Blackwater at Swallowfield and the Mole at Castle Mill. Chapter 2 reviews the catchments and the data sets used for model evaluation.

Chapter 3 describes the six models that were evaluated and Chapter 4 gives the evaluation procedures and results. The data period was divided into a calibration period and an evaluation period. Daily data were used, though a shorter time step could be used with some of the models.

Model evaluation was based on four measures of accuracy of prediction; mean absolute error, root mean square error, proportional mean square error and proportional root mean square error. Since the forecasting model is to be used throughout the year over a wide range of flows, the evaluation criteria did not focus upon flood peak prediction or peak timing.

For the Cherwell and Blackwater, the calibration period ran from October 1968 to September 1974 and the evaluation period from October 1974 to September 1980. For the Mole, the period February 1978 to September 1983 was used for calibration and evaluation was carried out over the period October 1972 to September 1975. To investigate the influence of the 1976 drought, a second evaluation period was formed for the Cherwell and Blackwater by removing the period January 1976 to October 1976.

### 1.3 Summary of Results

It is clear that the complex conceptual models, as a group, significantly outperformed the simple models. This finding is important for the seasonal risk and reliability analysis and for extended streamflow simulation - activities important for strategic management.

Within the complex conceptual models, the US National Weather Service Model generally works best. Table 1.3.1 summarizes the best performing model over the four seasonal periods. During dry periods (Summer and Autumn) and especially on the Cherwell which has a larger soil moisture storage, the Thames Water Model (TWM) performs very well.

It can probably be concluded that for strategic management, any of the complex conceptual rainfall-runoff models will perform well. Detailed discussion of the results are in Chapter 4.

| Catchment  | Period | Winter<br>(Dec - Feb) | Spring<br>(Mar - May) | Summer<br>(Jun - Aug) | Autumn<br>(Sept - Nov) |
|------------|--------|-----------------------|-----------------------|-----------------------|------------------------|
| Cherwell   | a      | NWS                   | NWS                   | TWM                   | NWS                    |
|            | b      | NWS                   | NWS                   | NWS                   | TWM                    |
|            | c      | NWS                   | NWS                   | TWM                   | TWM                    |
| Mole       | a      | NWS                   | NWS                   | NWS                   | NWS                    |
|            | b      | NWS                   | NWS                   | TWM                   | IHCM                   |
| Blackwater | a      | NWS                   | NWS                   | NWS                   | NWS                    |
|            | b      | NWS                   | NWS                   | NWS                   | NWS                    |
|            | c      | NWS                   | NWS                   | NWS                   | NWS                    |

a: calibration

b: evaluation

c: evaluation except 1/76 - 10/76

Table 1.3.1 Best performing model, using the proportional root mean square error criterion (see Section 4.1), during different seasons

## 2. CATCHMENTS AND DATA SETS FOR MODEL EVALUATION

### 2.1 Introduction

Three major subcatchments of the River Thames, chosen to cover a range of geological characteristics, were used to assess the candidate rainfall-runoff models. The tributaries selected were the Cherwell, Mole and Blackwater which drain catchments with, in very broad terms, limestone, clay, and mixed gravel/sand/clay lithologies respectively. A summary of some pertinent topographical and hydrological characteristics of these catchments is provided in Table 2.1; an explanation of the indices presented is contained in the Flood Studies Report (NERC, 1975) and its supplementary reports. The Cherwell is the largest and most rural catchment, the Mole the most poorly drained, the least affected by baseflow, and having the most dense stream network, and the Blackwater has the smallest slope and most permeable soils.

A more comprehensive description of the catchments, including some details of the flow measurement stations, will be presented next. This is followed by information on the flow, rainfall, and potential evaporation data sets employed for model evaluation.

### 2.2 Catchments used for model evaluation

#### 2.2.1 Cherwell at Enslow Mill

The Cherwell above Enslow Mill drains a predominantly rural area of 551.7 km<sup>2</sup> and is dominated by pervious lias lithology. A compound crump weir with a broad crested side weir is used to measure flows. The side weir comes into operation at higher flows (greater than 1.3 m<sup>3</sup>/s) and is associated with a separate stage recorder: both the rating and the maintenance of the side weir and recorder have been a cause for concern (eg. missing charts, inconsistent zeroing of level). By-passing of flood flows around the structure also occurs above about 17 m<sup>3</sup>/s, leading to underestimation of peak flows.

### **2.2.2 Mole at Castle Mill**

The Mole at Castle Mill drains an area of 316 km<sup>2</sup> with predominantly clay lithology. Flows are gauged by a crump weir which commenced operation in February 1978. Records available from October 1972 to February 1976 are from a previous mill structure and are considered less accurate.

### **2.2.3 Blackwater at Swallowfield**

The Blackwater at Swallowfield drains an area of 355 km<sup>2</sup>, rises on the chalk hills of the Hogs Back, and crosses sands, gravels and clays. Two gauging structures (a flume and side weir) were replaced in 1970 (30 November 1970) by two crump weirs which provide accurate measurement of low flows. A rippled hydrograph trace at low flows reflects significant abstractions and returns upstream.

## **2.3 Flow data and model calibration and evaluation periods**

Flow data for the 12 year period October 1968 to September 1980 in the form of daily totals were used in the modelling study for the Cherwell and Blackwater catchments. The first 6 years, from October 1968 to September 1974, were used for model calibration, and the last 6 years for model evaluation.

For the Mole catchment, flow data are not available until November 1971 and the quality of the earlier record is considered inferior to more recent records (see Section 2.2.2). The period from February 1978 to September 1983 was selected for model calibration, and the period from October 1972 to September 1975 was used for model evaluation. These periods were chosen to take account of a break in the record between March 1976 to January 1978, during which time there were improvements to the gauging station .

The measured daily total flow relates to the period from 9 am on the day in question to 9 am the next day.

#### 2.4 Rainfall data

Daily areal average rainfall for each basin was calculated according to a procedure based on standardisation of daily totals measured at each gauge by each gauge's long term average annual rainfall. If  $P_i$  denotes the daily rainfall measured by gauge  $i$ , and  $\bar{P}_i$  the long term average annual rainfall at gauge  $i$ , then the areal average daily rainfall formed by the use of  $n$  gauges is defined as

$$P = \left( \frac{P_1}{\bar{P}_1} + \frac{P_2}{\bar{P}_2} + \dots + \frac{P_n}{\bar{P}_n} \right) \frac{\bar{P}}{n} \quad (2.1)$$

where  $\bar{P}$  denotes the long-term areal average annual rainfall.

Table 2.2 indicates the gauges used to form the areal average daily rainfall totals for the Cherwell, Blackwater and Mole catchments; four in each case. Figures 2.1-2.3 indicate the location of these raingauges in relation to the catchments for which they are used to provide areal average rainfall totals.

Areal average rainfall totals computed by the above procedure were available for the period October 1968 to September 1983 inclusive. The daily values obtained relate to the period from 9 am on the day in question to 9 am the next day.

#### 2.5 Potential evaporation data

The procedure employed to calculate areal daily potential evaporation estimates for each catchment first derives monthly estimates based on reciprocal-distance weighting factors and standardisation by the long term average annual value for each station. Daily totals are then obtained from the monthly values

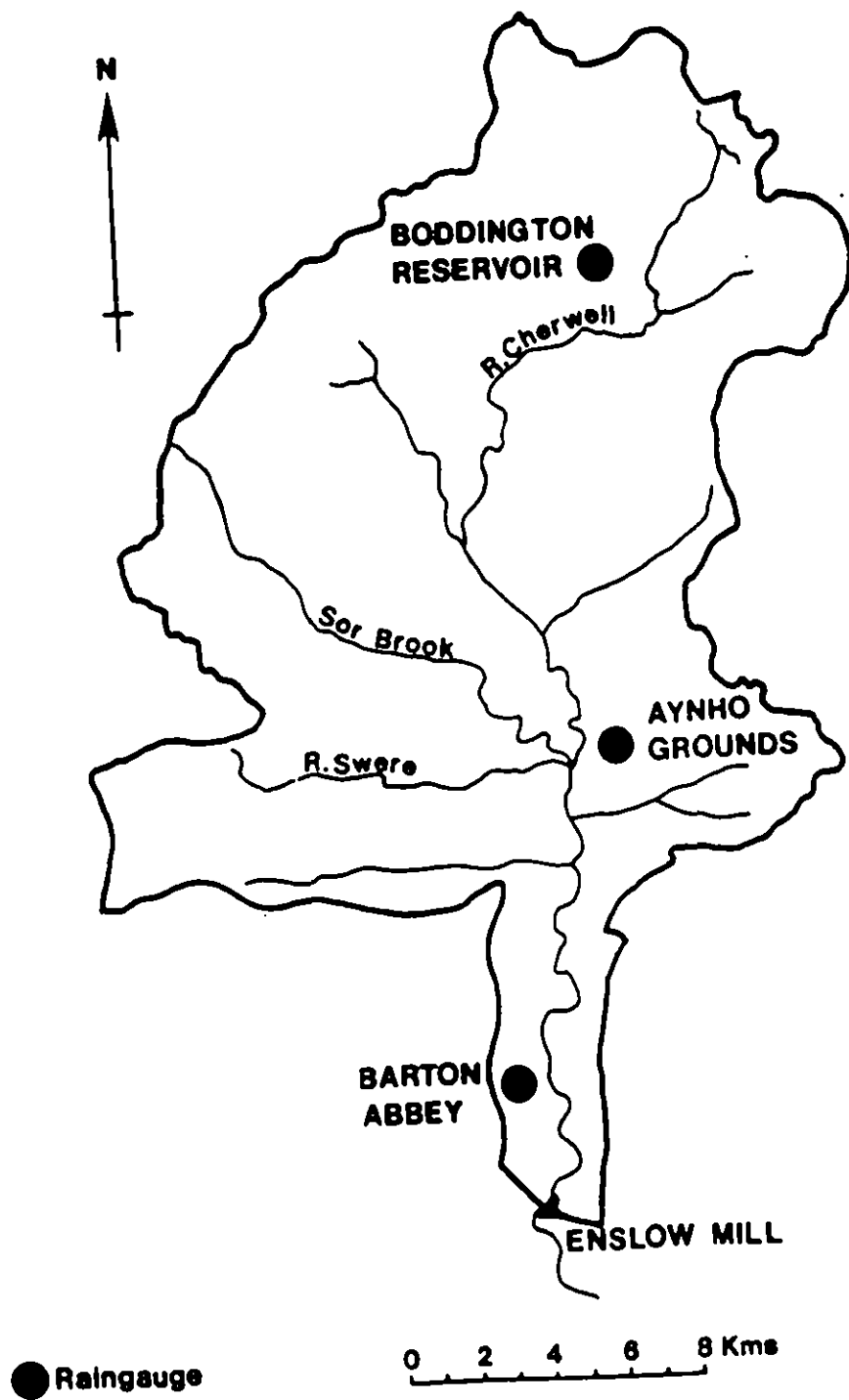


Figure 2.1 The Cherwell catchment

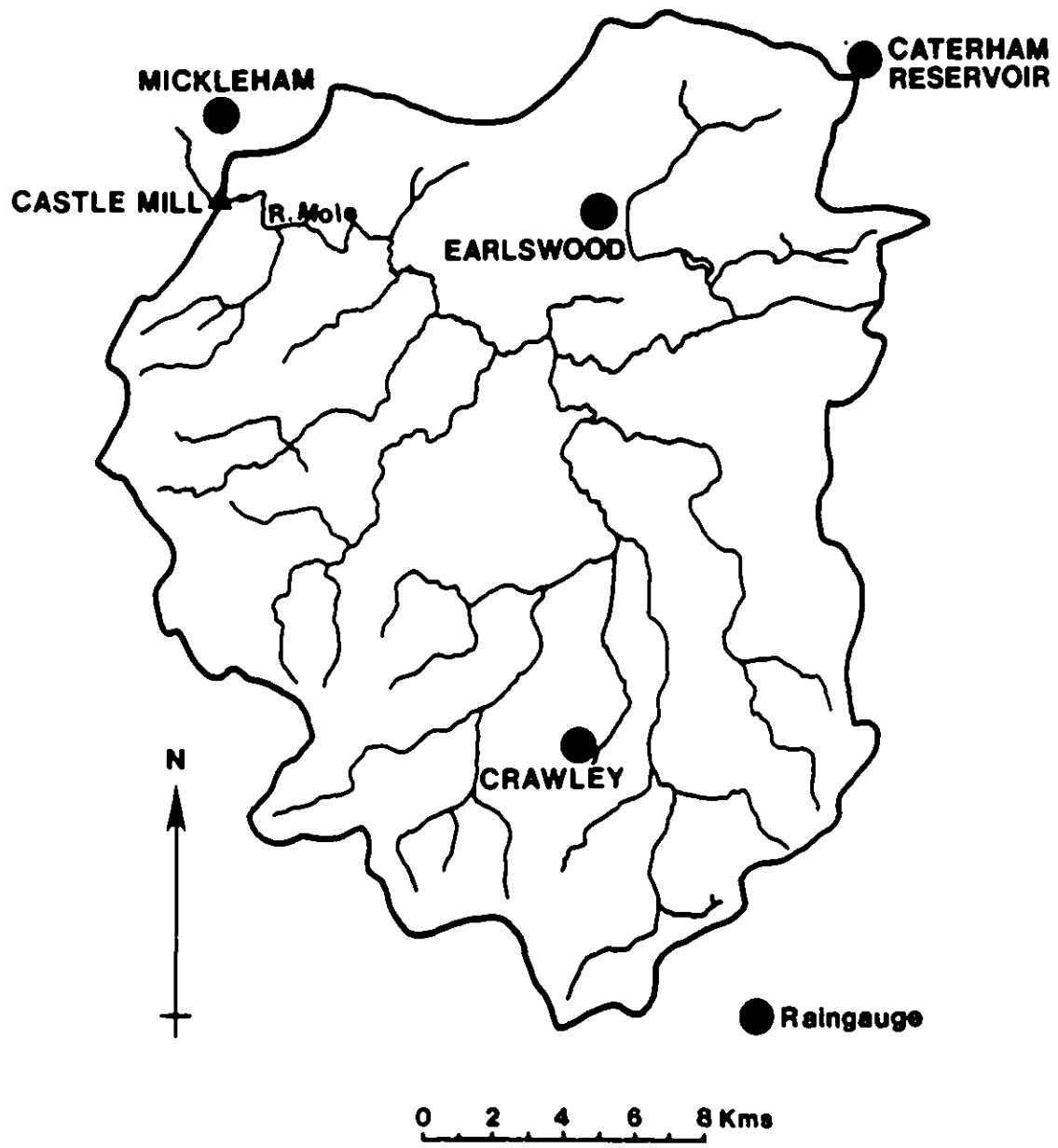


Figure 2.2 The Mole catchment

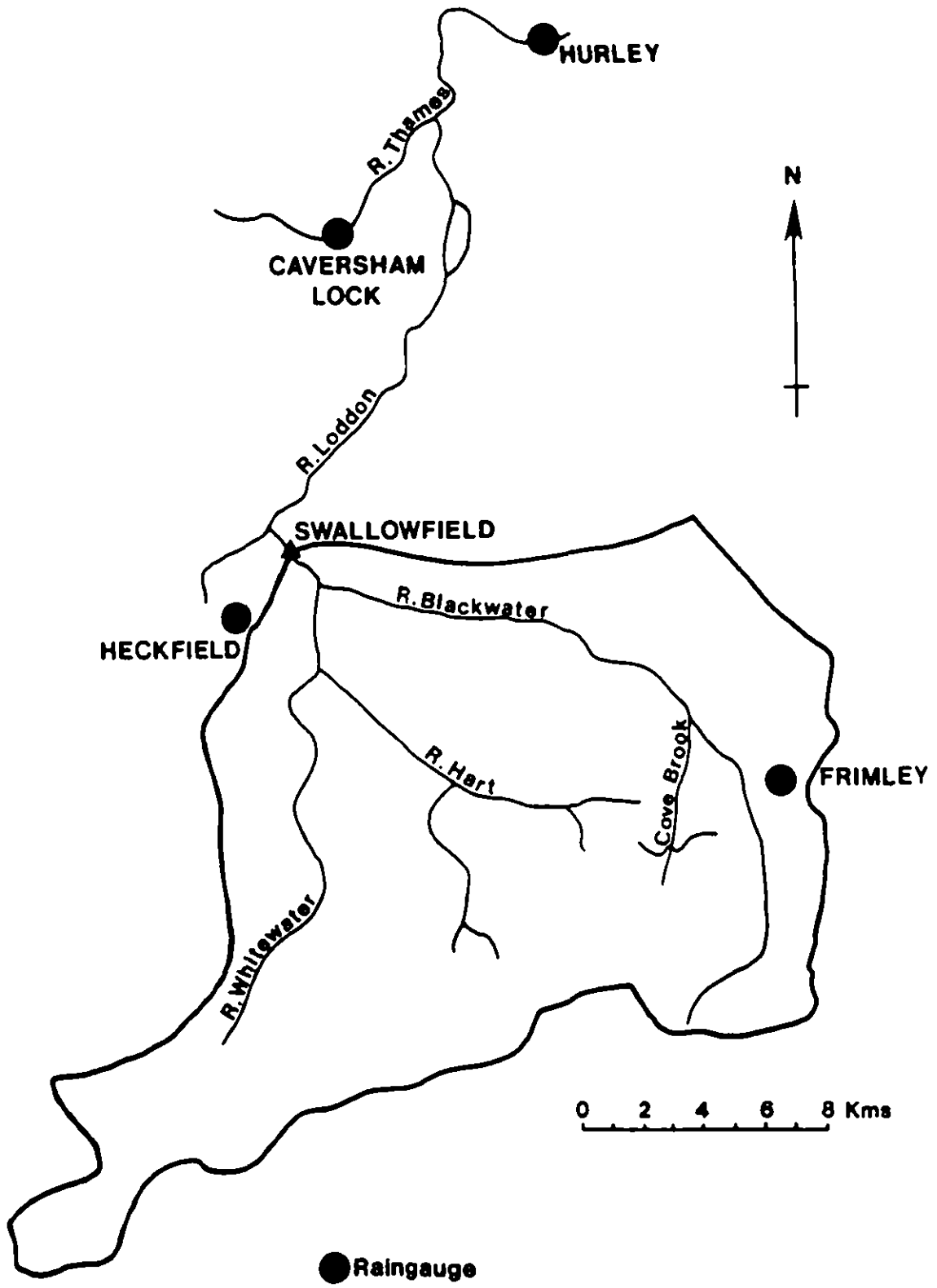


Figure 2.3 The Blackwater catchment

using a standard annual distribution. If  $d_i$  denotes the distance of station  $i$  from the catchment control, then a reciprocal distance weighting factor for the  $i$ th station may be formed as

$$w_i = \left( \frac{1}{d_i} \right) / \left( \frac{1}{d_1} + \frac{1}{d_2} + \dots + \frac{1}{d_n} \right) . \quad (2.2)$$

The reciprocal-distance weights for  $n$  stations may be used to define the areal average monthly evaporation as

$$E = \left( w_1 \frac{E_1}{\bar{E}_1} + w_2 \frac{E_2}{\bar{E}_2} + \dots + w_n \frac{E_n}{\bar{E}_n} \right) \bar{E} \quad (2.3)$$

where  $\bar{E}$  is the long term areal average annual potential evaporation , and  $\bar{E}_i$  is the long term average annual potential evaporation for station  $i$  (the standard long term period used is 1956 to 1975).

A standard annual profile of 365 daily values of potential evaporation is used to transform the monthly values to daily values. If this profile is denoted by  $e_d$ ,  $d = 1, 2, \dots, 365$  and the monthly standard series derived from it by  $\bar{e}_m$ ,  $m = 1, 2, \dots, 12$ , then daily areal average potential evaporation on day  $d$  in month  $m$ ,  $E_d$ , is derived from the monthly value,  $E$ , using

$$E_d = \frac{e_d}{\bar{e}_m} E . \quad (2.4)$$

Table 2.3 indicates the potential evaporation stations used to derive the catchment areal average values and Figure 2.4 shows their location with respect to the three Thames subcatchments.

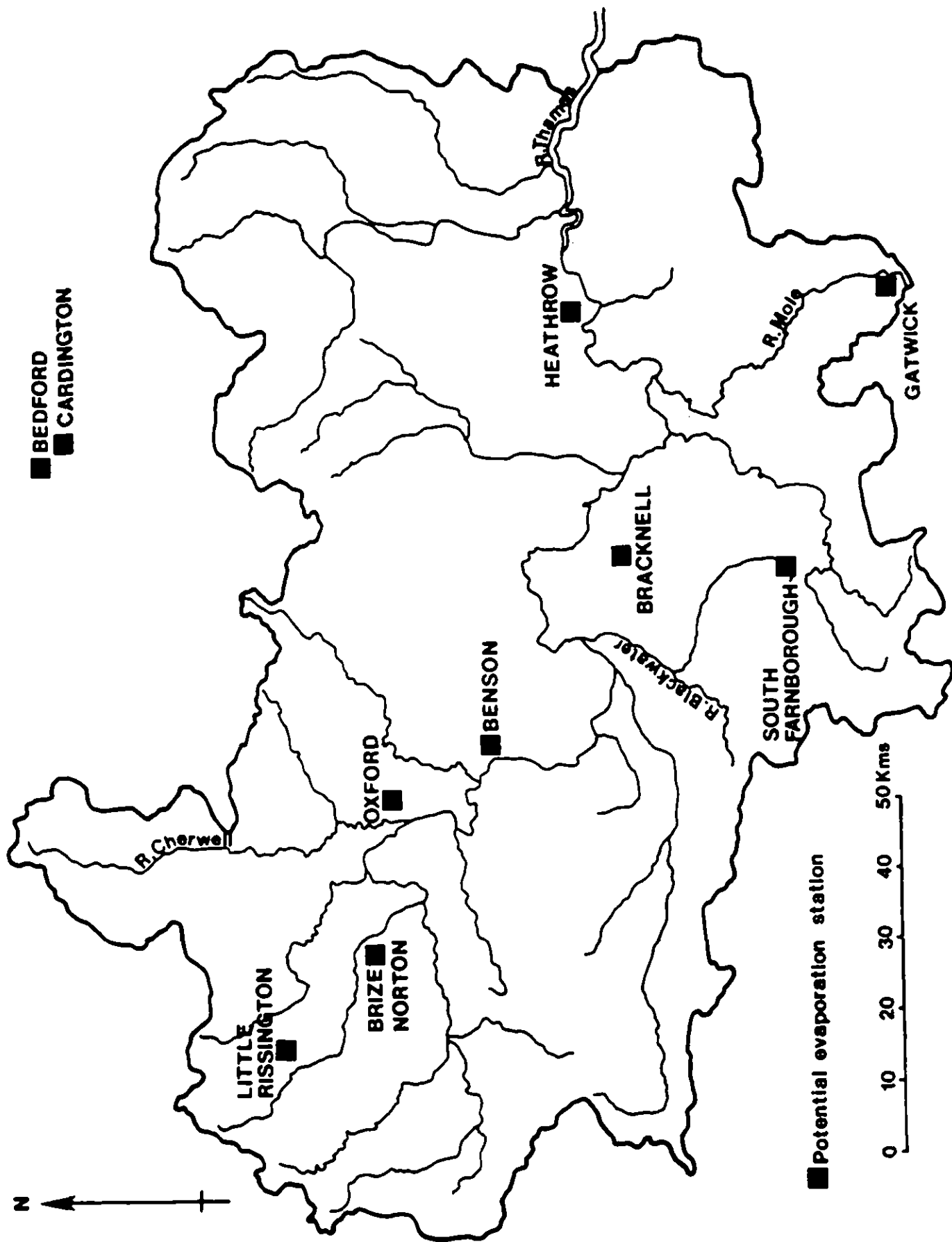


Figure 2.4. Evaporation stations

| Catchment                     | Area<br>km <sup>2</sup> | Average<br>daily flow<br>m <sup>3</sup> /s | Average<br>annual<br>rainfall, mm | Baseflow<br>index | Stream<br>frequency | Slope<br>(SL1085) Urban Lake Soil |
|-------------------------------|-------------------------|--|-----------------------------------|-------------------|---------------------|-----------------------------------|
| Cherwell at<br>Enslow Mill    | 551.7                   | 3.460                                      | 715                               | .638              | .71                 | 1.17 .008 0. .328                 |
| Mole at<br>Castle Mill        | 316.0                   | 3.509                                      | 800                               |                   | 1.25                | .986 .095 .420                    |
| Blackwater<br>at Swallowfield | 355                     | 2.728                                      | 719                               | .641              | .383                | .98 .075 .306                     |

Table 2.1 Catchment characteristics

---

| Catchment     | Rainfall stations employed |                      |
|---------------|----------------------------|----------------------|
| Cherwell at   | 255837                     | Barton Abbey         |
| Enslow Mill   | 256686                     | Boddington Reservoir |
|               | 257038                     | Grimsbury            |
|               | 258035                     | Aynho Grounds        |
| Mole at       | 284374                     | Crawley              |
| Castle Mill   | 284974                     | Earlswood            |
|               | 285587                     | Mickleham            |
|               | 287642                     | Caterham Reservoir   |
| Blackwater at | 265922                     | Caversham            |
| Swallowfield  | 271093 & 271095            | Heckfield            |
|               | 271300                     | Frimley              |
|               | 273992                     | Hurley               |

---

Table 2.2 Rainfall stations employed to calculate catchment average rainfalls

| Catchment                     | Areal average<br>PE, mm | P.E. stations employed           |  | Alternative P.E. Stations         |                         |                                    |                                   |
|-------------------------------|-------------------------|----------------------------------|--|-----------------------------------|-------------------------|------------------------------------|-----------------------------------|
|                               |                         | Number                           | Name                                       | Distance<br>from centroid<br>(km) | Number                  | Name                               | Distance<br>from centroid<br>(km) |
| Cherwell at<br>Enslow Mill    | 500                     | 94522<br>94504<br>94339          | Benson<br>Brize Norton<br>Bedford          | 33<br>39<br>63                    | 94995<br>93456          | Little Rissington<br>Cardington    | 33<br>61                          |
| Mole at<br>Castle Mill        | 535                     | 95271<br>95113<br>95592          | Gatwick<br>Heathrow<br>Bracknell           | 4<br>37<br>46                     | 95258<br>95696          | Kew<br>South Farnborough           | 32<br>40                          |
| Blackwater at<br>Swallowfield | 525                     | 95592<br>94552<br>95113<br>95271 | Bracknell<br>Benson<br>Heathrow<br>Gatwick | 9<br>33<br>33<br>55               | 95696<br>94522<br>95258 | South Farnborough<br>Oxford<br>Kew | 13<br>51<br>42                    |

Table 2.3 Stations used to calculate catchment average potential evaporation

### 3. MODEL DESCRIPTIONS

#### 3.1 National Weather Service Model

##### 3.1.1 Model Outline

The United States National Weather Service developed the NWS River Forecast System during the 1970's. It is described in a series of technical memoranda produced by the National Oceanic and Atmospheric Administration (Monro, 1971; National Weather Service, 1972; Fread 1973; Anderson, 1973; Morris, 1975; Peck, 1976). The system, which models the rainfall-runoff behaviour of river catchments, may be classified as conceptual, lumped and deterministic. This means, first, that some features of the model are taken to represent physical aspects of the catchment, in particular, moisture storage regions in the soil. Secondly, the model allows for no spatial variability in parameter values, with limited subdivision of the catchment into areas which behave differently from one another. Thirdly, no random components are present in the model.

The feature which is perhaps most associated with the NWS model is its soil moisture accounting component, based on an upper and a lower soil zone, each containing tension water and free water. Although these zones are purely conceptual there is some basis for believing them to represent features which are present in the field. The movement of water into and out of the storage regions is described using parameters which may be interpreted as percolation rates, depletion rates and so forth.

The NWS system uses as input daily rainfall measurements at discrete points (raingauges) within the catchment, and gives as output daily discharges at a downstream point, regarded as the outlet of the catchment. As well as soil moisture accounting, the model includes a unit hydrograph describing the movement of water within stream channels, allowance for evapotranspiration, and parameters describing the movement of water which does not enter the soil, but runs off directly into streams.

### 3.1.2 Hydrological Pathways

Rainfall entering a catchment is regarded in the NWS system as a lumped input, which may take one of the pathways shown schematically in Figure 3.1.1. The central part of the model is concerned with the movement of water between the upper and lower zones and between tension water and free water. The upper zone represents the upper soil layer and interception storage and the lower zone most of the soil moisture and longer term groundwater storage. Tension water is assumed to be closely bound to the soil particles, in contrast to water which is free to move. Each type of storage has a maximum content. Moisture entering the upper zone is stored as tension water until this is filled, while in the lower zone some transfer of water from unfilled tension water capacity to free water is allowed. Depletion of free water occurs as percolation and as channel flow or as evapotranspiration, whereas tension water is depleted only by evapotranspiration.

Water draining from the upper zone free water into the stream network is described as interflow. To model low flows adequately, free water in the lower zone is divided into primary water which drains slowly, giving rise to primary base flow, and supplementary water which drains faster, as supplementary base flow. These three types of flow are computed as the product of the contents of the appropriate storage region and one of three withdrawal parameters.

The water contents of the upper and lower zones are linked through percolation, whose rate depends on the lower and upper zone moisture contents. Some percolating water enters the lower zone free water directly, the remainder adding to the lower zone tension water.

It is assumed that a certain proportion of any catchment is impervious, and any rain falling onto this area reaches the stream network directly. The extent of the impermeable area allowed in the NWS system depends on the water content of the upper zone. Further surface runoff is assumed to occur once the upper zone is filled.

The total channel flow therefore has five components:

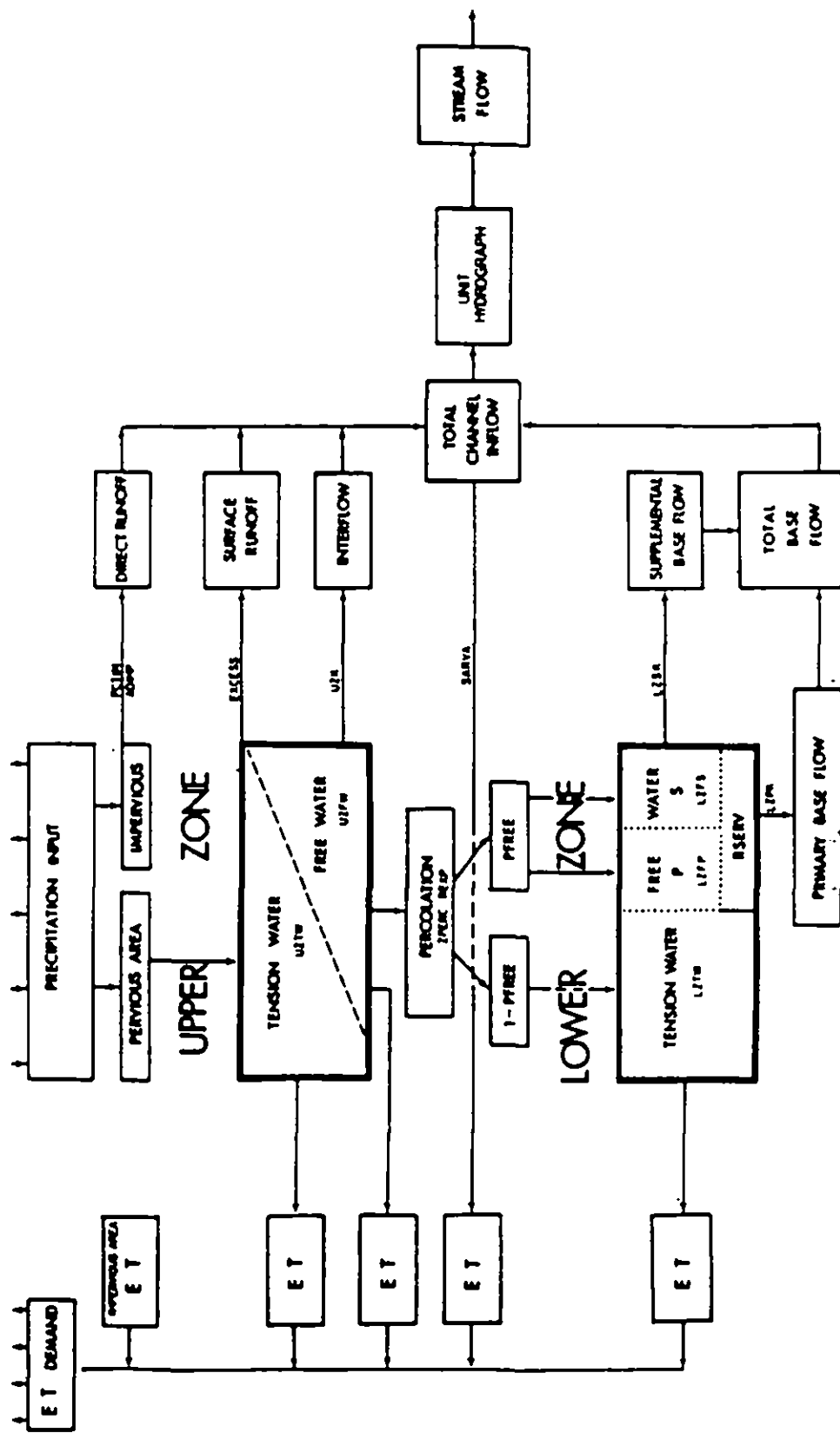


Figure 3.1.1 NWS Conceptual Catchment Representation

- (1) Direct runoff, from rain falling on the impervious area.
- (2) Surface runoff, present when rainfall is heavier than can be immediately accommodated in the upper zone.
- (3) Interflow, which is drainage from the upper zone free water.
- (4) Supplementary base flow which is drainage from the lower zone supplementary free water.
- (5) Primary base flow which is drainage from the lower zone primary free water.

### 3.1.3 Model parameters

The model parameters are considered here in six groups, and, where appropriate, these are named as in Figure 3.1.1.

UZK, LZPK, LZSK

These are depletion rates for upper zone free water, lower zone free water (primary component) and lower zone free water (secondary component). After suitable adjustments have been made, the contents, of for example,  $S_t$ , the upper zone free water storage region on day  $t$  are computed as  $S_t = (1 - UZK)S_{t-1}$

2. UZTWM, UZFWM, LZTWM, LZFPM, LZFSM

These parameters represent the maximum moisture content in inches of each of the five storage regions. For example LZFPM represents the lower zone primary free water maximum contents.

ZPERC, REXP, PFREE, RSERV

The percolation rate from the upper to the lower zone is calculated as

$$\text{RATE} = \text{PBASE} [1 + \text{ZPERC} \times \text{DEFR} \text{ REXP}]$$

where

$$PBASE = LZFPM \times LZPK + LZFSM \times LZSK$$

and DEFR is a deficit ratio calculated as the difference between the lower zone contents and capacity divided by its capacity. The rate therefore varies between PBASE when the deficit ratio is zero, and  $PBASE(1 + ZPERC)$  when the deficit ratio is 1.

The parameter PFREE represents the percentage of water percolating from the upper zone which enters the lower zone free water directly, and RSERV is the fraction of the lower zone free water which is not available for evapotranspiration.

PCTIM, ADIMP, SARVA

These are respectively the fraction of the basin contiguous with stream channels which is impervious; the fraction of the basin which becomes impervious when all tension water requirements are met; and the fraction of the basin which is covered by streams, lakes and riparian vegetation.

U1, U2, U3

Water entering the stream network from one of the storage regions will not reach the catchment outlet immediately. The parameters U1, U2 and U3 allow for a delay giving a form of unit hydrograph. For continuity, each should be greater than zero and their sum should be 1.

E1, E2, E3

These parameters allow for some adjustment to potential evaporation measurements, giving a better approximation to actual evaporation. Actual evaporation in April, August and December is taken to be E1, E2, E3 times the potential evaporation for those months. Factors for other months are found by interpolation.

### 3.1.4 Model Fitting

The National Weather Service (Peck, 1976) suggest how parameter estimates may be found by visually inspecting rainfall and runoff records and consulting a map of the catchment. Because of the large number of parameters in the NWS model it is usually thought inadvisable to attempt any optimization. Nevertheless, this has been done for the Cherwell, Blackwater and Mole catchments. The objective function was taken to be the sum of squares of the logarithms of the ratios of predicted to measured discharge values. This was minimized using a simplex algorithm (Nelder and Mead (1965)). A fully rigorous optimization would include a check on the global optimality of estimates, and give an estimate of the matrix of second derivatives of the objective function at the optimum. For the three catchments studied here, given starting values suggested by the nature of the catchments and their response behaviour, parameter optimization was continued until changes in the objective function became small. There is no guarantee of the adequacy of the parameter estimates, but predictions given using the values found have not been unreasonable.

Some changes were made to the NWS model to remove expected parameter redundancy. In view of the possibility of subsurface discharge it was not thought appropriate to retain continuity, so  $U_1$ ,  $U_2$  and  $U_3$  were not constrained to sum to 1. If this constraint is removed, then some restriction on the evaporation parameters is required; we have chosen to set  $E_2$  to 1.

Table 3.1.1 gives estimates of the parameters of the model for each subcatchment. Some interpretation of their values is of interest. Taking the parameters in six groups as before:

---

| Parameter | Cherwell | Blackwater | Mole  |
|-----------|----------|------------|-------|
| UZK       | .114     | .059       | .139  |
| LZPK      | .0142    | .0044      | .0036 |
| LZSK      | .015     | .004       | .014  |
| UZTWM     | 1.02     | .84        | 2.89  |
| UZFWM     | 1.14     | 1.04       | .78   |
| LZTWM     | 2.69     | 1.62       | 2.16  |
| LZFPM     | 3.39     | 3.77       | 4.11  |
| LZFSM     | 1.99     | 2.23       | 1.10  |
| ZPERC     | .8       | .7         | 1.1   |
| REXP      | .6       | .14        | .17   |
| PFREE     | .27      | .93        | .04   |
| RSERV     | .12      | .35        | .11   |
| PCTIM     | .009     | .042       | .081  |
| ADIMP     | .102     | .111       | .260  |
| SARVA     | .000     | .000       | .001  |
| U1        | .024     | .145       | .111  |
| U2        | .234     | .404       | .409  |
| U3        | .251     | .083       | .080  |
| E1        | .682     | .524       | .506  |
| E3        | 1.494    | .506       | .508  |

---

Table 3.1.1 Parameter Estimates

UZK, LZPK, LZSK

The fastest draining storage region is the upper zone, discharging about ten times as quickly as the lower zone secpmdaru free water. Estimates of LZK are similar to LZSK. There may be insufficient information to distinguish between the two conceptual zones. Without any movement of water between storage regions, primary base flow halves in about 100 days, and interflow halves in 10 days.

UZTWM, UZFWM, LZTWM, LZFPM, LZFSM

The values of these parameters are broadly similar for all catchments, giving a total maximum storage of about nine inches of water.

ZPERC, REXP, PFREE, RSERV

ZPERC and REXP are difficult to interpret directly, but are used to compute the percolation rate as a function of the deficit ratio in the lower zone. Values of the percolation rate are given below:

---

|            | Percolation rate, DEFR |      |       |       |       |
|------------|------------------------|------|-------|-------|-------|
|            | 0                      | .25  | .5    | .75   | ..    |
| Cherwell   | .078                   | .080 | .176  | 1.189 | 6.318 |
| Blackwater | .036                   | .287 | .716  | 1.243 | 1.846 |
| Mole       | .030                   | .343 | 1.046 | 2.054 | 3.330 |

---

Clearly, the behaviour of the Cherwell catchment at high deficit ratios is substantially different from the remaining catchments. The value of PFREE for the Blackwater is also very large, recalling that it represents the proportion of percolating water which enters the lower zone free water directly.

Whether these discrepancies represent any true difference in the soil properties of the catchments is a matter for further study.

PCTIM, ADIMP, SARVA

The higher values of PCTIM and ADIMP for the Mole are consistent with its being a clay catchment.

U1, U2, U3

These generally sum to about .6, suggesting that some water does not appear at the outlet, and is not accounted for by evapotranspiration calculated using the factor E1, E2, E3, with E2 set to 1. Some water may be lost through subsurface flow, and evaporation may need to be rescaled.

E1, E2, E3

Values for the Cherwell are quite different from those for the Mole and Blackwater. This is unexpected, since the parameters represent evaporation loss, and in theory are independent of catchment characteristics. Further study should reveal the cause of this discrepancy.

While the idea of using a conceptual model is sound, and the NWS system performs reasonably well, the interpretation put on some of the parameters is not necessarily correct. This is particularly true if parameter values are estimated using optimization. In this study, without recourse to further field measurements, it may be safest to regard the NWS model as empirical.

## 3.2 Thames Water Model

### 3.2.1 Introduction

A brief outline of the Thames Water model is included here. Predicted flows for periods of interest were kindly provided by Thames Water, who carried out the calibration.

In the Thames Water model, hydrological processes are represented by the movement of water between series of conceptual storages. It is used to generate river flow predictions at a given location from rainfall and evaporation estimates, and can reproduce many types of catchment response, ranging from storm runoff to base flow from an aquifer. A catchment may be considered as a whole or as a small number of component zones, each being defined by topographical, soil or geological properties, and having a characteristic response.

Examples of responses which might be recognised include:

- (a) groundwater flow from a permeable part of the catchment;
- (b) runoff from impermeable strata, such as clay, where the soil can develop a soil moisture deficit;
- (c) runoff from riparian areas which develop only very limited soil moisture deficits;
- (d) runoff from paved areas or water surfaces which drain directly to the river;
- (e) effluent discharged into the river.

It may be necessary to have more than one zone in the model representing areas of the same basic type. For example two separate aquifers or clay areas with different characteristics.

The model structure within each component zone is shown in Figure 3.2.1. Where several zones are present they are represented by a number of such structures operating in parallel, as shown in Figure 3.2.2. The soil moisture accounting process contains two storages through which water passes before reaching a river, independently of the type of zone being modelled. Responses appropriate to a particular zone are obtained by adjustment of the

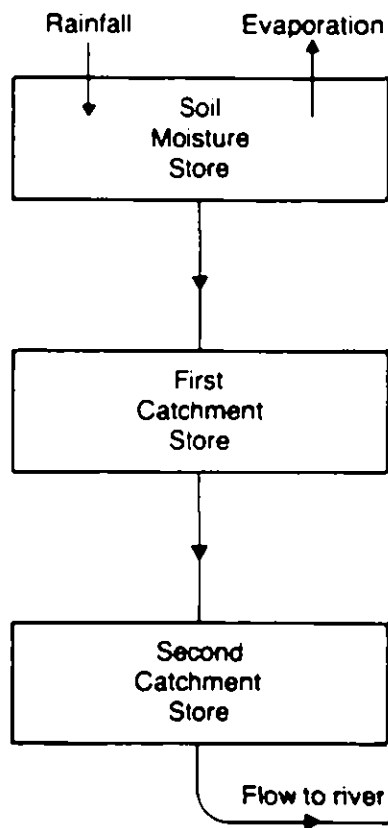


Figure 3.2.1 Model structure within each component zone

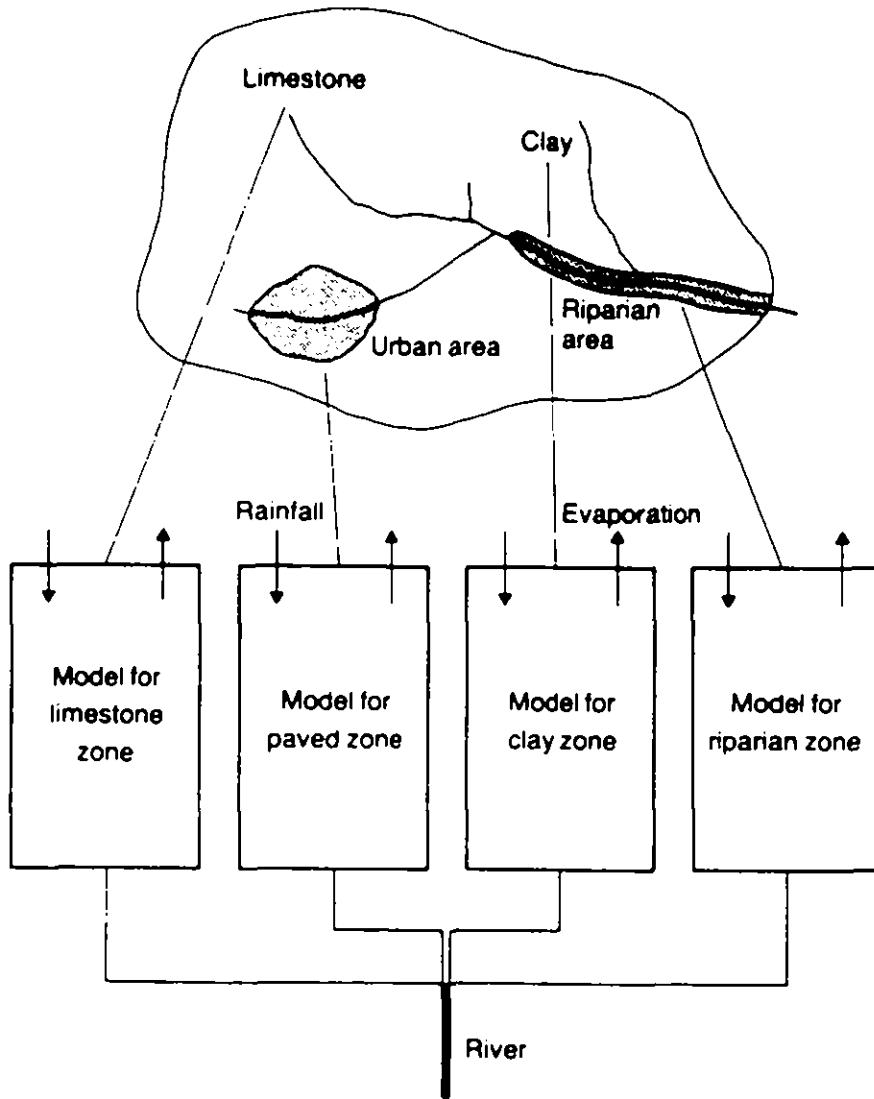


Figure 3.2.2 Operation of parallel zones

values of the parameters which define the relationship between the volume in storage and the outflow from the model's stores.

In some applications the storages of the model may be related to physical characteristics of the area being modelled. Where a soil is underlain by a permeable geological formation, excess water from the soil zone percolates to the aquifer below. The model's stores in this case can be taken to represent firstly the temporary storage of water in the unsaturated zone above the water table and secondly the main store of water below the water table.

Where a catchment has nominally impermeable geology, excess water from the soil zone becomes surface or near surface runoff and the model's stores represent the storage of water mainly over, but probably also within, the surface layers of the soil. The stores cannot be related to specific aspects of overland flow.

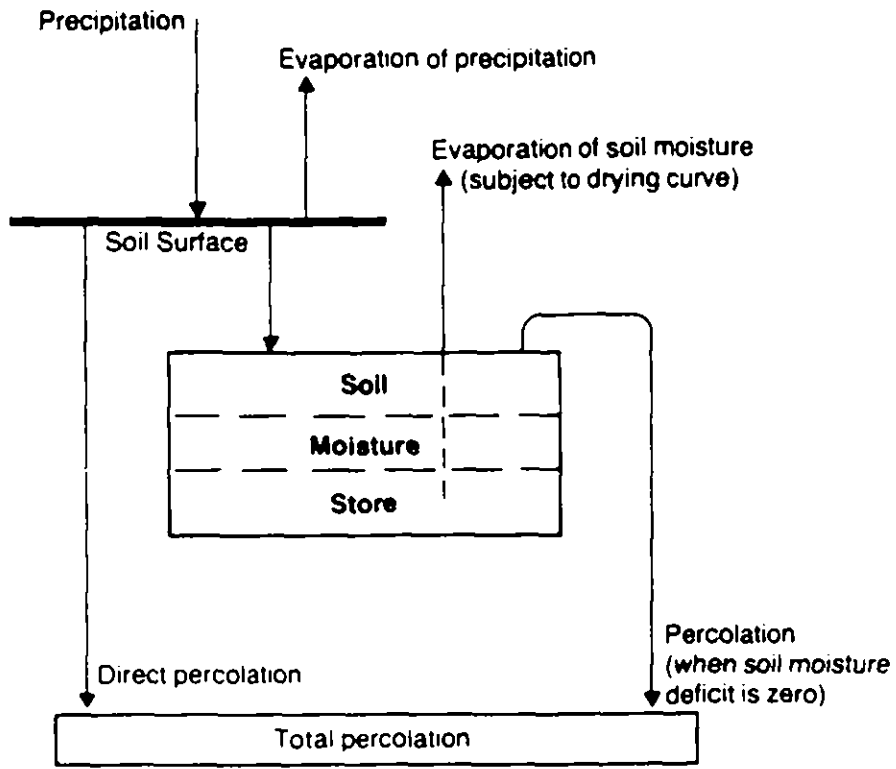
### 3.2.2 Model storages

#### (a) Soil moisture

The soil moisture model is shown schematically in Fig. 3.2.3. The model is based on Penman's concept of the drying curve (Penman 1941, 1949) but there are two important modifications.

The drying curve has been redefined as two straight lines (Fig. 3.2.4); one representing the situation in which evaporation occurs at the potential rate and the second representing the situation where the supply of moisture is limited and evaporation occurs at a constant proportion of the potential rate. This is almost identical in concept to Penman's drying curve in which the two straight lines are joined by a curve. The important difference is in the slope of the second line. Studies of a number of catchments (Hyoms 1980) have indicated that this slope should be close to 0.3 (i.e. the actual evaporation is 0.3 times the potential evaporation) rather than the value of 0.08 (Penman 1949). The deficit value above which evaporation occurs at the lower rate is termed the drying constant. It is one of the parameters evaluated during calibration of the model for a particular area.

### Soil Moisture Model Pervious Soils



### Soil Moisture Model Impervious Soils

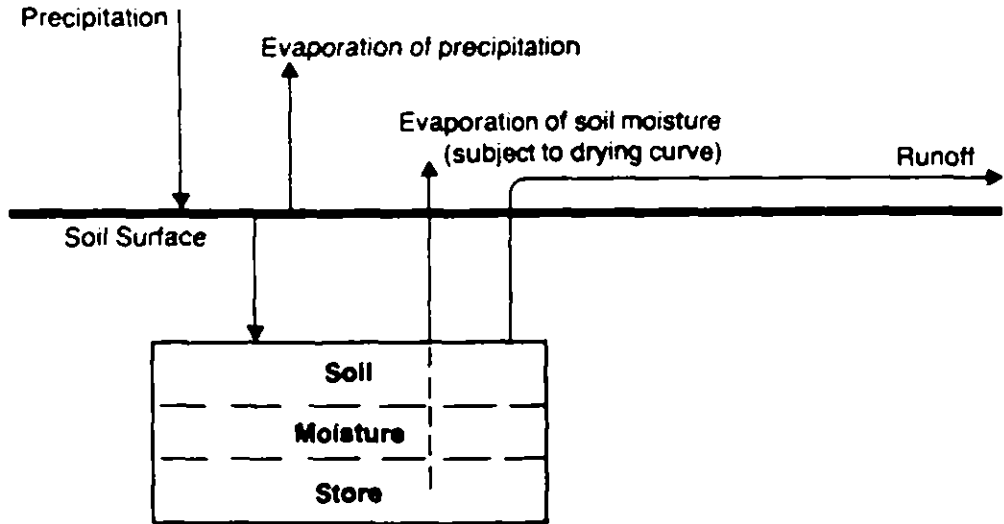


Figure 3.2.3 Soil moisture model

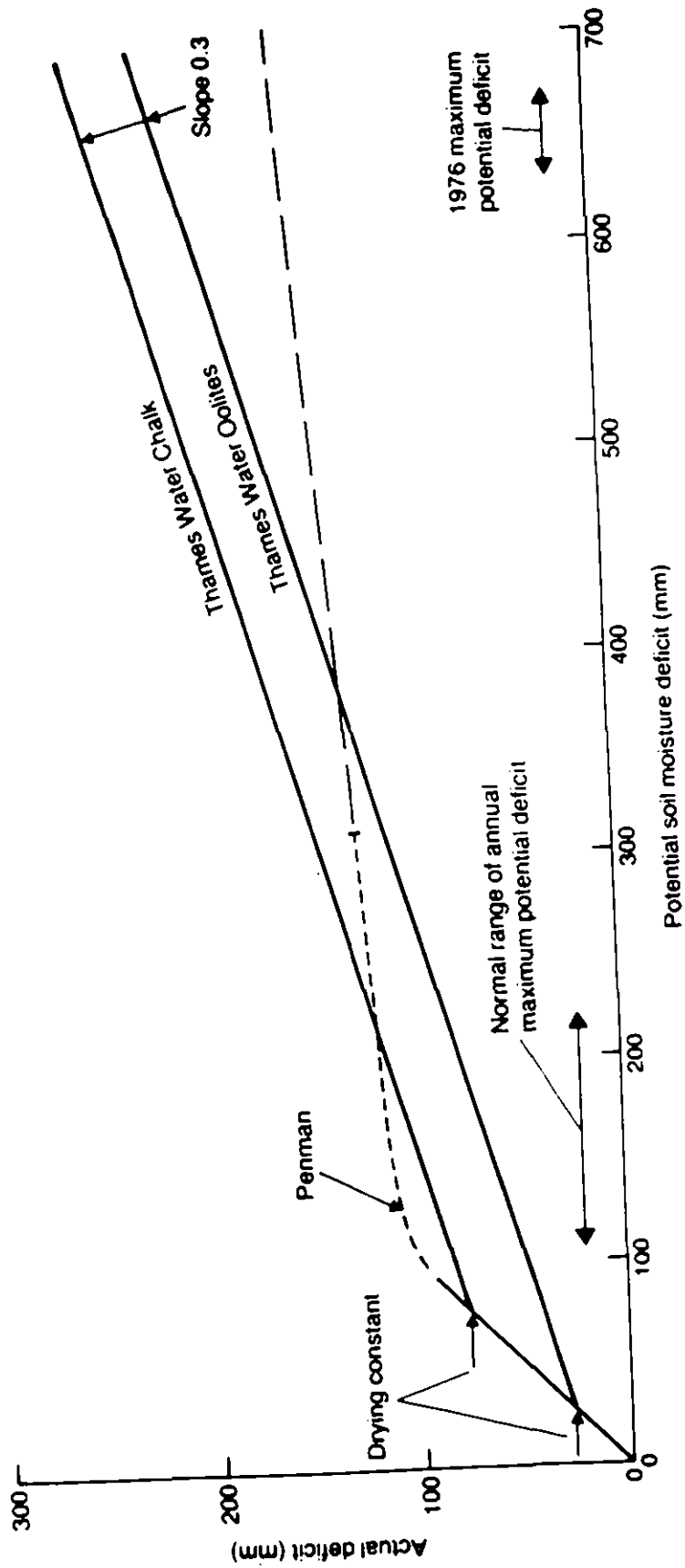


Figure 3.2.4 Modified drying curve

A mechanism, termed direct percolation, has been introduced which allows percolation to occur during periods when there is a soil moisture deficit. This phenomenon, which is apparent from a study of both groundwater levels and river discharge, is not accounted for by the basic Penman model. The method adopted here allows a proportion (usually 15%) of any daily rainfall which exceeds the potential evaporation for that day to bypass the soil moisture store and to become immediately effective as percolation. Direct percolation is taken to occur only in soils over permeable strata.

(b) Catchment storage

The remaining storages in the model represent all the storage regions that excess water from the soil zone passes through before reaching a river. This section of the model is shown in Fig. 3.2.5. The labels relate to the groundwater interpretation of the individual storages. Mathematically the model remains unchanged if it represents surface runoff.

The laws relating outflow to the volume in storage in each of the reservoirs are:

(1) Storage 1

Outflow (R) is proportional to the volume in storage ( $V_r$ )

$$R \cdot C_r = V_r$$

where  $C_r$  is a constant. This means that the first storage behaves as a linear reservoir.

(2) Storage 2

Outflow (Q) is proportional to the square of the volume in storage ( $V_q$ )

$$Q \cdot C_q = V_q^2$$

where  $C_q$  is a constant. The second storage therefore behaves as a non-linear reservoir.

### Ground Water Storage Model

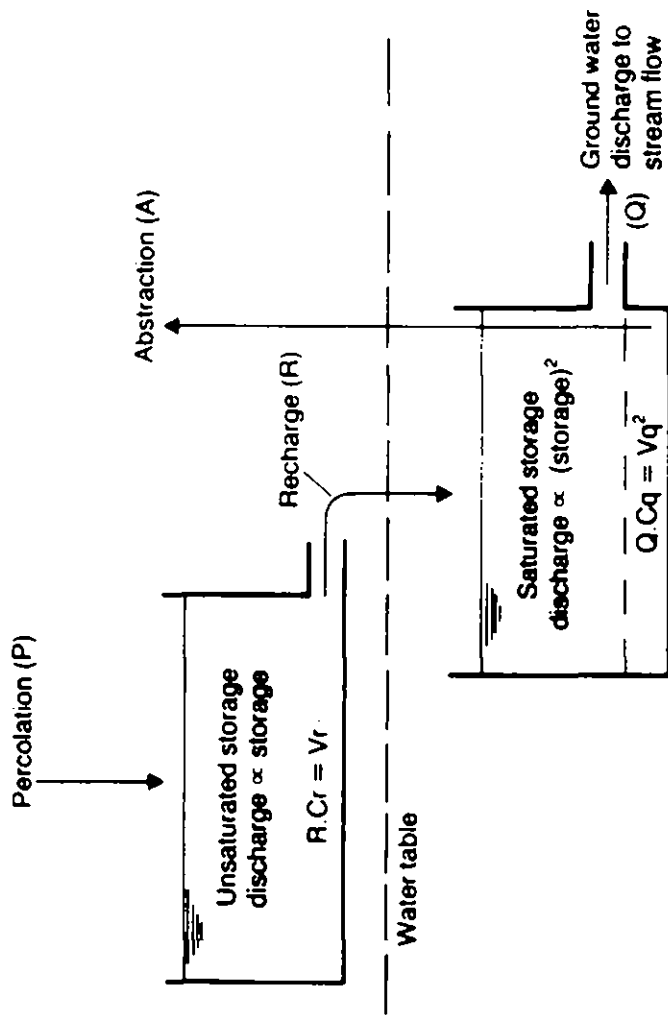


Figure 3.2.5 Ground water storage model

These relationships have been adopted because they have been found to be capable of producing river flows which correspond closely to observed sequences, particularly so far as recession of flow over a long period is concerned. A possible theoretical justification is given later.

### 3.2.3 Method of calculation

#### (a) Soil moisture

Soil moisture storage is represented by two reservoirs. An 'upper' finite reservoir, with a capacity equal to the drying constant, supplies water for evaporation at the potential rate. A 'lower' effectively infinite reservoir supplies water at a reduced rate defined by the slope of the drying curve.

The lower reservoir is depleted only when the upper is empty. Wetting by rainfall will fill the upper reservoir before any replenishment of the lower occurs.

#### (b) Linear reservoir

The law defining outflow (R) from the linear reservoir is:

$$R \cdot Cr = V_r$$

where  $V_r$  is the volume in storage and  $Cr$  is a constant (with units of time)

For a time interval  $\{t_0, t_1\}$  at the start of which the outflow is  $R_0$ , and during which there is a constant input (flow from the soil zone) of  $I$ , it can be shown that the mean outflow during the period is given by

$$R_m = I - Cr(I - R_0)(1 - \exp(b))/T$$

where  $b = -T/Cr$ .

The final outflow, R, is given by

$$R_1 = I - (I - R_0)\exp(b) .$$

The calculations are normally performed with I and R in units of mm/day or mm/hour. To obtain a flow rate it is necessary to multiply by the area of the zone being considered.

(c) Non-linear reservoir

The law defining outflow (Q) from the non-linear reservoir is

$$Q \cdot Cq = (Vq)^2$$

where Vq is the volume in storage, and Cq is a constant (with units of volume time).

The net inflow into this storage is the difference between outflow R from the linear reservoir and any abstraction A. It is possible to derive analytical solutions for the outflow  $Q_1$  at the end of a time interval T, during which the net inflow is I and the initial outflow  $Q_0$ .

To find  $Q_1$ , the differential equation to be solved is

$$\frac{d Vq}{dt} = \frac{(Vq)^2}{Cq} + I .$$

Using the transformed variable,  $z = Vq/\sqrt{I Cq}$ , the differential equation may be written

$$\frac{dz}{1-z^2} = \sqrt{I/Cq} dt ,$$

with solution

$$\tanh^{-1} z_1 = \tanh^{-1} z_0 + \sqrt{I/Cq} (t-t_0) ,$$

where  $z_0 = V_0/\sqrt{ICq} = \sqrt{Q_0/I}$ .

Taking hyperbolic tangents, and letting  $T = \sqrt{I/Cq} (t-t_0)$  gives

$$V_{q1} = (V_{q0} - \sqrt{ICq} \tanh T)/(1 + V_{q0}(\tanh T)/\sqrt{ICq}).$$

If I is negative the relationship  $\tan x = i \tanh (i x)$  can be used to give

$$V_{q1} = (V_{q0} - \sqrt{I'Cq} \tan T')/(1 + V_{q0} (\tan T')/\sqrt{I'Cq})$$

where  $I' = I$  and  $T' = \sqrt{I/Cq} (t_1-t_0)$ .

Note that in this case

$$V_{q1} = 0 \text{ when } V_{q0} < \sqrt{I' Cq} \tan T'.$$

The solution for  $I = 0$  can be found by taking limits as I or  $I' \rightarrow 0$ , using a series expansion for tanh or tan. It is

$$V_{q1} = \frac{Cq V_{q0}}{Cq + V_{q0} (t-t_0)}$$

The flow  $Q_1$  is simply  $V_{q1}^2/Cq$ .

#### 3.2.4 Model Parameters

As described in section 3.2.1, each catchment is divided into a number of regions or zones. The values of the parameters of the model vary between zones. The parameters used are as follows:

| Parameter | Units  | Interpretation                                 |
|-----------|--|--|
| DC        | mm   | Drying constant                                |
| DP        | %  | Direct percolation                             |
| Cr        | day  | Linear storage constant                        |
| Area      | km <sup>2</sup>  | Effective input area                           |
| CqU       | (m <sup>3</sup> sec <sup>-1</sup> )day <sup>2</sup> km <sup>-2</sup> | Non-linear storage constant<br>divided by area |
| D1        | mm   | Initial soil moisture deficit<br>(upper store) |
| D2        | mm   | Initial soil moisture deficit<br>(lower store) |
|           | mm day <sup>-1</sup>   | Initial outflow from<br>linear reservoir       |
|           | 1000 m <sup>3</sup> day <sup>-1</sup>                                | Initial outflow from<br>non-linear reservoir   |

The first five may be regarded as true parameters, the remainder describing the state of the catchment at the beginning of the period of interest.

The choice of zones is based broadly on the geology of the catchment, with some modification if the observed discharges show some pattern which is not apparently accounted for on these considerations only. Parameter fitting is carried out by visually comparing observed and computed hydrographs.

The number of zones used, and their parameter values, are shown in Table 3.2.1. The first zone for the Blackwater and Mole represents a sewage effluent, flowing at the constant rate Q. The final zone for each catchment represents paved areas or water surfaces for which no water deficit is allowed to develop. Note that, because of the parameterization used, high values of Cr and CqU correspond to low response rates and conversely.

For the Cherwell, zone 1 corresponds broadly with the pervious Oolitic limestone of the area, with some direct percolation and a slow response from both catchment stores representing base flow. The two

other major zones, 2 and 3 represent the remaining large clayey area of the catchment, where excess rainfall runs off quite rapidly.

About 40% of the Blackwater catchment has a very slow response, possibly associated with the area of the catchment underlain by sandy Bagshot beds. Another 25% responds rapidly, this corresponding with the clayey area of the Whitewater and Hart subcatchments. A further 15% has an intermediate response.

None of the zones given for the Mole catchment has a particularly slow response. About 15% has a rather slow response, the remainder being fast to very fast. This is to be expected on a predominantly clay catchment.

(a) Cherwell

| Zone | DC   | DP   | Cr  | Area  | CqU   | D1  | D2  | R    | Q      |
|------|------|------|-----|-------|-------|-----|-----|------|--------|
| 1    | 50.0 | 15.0 | 5.0 | 200.0 | 100.0 | 0.0 | 0.0 | 1.83 | 96.96  |
| 2    | 55.0 | 0.0  | 0.5 | 100.0 | 3.0   | 0.0 | 0.0 | 1.88 | 180.16 |
| 3    | 80.0 | 0.0  | 0.5 | 100.0 | 1.0   | 0.0 | 0.0 | 1.88 | 229.37 |
| 4    | 5.0  | 0.0  | 1.0 | 20.0  | 0.1   | 0.0 | 0.0 | 2.03 | 49.00  |
| 5    | 0.0  | 0.0  | 0.5 | 20.0  | 0.5   | 0.0 | 0.0 | 1.89 | 51.87  |

(b) Blackwater

| Zone | DC   | DP   | Cr   | Area  | CqU   | D1  | D2  | R    | Q      |
|------|------|------|------|-------|-------|-----|-----|------|--------|
| 1    | 0.0  | 0.0  | 0.0  | 0.0   | 0.0   | 0.0 | 0.0 | 0.0  | 20.0   |
| 2    | 40.0 | 15.0 | 10.0 | 110.0 | 500.0 | 1.4 | 0.0 | 1.87 | 69.45  |
| 3    | 10.0 | 15.0 | 1.0  | 50.0  | 20.0  | 1.4 | 0.0 | 1.29 | 123.20 |
| 4    | 40.0 | 0.0  | 0.5  | 70.0  | 0.05  | 1.4 | 0.0 | 0.50 | 142.70 |
| 5    | 1.0  | 0.0  | 0.3  | 30.0  | 0.20  | 1.0 | 0.1 | 0.13 | 61.34  |
| 6    | 0.0  | 0.0  | 0.3  | 30.0  | 0.20  | 0.0 | 0.0 | 0.13 | 64.93  |

(c) Mole

| Zone | DC    | DP   | Cr   | Area | CqU  | D1  | D2  | R   | Q    |
|------|-------|------|------|------|------|-----|-----|-----|------|
| 1    | 0.0   | 0.0  | 0.0  | 0.0  | 0.0  | 0.0 | 0.0 | 0.0 | 50.0 |
| 2    | 100.0 | 15.0 | 10.0 | 35.0 | 50.0 | 0.0 | 0.0 | 0.0 | 50.0 |
| 3    | 75.0  | 0.0  | 0.6  | 75.0 | 0.7  | 0.0 | 0.0 | 0.0 | 0.0  |
| 4    | 90.0  | 0.0  | 0.4  | 95.0 | 0.05 | 0.0 | 0.0 | 0.0 | 0.0  |
| 5    | 10.0  | 0.0  | 0.3  | 20.0 | 0.07 | 0.0 | 0.0 | 0.0 | 0.0  |
| 6    | 0.0   | 0.0  | 0.3  | 30.0 | 0.05 | 0.0 | 0.0 | 0.0 | 0.0  |

Table 3.2.1 Parameter values of the Thames Water model

### 3.3 Probability-distributed model

#### 3.3.1 Introduction

A rainfall-runoff model whose complexity is intermediate between physically-based models and simple "black-box" models will be developed in this section based on a consideration of the statistical distribution of hydrological variables over the basin. The approach to be employed essentially considers the frequency of occurrence of the magnitude of hydrological variables over the basin without regard to the location of a particular occurrence within the basin. Thus the random assemblage of different parts will be considered more important than the relation of the parts, one to another. Models of this type may be referred to as being based on a common probability-distributed principle and contrast distinctly with those physically-based models based on a geometrically distributed principle. The specific model developed here will be referred to as the probability-distributed model, or simply by the mnemonic, PDM.

By characterising the process of runoff generation at a point and the spatial distribution of the parameters defining the process over the entire basin, algebraic relations describing the integrated flow response from the basin will be obtained. To make the probability-distributed approach mathematically tractable it will be necessary to make certain simplifying assumptions with regard to the process operating at a point and the process interactions between neighbouring points. Direct runoff generation at a point, as a consequence, will be characterised by a simple reservoir: only a single parameter, the reservoir capacity, defines the response characteristics of the reservoir. In addition it is assumed that there is no interaction between neighbouring reservoir elements. Probability distributions will be used to describe (i) the variability in reservoir capacity over the basin, and (ii) the time for direct runoff generated at a point in the basin to reach the basin outlet.

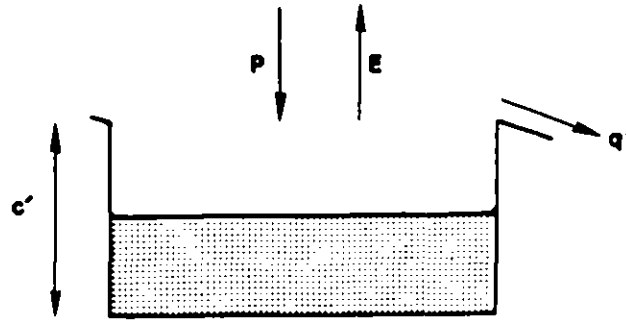
An important outcome of employing the probability-distributed principle is that the threshold-type overflow response from the reservoir, when observed at a point, gives rise to an integrated basin response which is no longer discontinuous in terms of its derivative with respect to the parameter(s) specifying the distribution of reservoir capacities. This attribute allows fast and reliable gradient-based optimisation procedures to be used for model parameter estimation. The probability-distributed model will be developed in detail in the following section.

### 3.3.2 The statistical distribution of stores

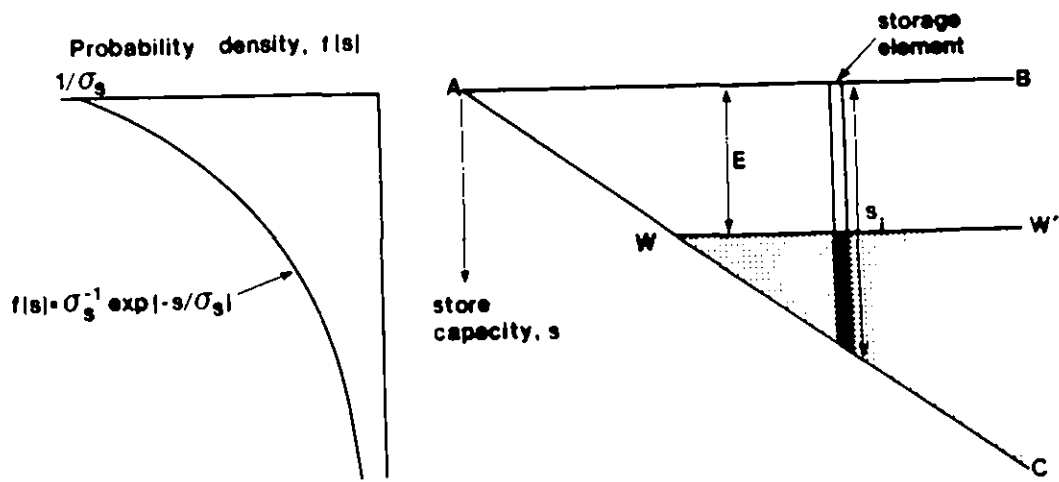
Consider that the simple reservoir in Figure 3.3.1a is used to represent the storage of water in a soil column at a point within a basin, and that it is characterised by its depth or capacity,  $C'$ . Rain falling into the reservoir at a rate  $P$  will be stored until its capacity is exceeded when spillage occurs in the form of direct runoff  $q'$ . Now imagine that the basin is made up of many such soil moisture stores, each characterised by a storage capacity,  $s$ , and that the distribution of  $s$  over the basin is  $f(s)$ : that is, stores in the depth range,  $(s, s+ds)$  occur with probability  $f(s)ds$ . If stores of different depth are ranked in ascending order of depth, with the shallowest on the left, then a wedge-shaped diagram results (Figure 3.3.1b) from drawing a horizontal line,  $AB$ , through the store tops and a sloping line,  $AC$ , through the closed store bottoms.

The assemblage of stores may be visualised as a bundle of capillary tubes of different lengths, and the ranked stores would resemble a set of organ pipes or pan pipes. If all stores are considered to be full of water initially and evaporation occurs at a constant potential rate  $E$  in a unit time interval, then the water level across the stores in the wedge-shaped diagram will be as indicated by the line  $WW'$  in Figure 3.3.1b, with stores of capacity less than  $E$  being empty. Rain falling at a uniform rate  $P$  in the next unit time interval will result in a water level profile across the stores which is made up of three segments: (i) a "capacity segment" (demarcated by  $AW$  in Figure 3.3.1c) in which stores are full, and corresponding to store capacities  $s < P$ , (ii) a sloping "contents segment" in which the water content of stores of increasing capacity is constant and equal to  $P$ , and (iii) a horizontal "deficit segment" in which the water deficit of stores of increasing capacity is constant and equal to  $E-P$ . Figure 3.3.2 shows how an alternating sequence of wet and dry periods gives rise to a number of content and deficit segments; here a sequence of net rainfalls,  $\{\pi_i\} = \{P_i - E_i\}$ , in the intervals  $i = 1, 2, \dots$ , are considered where  $P_i$ ,  $E_i$  are the rainfall and potential evaporation rates in the  $i$ 'th unit time interval. The water content of the  $j$ 'th sloping element is denoted by  $C_j$ , and the water deficit of the  $j$ 'th horizontal element is denoted by  $D_j$ . The capacity of the largest store full of water, and defining the extent of the capacity segment, is denoted by  $C^*$ .

(a) Point representation of runoff production by a simple store



(b) Basin representation by storage elements of different depth and their associated probability density function



(c) Direct runoff production from a population of stores

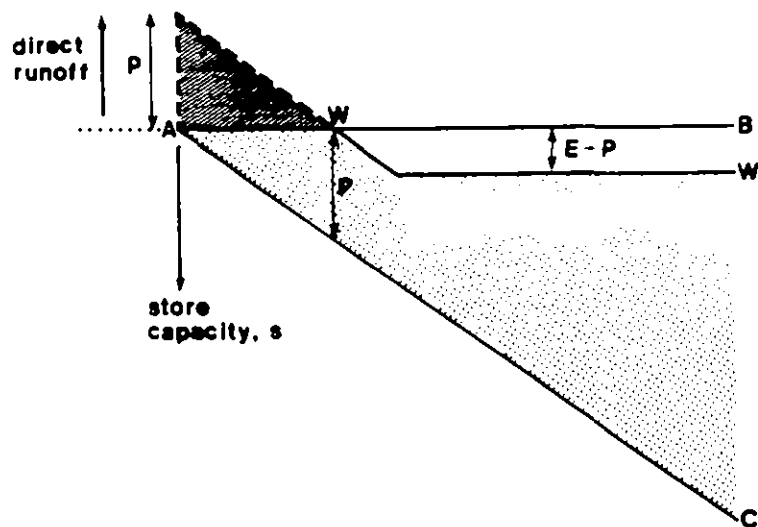
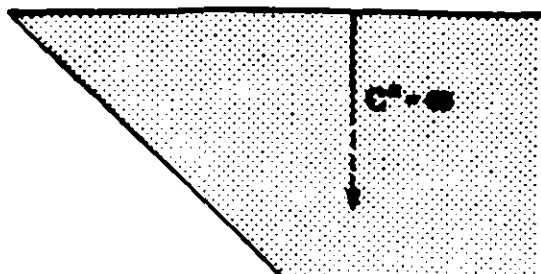
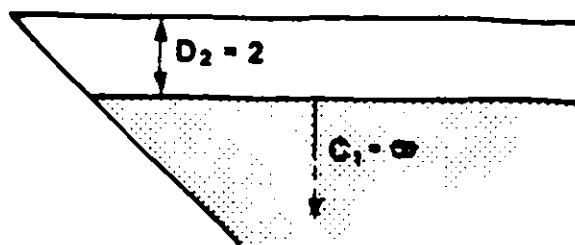


Figure 3.3.1 Definition diagrams of the statistical population of stores

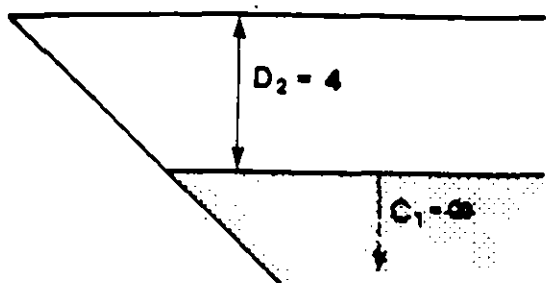
0.



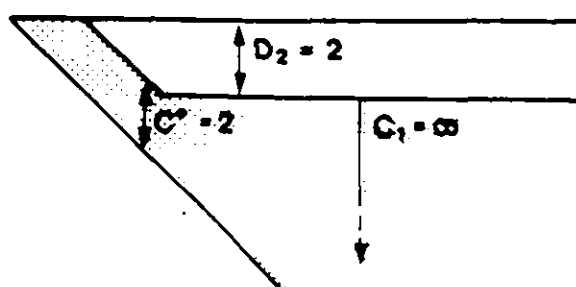
1.  $\Pi_1 = -2$



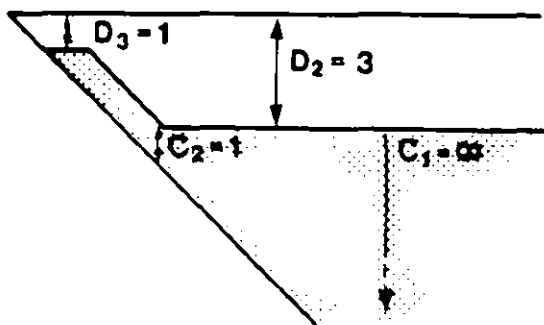
2.  $\Pi_2 = -2$



3.  $\Pi_3 = 2$



4.  $\Pi_4 = -1$



4.6 to 5.  $\Pi_5 = 5$

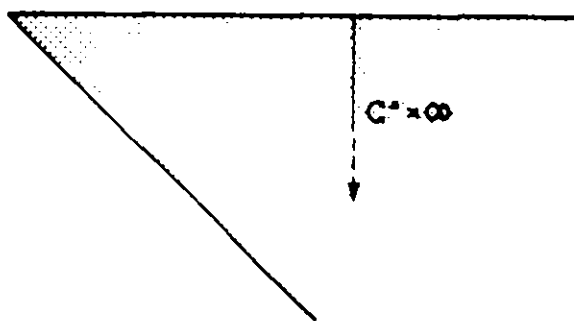


Figure 3.3.2 Updating of content segments,  $C_j$ , and deficit segments,  $D_j$ , for an initially saturated basin after five successive periods during which the net rainfalls,  $\pi_j$ , are  $(-2, -2, 2, -1, 5)$

Rain falling on areas of the basin with storage capacities less than  $C^*$ , and demarcated by the segment AW in Figure 3.3.1c, will spill and generate direct runoff. Considering runoff generation over the unit interval during which rainfall occurs at the uniform rate,  $P$ , initially runoff will be generated only from stores with zero capacity but at the end of the interval all stores with capacities less than or equal to  $C^* = P$  will be spilling and contributing to direct runoff. The volume of runoff generated in the interval is indicated by the triangular hachured area in Figure 3.3.1c. To obtain the true volume of direct runoff, this area requires to be weighted according to the frequency of occurrence of store capacities in a given range: the weighting is defined by the probability density function,  $f(s)$ , depicted on the left-hand side of Figure 3.3.1b. An expression for the volume of direct runoff generated in an interval will be given later.

In general consider net rainfall occurring at a constant rate  $\pi_1$  in the  $i$ 'th wet interval  $(t, t+\Delta t)$ . Then the extent of the capacity segment,  $C^*(t) \equiv C^*$ , generating direct runoff will vary linearly according to

$$C^*(\tau) = C^*(t) + \pi_1 (\tau - t) . \quad (3.3.1)$$

The time interval  $(t, t+\Delta t)$  is chosen such that (i) rainfall may be assumed constant over this interval, and (ii) a deficit segment is not fully replenished during this interval. Therefore  $\Delta t$  will often correspond to the sampling interval of rainfall, but may be shorter depending on the configuration of content and deficit segments. The need for a shorter interval is illustrated by considering the transition from interval 4 to interval 5 in Figure 3.3.2, when the content segment,  $C^*$ , abruptly increases at time 4.6 from 3 to  $\infty$  as the deficit segment,  $D_2$ , is fully replenished by rainfall.

Now since the net rainfall,  $\pi_1$ , at time  $t$  will spill and generate direct runoff from all stores with capacities less than or equal to  $C^*(t)$ , the proportion of the basin generating direct runoff

will be given by

$$\text{Prob}(s \leq C^*(t)) = F(C^*(t)) = \int_0^{C^*(t)} f(s) ds ; \quad (3.3.2)$$

the function,  $F(\cdot)$ , is the distribution function of store capacities. During the wet interval  $(t, t+\Delta t)$  the capacity segment will continue to expand according to (3.3.1), and the proportion of the basin generating direct runoff,  $F(C^*(t))$ , will continue to increase in accord with the contributing area concept of storm runoff generation. The contributing area at any instant of time will be given simply by

$$A_c(t) = A F(C^*(t)) , \quad (3.3.3)$$

where  $A$  is the basin area. If the net rainfall rate,  $\pi_1$ , is considered to be in units of depth of water over the basin in a unit time interval (for example mm/hr) then the direct runoff rate at a point within the contributing area (where the store capacities,  $s$ , are less than or equal to  $C^*(t)$ ) will also be  $\pi_1$ . Since the contributing area of direct runoff represents only a proportion,  $F(C^*(t))$ , of the total basin area, then the instantaneous direct runoff rate from the basin as a whole is obtained as

$$q(t) = F(C^*(t)) \pi_1 . \quad (3.3.4)$$

No assumption has yet been made with regard to the form of the probability density function of store capacities,  $f(s)$ . This will be taken here to be the exponential density,  $f(s) = \sigma_s^{-1} \exp(-s/\sigma_s)$ , so that the frequency of stores within a certain capacity range decreases exponentially with increasing capacity. Although not essential to the development of the model approach, this choice seems physically reasonable since it assumes that there will be many small capacity stores and few stores of large capacity. The exponential density also has the advantage that it is characterised by a single parameter,  $\sigma_s$ , which can be interpreted physically as the mean store capacity. However, Moore (1982) considers the use of a lognormal distribution of store capacity as being physically more plausible, and exploration of the utility of this distribution is continuing.

When the distribution of store capacity is taken to be exponential, then the proportion of the basin generating direct runoff (from (3.3.2)) is

$$F(C^*(t)) = \int_0^{C^*(t)} \sigma_S^{-1} \exp(-s/\sigma_S) ds = 1 - \exp(-C^*(t)/\sigma_S) \quad (3.3.5)$$

which is the expression for the distribution function of the exponential distribution. The basin direct runoff rate at time  $t$  according to (3.3.4) is then given by

$$q(t) = \pi_1 \{1 - \exp[-C^*(t)/\sigma_S]\} . \quad (3.3.6)$$

The volume of direct runoff generated in the  $i$ 'th wet interval  $(t, t+\Delta t)$  is then calculated as

$$\begin{aligned} V_i &= \int_t^{t+\Delta t} q(\tau) d\tau \\ &= \pi_1 \Delta t + \sigma_S \{ \exp[-C^*(t+\Delta t)/\sigma_S] - \exp[-C^*(t)/\sigma_S] \} \end{aligned} \quad (3.3.7)$$

Having now obtained algebraic expressions for the instantaneous rate of direct runoff generation in the basin, and the volume of direct runoff generated in a time interval, we may now proceed to consider how direct runoff is translated to the basin outlet to form total runoff from the basin.

### 3.3.3 Translation of direct runoff to the basin outlet

When direct runoff is generated from the spilling of a full storage element, this runoff will be assumed to travel independently of runoff from neighbouring elements, and to be routed to the basin outlet by means of a linear channel with constant delay  $t$ . Each member of the statistical population of stores will be characterised not only by its depth,  $s$ , but by its translation time  $t$ , and both  $s$  and  $t$  may be considered to be random variables from some distribution. The density of store depths,  $f(s)$ , may now be replaced by the bivariate density,  $f(s, t)$ , where  $t$  is the time

taken for direct runoff from stores of depth  $s$  to reach the basin outlet. It will be assumed here that  $s$  and  $t$  are independent so that the bivariate density factorises to the product of two independent densities  $f(s,t) = f(s)f(t)$ , where  $f(t)$  is the density of translation time. Note that to simplify notation, arguments of the function  $f(\cdot)$  are used to denote different probability density functions:  $f(s)$ ,  $f(t)$ , and  $f(s,t)$ .

The basin runoff rate at time  $t$  will be given by

$$Q(t) = \int_0^t \pi_1 \int_0^{C^*(\tau)} f(s) ds f(t-\tau) d\tau . \quad (3.3.8)$$

Substituting (3.3.2) and (3.3.4) reduces the above to

$$Q(t) = \int_0^t q(\tau) f(t-\tau) d\tau \quad (3.3.9)$$

which indicates that basin runoff is given simply by the convolution of the basin direct runoff,  $q(t)$ , with the probability density function of translation time,  $f(t)$ . Note the equivalence of  $f(t)$  to the instantaneous unit hydrograph or kernel function, and the probabilistic interpretation of  $f(t)dt$  as the probability of the travel time being in the range  $(t, t+dt)$ . We will consider the choice of an appropriate translation time distribution in the next section.

#### **3.3.4 Distribution of translation times**

Moore and Clarke (1983) suggested the use of the inverse Gaussian density as a suitable function to describe the distribution of translation times of direct runoff for the following reasons:-

- (i) Its shape is unimodal and positively skewed;
- (ii) The heavy-tailed nature of the density agrees well with observed hydrograph recessions, without the need for identifying and separating a baseflow component;

(iii) It may be derived as the solution of the convection-diffusion equation for a Dirac delta function input, and thereby related to the Saint Venant equation of open channel flow in linearised form;

(iv) It is characterised by only two parameters which can be related through the linearised Saint Venant equation to the physical characteristics of the stream channel.

The form of the density is

$$f(t; \mu, \lambda) = \left(\frac{\lambda}{2\pi t^3}\right)^{1/2} \exp\left\{\frac{-\lambda(t-\mu)^2}{2\mu^2 t}\right\}, \quad t > 0 \quad (3.3.10)$$

= 0 otherwise.

The parameters  $\mu$  and  $\lambda$  are positive, have units of time, and may be related to the linearised Saint Venant equations (for flow in a rectangular channel and neglecting inertia terms)

$$\frac{1}{2} \frac{A_0 C^2 H_0^2}{Q_0} \frac{\partial^2 p}{\partial x^2} - \frac{3}{2} \frac{Q_0}{A_0} \frac{\partial p}{\partial x} = \frac{\partial p}{\partial t} \quad (3.3.11)$$

at  $x = L_0$ , by the relations

$$\mu = \frac{2 L_0 A_0}{3 Q_0}, \quad (3.3.12)$$

$$= \frac{L_0^2 Q_0}{A_0 C^2 H_0} \quad (3.3.13)$$

here  $Q_0$ ,  $H_0$  and  $A_0$  are the reference flow, depth, and cross-sectional area,  $C$  is the Chezy coefficient, and  $L_0$  is the characteristic length. Equation (3.3.11) is of the form of the convection-diffusion equation

$$\frac{1}{2} \sigma^2 \frac{\partial^2 p}{\partial x^2} + \frac{\partial p}{\partial x} = \frac{\partial p}{\partial t} \quad (3.3.14)$$

for which the inverse Gaussian density (3.3.10) is a solution. The dependent variable  $p \equiv p(x,t)$  may be used to represent the translated flow ( $p \equiv Q(t)$ ) at time  $t$  and at a distance  $x$  from its point of origin. This distance may be taken as  $x = L_0$ , and regarded as a characteristic translation length of the basin. The parameters of the diffusion equation are related to those of the inverse Gaussian density by  $\mu = L_0/v$ ,  $\lambda = L_0^2/\sigma^2$  at  $x = L_0$ . The relative importance of convection and diffusion is governed by the ratio of  $\mu$  to  $\lambda$ , and may be represented by the dimensionless Peclet number

$$P_e = \frac{2\lambda}{\mu} = \frac{2L_0v}{\sigma^2} = \frac{3L_0}{C^2} \left( \frac{Q_0}{A_0 H_0} \right)^2 = 3L \left( \frac{v_0}{CH_0} \right)^2, \quad (3.3.15)$$

where  $v_0$  is the reference velocity.

The limiting case of perfect diffusion is obtained when  $\mu$  when  $P_e \rightarrow 0$ , and the inverse Gaussian density reduces to

$$f(t;\lambda) = \left( \frac{\lambda}{2\pi t^3} \right)^{1/2} \exp\left( \frac{-\lambda}{2t} \right) \quad (3.3.16)$$

which is the solution to the diffusion equation

$$D \frac{\partial^2 p}{\partial x^2} = \frac{\partial p}{\partial t}. \quad (3.3.17)$$

When  $p$  is used to denote the piezometric head,  $h(x,t)$ , we have the equation employed in groundwater hydrology to represent one dimensional flow in a homogeneous isotropic confined aquifer with  $D = T/S$ , and  $\lambda = x^2/2D = Sx^2/2T$ , where  $S$  and  $T$  are the storage coefficient and transmissivity of the aquifer respectively. Venetis (1968) shows that (3.3.16) is the impulse response function of an aquifer represented by (3.3.17) for specified boundary and initial conditions. This link provides a physical reason why the inverse Gaussian density, when used as a runoff translation function, is capable of representing the long-tailed hydrograph recessions derived from the drainage of subsurface water. It is therefore seen that the inverse Gaussian density has a physical basis in terms of its relations to the diffusion and convection-diffusion equations employed

in ground- and surface-water hydrology, and may be expected to provide a sound basis for representing the translation of water to the basin outlet.

The inverse Gaussian density function is plotted for various values of the drift parameter,  $\mu$ , with  $\lambda = 1$  in Figure 3.3.3. The term inverse Gaussian derives from its cumulant generating function's inverse relationship with that of the Gaussian density (Tweedie, 1945), and its properties and use are reviewed in Johnston and Kotz (1970) and Folks and Chhikara (1978).

### 3.3.5 Drainage from storage elements

In developing the probability-distributed approach to direct runoff generation it was assumed that the basin was made up of a statistical population of storage elements. Each element was envisaged as a narrow tube of depth  $s$ , having a closed bottom and an open top, spillage of water from a full tube giving rise to direct runoff. If the tube is now considered to be open at the bottom allowing drainage to occur at a constant rate  $\gamma$  until the tube is empty, then the instantaneous drainage rate,  $b(t)$ , from the population of storage elements at time  $t$  can be calculated as follows. Consider first of all a dry period. At some time  $t$  during this dry period let the water level surface across the population of stores be as depicted by the line  $WW'$  in Figure 3.3.4. Drainage occurs at the instantaneous rate,  $\gamma$ , from all stores containing water, that is from all stores of depth greater than  $D_{k_d}$ . Therefore the instantaneous drainage rate from the basin (prior to translation) at time  $t$  is

$$b(t) = \int_{D_{k_d}}^{\infty} \lambda f(s) ds \quad (3.3.18)$$

which for an exponential distribution of stores gives

$$b(t) = \gamma \exp(-D_k/\sigma_s) . \quad (3.3.19)$$

Now  $D_{k_d}$  is the minimum depth of store still containing water at time  $t$  : let this be denoted by  $D^*(t)$ . Then over a dry interval

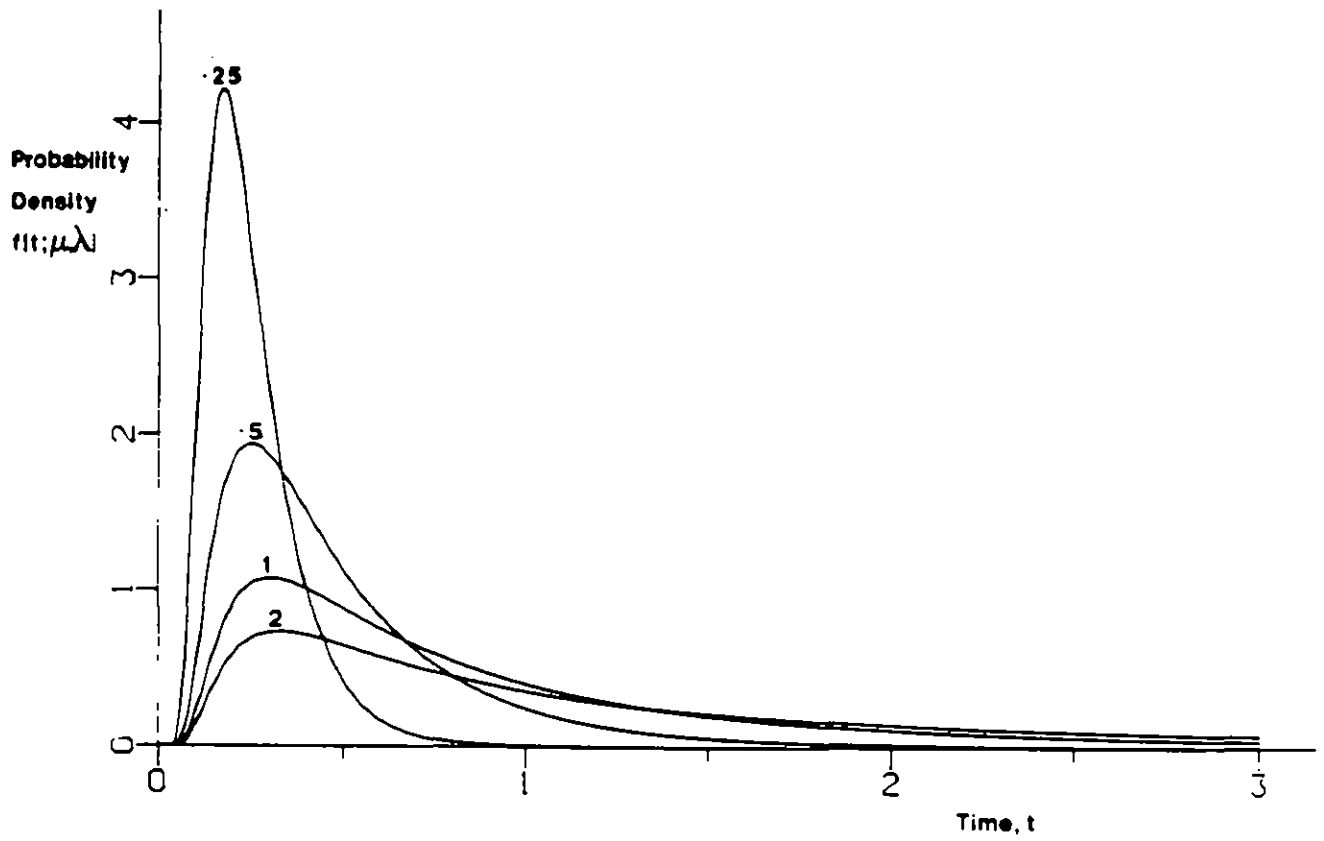


Figure 3.3.3 The inverse Gaussian probability density function for various values of the drift parameter,  $\mu$ , with  $\lambda = 1$

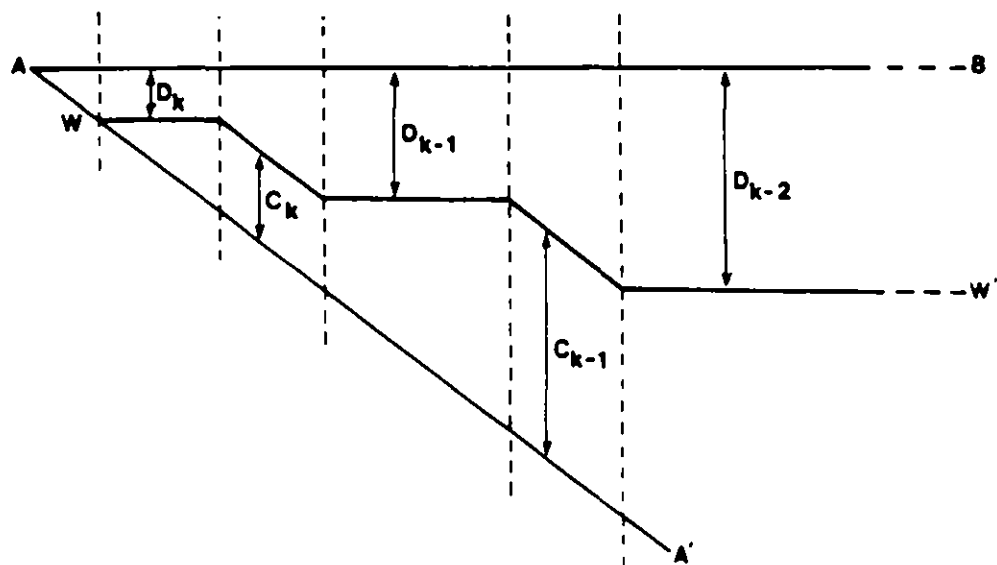


Figure 3.3.4 Definition diagram for deriving expressions for basin drainage

(t, t+Δt) this quantity will vary according to

$$D^*(\tau) = D^*(t) - (\pi_1 - \gamma)(\tau - t), \quad (3.3.21)$$

where the interval Δt is usually the sampling interval, but may be a shorter interval if a contents segment is fully depleted. Note that the emptying of a contents segment will result in an abrupt instantaneous increase in D\*(τ), in an analogous manner to replenishment of a deficit segment during a wet period causing C\*(τ) to change its value abruptly.

We may now calculate the volume of water drained in the interval (t, t+Δt) as follows for an exponential distribution of stores:-

$$\begin{aligned} B(t+\Delta t) &= \int_t^{t+\Delta t} b(\tau) d\tau = \int_t^{t+\Delta t} \gamma \exp[-\{D^*(t) - (\pi_1 - \gamma)(\tau - t)\} / \sigma_s] d\tau \\ &= \frac{\sigma_s \gamma}{(\pi_1 - \gamma)} \left[ \exp(-D^*(t+\Delta t) / \sigma_s) - \exp(-D^*(t) / \sigma_s) \right]. \quad (3.3.22) \end{aligned}$$

As an illustration of this result consider that saturated conditions prevail over the basin at time 0 and that  $P_1 = E_1 = 0$  over the unit interval (0,1). Then  $D^*(0) = 0$  and  $D^*(1) = \lambda$  and the volume of drainage is given simply by

$$B(1) = \sigma_s (1 - \exp(-\lambda / \sigma_s)). \quad (3.3.23)$$

Now consider the complications introduced when drainage occurs under raining conditions. Provided that the instantaneous rainfall rate is less than the evaporation rate ( $P_1 < E_1$ ) then results (3.3.20) and (3.3.22) clearly still hold. However when rainfall exceeds the evaporation rate then drainage from stores with depths less than  $D^*(\tau)$  must also be considered even though some or all may remain empty due to drainage losses. Two cases must be considered.

Case 1 :  $\pi_1 > \gamma$

When the net rainfall exceeds the drainage rate then all stores will drain at the instantaneous rate γ. Therefore the instantaneous

drainage rate from the basin over the wet interval  $(t, t+\Delta t)$  is

$$b(\tau) = \int_0^{\infty} \gamma f(s) ds = \gamma \quad (3.3.24)$$

that is it remains constant and equal to the maximum rate,  $\gamma$ . Also the volume of drainage over the interval  $(t, t+\Delta t)$  will be

$$B(t+\Delta t) = \gamma \Delta t . \quad (3.3.25)$$

Case 2 :  $\pi_1 < \gamma$

When the net rainfall rate is less than the drainage rate then stores with depths less than  $D^*(\tau)$  will lose water by drainage at a rate  $P_1 - E_1$ , whilst stores with depths greater than  $D^*(\tau)$  will drain at the maximum instantaneous rate,  $\gamma$ . Consequently the instantaneous basin drainage rate will be given by the sum of two integrals

$$b(\tau) = \int_{D^*(\tau)}^{\infty} \gamma f(s) ds + \int_0^{D^*(\tau)} (P_1 - E_1) f(s) ds \quad (3.3.26)$$

which for an exponential distribution of stores results in

$$b(\tau) = (\gamma - P_1 + E_1) \exp(-D^*(\tau)/\sigma_s) + P_1 - E_1. \quad (3.3.27)$$

This may be integrated over the interval  $(t, t+\Delta t)$  to obtain an expression for the volume of basin drainage

$$\begin{aligned} B(t+\Delta t) &= \int_t^{t+\Delta t} b(\tau) d\tau \\ &= \pi_1 \Delta t - \sigma_s \left[ \exp\{-D^*(t+\Delta t)/\sigma_s\} - \exp\{-D^*(t)/\sigma_s\} \right] . \end{aligned} \quad (3.3.28)$$

Note that since  $\pi_1 < \gamma$  then the minimum depth of store containing water,  $D^*(\tau)$ , will decrease over the interval  $(t, t+\Delta t)$  and  $\Delta t$  must be chosen such that (3.3.21) is satisfied; thus the time  $t+\Delta t$  may coincide with the time at which a contents segment is fully depleted and not the end of the sampling interval.

### 3.3.6 Translation of drainage to the basin outlet

Translation of drainage to the basin outlet is achieved by forming the sum of the instantaneous direct runoff and drainage rates and convoluting this quantity with the density of travel times. Then the basin runoff rate is given by

$$Q(t) = \int_0^t (q(\tau) + b(\tau)) f(t-\tau) d\tau. \quad (3.3.28)$$

Conceptually this might be justified by considering direct runoff and baseflow to be contributions from hillslope segments to the channel system, both undergoing the same translation mechanism from thereon as controlled by the channel network. Thus the characteristics of the density of travel times  $f(t)$  would be dictated by the characteristics of the channel network.

### 3.3.7 Calibration of the probability-distributed model

The probability-distributed model applied to the Thames basin data has four parameters; these are summarised below:

- $\sigma_s$  mean store depth, mm
- $\gamma$  groundwater drainage rate, day<sup>-1</sup>
- $\mu$  mean translation time, day
- $\lambda$  parameter of inverse Gaussian density, day .

In addition it will be useful when interpreting the parameter values from a physical viewpoint to consider the following derived quantities of the inverse Gaussian translation function:

- (i) mode (or time to peak) (day)

$$t_m = \frac{2\lambda}{3 + \{9 + 4(\lambda/\mu)^2\}} \quad (3.3.29)$$

- (ii) maximum (day<sup>-1</sup>)

$$f_m \equiv f(t_m) = \left( \frac{\lambda}{2\pi t_m^3} \right)^{1/2} \exp \left( \frac{-\lambda(t_m - \mu)^2}{2\mu^2 t_m} \right) \quad (3.3.30)$$

(iii) standard deviation of translation time (day)

$$\text{s.d.} = (\mu^3/\lambda)^{1/2}. \quad (3.3.31)$$

Values of the model parameters, and the above derived quantities, estimated using the calibration set of data are given in Table 3.3.1. Parameters were estimated by minimising the sum of the squares of the differences between observed and predicted flows using a gradient-based optimisation algorithm. Because no input data (rainfall and evaporation) were missing over the calibration set of data, continuous series of predicted flow values could be formed; however, at times when observed flows were missing or considered suspect the corresponding prediction error was omitted from the sum of squares objective function to be minimised. In addition the first year of data for each basin were used to "warm-up" the model to ensure that the store contents were not unduly influenced by a poor choice of starting values.

Inspection of the parameter values and their derived quantities in Table 3.3.1 allow the following observations to be made. The Blackwater model has the shortest response (time to peak equals .960 hours), the smallest peak magnitude, and the largest groundwater drainage rate indicating that the storm response is the most immediate of the 3 basins, but that subsequent contributions from groundwater drainage are important. However, the model for the Mole has the least protracted response, indicated by its low translation time standard deviation. Its response contrasts markedly with that of the Cherwell model which has the largest translation time standard deviation equal to 211 days, and also the longest time to peak of 1.56 days. The mean store depth parameter,  $\sigma_s$ , controls the amount of wetting-up a basin requires before a given proportion of the basin generates runoff, a high value indicating that more wetting up is required : it is in some senses analogous to a basin runoff coefficient. Thus the Blackwater model is seen to be least responsive and the Cherwell and Mole models about equal in their responsiveness to rainfall.

The parameter values presented in Table 3.1.1 were used to obtain the final predicted series employed in the model evaluation study (Chapter 4). No warm-up period was used so the results obtained in the first year will be influenced by the starting conditions

employed. The series were predicted over both calibration and evaluation periods without resetting using observed flow values.

| Basin      | Parameter estimates |                    | Derived quantities |                  |              |              |             |
|------------|---------------------|--------------------|--------------------|------------------|--------------|--------------|-------------|
|            | $\sigma_s$<br>mm    | $\gamma$<br>mm/day | $\mu$<br>day       | $\lambda$<br>day | $t_m$<br>day | $f_m$<br>day | s.d.<br>day |
| Cherwell   | 179                 | .21                | 59.3               | 4.68             | 1.56         | .11          | 211         |
| Mole       | 177                 | .54                | 1.65               | 4.93             | 1.16         | 1.02         | .61         |
| Blackwater | 279                 | .57                | 2.97               | 3.67             | .960         | .47          | 1.55        |

Table 3.3.1 Parameter estimates and derived quantities  
for the probability-distributed model

### 3.4 The Institute of Hydrology conceptual model

#### 3.4.1 Introduction

This model is based on generally accepted concepts of how precipitation moves through the catchment system, and of the constraints determining its emergence as evaporation, transpiration, rapid response runoff or baseflow. The continuity equation is implicitly built into the expressions used so that all inputs are accounted for. Rigorous analytical expressions describing the movement of water through the system are not employed: this is partly because of the difficulties of deriving accurate spatially averaged values for use within them, and partly because of the complexity of many of the expressions which would make their use prohibitively expensive, both in computer capacity and time. Instead, relatively simple expressions which simulate each process with as few parameters as possible are used.

The version of the model used originated in work described by Nash and Sutcliffe (1970), and by Mandeville et al (1970). It was subsequently modified by Douglas (1974), by Dickinson and Douglas (1972), by Blackie (1979), and by Eeles (1978, 1984), for specific applications. The model has produced acceptable results in the simulation of runoff from catchments in the UK and East Africa ranging in area from 37 ha to 1700 km<sup>2</sup> and in annual rainfall input from 500 mm to 2500 mm.

#### 3.4.2 Model concepts

The version of the model described here is designed to produce hourly estimates of streamflow from hourly catchment rainfall and hourly potential evaporation derived from meteorological data using the Penman (1948) expression. The use of this version at daily intervals is not therefore expected to give as good results as for hourly data.

A diagram of the model is shown in Fig. 3.4.1. It consists of four stores representing, notionally, the interception by vegetation, the soil moisture surface storage, the soil profile storage and the groundwater storage. Its range of applications therefore excludes catchments in which snowfall accumulates or those in which the soil



profiles contain horizons with significantly different moisture storages and conductivities. In this form the model has sixteen parameters whose values have to be determined either from field knowledge or by optimisation.

Incoming rainfall, RAIN, enters the interception store until its content, CS, reaches the store capacity, SS. The overflow from this store then enters the soil surface store until its content, CSTOR, reaches the store capacity, SSTOR. The residual rainfall, ERAIN, overflowing the surface store is split between surface runoff and infiltration to the soil moisture store.

The volume assigned to surface runoff, ROFF, is determined by the expression:

$$ROFF = ROP \cdot ERAIN$$

where ROP is a function of the soil moisture deficit, DC, and the rainfall intensity estimated by

$$ROP = RC (e^{-RS \cdot DC} + e^{RR \cdot ERAIN - 1})$$

where RC, RS and RR are parameters to be evaluated. The remaining rainfall, ERAIN - ROFF, infiltrates to the soil moisture store to reduce the soil moisture deficit, DC.

If soil moisture storage is less than field capacity, i.e. if DC is positive, no drainage to groundwater occurs. If DC is negative drainage to groundwater takes place at a rate GPR given by

$$GPR = -A \cdot DC.$$

The interception store is depleted by evaporation at a rate, ES, given by

$$ES = FS \cdot EO$$

where EO is Penman potential evaporation for the day interval.

ES cannot exceed the store content, CS. When FS.EO is greater than CS the residual potential evaporative demand, EEO, equal to  $EO-CS/FS$ , is applied to the soil surface store. This store is depleted in a similar fashion except that the factor applied to the Penman evaporation is FC and not FS as for the interception store. The residual potential demand, EEO', is then applied to the soil moisture store. This store is depleted by transpiration at a rate, EC, determined by

$$EC = FCP \cdot FC \cdot EEO'$$

where FCP is a function of the deficit, DC, given by

$$FCP = 1 \text{ when } DC < DCS$$
$$FCP = \frac{(DCT - DC)}{(DCT - DCS)} \text{ when } DCT > DC > DCS$$

where DCS and DCT represent, respectively, the soil moisture deficits at which transpiration begins to be constrained and finally ceases. Thus total evapotranspiration, relative to Penman EO and to soil moisture storage is determined by the four parameters FS, FC, DCS and DCT.

The surface runoff store is treated as a non-linear reservoir giving the volume contribution to flow as

$$RO = RK \cdot RSTOR^{RX}$$

where RSTOR is the reservoir content at the start of the interval. This in turn is delayed by RDEL time intervals.

The groundwater store is also treated as a non-linear reservoir. In each time interval the volume, GRO, from the store content, GS, is given by

$$GRO = (GS/GSU)^{GSP}$$

where GSU, and GSP are parameters to be evaluated. This output is delayed by GDEL time intervals. Thus total streamflow in time interval n comprises

$$FLOW(n) = RO(n - RDEL) + GRO(n - GDEL)$$

The sixteen parameters whose values have to be evaluated or optimised comprise SS and FS for the interception store, SSTOR for soil surface store, RC, RS, RR, RK, RX and RDEL for the surface runoff, FC, DCS, DCT, and A for the soil moisture store and GSU, GSP and GDEL for the groundwater store.

In addition the initial contents of the stores have to be fixed at the start of each model run. Whenever possible runs are started at a point preceded by several dry days so that CS, the interception store content, can be assumed to be zero, DC is a positive soil moisture deficit, and the contents of the surface runoff store, RSTOR, are close to zero. GS is computed from the initial observed flow, assumed in these conditions to be baseflow only, which leaves the initial value of DC to be estimated from field observations or optimised.

### 3.4.3 Parameter values

Estimates of the parameter values required in the model are shown in Table 3.4.1. These were obtained by minimising the error sum of squares of errors using an algorithm based on the simplex method described by Nelder and Mead (1965). This algorithm was found to be more effective than the one normally used with the IHCM based on the method of Rosenbrock (1960).

The most sensitive parameters are shown for each catchment ranked 1 to 6 in order of decreasing effect on the model explained variance ( $R^2$ ) in Table 3.4.2. These were obtained by setting each parameter to an inoperational value and noting the relative difference in  $R^2$ . From this table it can be seen that the relatively impervious Blackwater catchment has its greatest sensitivity in the parameters controlling surface runoff and evaporation. The Cherwell is considered pervious and this is supported by the higher relative importance of surface response and groundwater parameters. The Mole has mixed subsurface formations and here the evaporative parameters have a higher importance than in the other two catchments; the ratio of model predicted evaporation to Penman open water is 0.86 compared to the Blackwater (0.69) and Cherwell (0.67).

Groundwater parameters, AA and GSU, which affect percolation to the store and the volume output from it, play a significant role in the Cherwell and Mole simulations but are not important in the impermeable Blackwater catchment. The channel routing factor, RK, shows its importance in all three catchments but the routing exponent, RX, is only important in the Mole.

| Parameter | Blackwater | Cherwell | Mole     |
|-----------|------------|----------|----------|
| SS        | 2.4142     | 4.0187   | 0.7435   |
| FS        | 1.4648     | 0.6512   | 2.3735   |
| RC        | 0.2869     | 0.4675   | 0.5438   |
| RS        | 0.0243     | 0.0621   | 0.0310   |
| RR        | 0.0037     | 0.0030   | 0.0022   |
| RDEL      | 1.0132     | 3.9316   | 2.1245   |
| RX        | 1.3241     | 1.2674   | 1.0746   |
| RK        | 0.2638     | 0.2138   | 0.5658   |
| FC        | 0.6014     | 0.8036   | 0.7583   |
| SSTOR     | 0.0551     | 0.2837   | 4.8782   |
| DCT       | 107.5279   | 138.0666 | 361.7682 |
| DCS       | 15.2488    | 20.9483  | 16.1617  |
| AA        | 2.2641     | 2.5043   | 1.4971   |
| GSU       | 467.5642   | 234.9550 | 140.3999 |
| GSP       | 5.6313     | 11.0445  | 2.3548   |
| GDEL      | 3.7087     | 1.5437   | 8.5202   |

Table 3.4.1: IHCM optimised parameter values

---

| Sensitivity ranking | Blackwater | Cherwell | Mole |
|---------------------|------------|----------|------|
|                     | RS         | RS       | RS   |
|                     | RC         | RK       | FC   |
|                     | FC         | AA       | GSU  |
|                     | RK         | DCT      | DCT  |
|                     | DCT        | FC       | RX   |
|                     | SS         | RC       | RK   |

---

Parameters are ranked 1-6 in order of decreasing effect on the model explained variance

Table 3.4.2: IHCM parameter sensitivity

### 3.5. Recession model

#### 3.5.1 Model genesis

The recession model described here was developed into its current form during the course of the present project. It is based on a model structure proposed originally by O'Connell and Jones (1979): this was developed further in cooperation with C. Jelsma, a student visiting the Institute of Hydrology, although the results have not been published. The original structure was intended to be used within a stochastic simulation framework for simulating short-duration (daily) flows, with particular attention being paid to the recession behaviour of the simulated hydrographs. No use was made of observed rainfall data either in model-fitting or during the course of the simulations.

For the present project it was thought useful to try to develop the above structure for use in rainfall-runoff modelling, in view of its success in reproducing realistic recession behaviour. The aim was to arrive at a reasonably simple model which would also be simple to fit, so although some arguments based on conceptual models are used in its development, the final model should probably be regarded as being essentially empirical.

The stochastic simulation model was structured so as to define generated daily flows,  $\{q_t; t=1,2,3,\dots\}$ , recursively as

$$q_{t+1} = f(q_t) + \varepsilon_{t+1}$$

where  $\{\varepsilon_t\}$  were pseudo-random variables representing "effective rainfall" and  $f(\cdot)$  was a suitable function. Here, the recession behaviour of the flows is governed by the properties of the zero-input recursion

$$q_{t+1} = f(q_t),$$

and in particular by the properties of the function  $f(q)$  for small  $q$ . Thus, as stated by O'Connell and Jones (1979), if for some  $c > 1$ ,

$$f(q) = q - \alpha q^c + o(q^c) \quad (q \rightarrow 0) \quad (3.5.1)$$

then, for an appropriate constant  $K$ ,

$$q_t = \{K + \alpha t(c-1)\}^{-1/(c-1)} \quad (t \rightarrow \infty).$$

In later work on the simulation model, it was argued that a recession behaviour like

$$q_t = (K_1 + t)^{-3/2}$$

was a good choice to make. This was on the basis that this behaviour occurs for the impulse response function associated with a groundwater flow model for a homogenous aquifer (Gottschalk, 1977): some empirical checks of this value for the exponent were made although these could have justified exponents in the range  $-1.8$  to  $-1.2$ . Given the choice  $-1.5$ , the corresponding value for  $c$  in (3.5.1) is  $c = 5/3$ . The interim conclusions of the stochastic simulation model exercise were that a model with the nonlinear structure

$$f(q) = \frac{q}{1 + \alpha q^{2/3}} \quad (3.5.2)$$

was reasonable and that differences in behaviour over the year could be accommodated by allowing the coefficient  $\alpha$  to vary sinusoidally over the year.

For the present study, an attempt was made to fit models of the form

$$q_{t+1} = f(q_t) + b_0 r_t + b_1 r_{t-1}$$

Here  $f(\ )$  was the function (3.5.2),  $\{r_t\}$  is the observed daily rainfall series and the coefficients  $\alpha$ ,  $b_0$  and  $b_1$  varied sinusoidally. It was found that such a structure did not perform well, in that the modelled flows did not seem to respond realistically to "catchment

conditions" : thus the response to rainfall is essentially the same whether the flows are currently high or low. It seemed reasonable to adjust the model structure to be more like a non-linear storage model. It turns out that a recession behaviour of the desired form is the outcome of the single-store model with storage-flow relationship given by

$$\frac{dS}{dt} = -k S^3, \quad q = -\frac{dS}{dt},$$

where the input is assumed to be zero. The solution of these equations for (instantaneous) flow  $q$ , given initial flow  $q_0$ , is

$$q_t = q_0 (1 + 2k^{1/3} q_0^{2/3} t)^{-3/2},$$

which has the alternative form

$$q_t = k S_t^3, \text{ where } S_t = \left(\frac{q_0}{k}\right)^{1/3} (1 + 2k^{1/3} q_0^{2/3} t)^{-1/2}.$$

If now input  $R_t$  to the store is introduced just before the end of the period, the final storage is increased by  $R_t$  and hence the final flow would be

$$q_t = k S_t^3, \text{ where } S_t = \left(\frac{q_0}{k}\right)^{1/3} (1 + 2k^{1/3} q_0^{2/3} t)^{-1/2} + R_t$$

or

$$q_t^{1/3} = q_0^{1/3} (1 + 2k^{1/3} q_0^{2/3} t)^{-1/2} + k^{-1/3} R_t.$$

The model structure finally adopted was based on this result, even though the data concerned are for daily-total flows rather than instantaneous flows and in spite of the unrealistic assumption that the input occurs as a single pulse at the end of the interval. Two reasons for using the structure that was adopted are that there is a "catchment wetness effect" built in and that fitting of the model is made fairly easy because some of the parameters can be estimated using simple linear least-squares methods. Although the choice of underlying model in which the rainfall enters as a single pulse is implausible, it does allow this simple fitting procedure to be used.

The final form of the model for simulating flow from rainfall was, after reparameterising,

$$q_{t+1}^{1/3} = q_t^{1/3} (1 + a q_t^{2/3})^{-1/2} + b_0 r_t + b_1 r_{t-1}, \quad (3.5.3)$$

where the coefficients vary over the year as

$$a = a(t+1) = \exp\{-(\alpha_0 + \alpha_1 C_{t+1} + \alpha_2 S_{t+1})\} \quad (3.5.4a)$$

$$b_0 = b_0(t+1) = \beta_{00} + \beta_{01} C_{t+1} + \beta_{02} S_{t+1} \quad (3.5.4b)$$

$$b_1 = b_1(t+1) = \beta_{10} + \beta_{11} C_{t+1} + \beta_{12} S_{t+1}. \quad (3.5.4c)$$

Here the sinusoid terms are defined, for convenience, as

$$C_t = \cos\left(\frac{2\pi}{365}(i-1/2)\right), \quad S_t = \sin\left(\frac{2\pi}{365}(i-1/2)\right) \quad (i=1, \dots, 365)$$

and  $i = i(t)$  is the day number within the year corresponding to  $t$ , and for use in leap years,  $C_t = 1$ ,  $S_t = 0$  for  $i = 366$ .

### 3.5.2 Method of fitting the recession model

In contrast to the other models considered in this report, the recession model has been fitted by minimising an objective function based on one-step ahead forecasts as opposed to the simulation-mode forecasts. This was partly because the aim of later stages of the project will be to examine forecasts updated using the latest available flow information and in this context it is probably sensible to develop empirical models on the basis of forecasting rather than rainfall-runoff simulation. It is also true that for the present model it is rather easier to fit the model structure using one-step ahead errors rather than simulation-mode errors. The one-step ahead forecasting model that has been developed based on (3.5.3), not only uses the latest flow information but also includes an error-correction based on the last one-step ahead error.

For the purpose of this report, models are compared in terms of the simulation-mode forecasts. Now it is not generally true that a model fitted using one-step ahead errors would produce realistic simulation-mode behaviour, particularly if the one-step model includes error correction terms. However the current model did seem to perform reasonably well in this regard, and so it seems worth comparing it with other models in simulation-mode. In practical terms the simulation-mode forecasts can be regarded as being the forecasts one would obtain from the model at a high lead time with the assumption that future records of rainfall were already known, and so give at least an indication of the comparison between forecasting versions of the models at high lead times.

Because of the structure of (3.5.3), it is convenient to make the transformation to cube-root flows,  $y_t \equiv q_t^{1/3}$ . This gives the basic structure as

$$y_{t+1} = y_t (1 + a y_t^2)^{-1/2} + b_0 r_t + b_1 r_{t-1}.$$

Based on this, the one-step ahead forecast  $\hat{y}_{t+1|t}$  of flow  $y_{t+1}$ , given observed data up to time  $t$ , was chosen to be defined as

$$\hat{y}_{t+1|t} = y_t (1 + a y_t^2)^{-1/2} + b_0 r_t + b_1 r_{t-1} + f \varepsilon_{t|t-1}, \quad (3.5.5)$$

where  $\varepsilon_{t|t-1} = y_t - \hat{y}_{t|t-1}$ . Here  $f$  is a further parameter, constant over the year. Overall there are 10 parameters and values for these were obtained by minimising the objective function

$$\sum_t \varepsilon_{t|t-1}^2$$

over the specified fitting period. In practice this was done by noting that, for fixed values of the 3 parameters of  $a$ , the best values of the other 7 parameters are easily found. Thus the method

consisted of a simple manual search over the three parameters  $\alpha_0, \alpha_1, \alpha_2$  which relate to a via (3.5.4). With these values fixed, best values for  $\beta_{00}, \beta_{01}, \beta_{02}, \beta_{10}, \beta_{11}, \beta_{12}$  and  $f$  were obtained as follows. An initial estimate of the series  $\{\epsilon_{t|t-1}\}$  was defined as

$$\epsilon_{t+1|t}^{(0)} = y_{t+1} - y_t (1 + ay_t^2)^{-1/2}.$$

The method then proceeds iteratively to produce new estimates of the parameters and a new estimate of the error series  $\{\epsilon_{t|t-1}\}$ . Thus at stage  $j$ , the following linear regression problem is solved:

|              |                                     |                            |
|--------------|-------------------------------------|----------------------------|
| Regressor:   | $y_{t+1} - y_t (1 + ay_t^2)^{-1/2}$ |                            |
| Regressands: | $r_t$                               | Coefficients: $\beta_{00}$ |
|              | $C_{t+1} r_t$                       | $\beta_{01}$               |
|              | $S_{t+1} r_t$                       | $\beta_{02}$               |
|              | $r_{t-1}$                           | $\beta_{10}$               |
|              | $C_{t+1} r_{t-1}$                   | $\beta_{11}$               |
|              | $S_{t+1} r_{t-1}$                   | $\beta_{12}$               |
|              | $\epsilon_{t t-1}^{(j)}$            |                            |

The fitted regression coefficients are then used to construct  $\{\epsilon_{t|t-1}^{(j+1)}\}$  as the sequence of residuals from this regression. This iterative procedure was found to converge quickly, and the final sum of squares of errors for this regression is the value of the objective function for fixed values of  $\alpha_0, \alpha_1, \alpha_2$  while the coefficients are the best overall values for  $\beta_{00}, \dots, f$  if  $\alpha_0, \alpha_1$  and  $\alpha_2$  have their best values.

While the above procedure fits a model only for the one-step ahead forecasts, forecasts at higher lead times can be defined in an obvious way. Note that, as there is no stochastic model assumed for the errors of the forecasts, the higher lead time forecasts are derived in what seems to be an intuitively appealing way. Thus forecasts  $\hat{y}_{t+\lambda|t}$  of  $y_{t+\lambda}$  with lead time  $\lambda$  (i.e. given flow data to time  $t$ ) are defined recursively as

$$\hat{y}_{t+\lambda+1|t} = \hat{y}_{t+\lambda|t} (1 + a \hat{y}_{t+\lambda|t}^2)^{-1/2} + b_0 r_{t+\lambda} + b_1 r_{t+\lambda-1} \quad (\lambda = 1, 2, 3, \dots)$$

where  $a = a(t+\lambda-1)$ ,  $b_0 = b_0(t+\lambda+1)$ ,  $b_1 = b_1(t+\lambda+1)$ . It is clear that for large lead times,  $\lambda$ , the forecast  $\hat{y}_{t+\lambda|t}$  will be equivalent to the simulation mode forecast  $\hat{y}_{t+\lambda}^{(s)}$  defined recursively by

$$\hat{y}_{t+1}^{(s)} = \hat{y}_t^{(s)} (1 + a \hat{y}_t^{(s)2})^{-1/2} + b_0 r_t + b_1 r_{t-1}. \quad (3.5.6)$$

The above formula of course assumes that the appropriate values of  $r_t$  are available when required. In practice, for forecasting more than one day ahead such values would not exist and some adjustment of the procedure would have to be made. For a context such as forecasting for water resource system operations, rather than flood forecasting, it might be appropriate to set future unknown rainfalls to zero, at least over the immediately following time periods, since this would represent, in some sense, a worst case situation. However for the purposes of the present report, only the simulation-mode forecasts (3.5.6) are of immediate interest.

Because of the transformation to cube-roots of flow ( $q = y^3$ ), the objective function used for fitting is such that it reduces considerably the importance that would otherwise be given to errors associated with forecasting high flows if the objective function had

been the more usual choice of the sum of squared errors in the untransformed flows. This seems sensible in the present context where the aim is to be able to forecast well over the whole range of the flow regime. The model structure (3.5.3) turns out to be very convenient in this regard since the natural objective function for this model has this intuitively reasonable property : otherwise a rather more complicated fitting procedure would have been necessary.

For completeness, the forecasts of flow corresponding to  $\hat{y}_{t+l|t}$  and  $\hat{y}_t^{(s)}$  are given by

$$\hat{q}_{t+l|t} = \hat{y}_{t+l|t}^3,$$

$$\hat{q}_t^{(s)} = \hat{y}_t^{(s)3}.$$

Note that, if the regression-like structure of the model were taken seriously, it would be possible to derive another, rather different, way of transforming the forecasts of the series  $\{y_t\}$  back to the original space to produce an "unbiased" prediction. This has not been done here since the regression is not regarded as being in a statistical model framework.

### 3.5.3 Results of fitting the recession model

The recession model was fitted in the manner described above to the data sets and fitting periods described earlier. However, since the model relies to a considerable extent on the one-step ahead forecasting errors, it was felt advisable to remove from the data for model-fitting certain values which appeared, on visual inspection of the hydrographs and hietographs, to be doubtful. The days concerned are listed below:

#### Cherwell

- 25-27 Dec 1968
- 1 Oct-8 Nov 1969
- 1-31 Mar 1970
- 1- 31 Oct 1970
- 3-4 Sept 1972

Mole

None

Blackwater

26 June - 18 July 1970

There is little problem in handling periods of missing data with this model, except in starting up following such periods: the forecast error required from the previous time step is set to zero in calculating the forecast on the first day after a run of missing values for the value on the next day.

The above periods of data were treated as missing values only for fitting the model. For the model evaluation studies reported later, where the models are compared over the same fitting period, all the existing data was treated as real. This is because, in fact only a very cursory inspection of the data was possible and many more dubious points probably exist. No attempt was made to identify periods of doubtful data for the verification period. The models are compared on an equal footing on the basis of their ability to predict the observed data : periods of "dubious" data may be associated with abstractions or releases to the river or other artificial but real effects.

The values of the parameters for the models fitted to the three catchments are given in Table 3.5.1. Although some negative coefficients for the rainfall were found, in practice this did not lead to negative values for the predicted flows : the negative values are possibly associated with the sharp response to rainfall observed on the Mole and Blackwater catchments, while the Cherwell has a less sharp response.

In calculating the simulation-mode predictions of flow for these catchments, the models were started with an arbitrary initial value of flow on the first day of the initial year of the fitting period, using the first nine months of this year as a warm-up period.

|              | Cherwell | Mole      | Blackwater |
|--------------|----------|-----------|------------|
| $\alpha_0$   | 3.20     | 3.20      | 3.80       |
| $\alpha_1$   | 0.382    | 0.0       | 0.0        |
| $\alpha_2$   | 0.322    | 0.0       | 0.0        |
| $\beta_{00}$ | 0.00293  | 0.01282   | 0.00780    |
| $\beta_{01}$ | .00091   | 0.00423   | 0.00200    |
| $\beta_{02}$ | .00077   | - 0.00315 | 0.00184    |
| $\beta_{10}$ | .00135   | - 0.00553 | - 0.00410  |
| $\beta_{11}$ | .00064   | 0.00061   | - 0.00061  |
| $\beta_{12}$ | .00039   | - 0.00083 | - 0.00045  |
| $\tau$       | 0.208    | - 0.307   | - 0.462    |

Table 5.1 : Parameters of fitted recession model. Units of flow and rainfall data assumed to be in equivalent  $m^3/s$ .

### 3.6 Constrained Linear System Models

#### 3.6.1 Macro-Scale Models

In modelling the rainfall-runoff relationship at the catchment scale, it is useful to distinguish between three types of models: distributed physics-based models, lumped conceptual models and input-output (or 'black-box') models. Earlier sections of this report discussed the US National Weather Service model, Thames Water Model and IH conceptual rainfall-runoff models - all representing the lumped conceptual approach.

A classical example of the black-box model is the unit hydrograph which postulates a linear relationship between effective rainfall and storm runoff. The model can be identified using any one of a number of input-output system techniques. One efficient way is to formulate the model estimation problem as a quadratic optimization problem as proposed by Natale and Todini (1976). The resulting model, known as the constrained linear system (CLS) model is discussed in greater detail in the next section.

In engineering hydrology, linear unit hydrograph models of the rainfall-runoff process have been widely used, with favourable results. The basic assumption in using such models is that a 'law of large systems' can be applied to complex hydrological systems. The multitude of non-linear, distributed elements can often be represented in a lumped macro representation by a linear model.

The linearity assumption in the unit hydrograph approach applies to the response to effective or excess rainfall. Total rainfall must first be converted to effective rainfall through an appropriate soil moisture model. For severe rainfall flood forecasting conditions, the soil moisture component plays a diminished role and in this case total rainfall may be used in unit hydrograph models. For continuous modelling of both wet and dry periods, the role of soil moisture must be considered.

Figure 3.6.1 illustrates the major components of the basin water budget. There are three major sub-systems: (i) the direct storm response to excess rainfall, (ii) the soil moisture response system in the unsaturated zone which controls infiltration, the volume of excess

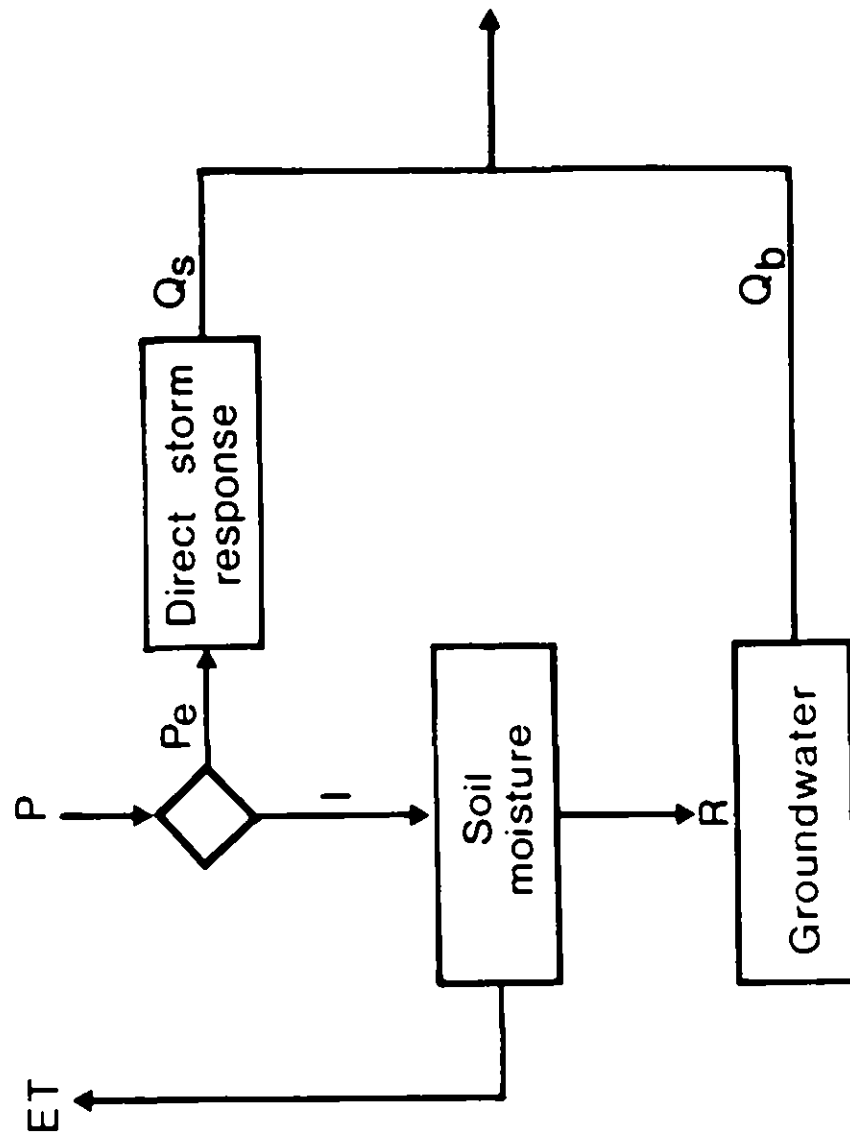


Figure 3.6.1 Major components of basin water budget

rainfall and actual evapotranspiration and (iii) the groundwater system which responds to recharge to produce base flow.

The two models reported here differ in the way the total rainfall is converted into excess rainfall. Both models then use the excess rainfall and the measured outflow to estimate the impulse response function (unit hydrograph) using the Constrained Linear System (CLS) model. The next section will describe CLS, followed by a description of the rainfall preprocessors.

### 3.6.2 Constrained Linear System (CLS) Model

The CLS model is based on the instantaneous unit hydrograph (IUH). The discharge at time  $t$  is calculated using a discrete time convolution operator

$$q_t = \sum_{j=0}^k p_{t-j} u_j \quad (3.6.1)$$

where  $p_{t-j}$  is the effective rainfall at time  $t-j$  and  $u_j$  is the  $j$ th ordinate value of the impulse response. The kernel length of the impulse response is  $k$ . Equation (3.6.1) can be written in vector notation

$$Q = P \cdot U \quad (3.6.2)$$

where  $Q$  is an  $m$ -dimensional vector of discharges,  $U$  a  $(k \times 1)$  vector of impulse response ordinates and  $P$  an  $(m \times k)$  matrix of effective rainfall values. Row  $\lambda$  of  $P$  consists of the rainfall values  $p_{\lambda-j}$ ,  $j=0, \dots, k$ , and are used to calculate  $q_{\lambda}$ .

Equation (3.6.2) can be generalized to consider  $n$  inputs each acting on a different impulse response function and through superposition results in the discharge  $q_t$ . This multiple input model can be written as

$$Q = \sum_{i=1}^n P_i U_i \quad (3.6.3a)$$

$$= \underline{P} \underline{U} \quad (3.6.3b)$$

where  $P_i$  and  $U_i$  represent the  $(m \times k)$  input matrix and  $(k \times 1)$  impulse response vector for input  $i$ ,  $\underline{P}$  is a  $(m \times n \cdot k)$  partitioned matrix made up as  $\underline{P} = [P_1 : P_2 : \dots : P_n]$ , and  $\underline{U}$  is the  $(n \cdot k \times 1)$  partitioned vector  $\underline{U} = [U_1 : U_2 : \dots : U_n]^T$ , where  $T$  denotes transposition.

The observed record  $Q$  and  $\underline{P}$  are used to estimate  $\underline{U}$ . The original CLS model considered, instead of (3.6.3b), the expression

$$Q = \underline{P} \underline{U} + E \quad (3.6.4)$$

where  $E$  is an  $(m \times 1)$  vector of errors which takes into account modeling errors and errors in the data.

CLS minimizes the functional

$$J(E^T E) = \frac{1}{2} \underline{U}^T \underline{P}^T V_E^{-1} \underline{P} \underline{U} - \underline{U}^T \underline{P}^T V_E^{-1} (Q - \bar{E}) \quad (3.6.5)$$

subject to some optional choice of constraints, listed below.  $V_E$  is the covariance matrix for  $E$ , assumed to be  $\sigma^2 I$  (temporally stationary) and  $\bar{E}$  is the mean of  $E$ . The possible constraints are:

1. No constraints; then (3.6.5) represents an unconstrained ordinary least-squares problem and reduces to : minimize

$$= 1/2 \underline{U}^T \underline{P}^T \underline{P} \underline{U} - \underline{U}^T \underline{P}^T Q \quad (3.6.6)$$

2. Non-negativity constraints on  $\underline{U}$ ; thus  $\underline{U} > 0$  requires only positive ordinates of the impulse response.

3. Constraints  $\underline{U} > 0$  and  $G \cdot \underline{U} = 1$ ; the latter linear equality constraints can be used to impose continuity upon the estimate of  $\underline{U}$ , (1 being the unity vector). Here the values and structure of  $G$  can be derived from the physics of the problem.

In the case of 2 and 3, equation (3.6.5) is minimized subject to the appropriate constraints.

The original model development of Natale and Todini (1976) was applied to flow routing with tributary inputs. For this application constraint 3 above was important. Further, linear models work quite well. When CLS was applied to rainfall-runoff modelling, it was recognized that the non-linear response of the catchment, due to varying pre-storm moisture conditions, could be approximated by estimating different impulse response function for varying soil conditions (for example, wet or dry). The actual precipitation data (time series) were assigned to different input vectors depending upon soil moisture conditions. The soil moisture condition was approximated by an antecedent precipitation index (API). Figure 3.6.2 illustrates the procedure.

This approach of using actual precipitation and varying the input response function due to moisture conditions was often satisfactory for large catchments or for flood prediction where the actual catchment response is quasi-linear. For those situations where soil moisture thresholds have a greater influence on catchment response (small catchments with large moisture storage after prolonged dry periods), the CLS/API approach gave poorer simulation performance (Datta and Lettenmaier, 1985).

In this study for Thames Water Authority, an alternative approach was taken - the input vector P was modified through a continuous soil moisture accounting model to provide effective precipitation. Two such preprocessors are described.

### **3.6.3 Precipitation - Soil Moisture Accounting Preprocessor**

The soil moisture system is of critical importance to the accuracy of continuous time rainfall-runoff simulations. Within this system there exists a feedback mechanism since the soil moisture level controls the rate of infiltration and evapotranspiration. There is a further complication due to non-linear threshold effects. For rainfall rates less than the infiltration rate, no surface runoff will be generated. This potential infiltration rate varies and is a function of the cumulative infiltration and initial soil moisture. On the other hand, if the precipitation rate exceeds the infiltration capacity at any point then infiltration will occur at this potential rate and the remainder of the precipitation will appear in the direct storm response.

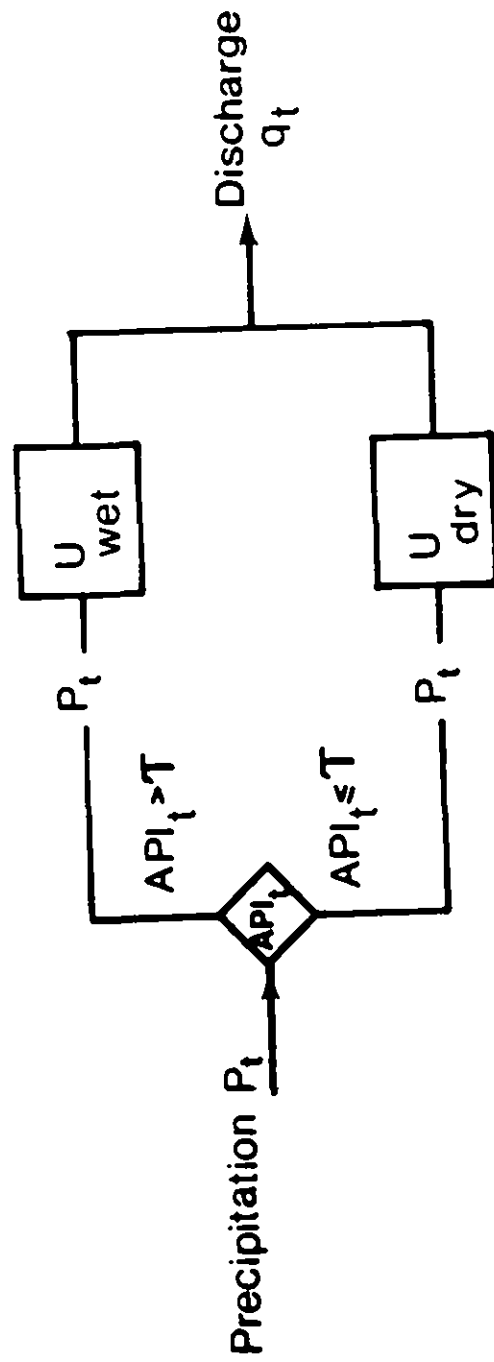


Figure 3.6.2 CLS model with API preprocessor

On the scale of an experimental plot it may be reasonable to assume that the potential infiltration rate is uniform. On the scale of a catchment this is unreasonable. In many hydrologic models, catchment scale infiltration models are based upon empirical relationships (eg Horton's model) or upon simplified storages (eg US Weather Service river forecasting model). Recently Moore and Clarke (1981) developed a model based on a distribution of storages. The model proposed herein follows a similar approach.

### 3.6.3.1 Catchment Scale Soil Moisture Model: Preprocessor I

In Figure 3.6.1, the soil moisture sub-system is composed of three processes. The first is the response to precipitation through infiltration, the second is the response to potential evapotranspiration and the third is drainage and recharge to groundwater. The proposed model has a sub-model for each process.

Over a catchment, the depth to groundwater and the soil moisture deficit will vary. This variation is due to variability in soil type, topography and vegetation. Runoff may occur in at least two ways: rainfall intensity exceeding the infiltration capacity on a variable area of near-saturated soils resulting in the partial area concept of Betson (1964) or rainfall on completely saturated soils adjacent to stream channels (Dunne and Black, 1970).

Both mechanisms produce a partial contributing area which generates the direct storm response. Following Pandolfi, et. al., (1983), let us define the variation in catchment infiltration capacity as

$$= i_m(1 - (1 - A)^{1/B}) \quad (3.6.7)$$

where  $i_m$  is the maximum point capacity within the catchment,  $A$ , is the fraction of the catchment with capacity less than or equal to  $i$ , and  $B$  is the catchment storage parameter. The total infiltration capacity,  $I$ , is obtained by integrating (3.6.7) over the basin, which results in  $I = i_m/(1 + B)$ . Figure 3.6.3 illustrates the infiltration capacity curve for  $B < 1$ . Notice that the area under the infiltration capacity curve represents the catchment storage capacity. Prior to a precipitation event of magnitude  $P$ , let the soil moisture within the catchment be  $I_0$ , as shown in Figure 3.6.4. The catchment fraction  $A_S$

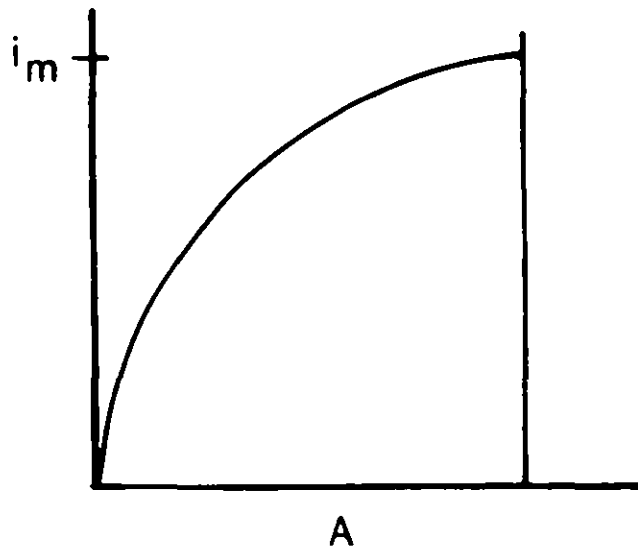


Figure 3.6.3 Catchment infiltration capacity curve

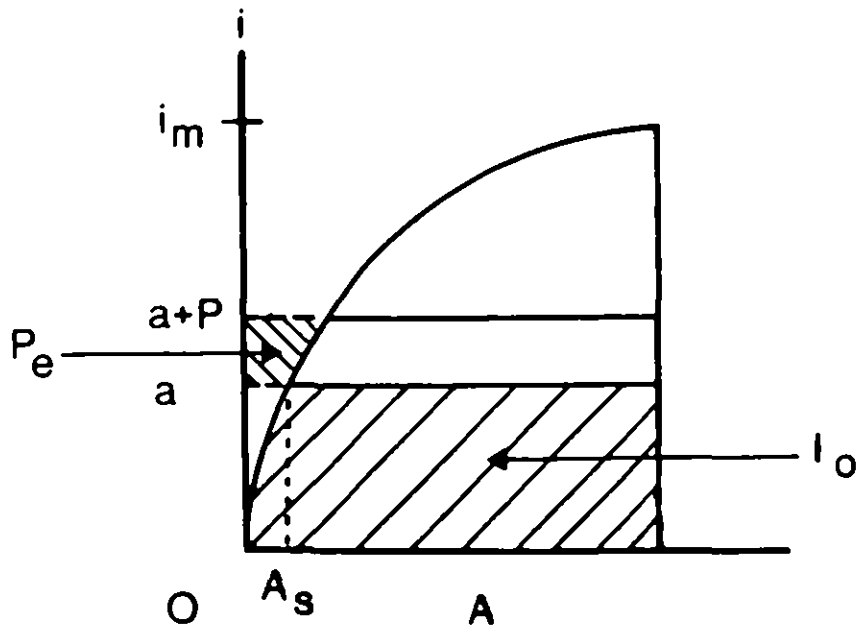


Figure 3.6.4 Effective precipitation computation

is assumed to be saturated and a contributing area at the onset of the event. The excess precipitation is that part of the precipitation that occurs over the saturated portion of the catchment and is calculated by

$$P_e = \int_a^{a+P} A \, di. \quad (3.6.8)$$

After integration,  $P_e$  is:

$$P_e = P + I_0 - I + I \left(1 - \frac{a + P}{i_m}\right)^{B+1}, \text{ for } a + P < i_m.$$

$$P_e = P + I_0 - \quad \text{for } a + P > i_m. \quad (3.6.9)$$

The catchment scale soil moisture is  $I_0 + P - P_e$  for  $P + a < i_m$  and is  $I$  for  $P + a > i_m$ .

In the infiltration-runoff (excess precipitation) equations,  $I_0/I$  represented catchment dryness to which one can relate the ratio of actual evaporation to potential evaporation. A function of the form

$$\frac{E}{E_p} = 1 - (1 - I_0/I)^{1/B_e} \quad (3.6.10)$$

is used and gives, for  $B_e = .6$ , evaporation values similar to those observed (Ripple, 1972).

The rainfall-runoff relationship behaves as a non-linear storage element. It can be assumed that the contents of the storage element,  $I_0$ , drains and contributes to base flow as a linear storage element. Thus the base flow can be represented as

$$R_b = B_d I_0/I. \quad (3.6.11)$$

The catchment water balance model consists of equations (3.6.9) - (3.6.11) and is represented by four parameters,  $B$ ,  $i_m$ ,  $B_e$  and  $B_d$ .

The total effective precipitation for the time interval  $t$  (from the direct storm response and base flow) is represented by

$$P_t^e = P_e + R_b. \quad (3.6.12)$$

Thus  $P_t^e$  is the input used by CLS and can be regarded as the total basin input for time interval  $t$ .

### 3.6.3.2 Catchment Scale Soil Moisture Model - Preprocessor II

The pre-processor reported in this section is based upon the work of Datta and Lettenmaier (1985). The preprocessing procedure consists of separately computing the contribution of total precipitation to depression storage, interception storage, and infiltration. The contribution to infiltration is computed on the basis of the existing soil conditions. The assumptions made are empirical and simplified compared to physics-based models. However, the calibration process of CLS has the advantage that systematic errors are offset through the input-output calibration procedure. Use of the preprocessor effectively incorporates time variance and nonlinearity in the catchment response.

The precipitation preprocessor assumes that the observed runoff results from precipitation after entering one of three storage elements, or the impervious area, as shown schematically in Figure 3.6.5. The overland flow caused by direct precipitation on impervious area together with the overflow from the storage elements, acts as the effective precipitation causing the observed runoff, when transformed by the impulse response function of CLS.

The contribution of precipitation to infiltration is computed as a function of the existing volume in infiltration storage. The fraction of total precipitation actually entering the ground as infiltration is assumed to decay exponentially as the contents of this storage volume increase.

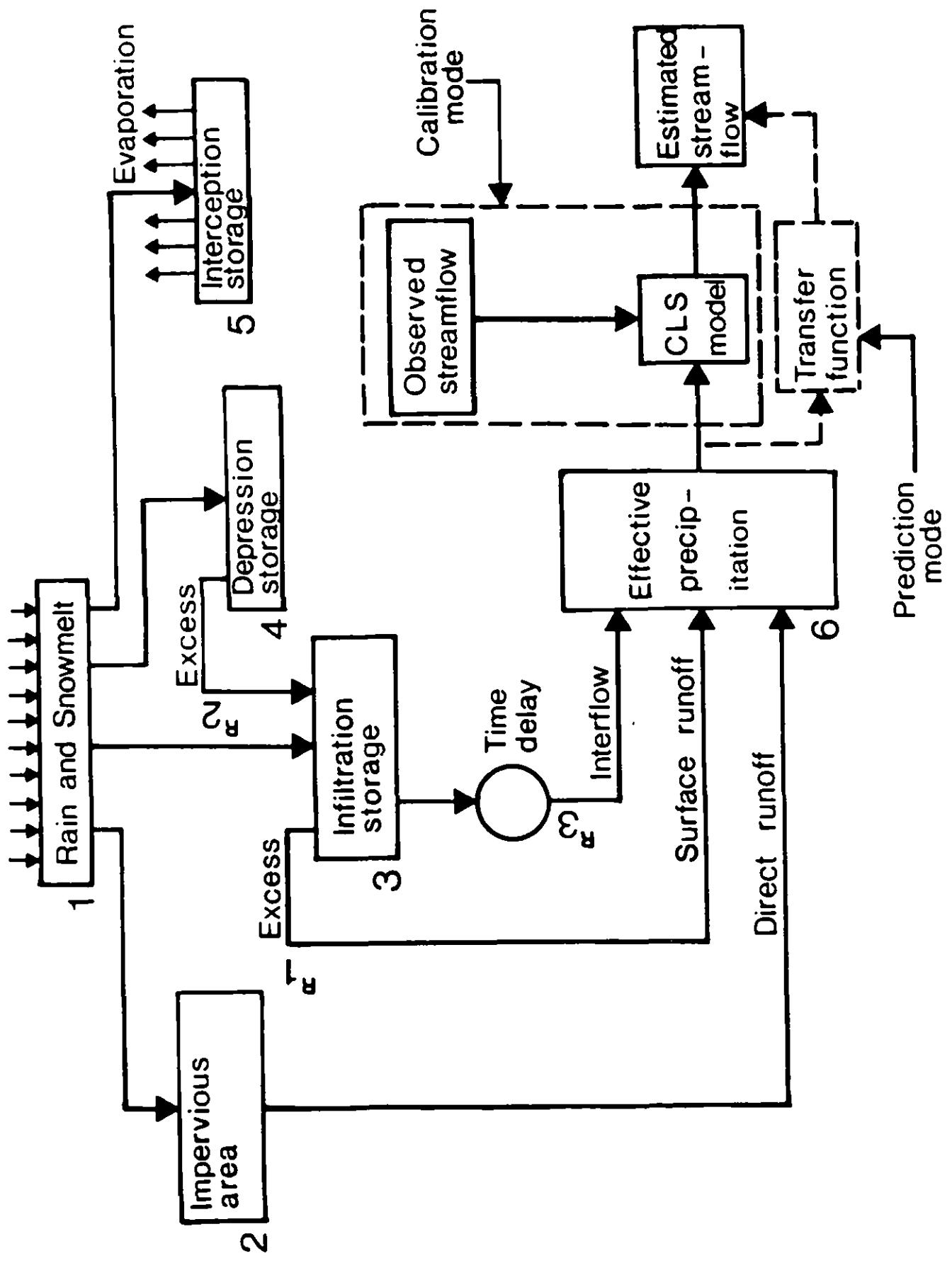


Figure 3.6.5 Schematic Diagram of Precipitation Preprocessor II after (Datta and Lettenmaier (1985))

The most important part of the model is the computation of the percentage contribution of total precipitation to infiltration. The amount of infiltration is assessed on the basis of the accumulated storage in the ground; this amount is therefore time-variant.

The following notation is used in the model:

- K = non-negative constant
- $\alpha$  = fraction of gross precipitation infiltrating into the ground
- $C_1$  = infiltration capacity when the existing infiltration storage is empty
- $C_2$  = infiltration capacity when the existing infiltration storage is full
- $S_t$  = infiltration storage at the end of time period  $t$
- CAP = maximum possible infiltration storage
- $peg_t$  = gross precipitation minus the infiltration during time period  $t$
- $D_t$  = contribution to depression storage during the time period  $t$
- $IC_t$  = contribution to interception storage during the time period  $t$
- $PG_t$  = gross precipitation during time period  $t$
- $I_t$  = infiltration during time period  $t$
- $V_d$  = depression storage capacity
- $V_i$  = interception storage capacity
- $Sd_t$  = depression storage at the end of the period  $t$
- $P_t$  = effective precipitation contributing to runoff
- $R_1, R_2, R_3$  = rate constants for controlling infiltration
- $\beta$  = rate constant for actual evaporation

The fraction of gross precipitation appearing as direct runoff is defined as a function of the two limiting values  $C_1$  and  $C_2$ . The infiltration capacity is assumed to decrease exponentially with increasing water content in infiltration storage. Because the model uses lumped parameters,  $\alpha$  can be considered equivalent to a fraction representing the ratio of the pervious to the total area of the catchment which varies with time:

$$\alpha = C_2 + (C_1 - C_2) e^{-K\left(\frac{S_{t-1}}{CAP}\right)} \quad (3.6.13)$$

The net precipitation, given by gross precipitation minus infiltration is given by:

$$P_t^{eg} = (1 - \alpha) P_t^g, \quad (3.6.14)$$

so the portion of total precipitation infiltrating into ground storage is

$$I_t = \alpha(P_t^g). \quad (3.6.15)$$

Infiltration storage at the end of time period  $t$  is defined as:

$$S_t = S_{t-1} + I_t - R_3(S_{t-1}) \quad \text{for } S_t \leq CAP. \quad (3.6.16a)$$

$$S_t = S_{t-1} + I_t - R_3(S_{t-1}) - R_1[S_{t-1} + I_t - R_3(S_{t-1}) - CAP]$$

$$\text{for } S_{t-1} + I_t - R_3(S_{t-1}) > CAP \quad (3.6.16b)$$

The contribution of precipitation to depression storage is defined as:

$$D_t = V_d [1 - e^{-(1/V_d)P_t^{eg}}] \quad (3.6.17)$$

and the mass balance equation for the depression storage is

$$S_t^d = S_{t-1}^d + D_t \quad \text{for } S_{t-1}^d \leq V_d \quad (3.6.18a)$$

$$S_t^d = S_{t-1}^d + D_t - R_2(S_{t-1}^d - V_d) \quad \text{for } S_{t-1}^d > V_d \quad (3.6.18b)$$

The contribution of precipitation to interception storage is defined as:

$$IC_t = V_i [1 - e^{-(1/V_i)P_t^{eg}}] \quad (3.6.19)$$

Because  $D_t$  and  $IC_t$  are computed independently, there is a possibility of  $IC_t + D_t$  exceeding  $P_t^{eg}$ . However, the maximum possible values of  $IC_t$  and  $D_t$  are  $V_i$  and  $V_d$  respectively. In a typical catchment  $V_d \gg V_i$  and therefore such a possibility does not arise. If under some circumstances mass balance is not satisfied by computing  $IC_t$  and  $D_t$  independently then it is evident that  $P_t^{eg} - (D_t + IC_t) = 0$ . No mass balance is accounted for in the interception storage computation; however, interception is negligible compared to the other storage elements. Alternatively, this implies that the contribution of precipitation to interception storage is lost in evaporation.

The total contribution to streamflow is therefore a function of the effective precipitation as well as the contents of the various storages, and consists of interflow, surface runoff and direct runoff. These components are shown schematically in Figure 3.6.5. The amount of precipitation contributing to direct runoff is strongly dependent on the infiltration storage contents. Surface runoff occurs as an overflow from the infiltration storage. Depression storage overflow contributes to infiltration storage, and subsequently to direct runoff if infiltration storage has reached capacity. Interflow occurs as an outflow from infiltration storage at a rate dependent on the contents of the infiltration storage in the previous time interval, with a time delay element. The various flow components contributed by the storage elements are defined as:

- (1) Contribution from depression storage to infiltration storage  
= excess in depression storage  $\times R_2$
- (2) Contribution to surface runoff = excess in infiltration  
storage  $\times R_1$
- (3) Interflow = storage in infiltration storage  $\times R_3$ .

The effective precipitation is now computed as :

$$P_t^e = (1 - \alpha)P_t^g - D_t - IC_t + R_1[S_{t-1} + I_t - R_3(S_{t-1}) - CAP]\delta + R_3(S_{t-1}) \quad (3.6.20)$$

where  $P_t^e$  = the net effective precipitation

and  $\delta = 1$  if  $S_{t-1} + I_t - R_3(S_{t-1}) > CAP$   
 $\delta = 0$  if  $S_{t-1} + I_t - R_3(S_{t-1}) < CAP$ .

$$\begin{aligned} \text{If } S_t^d > V_d \\ &= S_t + R_2 (S_t^d - V_d) \end{aligned} \quad (3.6.21)$$

### 3.6.3.3 Preprocessor Parameter Estimation

The parameters are estimated using the simplex optimization method of Nelder and Mead (1965) which does not require derivatives of  $g(O_t - \hat{Q}_t)$ , a user specified objective function dependent upon the errors between observed and estimated discharges.

Due to the general structure of the parameter optimization routine, the number of parameters being optimized and the objective function can easily be varied. For example, in the work reported in Chapter 4, the errors associated with low, middle and high streamflows were square root transformed and weighted. That is, for

$$\varepsilon_t^j = Q_t^j - \hat{Q}_t^j \quad \text{where } j \text{ refers to flow interval } j, j=1, 2, 3 \text{ and}$$

$t$  refers to time, the function  $g(\cdot)$  may be written

$$g(\varepsilon_t) = \sum_{j=1}^3 w^j \left( \frac{\hat{Q}_t^j}{Q_t^j} \right)^{1/2}$$

where  $\hat{Q}_t^j$  is the average estimated discharge in the flow interval  $j$ .

The weights are included to allow the user flexibility in calibrating the model. Besides the above objective function, the preprocessor program also allows for the following objective functions:

$$g(\epsilon) = \frac{1}{T-1} \left( \sum_{t=1}^T (\epsilon_t - \bar{\epsilon})^2 \right)^{1/2}$$

$$g(\hat{Q}) = \frac{1}{T-1} \sum_{t=1}^T [\ln(\hat{Q}_t) - \ln(Q_t)]^2$$

$$g(\epsilon) = 1/R^2$$

$$g(\epsilon) = \left[ \frac{\max(\hat{Q}_t) - \max(Q_t)}{\max(Q_t)} \right] \times 100\%$$

where T is the length of the calibration record and  $R^2$  is the explained sum-of-squares ratio.

The output of the preprocessor is the effective precipitation,  $P_t^e$ . If there are n precipitation zones (inputs) in the catchment and T time periods for which  $P_t^e$  is computed, these values will constitute the (Txn) matrix  $\underline{P}$  in equation (3.6.3) and (3.6.4).

It is now possible to find  $\underline{U}_i$ , the ith impulse response given by Equation (3.6.3) using the CLS model of section 3.6.2. Estimation of  $\underline{U}_i$  is performed using quadratic programming with a minimum squared error (between observed and estimated discharges) objective function, as given in Equation (3.6.5).

The outflow from the CLS module is computed using a simple impulse response for each precipitation input; thus assuming a linear and time invariant response. The non-linearities in catchment response are accommodated entirely by the precipitation - soil moisture accounting preprocessing model.

#### 3.6.4 Calibrated values for three Thames subcatchments

The two models described here were applied to the three Thames subcatchments described earlier in this report. An intercomparison of the models' performances is given in Chapter 4. In this section, the parameter values are reported from a calibration period 1.10.69 to 30.9.73. An initial year 1.10.68 - 30.9.69 was used to find the initial soil moisture.

The structure of CLS, being a multiple input-single output system, allows one to write equation (3.6.3) in the form where one of the inputs is a lagged value of the estimated discharge. That is  $P_t = \hat{Q}_{t-1}$ . For this CLS model structure, we will denote the model as 'CLS with autoregressive inputs'. While this form has no inherent advantages for rainfall-runoff modelling, its form is of great advantage when the rainfall-runoff model is used in real-time flow forecasting. In this case, the model can easily be incorporated within a Markovian state-space representation suitable for Kalman filtering. The use of the lagged flow estimate as an input allows for easy updating.

Tables 3.6.1 and 3.6.2 give the results for the first preprocessor, with and without an autoregressive input. Table 3.6.3 gives results for the second preprocessor. These three models are denoted CLS1, CLS2 and CLS3 respectively in Chapter 4.

(a) Preprocessor I parameters

| Preprocessor |             |             |             |
|--------------|-------------|-------------|-------------|
| Parameter    | Blackwater  | Cherwell    | Mole        |
| $i_m$        | 11.1 inches | 5.77 inches | 6.15 inches |
| B            | .37         | .73         | .31         |
| $B_e$        | .43         | .04         | .69         |
| $B_d$        | .03         | .02         | .021        |

(b) Parameters of impulse response

| Lag | Blackwater | Cherwell | Mole |
|-----|------------|----------|------|
| 1   | .15        | .03      | .13  |
| 2   | .44        | .12      | .46  |
| 3   | .15        | .17      | .12  |
| 4   | .13        | .12      | .04  |
| 5   | .07        | .08      |      |
| 6   | .06        | .05      |      |
| 7   | .03        | .03      |      |
| 8   | .02        | .03      |      |
| 9   |            | .03      |      |
| 10  |            | .03      |      |
| 11  |            | .03      |      |
| 12  |            | .02      |      |
| 13  |            | .02      |      |
| 17  |            | .02      |      |

Table 3.6.1 Parameter values for Preprocessor I and the impulse response (CLS1).

(a) Preprocessor I parameters

| Preprocessor<br>Parameter | Blackwater | Cherwell    | Mole        |
|---------------------------|------------|-------------|-------------|
| $i_m$                     | 12.0 inch  | 5.58 inches | 6.45 inches |
| B                         | .62        | .69         | .223        |
| $B_e$                     | .32        | .05         | 1.09        |
| $B_d$                     | .03        | .02         | .020        |

(b) Autoregressive CLS model parameters

| Lag | Blackwater |                 | Cherwell |                 | Mole   |             |
|-----|------------|-----------------|----------|-----------------|--------|-------------|
|     | $pe_t$     | $\hat{Q}_{t-1}$ | $pe_t$   | $\hat{Q}_{t-1}$ | $pe_t$ | $\hat{Q}_t$ |
| 1   | .13        | .40             | .01      | 1.00            | .11    | .43         |
| 2   | .35        | .11             | .09      | -.31            | .34    | .11         |
| 3   | 0          | .01             | .05      | .10             | 0      | 0           |

Table 3.6.2 Parameter values for Preprocessor 1 and the Autoregressive CLS model (CLS2).

(a) Preprocessor II parameters

| Preprocessor Parameter   | Blackwater | Cherwell | Mole |
|--------------------------|------------|----------|------|
| Initial storage fraction | .50        | .50      | .50  |
| R <sub>1</sub>           | .784       | .997     | .030 |
| R <sub>2</sub>           | .500       | .129     | .958 |
| C <sub>1</sub>           | .983       | .663     | .586 |
| C <sub>2</sub>           | 1.63       | 2.32     | 2.94 |
| R <sub>3</sub>           | .020       | .023     | .032 |
| CAP                      | 8.74       | 7.61     | 6.66 |
| V <sub>i</sub>           | 1.42       | .71      | 1.19 |
| V <sub>d</sub>           | 1.10       | 1.38     | 1.98 |
| β                        | .031       | .037     | .039 |

(b) Parameters of impulse response

| Lag | Blackwater | Cherwell | Mole |
|-----|------------|----------|------|
| 1   | .21        | .08      | .06  |
| 2   | .54        | .19      | .23  |
| 3   | .08        | .25      | .03  |
| 4   | .05        | .14      |      |
| 5   |            | .03      |      |

Table 3.6.3 Parameter values for Preprocessor II and the impulse response (CLS3).

#### 4. EVALUATION PROCEDURES AND RESULTS

##### 4.1 Model evaluation

As explained in chapter 1, the primary purpose of the work reported here was to compare a range of different rainfall-runoff models, with regard to their suitability for application to catchments having varied types of behavioural response. The present report is concerned with the models applied in simulation-mode only. The context in which the models are being compared is that of flow prediction across the whole range of flows and not simply that of flood event forecasting. Thus the comparison of the models has been made on the basis of overall average errors, suitably defined, rather than measures of errors in peaks, for example. Similarly, measures of timing-errors in peaks have not been considered.

Four measures of goodness of prediction have been used for the present study : these are mean absolute error (MABS), root mean square error (RMSE), proportional mean absolute error (PMABS) and proportional root mean square error (PRMSE). Thus if  $q_t$  denotes the flow on day  $t$ , and  $\hat{q}_t$  denotes the modelled flow for that day, the measures of overall error are defined as

$$\begin{aligned} \text{MABS} &= N^{-1} \sum_t | \epsilon_t | \\ \text{RMSE} &= \{ N^{-1} \sum_t \epsilon_t^2 \}^{1/2} \\ \text{PMABS} &= N^{-1} \sum_t | \eta_t | \\ \text{PRMSE} &= \{ N^{-1} \sum_t \eta_t^2 \}^{1/2} \end{aligned}$$

where  $\epsilon_t = q_t - \hat{q}_t$ ,  
 $\eta_t = \epsilon_t / q_t$ ,

and where  $N$  denotes the number of days included in the summation. These four measures are essentially similar, except for the obvious and well known properties that:

(i) compared with mean absolute errors, root mean square errors have the desirable feature of deflating the contribution of the smallest errors (errors which intuitively one might wish to ignore). However root mean square errors are numerically sensitive to the few largest errors in situations such as the present one where the preponderance of errors are small.

(ii) since large errors ( $\epsilon_t$ ) tend to be associated with high flows, the ordinary measures of fit tend to reflect the behaviour of the predictions at such high flows, and ipso facto, at peaks in flow. The use of proportional errors ( $\eta_t$ ) in the two proportional criteria compensates for this effect.

(iii) In the proportional criteria, occurrences of the situation where the actual flow is small and the modelled flow high tend to be the major contributors to the overall value. In contrast, errors of underprediction can make only a limited contribution to these criteria.

As well as considering the above four criteria calculated for the whole of the calibration and evaluation periods, each has been subdivided to provide separate measures of performance for the twelve calendar months. This enables distinction to be made between the models' performance during different seasons of the year, and also gives at least an idea of the reliability of any apparent difference between the overall measure of fit of different models. The use of four different measures of fit provides some assurance that any preference between models will not be tied to any one, possibly inappropriate, measure. In principle, a choice between models could be made within a framework closely allied to the use eventually to be made of the models : that is, by looking at the effects of the errors in predictions from the models on any control decisions or other consequences of the predictions. However such an approach cannot be implemented except in the context of a detailed case-study of specific situations.

## 4.2 Results of evaluation

### 4.2.1 Introduction

The results of applying the quantitative criteria described above to the three catchments are presented in Tables 4.2.1 to 4.2.8 (on pages 87 to 102) and these will be discussed in the following subsections. For each catchment, results are given both for the calibration data periods and for the evaluation period. In addition, for the Cherwell and Blackwater catchments results are given for essentially the same evaluation period but excluding January to October of 1976. This somewhat arbitrary exclusion period was chosen so that the effect of the 1976 drought and the immediately following recovery period could be separated if necessary: however it does not seem to be the case that any of the models are exceptionally good outside the drought period but exceptionally poor during it. Since there were no records for the Castle Mill gauging station on the Mole from March 1976 to 1978, no such analysis was possible for this catchment.

The tables of results for the model calibration periods are only of secondary interest compared with the tables for the evaluation period. One would generally expect the more flexible models, containing many parameters, to do best in the calibration period. If such models subsequently gave poor results for the evaluation period this would tend to suggest that the models were over-fitted; that is, trying to fit too many parameters to too few data. It should be noted that the various models were fitted using different error criteria: however, the tables for the calibration period do enable a direct comparison of the models for this period.

The results in Tables 4.2.1 to 4.2.8 are also shown in graphical form in Figures 4.2.1 to 4.2.8 (after page 102), which are perhaps easier to assess visually than the Tables. It can be seen that the proportional error criteria PMABS and PRMSE have relatively stable values over the year, in contrast to the ordinary criteria MABS and RMSE which generally have high values during the months of high average flow.

In all, eight different models are considered in the model comparison:-

|      |  |               |
|------|--|---------------|
| PDM1 | Probability-distributed model                        | (Section 3.3) |
| IHCM | Institute of Hydrology conceptual model              | (Section 3.4) |
| NWS1 | National Weather Service model                       | (Section 3.1) |
| TW1  | Thames Water model                                   | (Section 3.2) |
| CLS1 | CLS with Preprocessor I                              | (Section 3.6) |
| CLS2 | CLS with autoregressive inputs and<br>Preprocessor I | (Section 3.6) |
| CLS3 | CLS with Preprocessor II                             | (Section 3.6) |
| REC1 | Recession model                                      | (Section 3.5) |

For convenience in presenting the Figures these have been divided into two groups : the first four above, representing broadly conceptual soil water accounting and translation models, and the last four, representing black-box models, at least as far as the translation components are concerned.

The following subsections describe the quantitative results for the three catchments individually. Section 4.3 looks briefly at the predictions made by the models for a few typical periods of data.

#### 4.2.2 Results for the Cherwell

Tables 4.2.1-3 and Figures 4.2.1-3 give results for the Cherwell at Enslow Mill. On the basis of the criteria calculated for the whole of the year, given in the last lines of the tables, it appears that the Thames Water Model (TW1) is best over the evaluation period: it is the best model according to three of the four criteria and is beaten by only a small margin on the RMSE criterion. Examination of the monthly values reveals that TW1 gave large overpredictions in the Decembers of 1976 and 1977 and in January of 1979: however in general it performs particularly well, compared with the other models, during the dry months of the year, and also performs well at other times.

The National Weather Service Model (NWS1) is affected by isolated large overpredictions for the peaks of events in March 1975, February and March 1979 and June 1977: it also seems to recover poorly from the 1976 drought, with consistent overpredictions during September to November of that year. Given that this model apparently performs best out of all models for the calibration period there is perhaps some evidence of over-fitting of the model. According to the overall figures, the IH Catchment Model (IHCM) is second best to the Thames Water Model: while IHCM gives better error figures than TWMI for a few of the months, the reverse is true for most months. However one would ideally like to extend the model evaluation period in order to be more confident in claiming that TWMI would be best overall when applied in practice. As an example one may consider Figure 4.3.6(a) which shows the models' predictions for the immediate end of the 1976 drought. Here IHCM is certainly best when judged in terms of the size of response to the rainfall events, whereas it does relatively poorly at modelling the baseflow before and between the two events shown.

Of the three CLS-based models, CLS3 appears to perform very poorly, while the other two versions give very similar results. Both CLS1 and CLS2 suffer from consistent over-prediction of flow from October 1975 to March 1976 and from September 1976 to January 1977. They also tend to under-predict flows during May to July. The recession-based model RECI appears to perform slightly better than the CLS models and is perhaps the fifth-best model overall, behind the more physically based models TWMI, IHCM and NWS1 and PDMI. The general performance of the probability-distributed model (PDMI) is only slightly better than the best of the 'black-box' models: even so, the comparison for individual calendar months shows that PDMI is sometimes 'best', although this can probably be regarded as being due to a type of random sampling effect.

#### 4.2.3 Results for the Mole

Tables 4.2.4-5 and Figures 4.2.4-5 give results for the Mole at Castle Mill. The comparison here is based on only three years of data for the evaluation period and so the conclusions are slightly less reliable than for the other two catchments, where five years were used. It will be recalled that for this catchment there was a change in the gauging structure during 1976-77 and that data before this

change (the model evaluation period here) are considered to be less reliable than data obtained later (the model calibration period here). In fact all of the models, except for CLS3 which itself performs badly anyway, seem to generally overpredict flows throughout the evaluation period, and this may be related to the change in gauging structure. There is thus some doubt about the relevance of the results of model comparisons for this catchment.

For the model evaluation period, the National Weather Service model performs best according to all of the overall criteria and also for most of the months taken separately. The Thames Water and IH Catchment Models are next best, but surprisingly are not substantially better than the other models.

As for the Cherwell, CLS3 performs badly and is the worst of all the models here. Some of the predictions from CLS3 are actually negative at times: these negative values were not reset to zero before calculating the error criteria. CLS1 and CLS2 give similar results according to the error criteria, with CLS2 being just the better of the two.

The comparison on the basis of the overall figures for the criteria MABS and RMSE is greatly influenced by the results for just three or four events. One of these occurred during November 1974, for which the model predictions are shown in Figure 4.3.10. The following are the contributions to the four performance criteria for this individual month:

|       | PDM1 | IHCM | NWS1 | TWM1 | CLS1 | CLS2 | CLS3  | REC1 |
|-------|------|------|------|------|------|------|-------|------|
| MABS  | 4.16 | 3.05 | 2.52 | 3.53 | 3.62 | 3.42 | 6.70  | 3.98 |
| RMSE  | 7.11 | 5.14 | 4.24 | 6.38 | 6.17 | 6.01 | 10.95 | 7.01 |
| PMABS | .34  | .28  | .22  | .26  | .41  | .33  | .66   | .26  |
| PRMSE | .51  | .38  | .29  | .41  | .53  | .46  | .76   | .33  |

#### 4.2.4 Results for the Blackwater

Tables 4.2.6-8 and Figures 4.2.6-8 gives results for the Blackwater at Swallowfield. For this catchment, the National Weather Service model (NWS1) gives the best overall values for three of the error criteria calculated for the evaluation period: the remaining criterion (RMSE) is greatly influenced by the large overprediction resulting from NWS1 in November 1974. The Thames Water Model (TWMI) performs best according to the RMSE criterion and is second best overall for the others. There does not seem much to separate TWMI from the IH Catchment Model (IHCM) although TWMI is slightly better.

Once again the results for CLS1 and CLS2 are extremely similar while those for CLS3 are very poor: again CLS3 sometimes gave negative predictions of flow. The Recession model (RECI) seems to be slightly better than CLS1 and CLS2 overall and it is possibly the fourth best overall, just behind IHCM.

According to the proportional mean absolute error criterion (PMABS), the National Weather Service Model performs rather better than the other models, having an overall error of 15% whereas the others have errors of at least 22%.

#### 4.3 Qualitative comparison of models

In order that some impression of the different behaviours of the models can be gained, plots against time of observed and predicted flows are given in Figures 4.3.1 to 4.3.19. The periods chosen for plotting were selected so as to have comparatively large flow events (for the time of year) and also to give representatives of the different seasons. The behaviour of the models at low flows can be judged from the parts of the hydrographs before and after the peaks. Both the model calibration and evaluation periods are represented among the data chosen for plotting. The responses of the models to the first rainfall events following the 1976 drought are of some interest and so plots of these have been included.

The plots of observed and predicted flows give some indication of the variety of different responses produced by the models, compared with the difference of the model predictions from the observed flows. In some instances the behaviour of the observed flows is radically different from that predicted by all the models. There are several explanations for this: some winter events are affected by the precipitation falling as snow rather than rain, with possibly a delayed peak in flows if the snow melted quickly, while some of the periods of low flow may include abstraction, discharge and regulation effects. To the extent that these are present in the data, the quantitative measures of model fit are not so meaningful as they might be otherwise. In practice effects of this sort should ideally be accounted for by the flow-prediction model: however this would involve supplying the right data to the models. The lesser differences in modelled and observed behaviour, such as peaks occurring a day out of phase, are possibly attributable to the use of a daily time interval for the input data and model computations, and of course there is the possibility of storm cells completely missing the relatively sparse set of raingauges used.

In general terms the models all seem to give realistic responses, except for CLS3 which gives negative predictions for the Mole and Blackwater, and except also for PDM1 on the Blackwater following the drought of 1976 when the response is oddly behaved, as shown in the plot for August and September 1976. Apart from these it is difficult to distinguish between the models on a visual basis: for each of the models there are occasions when it considerably overpredicts the peak in observed flow while the other models give much closer predictions. Similarly, for the flow recession periods, no one model is better behaved (or, excluding CLS3, worse behaved) than all the others.

#### 4.4 Conclusions

It is extremely difficult to draw any clear-cut conclusions about the relative merits of the models from the current study, particularly because of the limited amount of data available to form the comparison period. There is also the further difficulty that the models tested have been fitted according to different optimisation criteria: for some of the models the optimisation criterion is an inbuilt part of

the model, but, for those cases where it could readily be changed, use of a different criterion for fitting could well lead to a different preference between models.

On taking the three catchments together, it could be argued that the National Weather Service Model (NWS1) is the best overall, with the Thames Water Model (TWM1) and perhaps the IH catchment model (IHCM) following in preference. Of course the conclusions here are limited to the models used in simulation-mode and any preference between models could change radically for updated models, depending both on the lead time and the method of updating.

Of the three CLS-based models, CLS3 (using Preprocessor II) appears to perform very poorly, while the other two versions, which differ in the implementation of the impulse response function component, give very similar results. This suggests that CLS2 has no disadvantages compared with CLS1, and thus will form a good basis for a model producing forecasts making use of latest observations of flow, to which the structure of CLS2 is more suited than CLS1. The Recession model (RECI) performs surprisingly well, considering that it was fitted in one-day ahead forecasting-mode. It may be noted that both CLS2 and RECI have a ready-made formulation for producing one step ahead forecasts, but this is no guarantee that they would do better than the other models in forecasting-mode.

|         | PDMI | IHCM | NWS1 | TWMI | CLS1 | CLS2 | CLS3 | RECI | BEST MODEL |
|---------|------|------|------|------|------|------|------|------|------------|
| JAN     | 1.26 | 1.38 | 1.26 | 1.33 | 1.25 | 1.24 | 2.00 | 1.74 | CLS2       |
| FEB     | 1.62 | 1.80 | 1.49 | 1.45 | 1.56 | 1.54 | 2.08 | 1.54 | TWMI       |
| MAR     | 1.09 | 1.12 | 1.20 | 1.09 | 1.37 | 1.32 | 1.32 | 1.49 | TWMI       |
| APR     | 0.66 | 0.53 | 0.41 | 0.59 | 1.05 | 1.00 | 1.12 | 1.15 | NWS1       |
| MAY     | 0.63 | 0.54 | 0.39 | 0.73 | 0.61 | 0.59 | 1.63 | 0.82 | NWS1       |
| JUN     | 0.54 | 0.47 | 0.53 | 0.73 | 0.75 | 0.72 | 1.49 | 0.72 | IHCM       |
| JUL     | 0.37 | 0.55 | 0.40 | 0.34 | 0.87 | 0.84 | 0.98 | 0.60 | TWMI       |
| AUG     | 0.46 | 0.43 | 0.34 | 0.44 | 0.69 | 0.67 | 0.85 | 0.42 | NWS1       |
| SEP     | 0.41 | 0.34 | 0.22 | 0.29 | 0.59 | 0.56 | 0.74 | 0.40 | NWS1       |
| OCT     | 0.50 | 0.36 | 0.30 | 0.31 | 0.95 | 0.72 | 1.03 | 1.13 | NWS1       |
| NOV     | 1.07 | 0.90 | 0.64 | 0.81 | 1.22 | 1.22 | 0.90 | 1.72 | NWS1       |
| DEC     | 1.26 | 1.39 | 0.90 | 1.05 | 1.12 | 1.13 | 1.45 | 1.33 | NWS1       |
| OVERALL | 0.82 | 0.82 | 0.67 | 0.76 | 1.00 | 0.96 | 1.30 | 1.09 | NWS1       |

Table 4.2.1(a) Statistics of errors of rainfall-runoff models in simulation-mode, calculated for calibration period October 1968 to September 1974.

Statistic = MABS (mean absolute error)  
 Units = m<sup>3</sup>/sec  
 Catchment = CHERWELL

|         | PDMI | IHCM | NWS1 | TWMI | CLS1 | CLS2 | CLS3 | RECI | BEST MODEL |
|---------|------|------|------|------|------|------|------|------|------------|
| JAN     | 1.76 | 1.77 | 1.77 | 1.83 | 1.79 | 1.81 | 2.82 | 2.55 | PDMI       |
| FEB     | 2.22 | 2.53 | 2.45 | 2.05 | 2.22 | 2.19 | 3.10 | 2.44 | TWMI       |
| MAR     | 1.89 | 1.70 | 2.08 | 1.79 | 1.93 | 1.86 | 2.05 | 2.17 | IHCM       |
| APR     | 1.21 | 1.02 | 0.62 | 1.10 | 1.23 | 1.17 | 1.60 | 1.36 | NWS1       |
| MAY     | 1.18 | 0.94 | 0.63 | 1.23 | 0.78 | 0.77 | 1.91 | 1.12 | NWS1       |
| JUN     | 1.00 | 0.73 | 1.31 | 1.20 | 0.99 | 0.97 | 1.83 | 0.96 | IHCM       |
| JUL     | 0.59 | 0.86 | 0.51 | 0.52 | 1.00 | 0.96 | 1.13 | 0.74 | NWS1       |
| AUG     | 0.71 | 0.79 | 0.58 | 0.76 | 0.91 | 0.88 | 1.01 | 0.67 | NWS1       |
| SEP     | 0.52 | 0.54 | 0.36 | 0.48 | 0.77 | 0.75 | 0.91 | 0.57 | NWS1       |
| OCT     | 0.61 | 0.68 | 0.61 | 0.45 | 1.61 | 1.11 | 1.71 | 2.12 | TWMI       |
| NOV     | 1.52 | 1.67 | 1.16 | 1.54 | 1.83 | 1.86 | 1.45 | 2.62 | NWS1       |
| DEC     | 2.23 | 1.86 | 1.35 | 1.76 | 1.53 | 1.59 | 2.25 | 1.89 | NWS1       |
| OVERALL | 1.29 | 1.26 | 1.12 | 1.23 | 1.38 | 1.33 | 1.81 | 1.60 | NWS1       |

Table 4.2.1(b) Statistics of errors of rainfall-runoff models in simulation-mode, calculated for calibration period October 1968 to September 1974.

Statistic = RMSE (root mean square error)  
 Units = m<sup>3</sup>/sec  
 Catchment = CHERWELL

|         | PDMI | IHCM | NWS1 | TWMI | CLS1 | CLS2 | CLS3 | RECI | BEST MODEL |
|---------|------|------|------|------|------|------|------|------|------------|
| JAN     | 0.17 | 0.25 | 0.20 | 0.21 | 0.20 | 0.20 | 0.30 | 0.24 | PDMI       |
| FEB     | 0.21 | 0.26 | 0.18 | 0.21 | 0.23 | 0.23 | 0.27 | 0.18 | RECI       |
| MAR     | 0.17 | 0.19 | 0.17 | 0.16 | 0.26 | 0.25 | 0.24 | 0.23 | TWMI       |
| APR     | 0.15 | 0.13 | 0.11 | 0.14 | 0.35 | 0.34 | 0.36 | 0.41 | NWS1       |
| MAY     | 0.18 | 0.18 | 0.17 | 0.22 | 0.30 | 0.30 | 0.68 | 0.41 | NWS1       |
| JUN     | 0.23 | 0.21 | 0.24 | 0.28 | 0.45 | 0.42 | 0.77 | 0.40 | IHCM       |
| JUL     | 0.27 | 0.41 | 0.32 | 0.21 | 0.68 | 0.66 | 0.73 | 0.43 | TWMI       |
| AUG     | 0.33 | 0.28 | 0.25 | 0.26 | 0.53 | 0.51 | 0.68 | 0.28 | NWS1       |
| SEP     | 0.40 | 0.31 | 0.20 | 0.22 | 0.53 | 0.50 | 0.73 | 0.36 | NWS1       |
| OCT     | 0.47 | 0.23 | 0.16 | 0.22 | 0.57 | 0.51 | 0.66 | 0.53 | NWS1       |
| NOV     | 0.61 | 0.32 | 0.25 | 0.30 | 0.55 | 0.54 | 0.39 | 0.74 | NWS1       |
| DEC     | 0.34 | 0.37 | 0.23 | 0.22 | 0.35 | 0.34 | 0.30 | 0.38 | TWMI       |
| OVERALL | 0.29 | 0.26 | 0.21 | 0.22 | 0.42 | 0.40 | 0.51 | 0.38 | NWS1       |

Table 4.2.1(c) Statistics of errors of rainfall-runoff models in simulation-mode, calculated for calibration period October 1968 to September 1974.

Statistic = PMABS (proportional mean absolute error)  
 Independent of units  
 Catchment = CHERWELL

|         | PDMI | IHCM | NWS1 | TWMI | CLS1 | CLS2 | CLS3 | RECI | BEST MODEL |
|---------|------|------|------|------|------|------|------|------|------------|
| JAN     | 0.21 | 0.32 | 0.25 | 0.27 | 0.27 | 0.26 | 0.39 | 0.32 | PDMI       |
| FEB     | 0.28 | 0.33 | 0.24 | 0.26 | 0.31 | 0.30 | 0.37 | 0.23 | RECI       |
| MAR     | 0.24 | 0.23 | 0.21 | 0.21 | 0.33 | 0.32 | 0.33 | 0.28 | NWS1       |
| APR     | 0.19 | 0.17 | 0.13 | 0.18 | 0.43 | 0.42 | 0.48 | 0.51 | NWS1       |
| MAY     | 0.23 | 0.23 | 0.21 | 0.27 | 0.40 | 0.39 | 0.73 | 0.62 | NWS1       |
| JUN     | 0.30 | 0.24 | 0.31 | 0.35 | 0.55 | 0.52 | 0.83 | 0.49 | IHCM       |
| JUL     | 0.38 | 0.64 | 0.38 | 0.25 | 0.76 | 0.73 | 0.80 | 0.49 | TWMI       |
| AUG     | 0.44 | 0.38 | 0.35 | 0.39 | 0.62 | 0.59 | 0.77 | 0.34 | NWS1       |
| SEP     | 0.50 | 0.41 | 0.26 | 0.26 | 0.62 | 0.60 | 0.83 | 0.42 | NWS1       |
| OCT     | 0.58 | 0.28 | 0.21 | 0.27 | 0.62 | 0.56 | 0.76 | 0.61 | NWS1       |
| NOV     | 0.73 | 0.43 | 0.35 | 0.42 | 0.65 | 0.63 | 0.49 | 0.96 | NWS1       |
| DEC     | 0.50 | 0.46 | 0.31 | 0.32 | 0.51 | 0.49 | 0.39 | 0.49 | NWS1       |
| OVERALL | 0.38 | 0.34 | 0.27 | 0.29 | 0.51 | 0.49 | 0.60 | 0.48 | NWS1       |

Table 4.2.1(d) Statistics of errors of rainfall-runoff models in simulation-mode, calculated for calibration period October 1968 to September 1974.

Statistic = PRMSE (proportional root mean square error)  
 Independent of units  
 Catchment = CHERWELL

|         | PDMI | IHCM | NWS1 | TWMI | CLS1 | CLS2 | CLS3 | RECI | BEST MODEL |
|---------|------|------|------|------|------|------|------|------|------------|
| JAN     | 1.66 | 1.66 | 1.55 | 1.61 | 1.78 | 1.83 | 2.87 | 1.86 | NWS1       |
| FEB     | 1.76 | 1.36 | 1.60 | 1.29 | 1.84 | 1.76 | 4.41 | 1.80 | TWMI       |
| MAR     | 1.58 | 1.20 | 1.50 | 1.26 | 1.56 | 1.47 | 3.09 | 1.82 | IHCM       |
| APR     | 0.70 | 0.47 | 0.68 | 0.66 | 0.76 | 0.70 | 2.57 | 1.35 | IHCM       |
| MAY     | 1.12 | 0.90 | 0.58 | 1.13 | 0.90 | 0.84 | 1.82 | 1.49 | NWS1       |
| JUN     | 0.44 | 0.48 | 0.56 | 0.64 | 1.03 | 0.97 | 1.37 | 1.25 | PDMI       |
| JUL     | 0.15 | 0.37 | 0.37 | 0.16 | 0.81 | 0.78 | 0.87 | 0.64 | PDMI       |
| AUG     | 0.71 | 0.38 | 0.67 | 0.34 | 0.99 | 0.95 | 0.76 | 0.42 | TWMI       |
| SEP     | 0.97 | 0.13 | 0.50 | 0.19 | 1.17 | 1.12 | 0.87 | 0.77 | IHCM       |
| OCT     | 1.63 | 0.69 | 1.08 | 0.39 | 1.81 | 1.82 | 1.74 | 1.10 | TWMI       |
| NOV     | 1.24 | 1.05 | 1.03 | 0.69 | 1.31 | 1.31 | 1.82 | 1.19 | TWMI       |
| DEC     | 1.61 | 1.20 | 1.06 | 1.29 | 1.60 | 1.50 | 1.80 | 1.96 | NWS1       |
| OVERALL | 1.13 | 0.83 | 0.93 | 0.80 | 1.30 | 1.25 | 2.00 | 1.30 | TWMI       |

Table 4.2.2(a) Statistics of errors of rainfall-runoff models in simulation-mode, calculated for evaluation period October 1974 to September 1979.

Statistic = MABS (mean absolute error)  
 Units = m<sup>3</sup>/sec  
 Catchment = CHERWELL

|         | PDMI | IHCM | NWS1 | TWMI | CLS1 | CLS2 | CLS3 | RECI | BEST MODEL |
|---------|------|------|------|------|------|------|------|------|------------|
| JAN     | 2.19 | 2.38 | 2.43 | 2.30 | 2.39 | 2.46 | 4.21 | 2.34 | PDMI       |
| FEB     | 2.39 | 1.84 | 2.42 | 1.97 | 2.56 | 2.45 | 9.89 | 2.35 | IHCM       |
| MAR     | 2.60 | 1.90 | 2.52 | 2.20 | 2.18 | 2.03 | 5.18 | 2.24 | IHCM       |
| APR     | 0.91 | 0.63 | 1.24 | 1.00 | 0.97 | 0.88 | 3.40 | 1.72 | IHCM       |
| MAY     | 2.17 | 1.61 | 1.09 | 1.96 | 1.32 | 1.32 | 2.78 | 2.09 | NWS1       |
| JUN     | 1.22 | 1.30 | 1.18 | 1.70 | 1.53 | 1.49 | 2.11 | 1.79 | NWS1       |
| JUL     | 0.20 | 0.43 | 0.44 | 0.22 | 0.95 | 0.92 | 1.04 | 0.77 | PDMI       |
| AUG     | 1.29 | 0.57 | 1.22 | 0.69 | 1.68 | 1.58 | 1.16 | 0.74 | IHCM       |
| SEP     | 1.72 | 0.18 | 1.00 | 0.37 | 2.04 | 1.95 | 1.11 | 1.05 | IHCM       |
| OCT     | 2.93 | 1.16 | 2.11 | 0.67 | 3.29 | 3.30 | 2.49 | 1.60 | TWMI       |
| NOV     | 1.94 | 1.60 | 1.83 | 1.38 | 1.96 | 1.96 | 3.14 | 2.32 | TWMI       |
| DEC     | 2.18 | 1.72 | 1.67 | 2.11 | 2.19 | 2.07 | 2.68 | 2.80 | NWS1       |
| OVERALL | 1.81 | 1.28 | 1.60 | 1.38 | 1.92 | 1.87 | 3.27 | 1.82 | IHCM       |

Table 4.2.2(b) Statistics of errors of rainfall-runoff models in simulation-mode, calculated for evaluation period October 1974 to September 1979.

Statistic = RMSE (root mean square error)  
 Units = m<sup>3</sup>/sec  
 Catchment = CHERWELL

|         | PDMI | IHCM | NWS1 | TWM1 | CLS1 | CLS2 | CLS3 | RECI | BEST MODEL |
|---------|------|------|------|------|------|------|------|------|------------|
| JAN     | 0.45 | 0.26 | 0.23 | 0.27 | 0.52 | 0.52 | 0.42 | 0.57 | NWS1       |
| FEB     | 0.31 | 0.23 | 0.17 | 0.19 | 0.43 | 0.42 | 0.33 | 0.47 | NWS1       |
| MAR     | 0.26 | 0.24 | 0.17 | 0.19 | 0.43 | 0.42 | 0.43 | 0.57 | NWS1       |
| APR     | 0.26 | 0.17 | 0.15 | 0.18 | 0.22 | 0.21 | 0.63 | 0.47 | NWS1       |
| MAY     | 0.27 | 0.25 | 0.17 | 0.24 | 0.31 | 0.28 | 0.51 | 0.63 | NWS1       |
| JUN     | 0.16 | 0.31 | 0.27 | 0.20 | 0.54 | 0.50 | 0.72 | 0.82 | PDMI       |
| JUL     | 0.21 | 0.66 | 0.34 | 0.18 | 0.72 | 0.69 | 0.81 | 0.82 | TWM1       |
| AUG     | 0.73 | 0.85 | 0.56 | 0.51 | 0.90 | 0.85 | 1.07 | 0.47 | RECI       |
| SEP     | 1.62 | 0.22 | 0.72 | 0.35 | 2.07 | 1.98 | 1.26 | 1.17 | IHCM       |
| OCT     | 1.11 | 0.34 | 0.61 | 0.21 | 1.23 | 1.23 | 1.02 | 0.60 | TWM1       |
| NOV     | 0.67 | 0.43 | 0.43 | 0.24 | 0.67 | 0.67 | 0.69 | 0.44 | TWM1       |
| DEC     | 0.59 | 0.27 | 0.26 | 0.26 | 0.56 | 0.54 | 0.46 | 0.70 | NWS1       |
| OVERALL | 0.55 | 0.35 | 0.34 | 0.25 | 0.72 | 0.69 | 0.70 | 0.65 | TWM1       |

Table 4.2.2(c) Statistics of errors of rainfall-runoff models in simulation-mode, calculated for evaluation period October 1974 to September 1979.

Statistic = PMABS (proportional mean absolute error)  
 Independent of units  
 Catchment = CHERWELL

|         | PDMI | IHCM | NWS1 | TWM1 | CLS1 | CLS2 | CLS3 | RECI | BEST MODEL |
|---------|------|------|------|------|------|------|------|------|------------|
| JAN     | 0.70 | 0.35 | 0.34 | 0.35 | 0.84 | 0.83 | 0.51 | 0.93 | NWS1       |
| FEB     | 0.39 | 0.34 | 0.23 | 0.25 | 0.69 | 0.67 | 0.57 | 0.78 | NWS1       |
| MAR     | 0.36 | 0.35 | 0.20 | 0.25 | 0.73 | 0.72 | 0.59 | 0.98 | NWS1       |
| APR     | 0.37 | 0.25 | 0.19 | 0.23 | 0.28 | 0.28 | 0.72 | 0.67 | NWS1       |
| MAY     | 0.35 | 0.32 | 0.22 | 0.29 | 0.40 | 0.36 | 0.61 | 0.98 | NWS1       |
| JUN     | 0.20 | 0.52 | 0.33 | 0.25 | 0.61 | 0.58 | 0.86 | 1.13 | PDMI       |
| JUL     | 0.29 | 1.02 | 0.38 | 0.24 | 0.76 | 0.73 | 0.88 | 1.08 | TWM1       |
| AUG     | 2.30 | 1.57 | 1.10 | 2.11 | 1.97 | 1.69 | 3.21 | 0.85 | RECI       |
| SEP     | 2.92 | 0.37 | 1.31 | 0.77 | 3.77 | 3.61 | 1.90 | 1.88 | IHCM       |
| OCT     | 1.91 | 0.61 | 1.20 | 0.30 | 2.13 | 2.11 | 1.28 | 0.80 | TWM1       |
| NOV     | 0.90 | 0.58 | 0.68 | 0.36 | 0.89 | 0.88 | 0.97 | 0.56 | TWM1       |
| DEC     | 0.84 | 0.33 | 0.36 | 0.37 | 0.81 | 0.79 | 0.57 | 1.03 | IHCM       |
| OVERALL | 0.96 | 0.55 | 0.54 | 0.48 | 1.16 | 1.11 | 1.06 | 0.97 | TWM1       |

Table 4.2.2(d) Statistics of errors of rainfall-runoff models in simulation-mode, calculated for evaluation period October 1974 to September 1979.

Statistic = PRMSE (proportional root mean square error)  
 Independent of units  
 Catchment = CHERWELL

|         | PDM1 | IHCM | NWS1 | TWM1 | CLS1 | CLS2 | CLS3 | REC1 | BEST MODEL |
|---------|------|------|------|------|------|------|------|------|------------|
| JAN     | 1.74 | 2.00 | 1.84 | 1.94 | 1.81 | 1.88 | 3.43 | 1.88 | PDM1       |
| FEB     | 2.05 | 1.57 | 1.97 | 1.53 | 1.98 | 1.88 | 5.51 | 1.88 | TWM1       |
| MAR     | 1.86 | 1.38 | 1.84 | 1.51 | 1.66 | 1.55 | 3.74 | 1.88 | IHCM       |
| APR     | 0.78 | 0.52 | 0.81 | 0.77 | 0.89 | 0.81 | 3.09 | 1.50 | IHCM       |
| MAY     | 1.35 | 1.07 | 0.69 | 1.38 | 1.07 | 1.00 | 2.21 | 1.65 | NWS1       |
| JUN     | 0.53 | 0.53 | 0.67 | 0.79 | 1.24 | 1.17 | 1.63 | 1.39 | PDM1       |
| JUL     | 0.17 | 0.38 | 0.46 | 0.18 | 1.00 | 0.96 | 1.05 | 0.72 | PDM1       |
| AUG     | 0.80 | 0.39 | 0.80 | 0.35 | 1.15 | 1.10 | 0.82 | 0.48 | TWM1       |
| SEP     | 0.49 | 0.11 | 0.29 | 0.10 | 0.58 | 0.54 | 0.71 | 0.55 | TWM1       |
| OCT     | 0.47 | 0.41 | 0.25 | 0.35 | 0.50 | 0.50 | 1.09 | 0.92 | NWS1       |
| NOV     | 1.24 | 1.05 | 1.03 | 0.69 | 1.31 | 1.31 | 1.82 | 1.19 | TWM1       |
| DEC     | 1.61 | 1.20 | 1.06 | 1.29 | 1.60 | 1.50 | 1.80 | 1.96 | NWS1       |
| OVERALL | 1.09 | 0.88 | 0.98 | 0.91 | 1.23 | 1.18 | 2.24 | 1.33 | IHCM       |

Table 4.2.3(a) Statistics of errors of rainfall-runoff models in simulation-mode, calculated for evaluation period October 1974 to September 1979, omitting Jan-Oct of 1976.

Statistic = MABS (mean absolute error)  
 Units = m<sup>3</sup>/sec  
 Catchment = CHERWELL

|         | PDM1 | IHCM | NWS1 | TWM1 | CLS1 | CLS2 | CLS3  | REC1 | BEST MODEL |
|---------|------|------|------|------|------|------|-------|------|------------|
| JAN     | 2.33 | 2.64 | 2.70 | 2.56 | 2.52 | 2.61 | 4.70  | 2.43 | PDM1       |
| FEB     | 2.66 | 2.03 | 2.70 | 2.20 | 2.77 | 2.66 | 11.10 | 2.50 | IHCM       |
| MAR     | 2.90 | 2.11 | 2.82 | 2.46 | 2.36 | 2.19 | 5.79  | 2.36 | IHCM       |
| APR     | 0.99 | 0.69 | 1.38 | 1.11 | 1.08 | 0.97 | 3.79  | 1.88 | IHCM       |
| MAY     | 2.43 | 1.80 | 1.22 | 2.19 | 1.46 | 1.47 | 3.11  | 2.29 | NWS1       |
| JUN     | 1.36 | 1.44 | 1.32 | 1.90 | 1.71 | 1.66 | 2.35  | 1.96 | NWS1       |
| JUL     | 0.22 | 0.45 | 0.49 | 0.24 | 1.06 | 1.02 | 1.16  | 0.84 | PDM1       |
| AUG     | 1.34 | 0.60 | 1.34 | 0.66 | 1.80 | 1.69 | 1.07  | 0.80 | IHCM       |
| SEP     | 0.59 | 0.15 | 0.33 | 0.18 | 0.68 | 0.67 | 0.81  | 0.65 | IHCM       |
| OCT     | 0.65 | 0.80 | 0.49 | 0.66 | 0.65 | 0.66 | 1.59  | 1.49 | NWS1       |
| NOV     | 1.94 | 1.60 | 1.83 | 1.38 | 1.96 | 1.96 | 3.14  | 2.32 | TWM1       |
| DEC     | 2.18 | 1.72 | 1.67 | 2.11 | 2.19 | 2.07 | 2.68  | 2.80 | NWS1       |
| OVERALL | 1.63 | 1.34 | 1.52 | 1.47 | 1.69 | 1.64 | 3.44  | 1.86 | IHCM       |

Table 4.2.3(b) Statistics of errors of rainfall-runoff models in simulation-mode, calculated for evaluation period October 1974 to September 1979, omitting Jan-Oct of 1976.

Statistic = RMSE (root mean square error)  
 Units = m<sup>3</sup>/sec  
 Catchment = CHERWELL

|         | PDM1 | IHCM | NWS1 | TWM1 | CLS1 | CLS2 | CLS3 | RECI | BEST MODEL |
|---------|------|------|------|------|------|------|------|------|------------|
| JAN     | 0.21 | 0.25 | 0.19 | 0.26 | 0.22 | 0.22 | 0.36 | 0.23 | NWS1       |
| FEB     | 0.21 | 0.15 | 0.16 | 0.14 | 0.18 | 0.17 | 0.38 | 0.19 | TWM1       |
| MAR     | 0.17 | 0.14 | 0.15 | 0.14 | 0.17 | 0.16 | 0.38 | 0.20 | IHCM       |
| APR     | 0.14 | 0.09 | 0.11 | 0.12 | 0.17 | 0.16 | 0.56 | 0.25 | IHCM       |
| MAY     | 0.21 | 0.18 | 0.13 | 0.23 | 0.25 | 0.22 | 0.49 | 0.33 | NWS1       |
| JUN     | 0.14 | 0.14 | 0.24 | 0.18 | 0.54 | 0.51 | 0.64 | 0.45 | IHCM       |
| JUL     | 0.14 | 0.29 | 0.36 | 0.13 | 0.76 | 0.73 | 0.79 | 0.51 | TWM1       |
| AUG     | 0.43 | 0.26 | 0.47 | 0.18 | 0.70 | 0.69 | 0.62 | 0.31 | TWM1       |
| SEP     | 0.45 | 0.10 | 0.27 | 0.10 | 0.57 | 0.53 | 0.72 | 0.47 | IHCM       |
| OCT     | 0.44 | 0.15 | 0.13 | 0.17 | 0.46 | 0.46 | 0.67 | 0.46 | NWS1       |
| NOV     | 0.67 | 0.43 | 0.43 | 0.24 | 0.67 | 0.67 | 0.69 | 0.44 | TWM1       |
| DEC     | 0.59 | 0.27 | 0.26 | 0.26 | 0.56 | 0.54 | 0.46 | 0.70 | NWS1       |
| OVERALL | 0.32 | 0.20 | 0.24 | 0.18 | 0.44 | 0.42 | 0.56 | 0.38 | TWM1       |

Table 4.2.3(c) Statistics of errors of rainfall-runoff models in simulation-mode, calculated for evaluation period October 1974 to September 1979, omitting Jan-Oct of 1976.

Statistic = PMABS (proportional mean absolute error)  
 Independent of units  
 Catchment = CHERWELL

|         | PDM1 | IHCM | NWS1 | TWM1 | CLS1 | CLS2 | CLS3 | RECI | BEST MODEL |
|---------|------|------|------|------|------|------|------|------|------------|
| JAN     | 0.28 | 0.31 | 0.25 | 0.35 | 0.28 | 0.29 | 0.44 | 0.28 | NWS1       |
| FEB     | 0.25 | 0.18 | 0.20 | 0.18 | 0.22 | 0.20 | 0.63 | 0.23 | TWM1       |
| MAR     | 0.24 | 0.18 | 0.19 | 0.20 | 0.23 | 0.21 | 0.54 | 0.23 | IHCM       |
| APR     | 0.18 | 0.11 | 0.14 | 0.15 | 0.20 | 0.19 | 0.66 | 0.29 | IHCM       |
| MAY     | 0.28 | 0.22 | 0.17 | 0.28 | 0.31 | 0.28 | 0.59 | 0.36 | NWS1       |
| JUN     | 0.18 | 0.19 | 0.30 | 0.23 | 0.62 | 0.59 | 0.72 | 0.47 | PDM1       |
| JUL     | 0.17 | 0.33 | 0.40 | 0.16 | 0.80 | 0.77 | 0.84 | 0.55 | TWM1       |
| AUG     | 0.58 | 0.32 | 0.57 | 0.26 | 0.86 | 0.84 | 0.71 | 0.37 | TWM1       |
| SEP     | 0.53 | 0.13 | 0.31 | 0.20 | 0.65 | 0.61 | 0.82 | 0.53 | IHCM       |
| OCT     | 0.66 | 0.22 | 0.17 | 0.21 | 0.62 | 0.62 | 0.73 | 0.55 | NWS1       |
| NOV     | 0.90 | 0.58 | 0.68 | 0.36 | 0.89 | 0.88 | 0.97 | 0.56 | TWM1       |
| DEC     | 0.84 | 0.33 | 0.36 | 0.37 | 0.81 | 0.79 | 0.57 | 1.03 | IHCM       |
| OVERALL | 0.42 | 0.26 | 0.31 | 0.25 | 0.54 | 0.52 | 0.69 | 0.45 | TWM1       |

Table 4.2.3(d) Statistics of errors of rainfall-runoff models in simulation-mode, calculated for evaluation period October 1974 to September 1979, omitting Jan-Oct of 1976.

Statistic = PRMSE (proportional root mean square error)  
 Independent of units  
 Catchment = CHERWELL

|         | PDMI | IHCM | NWS1 | TWMI | CLS1 | CLS2 | CLS3 | RECI | BEST MODEL |
|---------|------|------|------|------|------|------|------|------|------------|
| JAN     | 1.52 | 1.51 | 1.55 | 1.49 | 1.45 | 1.55 | 1.67 | 1.87 | CLS1       |
| FEB     | 1.48 | 1.09 | 0.98 | 1.04 | 1.05 | 1.08 | 1.29 | 1.20 | NWS1       |
| MAR     | 2.18 | 1.38 | 1.49 | 1.47 | 1.53 | 1.59 | 3.07 | 1.59 | IHCM       |
| APR     | 1.35 | 1.25 | 0.92 | 1.21 | 1.25 | 1.22 | 2.80 | 0.94 | NWS1       |
| MAY     | 1.58 | 1.16 | 0.78 | 1.26 | 0.92 | 0.90 | 2.43 | 0.98 | NWS1       |
| JUN     | 0.89 | 0.63 | 0.72 | 1.05 | 0.78 | 0.76 | 1.79 | 0.88 | IHCM       |
| JUL     | 0.39 | 0.48 | 0.28 | 0.49 | 0.41 | 0.35 | 1.29 | 0.51 | NWS1       |
| AUG     | 0.64 | 0.36 | 0.28 | 0.29 | 0.43 | 0.41 | 1.06 | 0.35 | NWS1       |
| SEP     | 0.70 | 0.50 | 0.30 | 0.47 | 0.46 | 0.43 | 1.24 | 0.53 | NWS1       |
| OCT     | 1.32 | 1.16 | 0.92 | 1.73 | 1.28 | 1.39 | 1.97 | 1.83 | NWS1       |
| NOV     | 1.14 | 1.05 | 0.74 | 0.93 | 0.89 | 0.76 | 1.45 | 1.44 | NWS1       |
| DEC     | 2.28 | 2.32 | 1.97 | 2.42 | 2.01 | 2.07 | 3.40 | 3.53 | NWS1       |
| OVERALL | 1.28 | 1.07 | 0.91 | 1.15 | 1.04 | 1.04 | 1.96 | 1.30 | NWS1       |

Table 4.2.4(a) Statistics of errors of rainfall-runoff models in simulation mode, calculated for calibration period October 1978 to September 1983.

Statistic = MABS (mean absolute error)  
 Units = m<sup>3</sup>/sec  
 Catchment = MOLE

|         | PDMI | IHCM | NWS1 | TWMI | CLS1 | CLS2 | CLS3 | RECI | BEST MODEL |
|---------|------|------|------|------|------|------|------|------|------------|
| JAN     | 2.40 | 2.50 | 2.72 | 2.30 | 2.33 | 2.39 | 2.37 | 3.18 | TWMI       |
| FEB     | 2.43 | 2.06 | 1.77 | 1.55 | 1.54 | 1.58 | 1.91 | 2.02 | CLS1       |
| MAR     | 3.10 | 2.20 | 2.42 | 2.07 | 2.29 | 2.40 | 5.00 | 2.54 | TWMI       |
| APR     | 2.51 | 2.21 | 2.19 | 2.80 | 2.27 | 2.29 | 4.74 | 1.97 | RECI       |
| MAY     | 3.41 | 2.03 | 1.74 | 2.33 | 2.28 | 2.37 | 4.26 | 2.53 | NWS1       |
| JUN     | 2.28 | 1.32 | 1.71 | 2.28 | 1.67 | 1.72 | 3.12 | 2.00 | IHCM       |
| JUL     | 0.81 | 0.98 | 0.48 | 1.06 | 0.59 | 0.60 | 1.80 | 0.91 | NWS1       |
| AUG     | 1.02 | 1.13 | 0.86 | 0.65 | 0.89 | 0.85 | 1.57 | 1.07 | TWMI       |
| SEP     | 0.95 | 1.13 | 0.67 | 1.53 | 1.02 | 1.13 | 2.45 | 1.46 | NWS1       |
| OCT     | 2.53 | 2.32 | 2.07 | 3.42 | 2.31 | 2.58 | 3.94 | 4.28 | NWS1       |
| NOV     | 1.88 | 1.78 | 1.46 | 1.60 | 1.63 | 1.50 | 2.60 | 2.80 | NWS1       |
| DEC     | 3.77 | 4.18 | 3.76 | 4.21 | 3.36 | 3.57 | 6.12 | 7.53 | CLS1       |
| OVERALL | 2.26 | 1.99 | 1.82 | 2.15 | 1.85 | 1.92 | 3.32 | 2.69 | NWS1       |

Table 4.2.4(b) Statistics of errors of rainfall-runoff models in simulation-mode, calculated for calibration period October 1978 to September 1983.

Statistic = RMSE (root mean square error)  
 Units = m<sup>3</sup>/sec  
 Catchment = MOLE

|         | PDMI | IHCM | NWS1 | TWMI | CLS1 | CLS2 | CLS3 | RECI | BEST MODEL |
|---------|------|------|------|------|------|------|------|------|------------|
| JAN     | 0.30 | 0.31 | 0.26 | 0.34 | 0.32 | 0.34 | 0.39 | 0.35 | NWS1       |
| FEB     | 0.30 | 0.19 | 0.17 | 0.25 | 0.23 | 0.23 | 0.31 | 0.25 | NWS1       |
| MAR     | 0.33 | 0.21 | 0.19 | 0.26 | 0.24 | 0.24 | 0.42 | 0.23 | NWS1       |
| APR     | 0.25 | 0.31 | 0.14 | 0.24 | 0.26 | 0.24 | 0.62 | 0.20 | NWS1       |
| MAY     | 0.29 | 0.35 | 0.18 | 0.29 | 0.24 | 0.21 | 0.76 | 0.25 | NWS1       |
| JUN     | 0.24 | 0.21 | 0.20 | 0.31 | 0.27 | 0.24 | 0.70 | 0.29 | NWS1       |
| JUL     | 0.23 | 0.26 | 0.19 | 0.26 | 0.31 | 0.24 | 0.90 | 0.36 | NWS1       |
| AUG     | 0.51 | 0.19 | 0.16 | 0.20 | 0.28 | 0.28 | 0.83 | 0.21 | NWS1       |
| SEP     | 0.52 | 0.25 | 0.17 | 0.20 | 0.25 | 0.22 | 0.78 | 0.27 | NWS1       |
| OCT     | 0.45 | 0.24 | 0.20 | 0.33 | 0.31 | 0.30 | 0.54 | 0.41 | NWS1       |
| NOV     | 0.40 | 0.27 | 0.19 | 0.25 | 0.25 | 0.20 | 0.42 | 0.32 | NWS1       |
| DEC     | 0.39 | 0.33 | 0.23 | 0.35 | 0.33 | 0.32 | 0.40 | 0.48 | NWS1       |
| OVERALL | 0.35 | 0.26 | 0.19 | 0.27 | 0.27 | 0.25 | 0.59 | 0.30 | NWS1       |

Table 4.2.4(c) Statistics of errors of rainfall-runoff models in simulation-mode, calculated for calibration period October 1978 to September 1983.

Statistic = PMABS (proportional mean absolute error)  
 Independent of units  
 Catchment = MOLE

|         | PDMI | IHCM | NWS1 | TWMI | CLS1 | CLS2 | CLS3 | RECI | BEST MODEL |
|---------|------|------|------|------|------|------|------|------|------------|
| JAN     | 0.44 | 0.42 | 0.35 | 0.55 | 0.50 | 0.49 | 0.48 | 0.52 | NWS1       |
| FEB     | 0.39 | 0.27 | 0.22 | 0.31 | 0.28 | 0.28 | 0.37 | 0.30 | NWS1       |
| MAR     | 0.38 | 0.28 | 0.24 | 0.35 | 0.30 | 0.29 | 0.49 | 0.28 | NWS1       |
| APR     | 0.32 | 0.38 | 0.19 | 0.32 | 0.31 | 0.29 | 0.73 | 0.24 | NWS1       |
| MAY     | 0.37 | 0.44 | 0.23 | 0.34 | 0.29 | 0.25 | 0.80 | 0.31 | NWS1       |
| JUN     | 0.34 | 0.27 | 0.28 | 0.40 | 0.34 | 0.30 | 0.76 | 0.40 | IHCM       |
| JUL     | 0.30 | 0.32 | 0.24 | 0.32 | 0.36 | 0.29 | 0.91 | 0.41 | NWS1       |
| AUG     | 0.61 | 0.25 | 0.23 | 0.33 | 0.37 | 0.36 | 0.86 | 0.27 | NWS1       |
| SEP     | 0.61 | 0.30 | 0.21 | 0.25 | 0.31 | 0.28 | 0.81 | 0.34 | NWS1       |
| OCT     | 0.59 | 0.31 | 0.28 | 0.48 | 0.39 | 0.40 | 0.63 | 0.49 | NWS1       |
| NOV     | 0.58 | 0.32 | 0.24 | 0.42 | 0.37 | 0.32 | 0.54 | 0.41 | NWS1       |
| DEC     | 0.54 | 0.41 | 0.33 | 0.56 | 0.47 | 0.47 | 0.48 | 0.82 | NWS1       |
| OVERALL | 0.46 | 0.33 | 0.25 | 0.39 | 0.36 | 0.34 | 0.65 | 0.40 | NWS1       |

Table 4.2.4(d) Statistics of errors of rainfall-runoff models in simulation-mode, calculated for calibration period October 1978 to September 1983.

Statistic = PRMSE (proportional root mean square error)  
 Independent of units  
 Catchment = MOLE

|         | PDMI | IHCM | NWS1 | TWM1 | CLS1 | CLS2 | CLS3 | RECI | BEST MODEL |
|---------|------|------|------|------|------|------|------|------|------------|
| JAN     | 2.78 | 2.53 | 1.85 | 2.91 | 2.48 | 2.56 | 2.95 | 2.72 | NWS1       |
| FEB     | 1.69 | 1.82 | 0.90 | 1.97 | 1.90 | 1.76 | 2.49 | 1.92 | NWS1       |
| MAR     | 1.27 | 1.42 | 0.68 | 0.97 | 0.93 | 0.76 | 1.65 | 0.88 | NWS1       |
| APR     | 0.84 | 1.16 | 0.64 | 0.65 | 0.70 | 0.65 | 1.16 | 0.81 | NWS1       |
| MAY     | 1.11 | 0.91 | 0.46 | 0.76 | 0.93 | 0.94 | 1.88 | 1.08 | NWS1       |
| JUN     | 0.51 | 0.64 | 0.55 | 0.29 | 0.51 | 0.47 | 1.00 | 0.58 | TWM1       |
| JUL     | 0.55 | 0.37 | 0.26 | 0.13 | 0.59 | 0.57 | 0.80 | 0.58 | TWM1       |
| AUG     | 0.44 | 0.23 | 0.20 | 0.14 | 0.44 | 0.43 | 0.68 | 0.22 | TWM1       |
| SEP     | 2.37 | 1.04 | 0.97 | 1.54 | 1.59 | 1.42 | 2.02 | 2.11 | NWS1       |
| OCT     | 0.99 | 0.79 | 0.51 | 0.80 | 1.09 | 1.05 | 0.75 | 0.87 | NWS1       |
| NOV     | 2.36 | 1.35 | 1.27 | 1.51 | 1.85 | 1.69 | 2.58 | 2.21 | NWS1       |
| DEC     | 1.74 | 1.79 | 1.00 | 2.00 | 1.43 | 1.51 | 1.91 | 1.80 | NWS1       |
| OVERALL | 1.39 | 1.17 | 0.78 | 1.14 | 1.20 | 1.15 | 1.66 | 1.32 | NWS1       |

Table 4.2.5(a) Statistics of errors of rainfall-runoff models in simulation-mode, calculated for evaluation period October 1972 to September 1975

Statistic = MABS (mean absolute error)  
 Units = m<sup>3</sup>/sec  
 Catchment = MOLE

|         | PDMI | IHCM | NWS1 | TWM1 | CLS1 | CLS2 | CLS3 | RECI | BEST MODEL |
|---------|------|------|------|------|------|------|------|------|------------|
| JAN     | 5.97 | 4.82 | 3.77 | 4.77 | 4.71 | 4.91 | 5.19 | 5.52 | NWS1       |
| FEB     | 3.45 | 2.37 | 1.65 | 3.99 | 3.61 | 3.39 | 4.41 | 5.72 | NWS1       |
| MAR     | 2.50 | 2.23 | 1.06 | 1.56 | 1.40 | 1.19 | 2.34 | 1.39 | NWS1       |
| APR     | 1.37 | 1.55 | 1.16 | 1.22 | 1.24 | 1.23 | 1.65 | 1.40 | NWS1       |
| MAY     | 3.36 | 1.31 | 0.73 | 2.32 | 2.05 | 2.25 | 4.34 | 1.55 | NWS1       |
| JUN     | 0.96 | 1.06 | 0.94 | 0.72 | 0.94 | 0.85 | 1.24 | 1.01 | TWM1       |
| JUL     | 0.65 | 0.57 | 0.35 | 0.24 | 0.81 | 0.76 | 0.84 | 0.70 | TWM1       |
| AUG     | 0.54 | 0.31 | 0.26 | 0.23 | 0.64 | 0.62 | 0.71 | 0.26 | TWM1       |
| SEP     | 4.21 | 2.06 | 1.84 | 3.48 | 2.57 | 2.42 | 4.80 | 4.37 | NWS1       |
| OCT     | 1.28 | 1.71 | 0.99 | 1.70 | 2.00 | 2.06 | 1.13 | 1.92 | NWS1       |
| NOV     | 4.31 | 3.04 | 2.60 | 3.74 | 3.70 | 3.57 | 6.36 | 4.38 | NWS1       |
| DEC     | 2.89 | 2.50 | 1.79 | 3.63 | 2.55 | 2.94 | 2.58 | 2.92 | NWS1       |
| OVERALL | 2.62 | 1.96 | 1.43 | 2.30 | 2.18 | 2.18 | 2.96 | 2.59 | NWS1       |

Table 4.2.5(b) Statistics of errors of rainfall-runoff models in simulation-mode, calculated for evaluation period October 1972 to September 1975

Statistic = RMSE (root mean square error)  
 Units = m<sup>3</sup>/sec  
 Catchment = MOLE

|         | PDMI | IHCM | NWS1 | TWMI | CLS1 | CLS2 | CLS3 | RECI | BEST MODEL |
|---------|------|------|------|------|------|------|------|------|------------|
| JAN     | 0.42 | 0.38 | 0.26 | 0.46 | 0.42 | 0.38 | 0.54 | 0.36 | NWS1       |
| FEB     | 0.33 | 0.50 | 0.20 | 0.36 | 0.36 | 0.32 | 0.51 | 0.28 | NWS1       |
| MAR     | 0.34 | 0.40 | 0.23 | 0.27 | 0.32 | 0.26 | 0.62 | 0.25 | NWS1       |
| APR     | 0.36 | 0.54 | 0.26 | 0.23 | 0.28 | 0.26 | 0.54 | 0.34 | TWMI       |
| MAY     | 0.28 | 0.46 | 0.22 | 0.20 | 0.35 | 0.33 | 0.67 | 0.59 | TWMI       |
| JUN     | 0.36 | 0.49 | 0.41 | 0.19 | 0.33 | 0.32 | 0.86 | 0.44 | TWMI       |
| JUL     | 0.62 | 0.37 | 0.27 | 0.12 | 0.56 | 0.55 | 0.86 | 0.62 | TWMI       |
| AUG     | 0.55 | 0.26 | 0.25 | 0.16 | 0.45 | 0.45 | 0.85 | 0.27 | TWMI       |
| SEP     | 1.01 | 0.30 | 0.37 | 0.47 | 0.69 | 0.58 | 0.58 | 0.66 | IHCM       |
| OCT     | 0.94 | 0.30 | 0.21 | 0.27 | 0.52 | 0.50 | 0.47 | 0.45 | NWS1       |
| NOV     | 1.09 | 0.37 | 0.40 | 0.38 | 0.71 | 0.63 | 0.50 | 0.78 | IHCM       |
| DEC     | 0.49 | 0.49 | 0.26 | 0.43 | 0.37 | 0.35 | 0.59 | 0.45 | NWS1       |
| OVERALL | 0.57 | 0.41 | 0.28 | 0.30 | 0.45 | 0.41 | 0.63 | 0.46 | NWS1       |

Table 4.2.5(c) Statistics of errors of rainfall-runoff models in simulation mode, calculated for evaluation period October 1972 to September 1975

Statistic = PMABS (proportional mean absolute error)  
 Independent of units  
 Catchment = MOLE

|         | PDMI | IHCM | NWS1 | TWMI | CLS1 | CLS2 | CLS3 | RECI | BEST MODEL |
|---------|------|------|------|------|------|------|------|------|------------|
| JAN     | 0.62 | 0.46 | 0.40 | 0.85 | 0.64 | 0.57 | 0.72 | 0.47 | NWS1       |
| FEB     | 0.44 | 0.60 | 0.30 | 0.52 | 0.51 | 0.43 | 0.63 | 0.39 | NWS1       |
| MAR     | 0.42 | 0.48 | 0.29 | 0.45 | 0.46 | 0.37 | 0.77 | 0.31 | NWS1       |
| APR     | 0.42 | 0.61 | 0.36 | 0.32 | 0.44 | 0.38 | 0.63 | 0.42 | TWMI       |
| MAY     | 0.36 | 0.52 | 0.29 | 0.23 | 0.50 | 0.46 | 0.73 | 0.71 | TWMI       |
| JUN     | 0.56 | 0.60 | 0.49 | 0.47 | 0.45 | 0.44 | 0.89 | 0.55 | CLS2       |
| JUL     | 0.75 | 0.50 | 0.34 | 0.19 | 0.63 | 0.62 | 0.88 | 0.73 | TWMI       |
| AUG     | 0.66 | 0.32 | 0.31 | 0.27 | 0.57 | 0.56 | 0.86 | 0.32 | TWMI       |
| SEP     | 1.56 | 0.37 | 0.56 | 0.96 | 0.96 | 0.81 | 0.67 | 0.88 | IHCM       |
| OCT     | 1.18 | 0.35 | 0.32 | 0.51 | 0.72 | 0.68 | 0.59 | 0.62 | NWS1       |
| NOV     | 1.28 | 0.44 | 0.60 | 0.54 | 0.87 | 0.77 | 0.57 | 1.18 | IHCM       |
| DEC     | 0.66 | 0.57 | 0.38 | 0.72 | 0.47 | 0.45 | 0.73 | 0.55 | NWS1       |
| OVERALL | 0.74 | 0.49 | 0.39 | 0.50 | 0.60 | 0.55 | 0.72 | 0.60 | NWS1       |

Table 4.2.5(d) Statistics of errors of rainfall-runoff models in simulation-mode, calculated for evaluation period October 1972 to September 1975

Statistic = PRMSE (proportional root mean square error)  
 Independent of units  
 Catchment = MOLE

|         | PDMI | IHCM | NWS1 | TWMI | CLS1 | CLS2 | CLS3 | RECI | BEST MODEL |
|---------|------|------|------|------|------|------|------|------|------------|
| JAN     | 1.31 | 1.01 | 0.91 | 0.95 | 0.90 | 0.85 | 0.91 | 1.35 | CLS2       |
| FEB     | 1.18 | 0.97 | 0.73 | 0.91 | 0.85 | 0.81 | 1.03 | 0.97 | NWS1       |
| MAR     | 1.12 | 0.78 | 0.58 | 0.85 | 0.80 | 0.79 | 0.97 | 0.85 | NWS1       |
| APR     | 0.82 | 0.71 | 0.41 | 0.94 | 0.57 | 0.59 | 1.19 | 0.71 | NWS1       |
| MAY     | 0.45 | 0.43 | 0.25 | 0.83 | 0.61 | 0.63 | 1.86 | 0.55 | NWS1       |
| JUN     | 0.77 | 0.52 | 0.42 | 0.64 | 0.56 | 0.60 | 1.85 | 0.74 | NWS1       |
| JUL     | 0.57 | 0.47 | 0.26 | 0.41 | 0.38 | 0.42 | 1.34 | 0.40 | NWS1       |
| AUG     | 0.70 | 0.38 | 0.23 | 0.39 | 0.48 | 0.46 | 1.10 | 0.28 | NWS1       |
| SEP     | 0.71 | 0.42 | 0.37 | 0.64 | 0.56 | 0.64 | 1.19 | 0.59 | NWS1       |
| OCT     | 0.94 | 0.40 | 0.32 | 0.56 | 0.73 | 0.70 | 1.11 | 1.11 | NWS1       |
| NOV     | 1.10 | 0.77 | 0.56 | 0.87 | 0.73 | 0.72 | 0.82 | 1.11 | NWS1       |
| DEC     | 1.50 | 0.34 | 0.75 | 1.07 | 0.92 | 0.85 | 1.00 | 1.05 | NWS1       |
| OVERALL | 0.93 | 0.64 | 0.48 | 0.76 | 0.67 | 0.67 | 1.20 | 0.81 | NWS1       |

Table 4.2.6(a) Statistics of errors of rainfall-runoff models in simulation-mode, calculated for calibration period October 1968 to September 1974

Statistic = MABS (mean absolute error)  
 Units = m<sup>3</sup>/sec  
 Catchment = BLACKWATER

|         | PDMI | IHCM | NWS1 | TWMI | CLS1 | CLS2 | CLS3 | RECI | BEST MODEL |
|---------|------|------|------|------|------|------|------|------|------------|
| JAN     | 2.41 | 1.51 | 1.55 | 1.34 | 1.40 | 1.35 | 1.35 | 2.17 | TWMI       |
| FEB     | 1.99 | 1.42 | 1.26 | 1.31 | 1.30 | 1.27 | 1.47 | 1.44 | NWS1       |
| MAR     | 1.77 | 1.45 | 1.25 | 1.33 | 1.33 | 1.34 | 1.63 | 1.85 | NWS1       |
| APR     | 1.69 | 1.17 | 1.06 | 1.48 | 0.91 | 0.92 | 1.72 | 1.26 | CLS1       |
| MAY     | 0.70 | 0.57 | 0.43 | 0.96 | 0.93 | 0.95 | 1.92 | 0.73 | NWS1       |
| JUN     | 2.03 | 1.30 | 1.10 | 1.12 | 1.01 | 1.03 | 2.75 | 1.65 | CLS1       |
| JUL     | 0.79 | 0.66 | 0.45 | 0.55 | 0.53 | 0.56 | 1.53 | 0.58 | NWS1       |
| AUG     | 0.81 | 0.57 | 0.42 | 0.60 | 0.66 | 0.62 | 1.32 | 0.44 | NWS1       |
| SEP     | 1.01 | 0.83 | 1.31 | 1.33 | 0.91 | 0.95 | 1.44 | 1.12 | IHCM       |
| OCT     | 2.00 | 0.64 | 0.60 | 0.85 | 1.23 | 1.06 | 1.48 | 1.96 | NWS1       |
| NOV     | 2.21 | 1.25 | 1.04 | 1.42 | 1.15 | 1.10 | 1.25 | 1.80 | NWS1       |
| DEC     | 3.74 | 1.26 | 1.29 | 1.71 | 1.55 | 1.42 | 1.41 | 1.84 | IHCM       |
| OVERALL | 1.76 | 1.05 | 0.98 | 1.17 | 1.08 | 1.05 | 1.61 | 1.40 | NWS1       |

Table 4.2.6(b) Statistics of errors of rainfall-runoff models in simulation-mode, calculated for calibration period October 1968 to September 1974.

Statistic = RMSE (root mean square error)  
 Units = m<sup>3</sup>/sec  
 Catchment = BLACKWATER

|         | PDMI | IHCM | NWS1 | TWMI | CLS1 | CLS2 | CLS3 | REC1 | BEST MODEL |
|---------|------|------|------|------|------|------|------|------|------------|
| JAN     | 0.21 | 0.19 | 0.14 | 0.20 | 0.15 | 0.15 | 0.19 | 0.23 | NWS1       |
| FEB     | 0.24 | 0.20 | 0.13 | 0.21 | 0.17 | 0.16 | 0.22 | 0.20 | NWS1       |
| MAR     | 0.24 | 0.18 | 0.11 | 0.23 | 0.19 | 0.18 | 0.25 | 0.19 | NWS1       |
| APR     | 0.20 | 0.22 | 0.10 | 0.29 | 0.18 | 0.19 | 0.42 | 0.23 | NWS1       |
| MAY     | 0.15 | 0.17 | 0.09 | 0.33 | 0.22 | 0.23 | 0.79 | 0.24 | NWS1       |
| JUN     | 0.24 | 0.17 | 0.13 | 0.26 | 0.21 | 0.23 | 0.83 | 0.23 | NWS1       |
| JUL     | 0.37 | 0.30 | 0.18 | 0.25 | 0.24 | 0.26 | 0.83 | 0.25 | NWS1       |
| AUG     | 0.47 | 0.20 | 0.13 | 0.24 | 0.28 | 0.28 | 0.68 | 0.16 | NWS1       |
| SEP     | 0.43 | 0.20 | 0.14 | 0.31 | 0.29 | 0.35 | 0.73 | 0.29 | NWS1       |
| OCT     | 0.45 | 0.21 | 0.14 | 0.31 | 0.32 | 0.34 | 0.64 | 0.46 | NWS1       |
| NOV     | 0.38 | 0.27 | 0.18 | 0.30 | 0.24 | 0.24 | 0.29 | 0.35 | NWS1       |
| DEC     | 0.28 | 0.23 | 0.18 | 0.29 | 0.22 | 0.21 | 0.29 | 0.23 | NWS1       |
| OVERALL | 0.31 | 0.21 | 0.14 | 0.27 | 0.23 | 0.24 | 0.51 | 0.26 | NWS1       |

Table 4.2.6(c) Statistics of errors of rainfall-runoff models in simulation-mode, calculated for calibration period October 1968 to September 1974.

Statistic = PMABS (proportional mean absolute error)  
 Independent of units  
 Catchment = BLACKWATER

|         | PDMI | IHCM | NWS1 | TWMI | CLS1 | CLS2 | CLS3 | REC1 | BEST MODEL |
|---------|------|------|------|------|------|------|------|------|------------|
| JAN     | 0.30 | 0.23 | 0.19 | 0.27 | 0.19 | 0.18 | 0.25 | 0.28 | CLS2       |
| FEB     | 0.32 | 0.25 | 0.18 | 0.27 | 0.23 | 0.22 | 0.29 | 0.25 | NWS1       |
| MAR     | 0.28 | 0.23 | 0.14 | 0.28 | 0.25 | 0.24 | 0.34 | 0.25 | NWS1       |
| APR     | 0.25 | 0.27 | 0.14 | 0.33 | 0.26 | 0.27 | 0.50 | 0.28 | NWS1       |
| MAY     | 0.18 | 0.21 | 0.12 | 0.35 | 0.31 | 0.32 | 0.81 | 0.31 | NWS1       |
| JUN     | 0.35 | 0.23 | 0.16 | 0.29 | 0.26 | 0.28 | 0.87 | 0.28 | NWS1       |
| JUL     | 0.47 | 0.40 | 0.29 | 0.30 | 0.31 | 0.31 | 0.87 | 0.31 | NWS1       |
| AUG     | 0.55 | 0.28 | 0.19 | 0.34 | 0.36 | 0.35 | 0.75 | 0.20 | NWS1       |
| SEP     | 0.51 | 0.24 | 0.27 | 0.41 | 0.36 | 0.41 | 0.81 | 0.33 | IHCM       |
| OCT     | 0.55 | 0.26 | 0.17 | 0.35 | 0.38 | 0.39 | 0.75 | 0.55 | NWS1       |
| NOV     | 0.51 | 0.34 | 0.25 | 0.39 | 0.30 | 0.30 | 0.39 | 0.44 | NWS1       |
| DEC     | 0.43 | 0.30 | 0.24 | 0.42 | 0.27 | 0.26 | 0.41 | 0.30 | NWS1       |
| OVERALL | 0.39 | 0.27 | 0.19 | 0.33 | 0.29 | 0.29 | 0.59 | 0.31 | NWS1       |

Table 4.2.6(d) Statistics of errors of rainfall-runoff models in simulation-mode, calculated for calibration period October 1968 to September 1974.

Statistic = PRMSE (proportional root mean square error)  
 Independent of units  
 Catchment = BLACKWATER

|         | PDMI | IHCM | NWS1 | TWMI | CLS1 | CLS2 | CLS3 | RECI | BEST MODEL |
|---------|------|------|------|------|------|------|------|------|------------|
| JAN     | 1.37 | 1.27 | 1.01 | 1.09 | 1.45 | 1.28 | 1.38 | 1.35 | NWS1       |
| FEB     | 1.57 | 1.25 | 0.89 | 0.92 | 1.53 | 1.26 | 1.08 | 0.98 | NWS1       |
| MAR     | 1.40 | 0.95 | 0.76 | 0.71 | 1.32 | 1.24 | 1.04 | 0.98 | TWMI       |
| APR     | 1.31 | 0.68 | 0.49 | 0.77 | 0.85 | 0.87 | 0.85 | 0.70 | NWS1       |
| MAY     | 1.48 | 0.99 | 0.64 | 1.00 | 1.02 | 1.12 | 1.67 | 0.88 | NWS1       |
| JUN     | 0.51 | 0.48 | 0.22 | 0.39 | 0.52 | 0.59 | 1.45 | 0.39 | NWS1       |
| JUL     | 0.33 | 0.48 | 0.16 | 0.22 | 0.35 | 0.43 | 1.42 | 0.47 | NWS1       |
| AUG     | 0.68 | 0.62 | 0.45 | 0.51 | 0.64 | 0.72 | 1.26 | 0.43 | RECI       |
| SEP     | 0.74 | 0.39 | 0.33 | 0.38 | 0.48 | 0.55 | 1.13 | 0.52 | NWS1       |
| OCT     | 0.85 | 0.57 | 0.45 | 0.59 | 0.68 | 0.80 | 1.37 | 0.61 | NWS1       |
| NOV     | 1.25 | 0.97 | 1.28 | 1.12 | 1.02 | 1.02 | 1.30 | 1.29 | IHCM       |
| DEC     | 1.24 | 1.22 | 1.01 | 1.25 | 0.99 | 0.95 | 1.52 | 1.27 | CLS2       |
| OVERALL | 1.06 | 0.82 | 0.64 | 0.75 | 0.91 | 0.90 | 1.29 | 0.82 | NWS1       |

Table 4.2.7(a) Statistics of errors of rainfall-runoff models in simulation-mode, calculated for evaluation period October 1974 to September 1979.

Statistic = MABS (mean absolute error)  
 Units =  $m^3/sec$   
 Catchment = BLACKWATER

|         | PDMI | IHCM | NWS1 | TWMI | CLS1 | CLS2 | CLS3 | RECI | BEST MODEL |
|---------|------|------|------|------|------|------|------|------|------------|
| JAN     | 2.26 | 2.16 | 1.95 | 1.69 | 2.41 | 2.08 | 2.05 | 2.58 | TWMI       |
| FEB     | 2.63 | 1.73 | 1.73 | 1.42 | 2.83 | 2.19 | 1.56 | 1.58 | TWMI       |
| MAR     | 1.89 | 1.39 | 1.33 | 0.98 | 2.02 | 1.81 | 1.34 | 1.52 | TWMI       |
| APR     | 1.75 | 0.95 | 0.93 | 1.06 | 1.28 | 1.27 | 1.11 | 1.08 | NWS1       |
| MAY     | 2.49 | 2.03 | 1.52 | 1.73 | 1.74 | 1.81 | 2.50 | 2.09 | NWS1       |
| JUN     | 0.75 | 0.60 | 0.39 | 0.55 | 0.87 | 0.96 | 1.56 | 0.49 | NWS1       |
| JUL     | 0.51 | 0.69 | 0.36 | 0.35 | 0.42 | 0.50 | 1.55 | 0.74 | TWMI       |
| AUG     | 1.09 | 1.40 | 1.51 | 1.31 | 1.10 | 1.17 | 1.53 | 0.65 | RECI       |
| SEP     | 1.07 | 0.68 | 0.64 | 0.64 | 0.74 | 0.79 | 1.48 | 0.87 | TWMI       |
| OCT     | 1.32 | 1.01 | 0.66 | 0.89 | 0.94 | 1.09 | 1.88 | 0.90 | NWS1       |
| NOV     | 2.34 | 1.90 | 3.21 | 1.96 | 1.79 | 1.67 | 1.80 | 2.60 | CLS2       |
| DEC     | 2.20 | 2.03 | 2.58 | 2.27 | 1.65 | 1.52 | 2.20 | 2.07 | CLS2       |
| OVERALL | 1.69 | 1.38 | 1.40 | 1.24 | 1.48 | 1.41 | 1.71 | 1.43 | TWMI       |

Table 4.2.7(b) Statistics of errors of rainfall-runoff models in simulation-mode, calculated for evaluation period October 1974 to September 1979.

Statistic = RMSE (root mean square error)  
 Units =  $m^3/sec$   
 Catchment = BLACKWATER

|         | PDMI | IHCM | NWS1 | TWMI | CLS1 | CLS2 | CLS3 | REC1 | BEST MODEL |
|---------|------|------|------|------|------|------|------|------|------------|
| JAN     | 0.24 | 0.21 | 0.15 | 0.21 | 0.22 | 0.21 | 0.25 | 0.23 | NWS1       |
| FEB     | 0.29 | 0.24 | 0.14 | 0.20 | 0.25 | 0.22 | 0.22 | 0.19 | NWS1       |
| MAR     | 0.29 | 0.19 | 0.12 | 0.18 | 0.24 | 0.23 | 0.27 | 0.18 | NWS1       |
| APR     | 0.32 | 0.18 | 0.10 | 0.22 | 0.22 | 0.23 | 0.32 | 0.19 | NWS1       |
| MAY     | 0.39 | 0.20 | 0.13 | 0.25 | 0.24 | 0.28 | 0.53 | 0.18 | NWS1       |
| JUN     | 0.28 | 0.23 | 0.10 | 0.18 | 0.24 | 0.28 | 0.79 | 0.19 | NWS1       |
| JUL     | 0.28 | 0.30 | 0.10 | 0.15 | 0.26 | 0.31 | 0.94 | 0.28 | NWS1       |
| AUG     | 0.44 | 0.28 | 0.18 | 0.23 | 0.35 | 0.40 | 0.79 | 0.24 | NWS1       |
| SEP     | 0.45 | 0.19 | 0.16 | 0.21 | 0.26 | 0.31 | 0.67 | 0.29 | NWS1       |
| OCT     | 0.34 | 0.19 | 0.16 | 0.24 | 0.26 | 0.31 | 0.53 | 0.26 | NWS1       |
| NOV     | 0.32 | 0.23 | 0.23 | 0.30 | 0.25 | 0.27 | 0.43 | 0.30 | NWS1       |
| DEC     | 0.25 | 0.24 | 0.17 | 0.25 | 0.19 | 0.19 | 0.35 | 0.26 | NWS1       |
| OVERALL | 0.32 | 0.22 | 0.15 | 0.22 | 0.25 | 0.27 | 0.51 | 0.23 | NWS1       |

Table 4.2.7(c) Statistics of errors of rainfall-runoff models in simulation-mode, calculated for evaluation period October 1974 to September 1979.

Statistic = PMABS (proportional mean absolute error)  
 Independent of units  
 Catchment = BLACKWATER

|         | PDMI | IHCM | NWS1 | TWMI | CLS1 | CLS2 | CLS3 | REC1 | BEST MODEL |
|---------|------|------|------|------|------|------|------|------|------------|
| JAN     | 0.30 | 0.28 | 0.21 | 0.29 | 0.30 | 0.27 | 0.30 | 0.30 | NWS1       |
| FEB     | 0.36 | 0.31 | 0.21 | 0.28 | 0.37 | 0.31 | 0.26 | 0.24 | NWS1       |
| MAR     | 0.32 | 0.26 | 0.16 | 0.23 | 0.33 | 0.31 | 0.36 | 0.23 | NWS1       |
| APR     | 0.35 | 0.23 | 0.14 | 0.26 | 0.31 | 0.32 | 0.46 | 0.23 | NWS1       |
| MAY     | 0.47 | 0.24 | 0.16 | 0.28 | 0.34 | 0.37 | 0.62 | 0.23 | NWS1       |
| JUN     | 0.40 | 0.27 | 0.13 | 0.21 | 0.31 | 0.36 | 0.85 | 0.22 | NWS1       |
| JUL     | 0.43 | 0.33 | 0.15 | 0.20 | 0.30 | 0.35 | 0.96 | 0.32 | NWS1       |
| AUG     | 0.57 | 0.41 | 0.39 | 0.37 | 0.44 | 0.50 | 0.84 | 0.27 | REC1       |
| SEP     | 0.60 | 0.23 | 0.21 | 0.25 | 0.32 | 0.36 | 0.76 | 0.34 | NWS1       |
| OCT     | 0.43 | 0.25 | 0.21 | 0.28 | 0.33 | 0.38 | 0.65 | 0.32 | NWS1       |
| NOV     | 0.41 | 0.35 | 0.31 | 0.42 | 0.34 | 0.36 | 0.57 | 0.37 | NWS1       |
| DEC     | 0.34 | 0.32 | 0.28 | 0.37 | 0.25 | 0.24 | 0.48 | 0.36 | CLS2       |
| OVERALL | 0.41 | 0.29 | 0.21 | 0.29 | 0.33 | 0.34 | 0.59 | 0.29 | NWS1       |

Table 4.2.7(d) Statistics of errors of rainfall-runoff models in simulation-mode, calculated for evaluation period October 1974 to September 1979.

Statistic = PRMSE (proportional root mean square error)  
 Independent of units  
 Catchment = BLACKWATER

|         | PDMI | IHCM | NWS1  | TWM1 | CLS1 | CLS2 | CLS3 | RECI | BEST MODEL |
|---------|------|------|-------|------|------|------|------|------|------------|
| JAN     | 1.61 | 1.52 | 1.21  | 1.22 | 1.74 | 1.53 | 1.66 | 1.56 | NWS1       |
| FEB     | 1.85 | 1.42 | 1.05  | 0.91 | 1.82 | 1.48 | 1.24 | 1.09 | TWM1       |
| MAR     | 1.65 | 1.13 | 0.93  | 0.71 | 1.59 | 1.48 | 1.04 | 1.12 | TWM1       |
| APR     | 1.54 | 0.80 | 0.60  | 0.80 | 1.01 | 1.02 | 0.70 | 0.76 | NWS1       |
| MAY     | 1.63 | 1.21 | 0.76  | 1.14 | 1.23 | 1.34 | 1.80 | 1.01 | NWS1       |
| JUN     | 0.45 | 0.58 | 0.24  | 0.40 | 0.57 | 0.64 | 1.57 | 0.46 | NWS1       |
| JUL     | 0.23 | 0.56 | 0.16  | 0.21 | 0.35 | 0.42 | 1.57 | 0.56 | NWS1       |
| AUG     | 0.67 | 0.75 | 0.53  | 0.59 | 0.69 | 0.77 | 1.39 | 0.49 | NWS1       |
| SEP     | 0.55 | 0.39 | 0.30  | 0.36 | 0.46 | 0.53 | 1.16 | 0.58 | NWS1       |
| OCT     | 0.53 | 0.38 | 0.32  | 0.58 | 0.54 | 0.61 | 0.85 | 0.55 | NWS1       |
| NOV     | 1.25 | 0.97 | 1.29  | 1.12 | 1.02 | 1.02 | 1.30 | 1.29 | IHCM       |
| DEC     | 1.24 | 1.22 | 1.01  | 1.25 | 0.99 | 0.95 | 1.52 | 1.27 | CLS2       |
| OVERALL | 1.10 | 0.91 | 0.701 | 0.77 | 1.00 | 0.98 | 1.32 | 0.89 | NWS1       |

Table 4.2.8(a) Statistics of errors of rainfall-runoff models in simulation-mode, calculated for evaluation period October 1974 to September 1979, omitting Jan-Oct of 1976.

Statistic = MABS (mean absolute error)  
 Units = m<sup>3</sup>/sec  
 Catchment = BLACKWATER

|         | PDMI | IHCM | NWS1 | TWM1 | CLS1 | CLS2 | CLS3 | RECI | BEST MODEL |
|---------|------|------|------|------|------|------|------|------|------------|
| JAN     | 2.51 | 2.40 | 2.17 | 1.86 | 2.68 | 2.31 | 2.28 | 2.87 | TWM1       |
| FEB     | 2.93 | 1.82 | 1.92 | 1.42 | 3.14 | 2.43 | 1.72 | 1.72 | TWM1       |
| MAR     | 2.10 | 1.54 | 1.49 | 1.04 | 2.24 | 2.01 | 1.40 | 1.69 | TWM1       |
| APR     | 1.95 | 1.06 | 1.04 | 1.14 | 1.42 | 1.40 | 1.00 | 1.18 | CLS3       |
| MAY     | 2.74 | 2.27 | 1.69 | 1.92 | 1.94 | 2.02 | 2.73 | 2.32 | NWS1       |
| JUN     | 0.74 | 0.66 | 0.43 | 0.59 | 0.96 | 1.04 | 1.67 | 0.55 | NWS1       |
| JUL     | 0.40 | 0.77 | 0.39 | 0.35 | 0.43 | 0.50 | 1.68 | 0.82 | TWM1       |
| AUG     | 1.16 | 1.56 | 1.68 | 1.46 | 1.20 | 1.28 | 1.67 | 0.71 | RECI       |
| SEP     | 0.75 | 0.68 | 0.58 | 0.64 | 0.73 | 0.78 | 1.46 | 0.94 | NWS1       |
| OCT     | 0.64 | 0.66 | 0.48 | 0.86 | 0.78 | 0.85 | 1.06 | 0.77 | NWS1       |
| NOV     | 2.34 | 1.90 | 3.21 | 1.96 | 1.79 | 1.67 | 1.80 | 2.60 | CLS2       |
| DEC     | 2.20 | 2.03 | 2.59 | 2.27 | 1.65 | 1.52 | 2.20 | 2.07 | CLS2       |
| OVERALL | 1.70 | 1.45 | 1.47 | 1.29 | 1.58 | 1.49 | 1.72 | 1.52 | TWM1       |

Table 4.2.8(b) Statistics of errors of rainfall-runoff models in simulation-mode, calculated for evaluation period October 1974 to September 1979, omitting Jan-Oct of 1976.

Statistic = RMSE (root mean square error)  
 Units = m<sup>3</sup>/sec  
 Catchment = BLACKWATER

|         | PDMI | IHCM | NWS1 | TWMI | CLS1 | CLS2 | CLS3 | RECI | BEST MODEL |
|---------|------|------|------|------|------|------|------|------|------------|
| JAN     | 0.24 | 0.23 | 0.17 | 0.19 | 0.24 | 0.22 | 0.28 | 0.22 | NWS1       |
| FEB     | 0.31 | 0.25 | 0.15 | 0.14 | 0.28 | 0.23 | 0.22 | 0.17 | TWMI       |
| MAR     | 0.29 | 0.21 | 0.13 | 0.12 | 0.27 | 0.26 | 0.20 | 0.18 | TWMI       |
| APR     | 0.33 | 0.20 | 0.11 | 0.17 | 0.24 | 0.25 | 0.16 | 0.16 | NWS1       |
| MAY     | 0.31 | 0.23 | 0.13 | 0.22 | 0.26 | 0.29 | 0.42 | 0.16 | NWS1       |
| JUN     | 0.15 | 0.27 | 0.09 | 0.15 | 0.21 | 0.24 | 0.74 | 0.21 | NWS1       |
| JUL     | 0.13 | 0.34 | 0.08 | 0.12 | 0.21 | 0.26 | 0.96 | 0.32 | NWS1       |
| AUG     | 0.31 | 0.33 | 0.18 | 0.22 | 0.28 | 0.33 | 0.75 | 0.24 | NWS1       |
| SEP     | 0.30 | 0.19 | 0.14 | 0.19 | 0.25 | 0.30 | 0.70 | 0.33 | NWS1       |
| OCT     | 0.29 | 0.16 | 0.13 | 0.26 | 0.24 | 0.28 | 0.43 | 0.28 | NWS1       |
| NOV     | 0.32 | 0.23 | 0.23 | 0.30 | 0.25 | 0.27 | 0.43 | 0.30 | IHCM       |
| DEC     | 0.25 | 0.24 | 0.17 | 0.25 | 0.19 | 0.19 | 0.35 | 0.26 | NWS1       |
| OVERALL | 0.27 | 0.24 | 0.14 | 0.19 | 0.24 | 0.26 | 0.47 | 0.24 | NWS1       |

Table 4.2.8(c) Statistics of errors of rainfall-runoff models in simulation-mode, calculated for evaluation period October 1974 to September 1979, omitting Jan-Oct of 1976.

Statistic = PMABS (proportional mean absolute error)  
 Independent of units  
 Catchment = BLACKWATER

|         | PDMI | IHCM | NWS1 | TWMI | CLS1 | CLS2 | CLS3 | RECI | BEST MODEL |
|---------|------|------|------|------|------|------|------|------|------------|
| JAN     | 0.31 | 0.29 | 0.22 | 0.27 | 0.32 | 0.29 | 0.32 | 0.31 | NWS1       |
| FEB     | 0.39 | 0.29 | 0.22 | 0.19 | 0.40 | 0.32 | 0.26 | 0.22 | TWMI       |
| MAR     | 0.34 | 0.28 | 0.18 | 0.16 | 0.36 | 0.33 | 0.28 | 0.22 | TWMI       |
| APR     | 0.36 | 0.24 | 0.16 | 0.20 | 0.33 | 0.34 | 0.19 | 0.20 | NWS1       |
| MAY     | 0.34 | 0.27 | 0.16 | 0.25 | 0.37 | 0.39 | 0.50 | 0.21 | NWS1       |
| JUN     | 0.19 | 0.30 | 0.12 | 0.17 | 0.30 | 0.33 | 0.81 | 0.24 | NWS1       |
| JUL     | 0.16 | 0.36 | 0.11 | 0.14 | 0.24 | 0.29 | 0.96 | 0.35 | NWS1       |
| AUG     | 0.42 | 0.46 | 0.42 | 0.39 | 0.38 | 0.42 | 0.80 | 0.28 | RECI       |
| SEP     | 0.35 | 0.22 | 0.17 | 0.21 | 0.30 | 0.35 | 0.78 | 0.37 | NWS1       |
| OCT     | 0.34 | 0.28 | 0.18 | 0.30 | 0.31 | 0.34 | 0.54 | 0.33 | NWS1       |
| NOV     | 0.41 | 0.35 | 0.31 | 0.42 | 0.34 | 0.36 | 0.57 | 0.37 | NWS1       |
| DEC     | 0.34 | 0.32 | 0.28 | 0.37 | 0.25 | 0.24 | 0.46 | 0.35 | CLS2       |
| OVERALL | 0.33 | 0.30 | 0.21 | 0.26 | 0.32 | 0.33 | 0.54 | 0.29 | NWS1       |

Table 4.2.8(d) Statistics of errors of rainfall-runoff models in simulation-mode, calculated for evaluation period October 1974 to September 1979, omitting Jan-Oct of 1976.

Statistic = PRMSE (proportional root mean square error)  
 Independent of units  
 Catchment = BLACKWATER

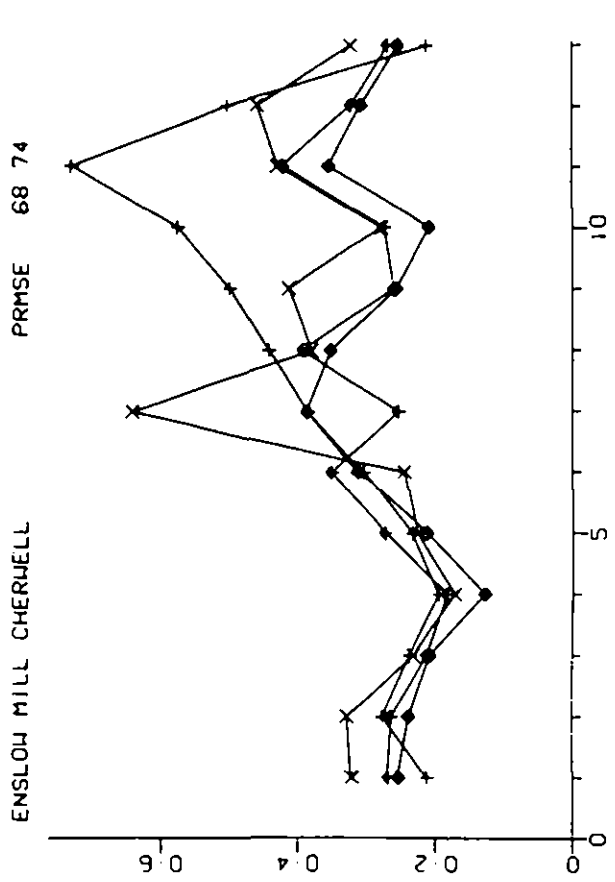
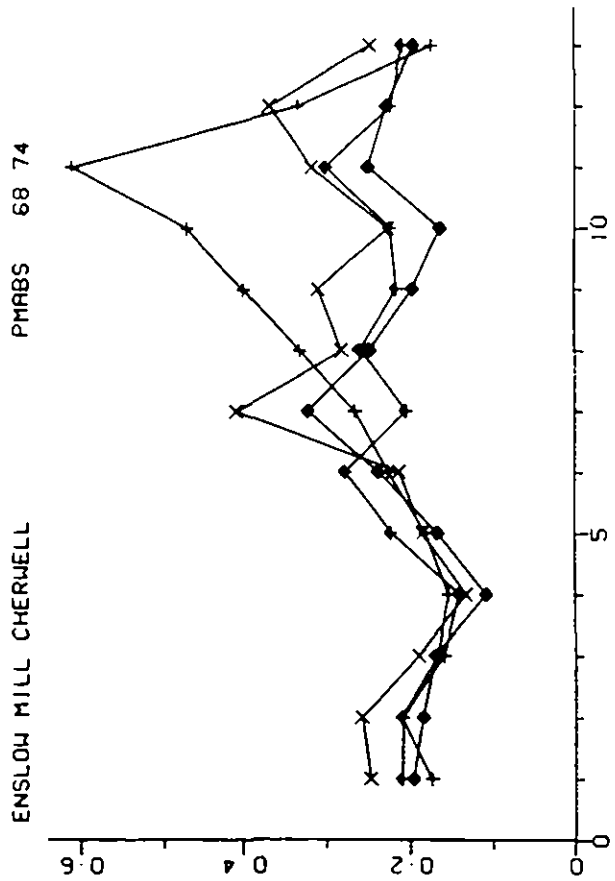
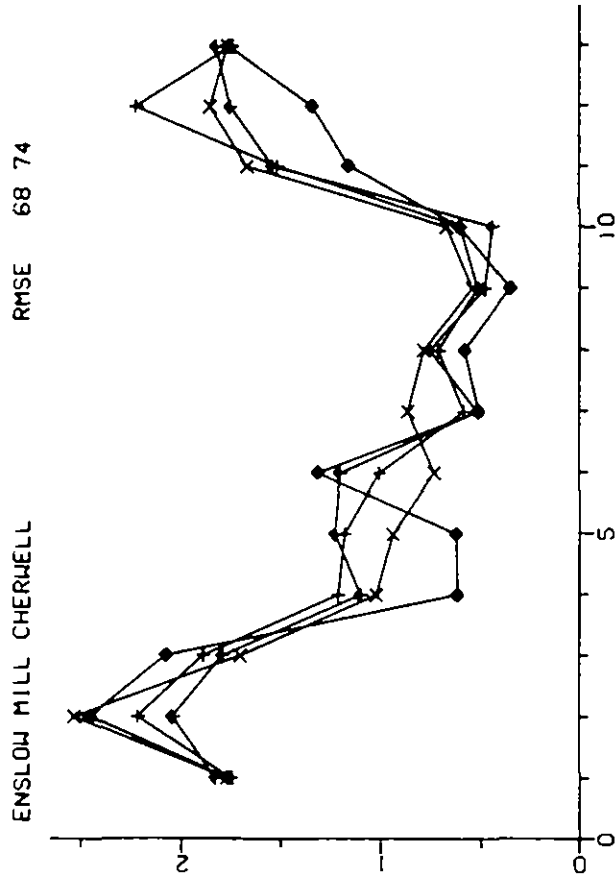
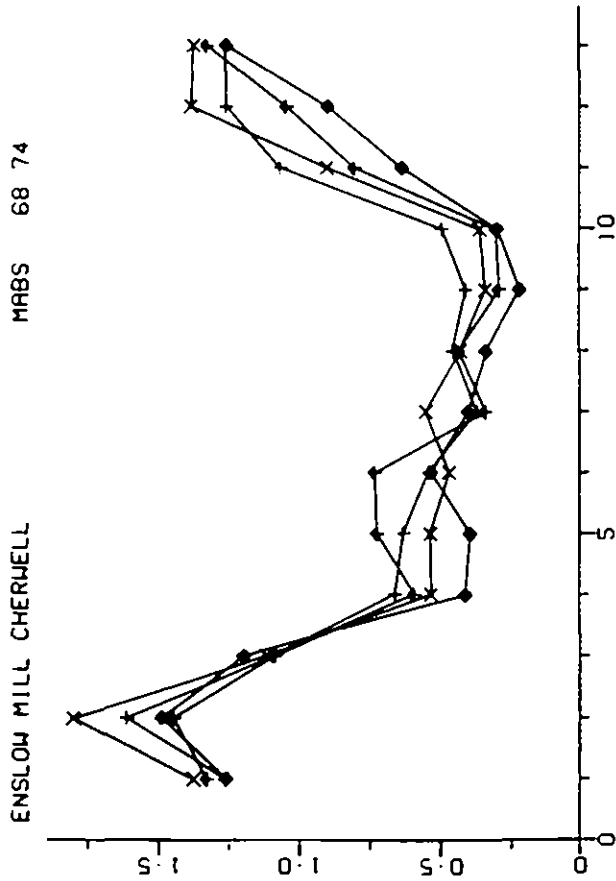
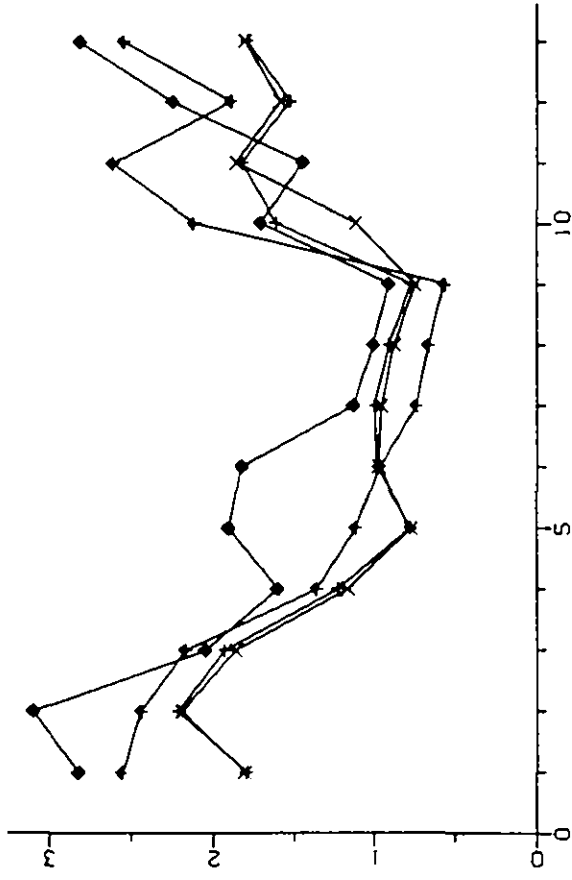


Figure 4.2.1(a). Error criteria for the Cherwell. Calibration period October 1968 to September 1974.

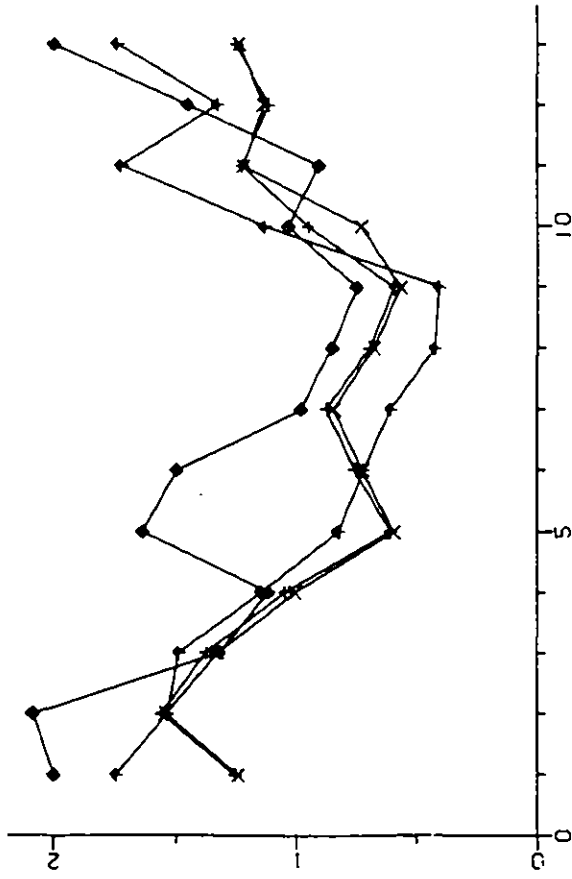
Months: 1 and 13 = Jan, 2 = Feb, etc.

Models: + = PDM1, X = IICM, ◆ = NWS1, † = TWM1

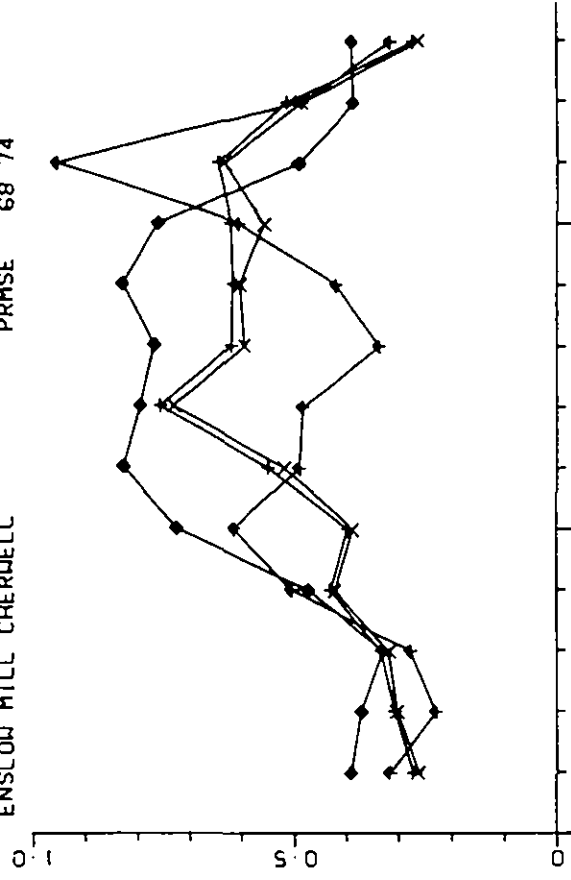
ENSLOW MILL CHERWELL RMSE 68 74



MABS 68 74



ENSLOW MILL CHERWELL PRMSE 68 74



PMABS 68 74

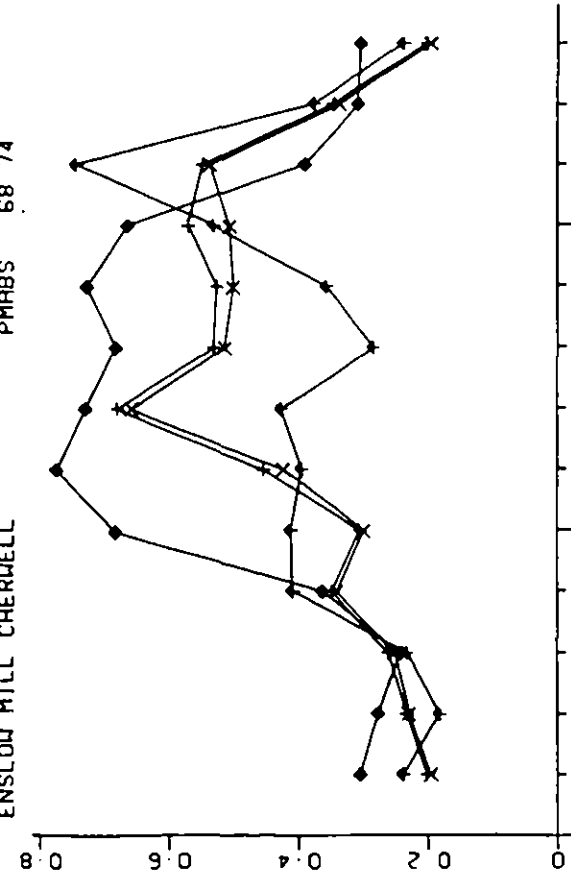


Figure 4.2.1(b). Error criteria for the Cherwell. Calibration period October 1968 to September 1974.

Months: 1 and 13 = Jan, 2 = Feb, etc.

Models: + = CLS1, -X = CLS2, ◆ = CLS3, ♣ = REC1

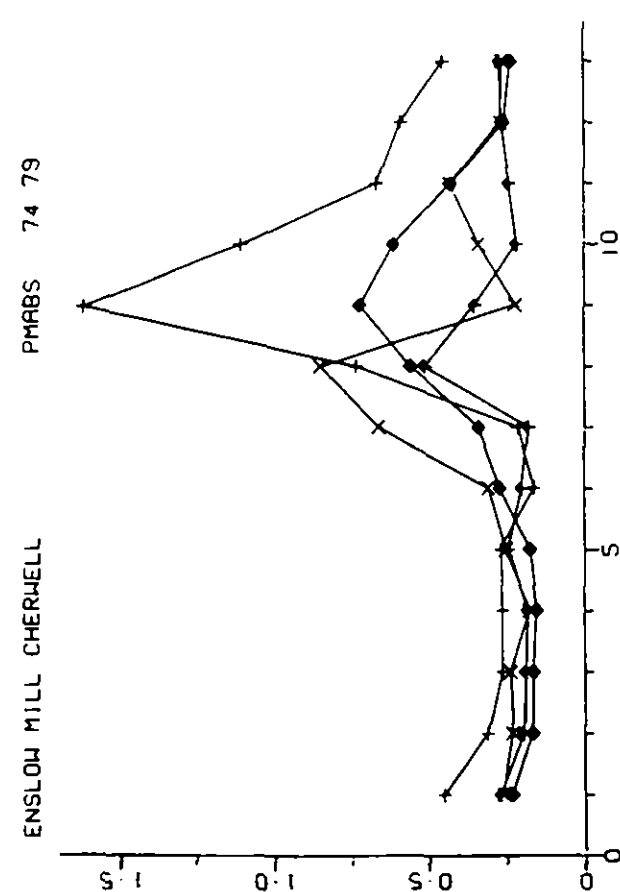
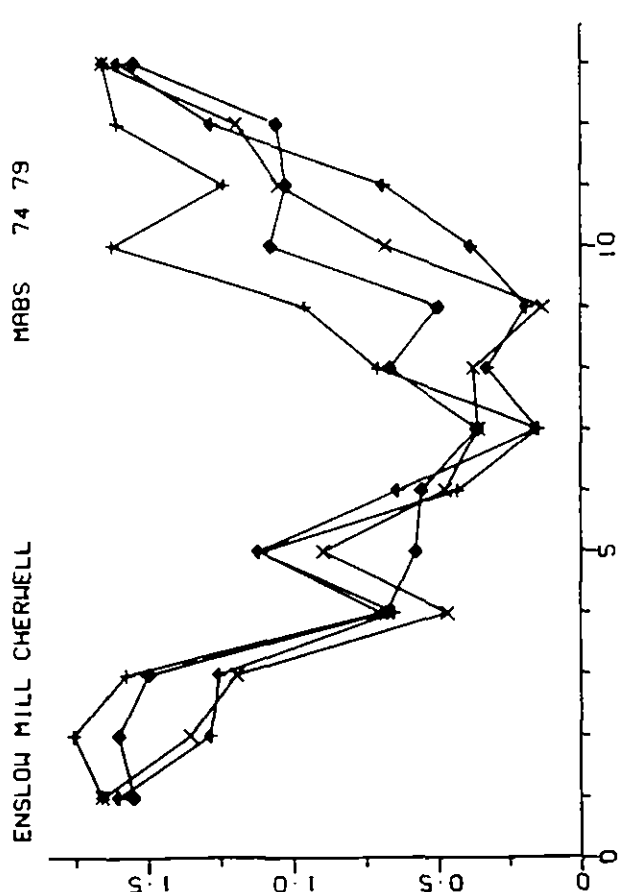
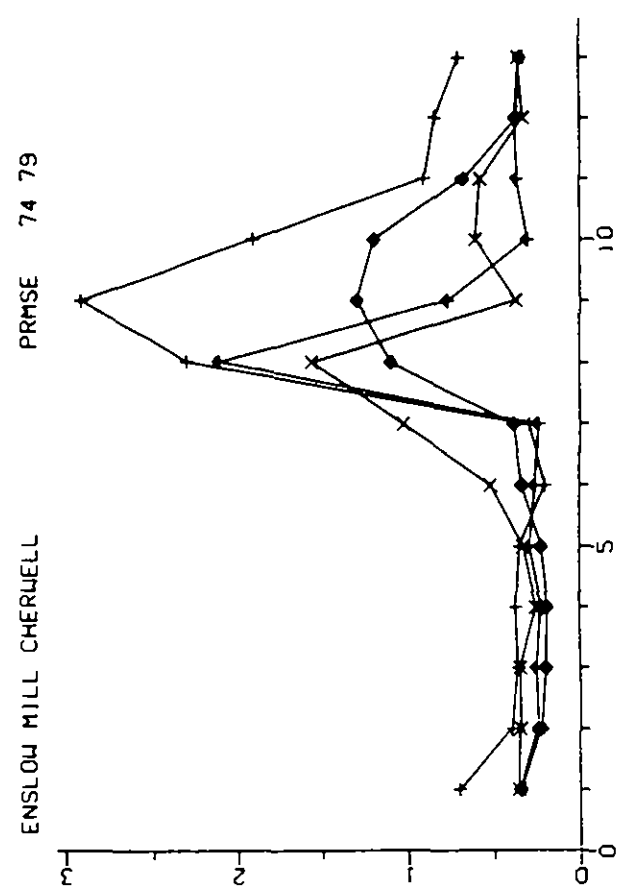
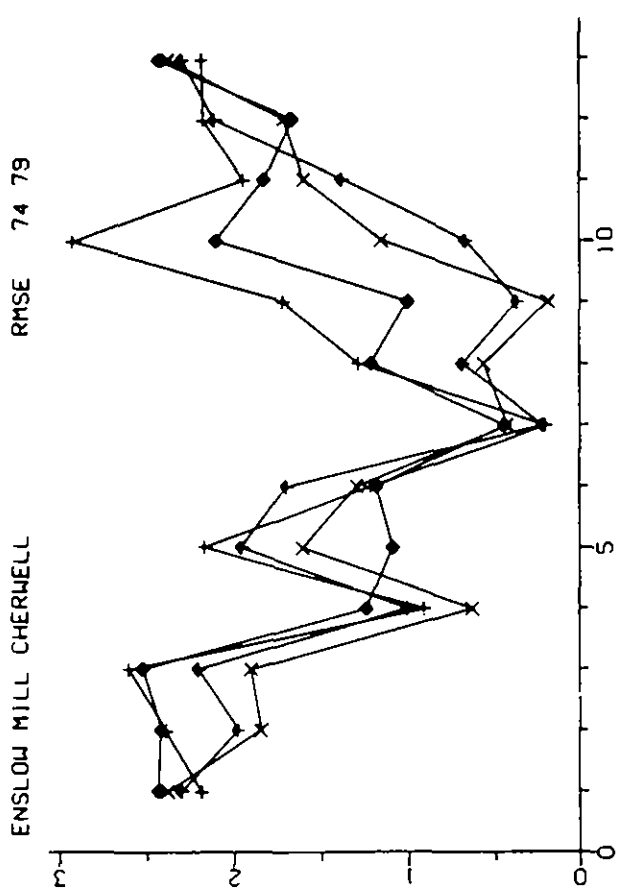


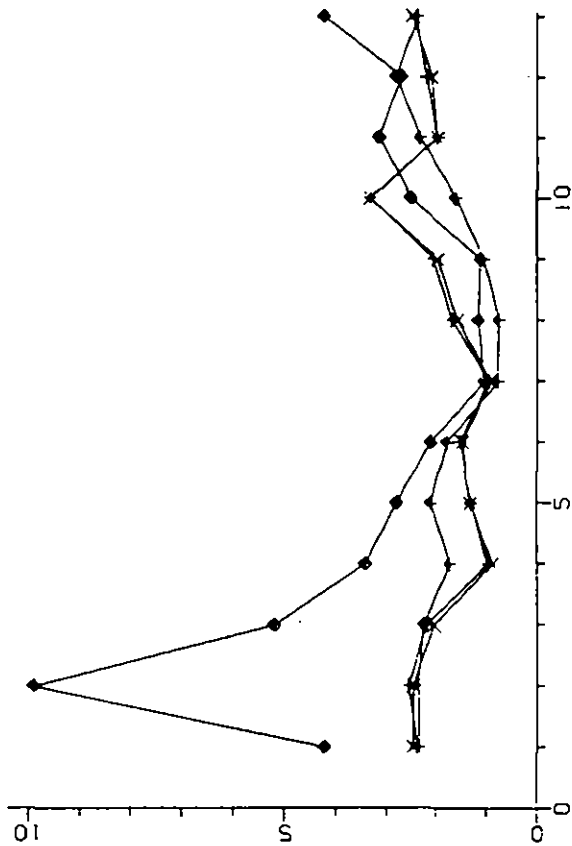
Figure 4.2.2(a). Error criteria for the Cherwell. Evaluation period October 1974 to September 1979.

Months: 1 and 13 = Jan, 2 = Feb, etc.

Models: + = PDM1, X = IHCM, ◆ = NWS1, † = TMM1

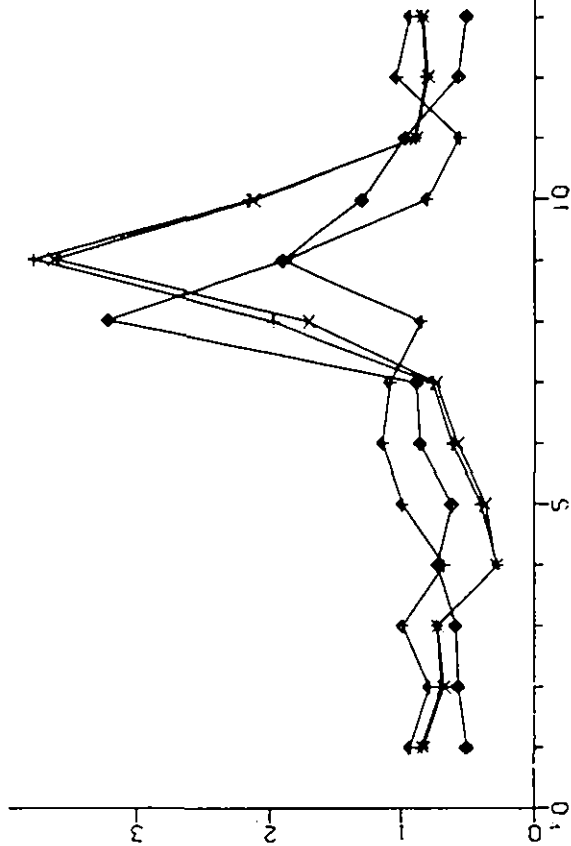
RMSE 74 79

ENSLOW MILL CHERWELL



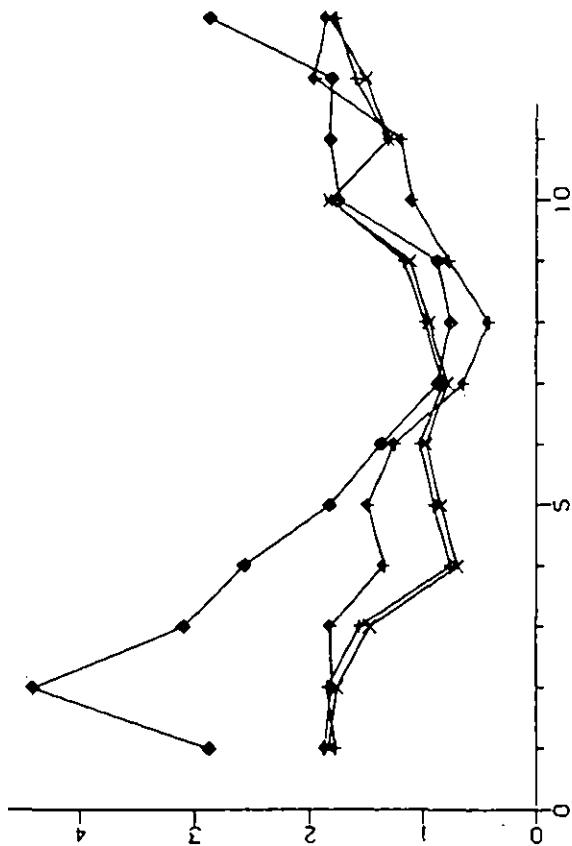
PRMSE 74 79

ENSLOW MILL CHERWELL



MABS 74 79

ENSLOW MILL CHERWELL



PMABS 74 79

ENSLOW MILL CHERWELL

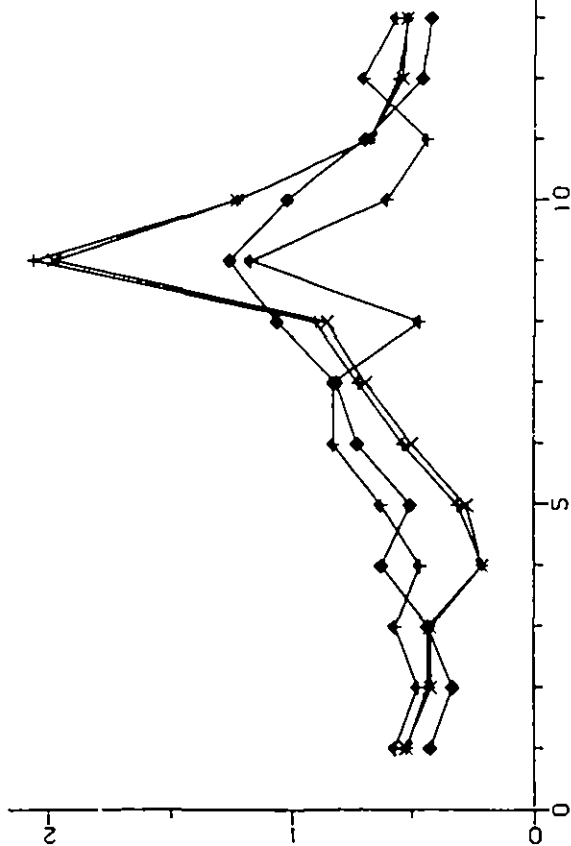


Figure 4.2.2(b). Error criteria for the Cherwell. Evaluation period October 1974 to September 1979.

Months: 1 and 13 = Jan, 2 = Feb, etc.

Models: + = CLS1, X = CLS2, ◆ = RECI

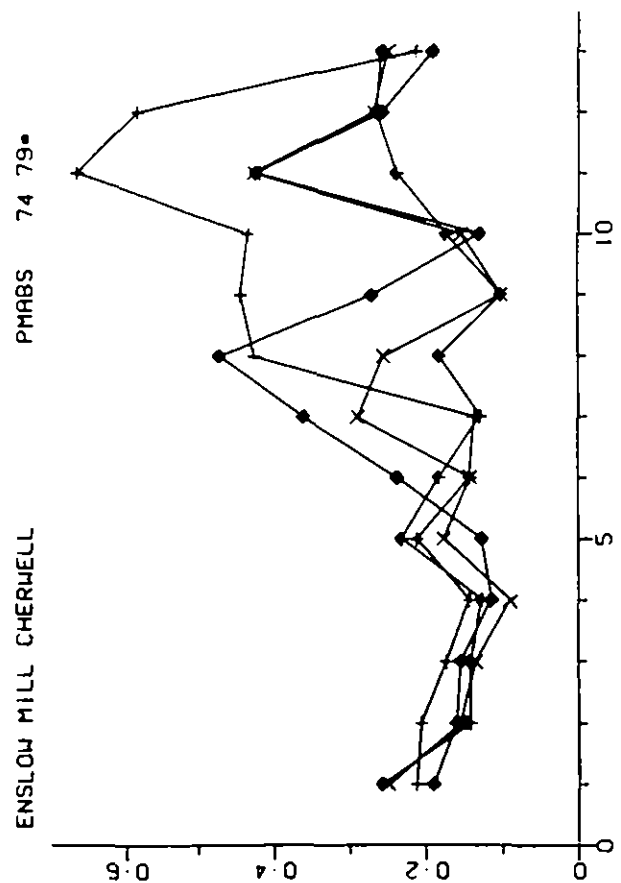
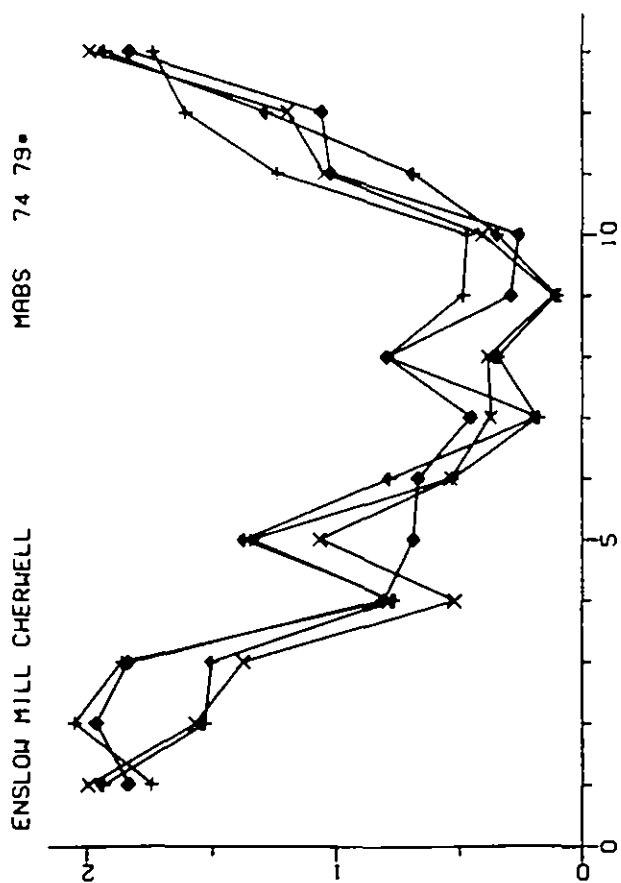
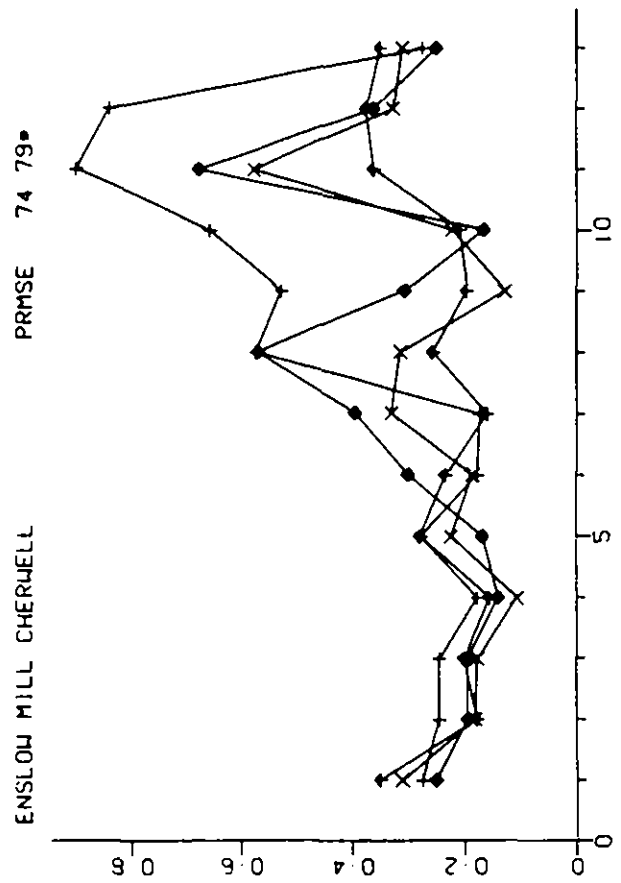
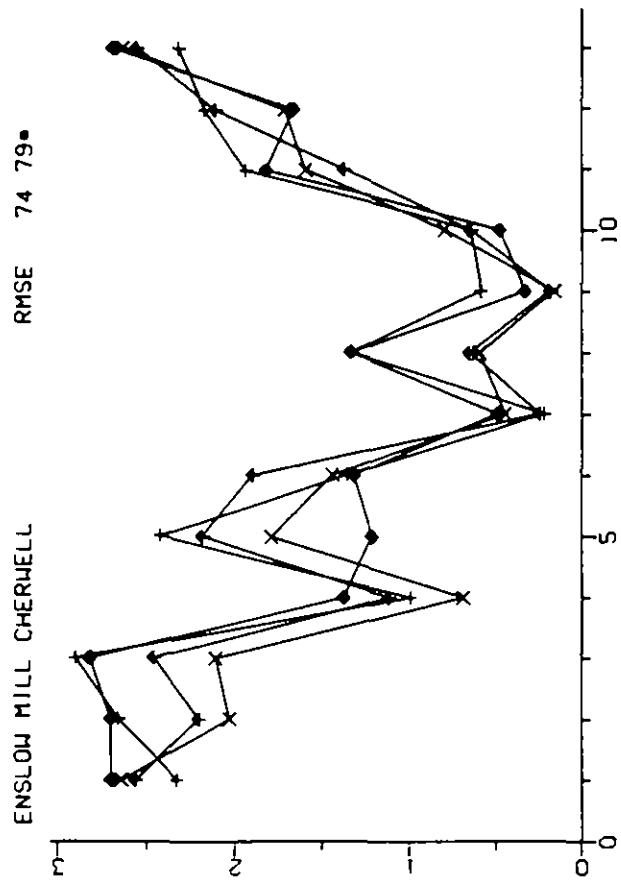


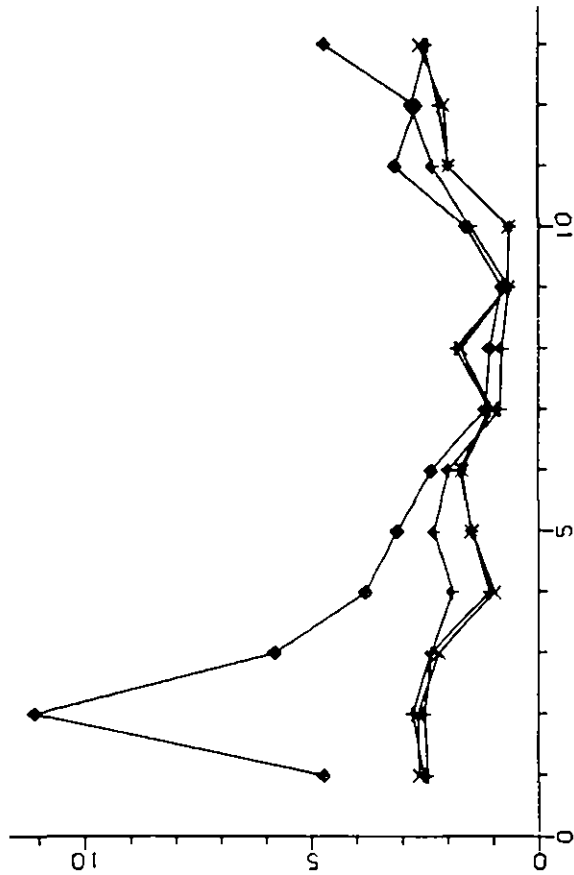
Figure 4.2.3(a). Error criteria for the Cherwell. Evaluation period October 1974 to September 1979, excluding Jan-Oct of 1976. Months: 1 and 13 = Jan, 2 = Feb, etc.

Models: + = PDM1, X = IHCM, ◆ = NWSI, ↑ = TWMI

MABS 74 79\*

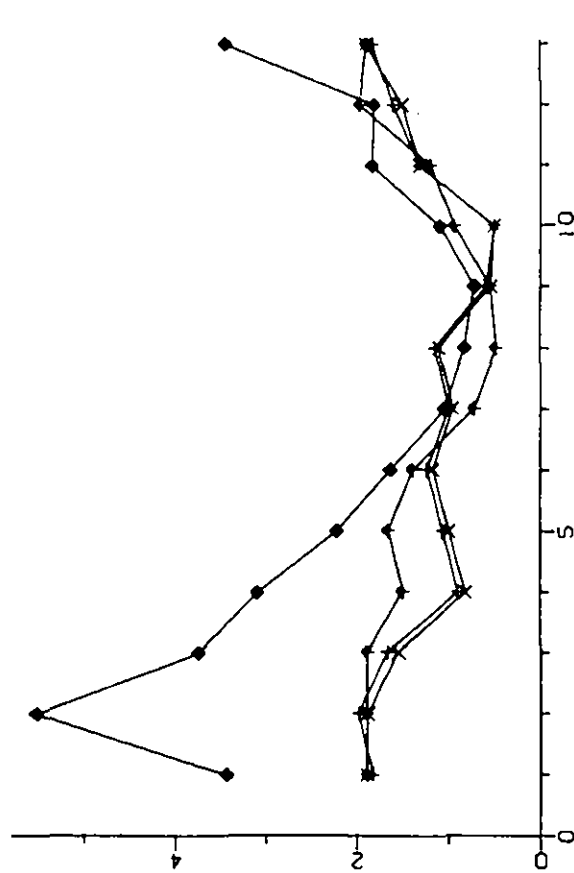
ENSLOW MILL CHERWELL

RMSE 74 79\*



ENSLOW MILL CHERWELL

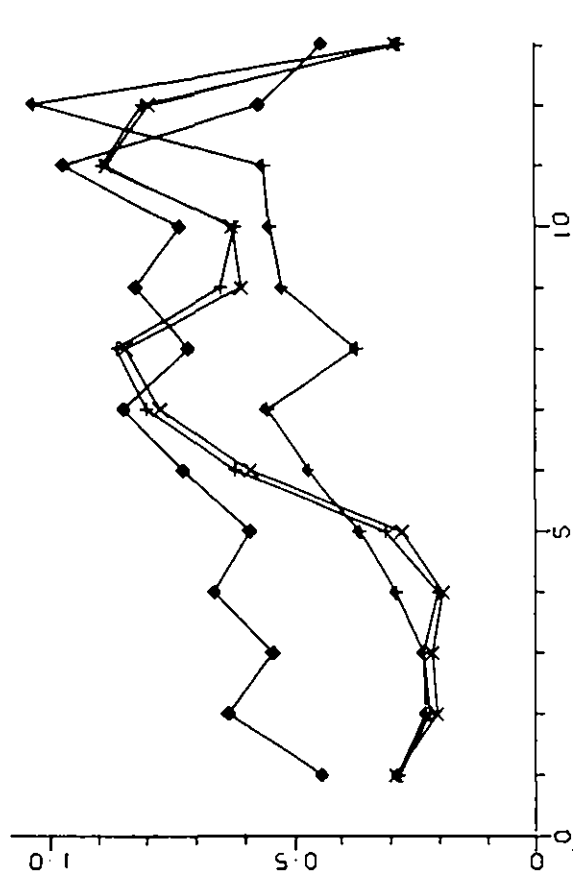
MABS 74 79\*



PMABS 74 79\*

ENSLOW MILL CHERWELL

PRMSE 74 79\*



ENSLOW MILL CHERWELL

PMABS 74 79\*

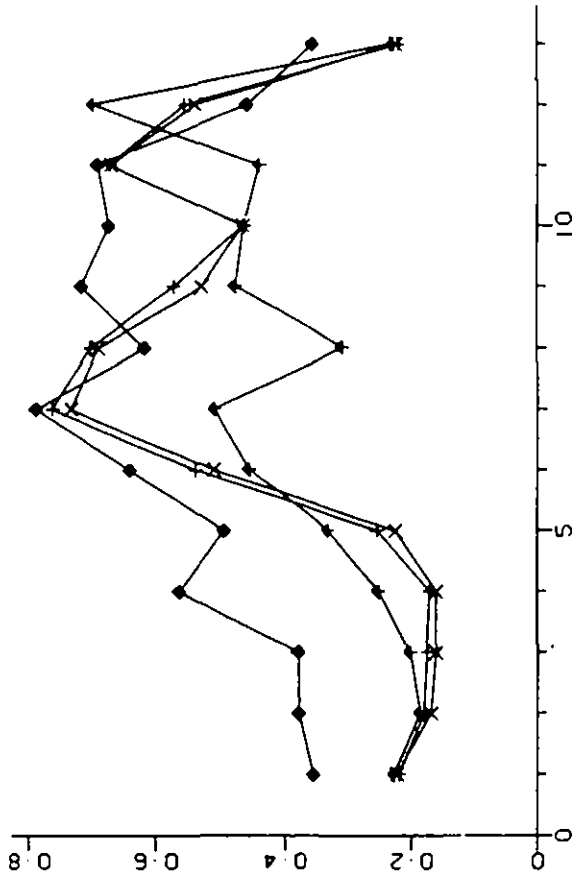
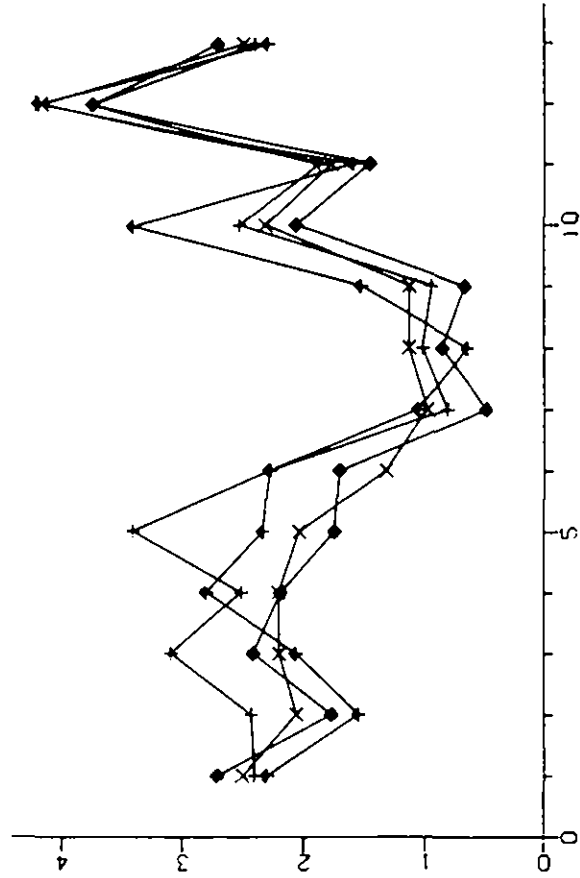


Figure 4.2.3(b). Error criteria for the Cherwell. Evaluation period October 1974 to September 1979, excluding Jan-Oct of 1976. Months: 1 and 13 = Jan, 2 = Feb, etc.

Models: + = CLS1, X = CLS2, ◆ = CLS3, ↑ = RECI

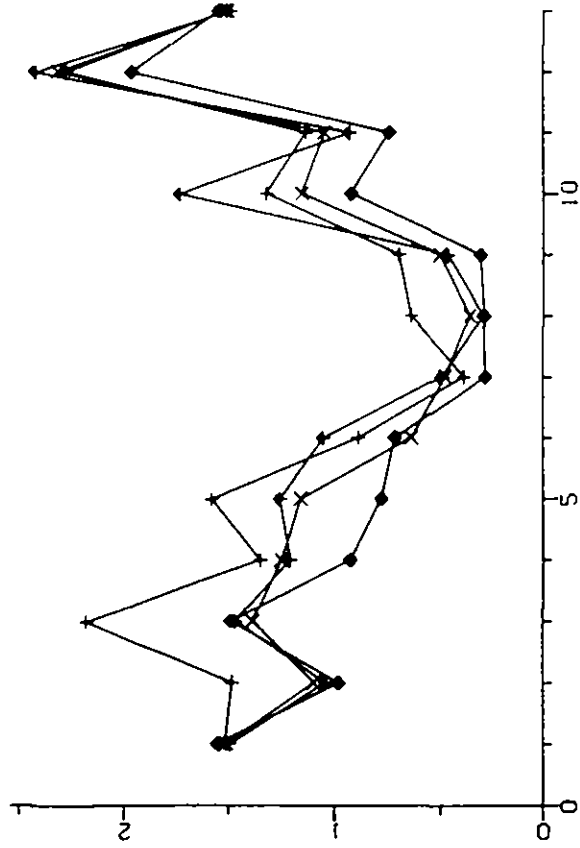
RMSE 78 83

CASTLE MILL MOLE



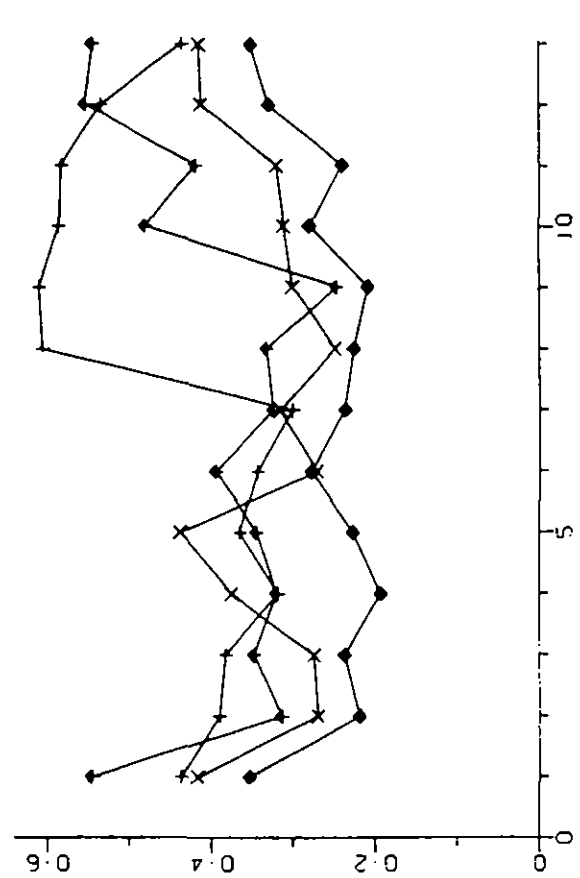
MABS 78 83

CASTLE MILL MOLE



PRMSE 78 83

CASTLE MILL MOLE



PMABS 78 83

CASTLE MILL MOLE

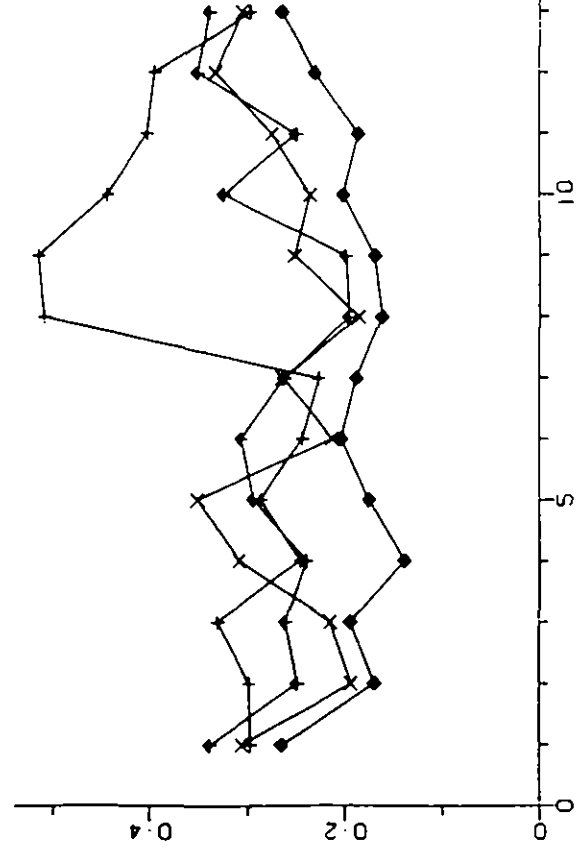


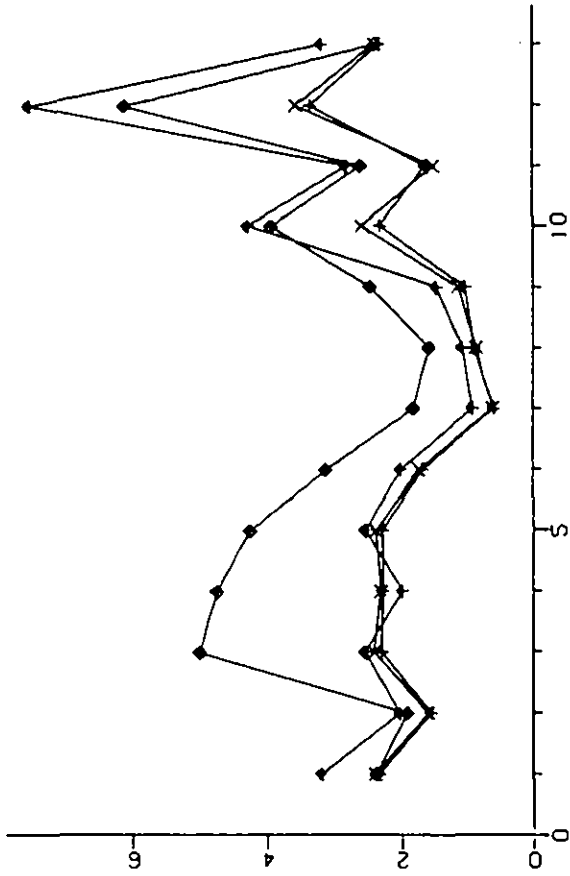
Figure 4.2.4(a). Error criteria for the Mole. Calibration period October 1978 to September 1983.

Months: 1 and 13 = Jan, 2 = Feb, etc.

Models: + = PDML, X = IHCM, ◆ = NWS1, ◆ = TWMI

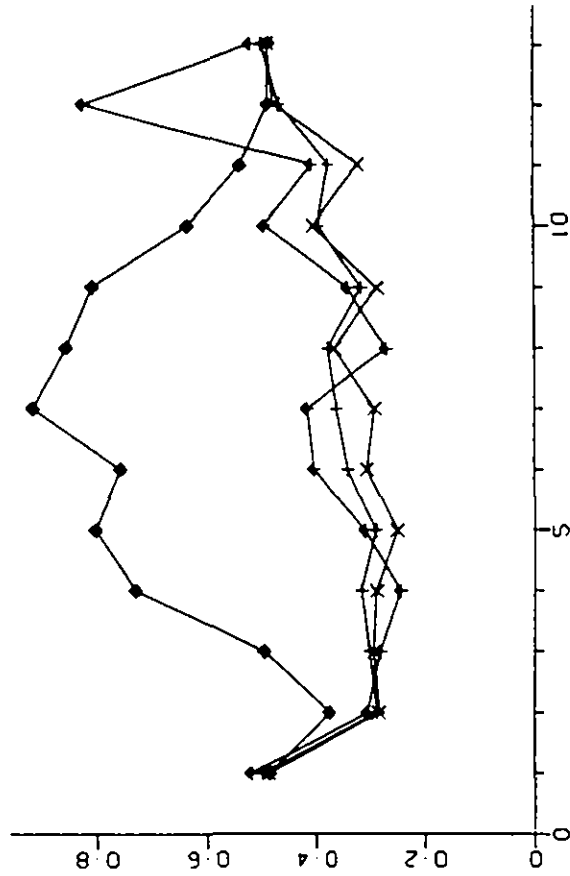
RMSE 78 83

CASTLE MILL MOLE



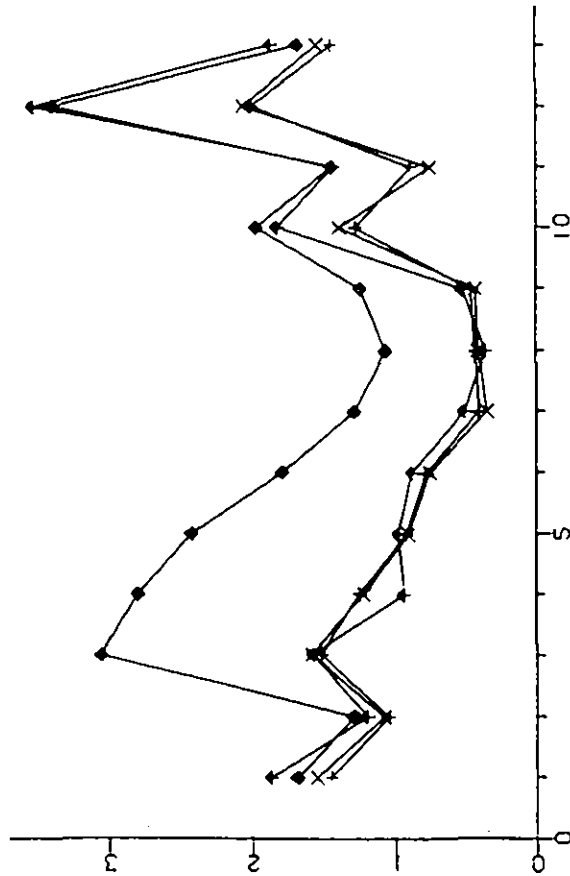
PRMSE 78 83

CASTLE MILL MOLE



MABS 78 83

CASTLE MILL MOLE



PMABS 78 83

CASTLE MILL MOLE

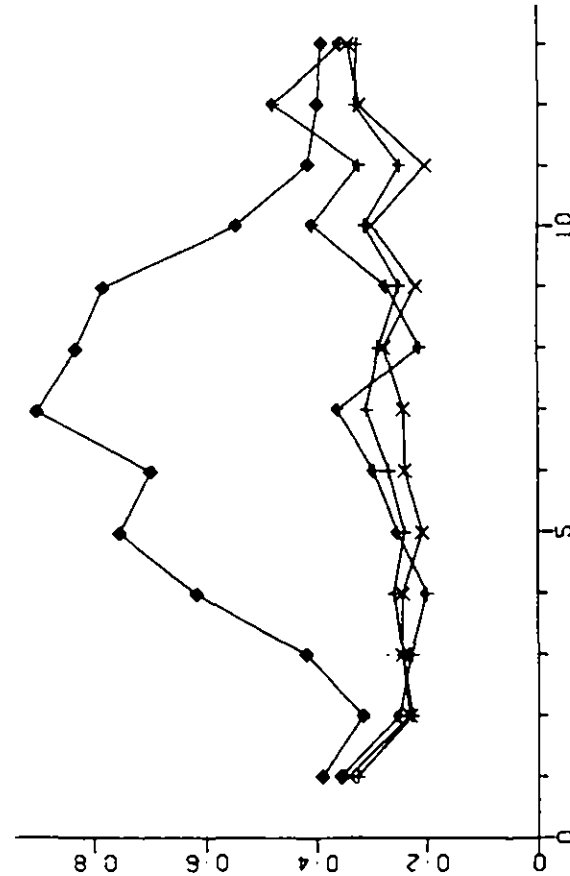


Figure 4.2.4(b). Error criteria for the Mole. Calibration period October 1978 to September 1983.

Months: 1 and 13 = Jan, 2 = Feb, etc.

Models: + = CLS1, X = CLS2, ◆ = CLS3, ↗ = RECI

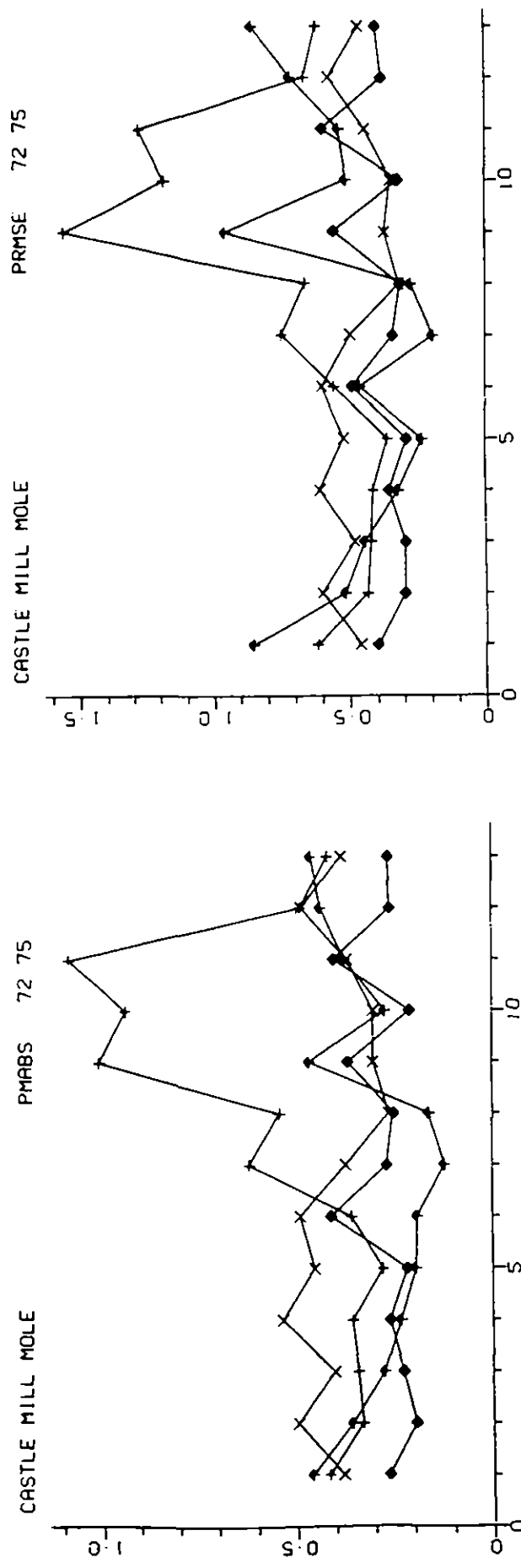
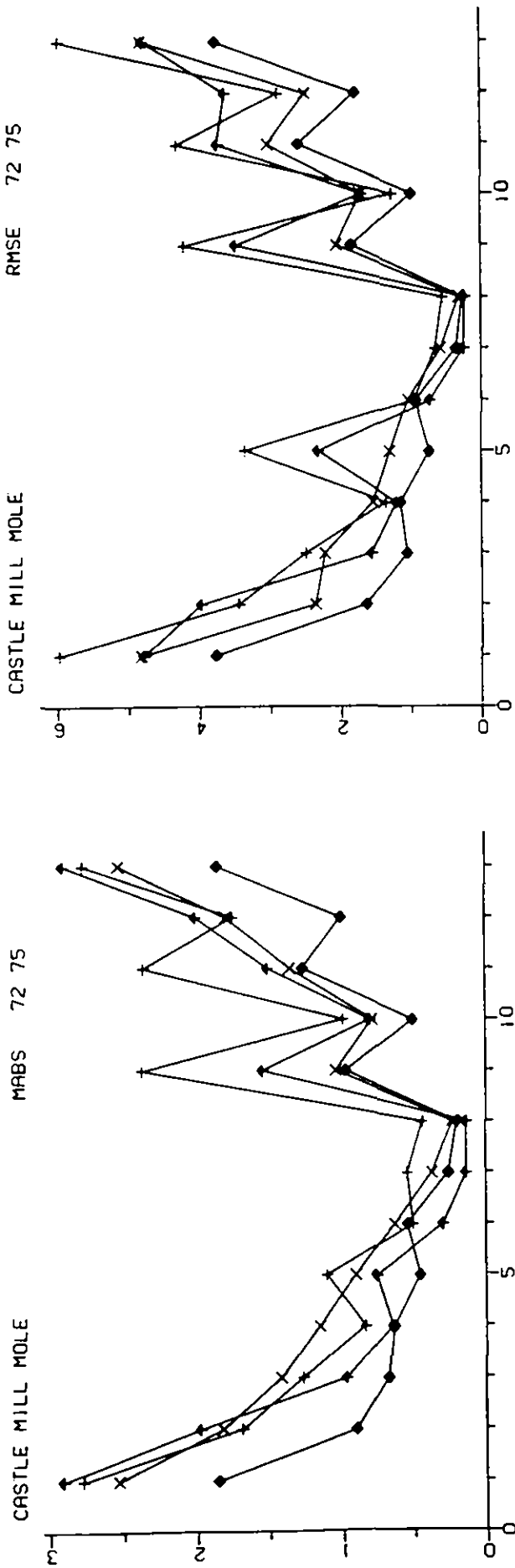


Figure 4.2.5(a). Error criteria for the Mole. Evaluation period October 1972 to September 1975.

Months: 1 and 13 = Jan, 2 = Feb, etc.  
 Models: + = PDM1, X = IHCM, ◆ = NWS1, † = TWMI

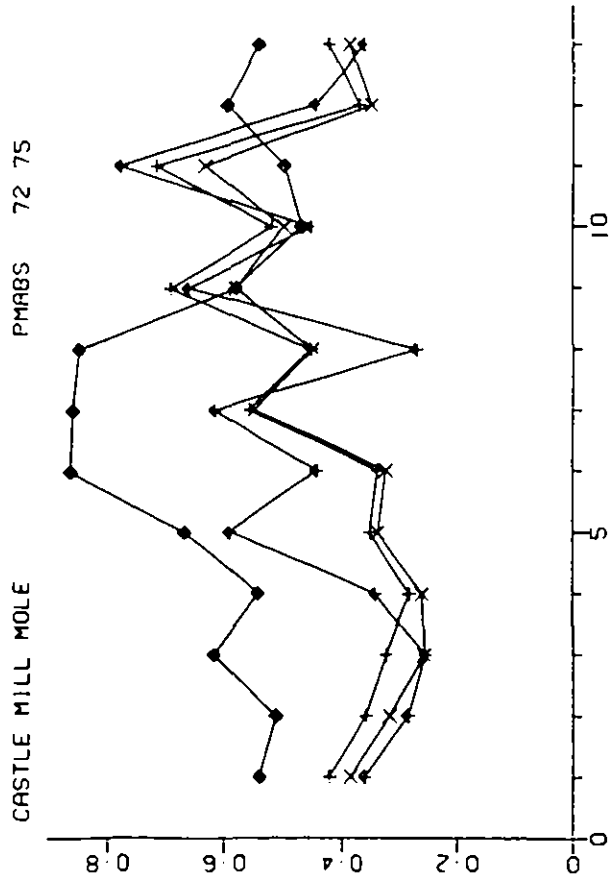
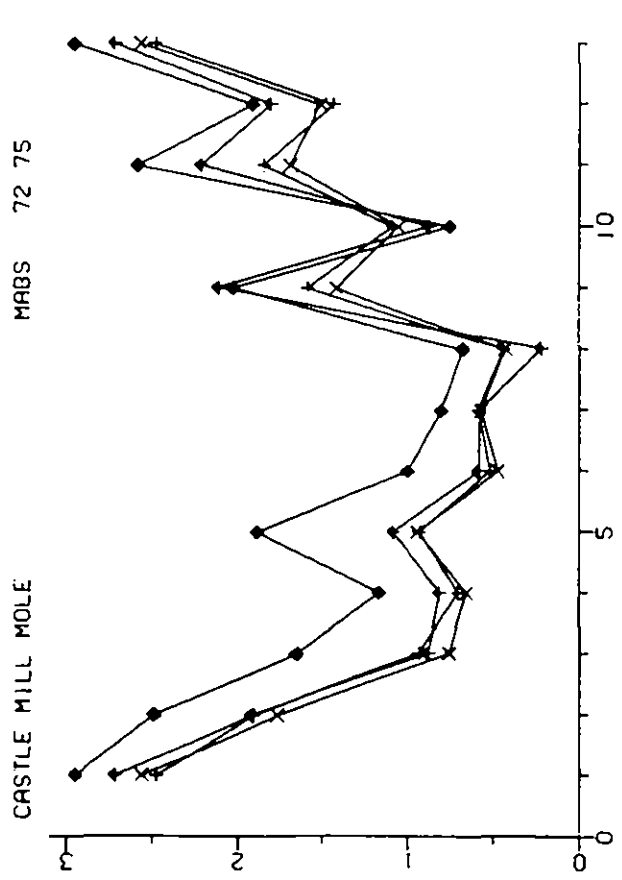
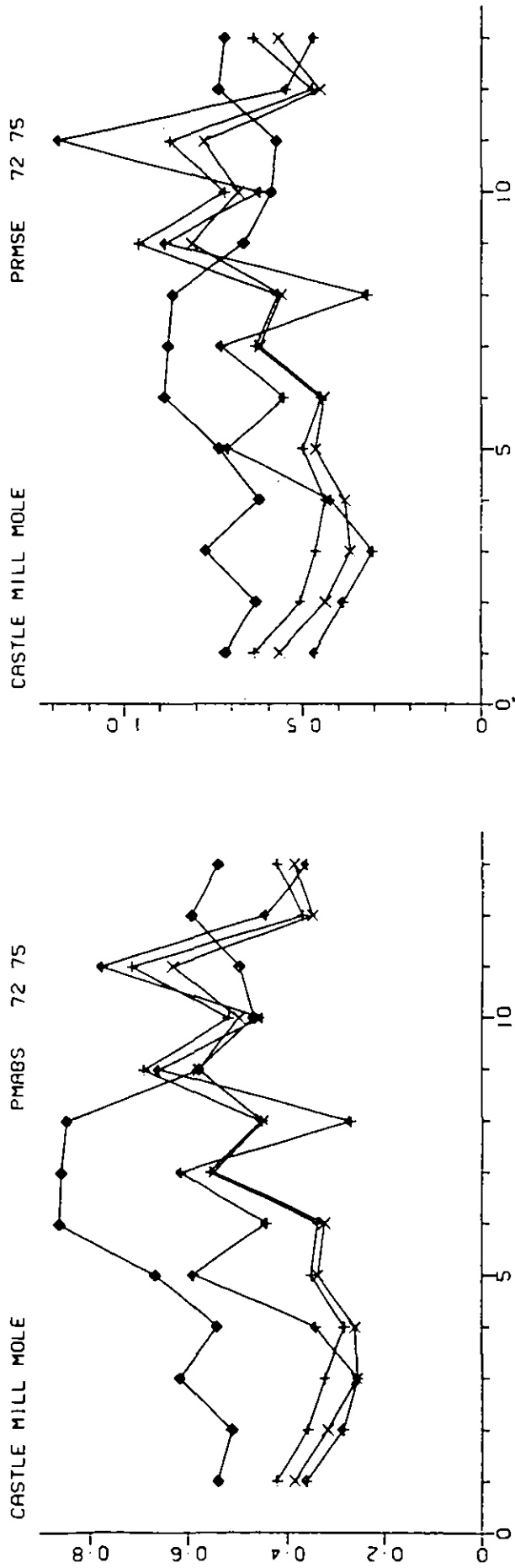
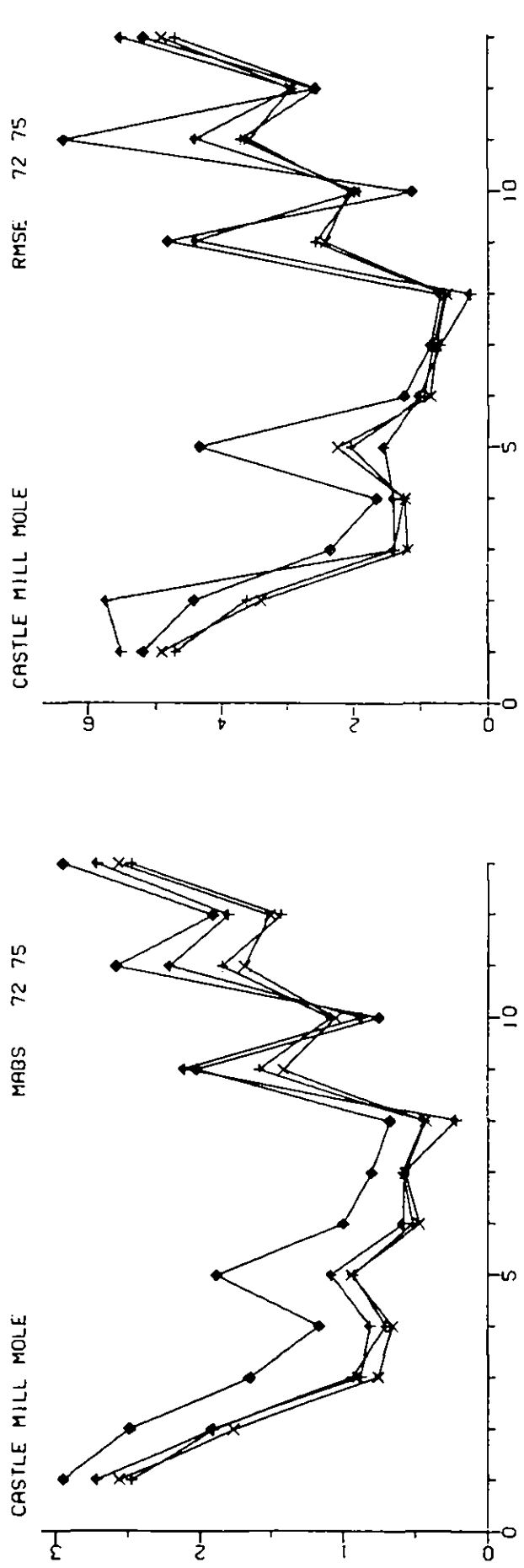


Figure 4.2.5(b). Error criteria for the Mole. Evaluation period October 1972 to September 1975.

Months: 1 and 13 = Jan, 2 = Feb, etc.

Models: + = CLS1, X = CLS2, ◆ = CLS3, ↑ = RECI.

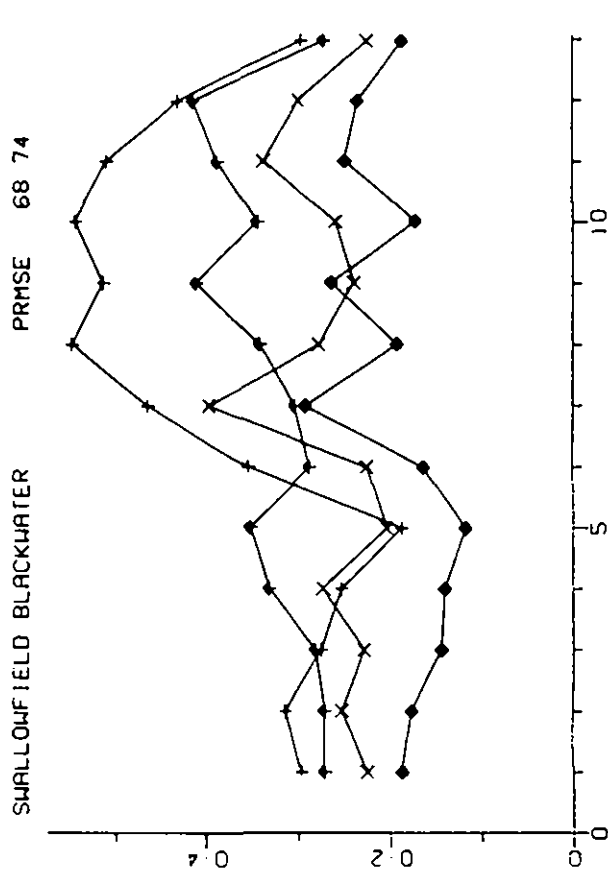
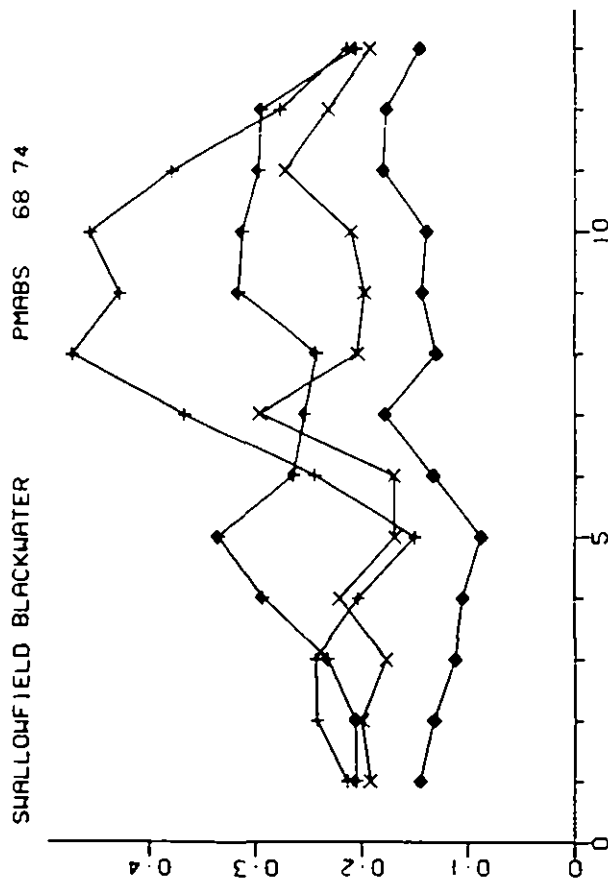
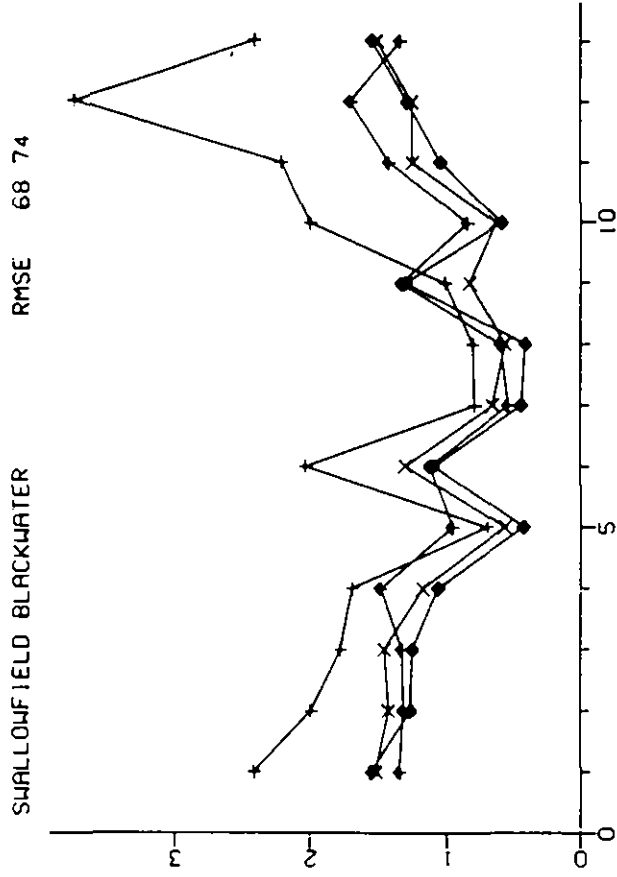
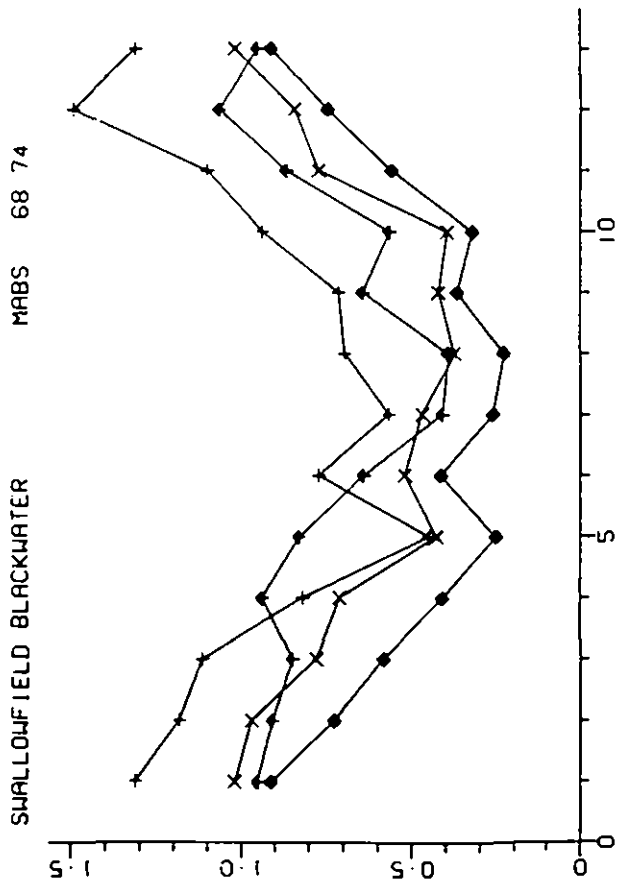


Figure 4.2.6(a). Error criteria for the Blackwater. Calibration period October 1968 to September 1974.

Months: 1 and 13 = Jan, 2 = Feb, etc.

Models: + = PDMI, X = IHCM, ◆ = NWSI, ◀ = TMMI

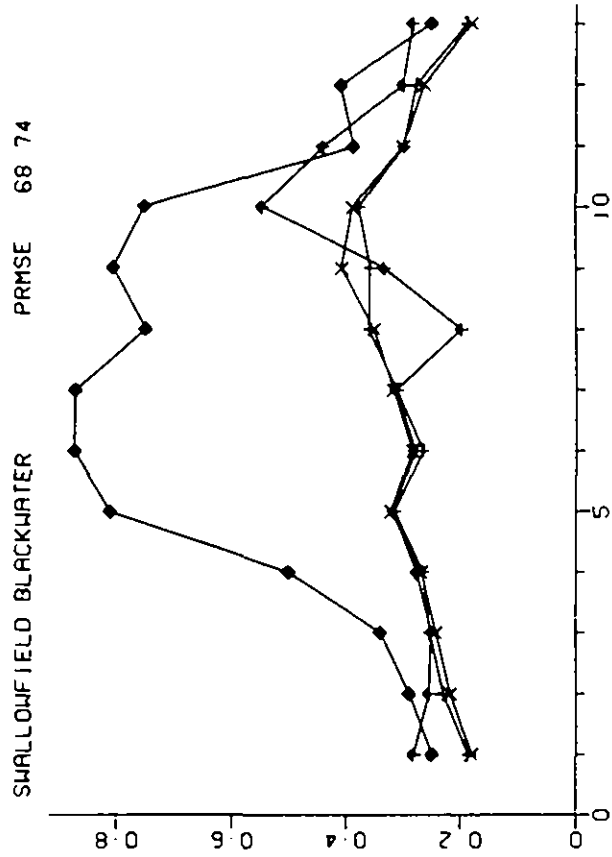
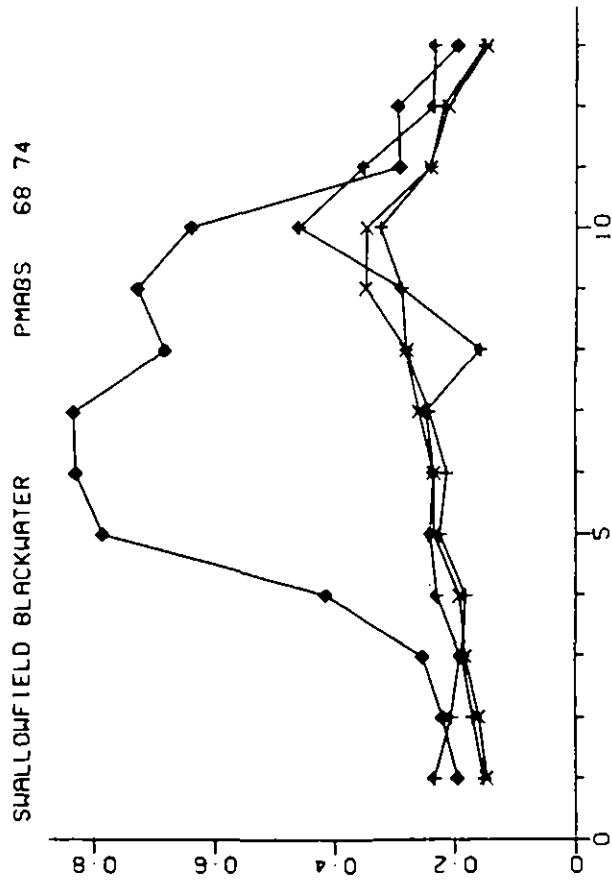
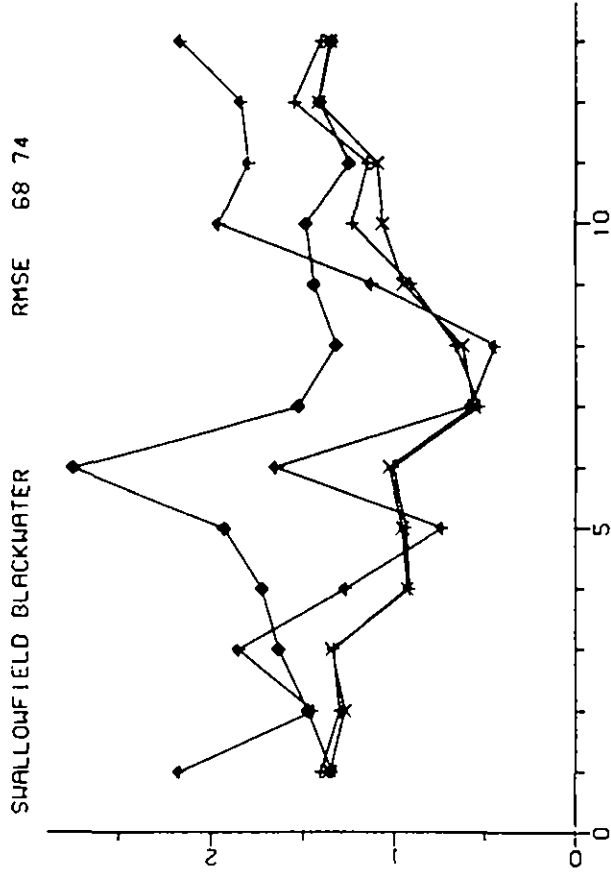
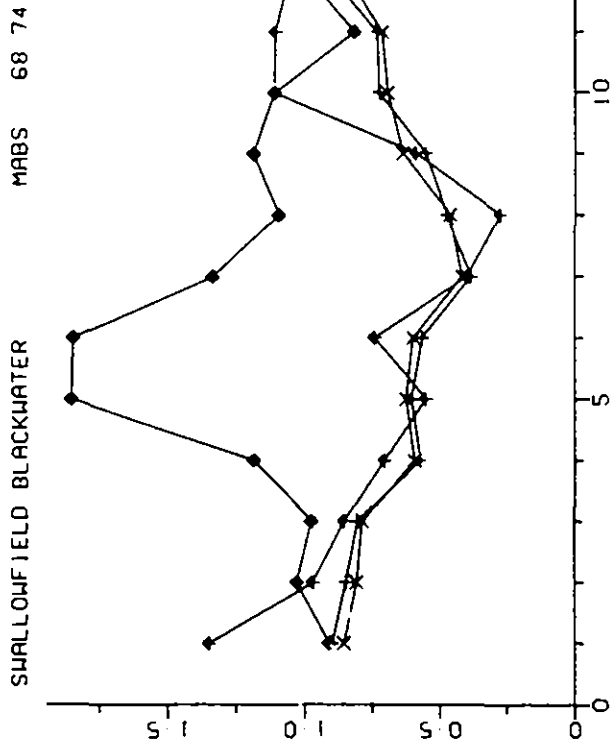


Figure 4.2.6(b). Error criteria for the Blackwater. Calibration period October 1968 to September 1974.

Months: 1 and 13=Jan, 2 = Feb, etc.

Models: + = CLS1, X = CLS2, ◆ = CLS3, ↑ = RECI

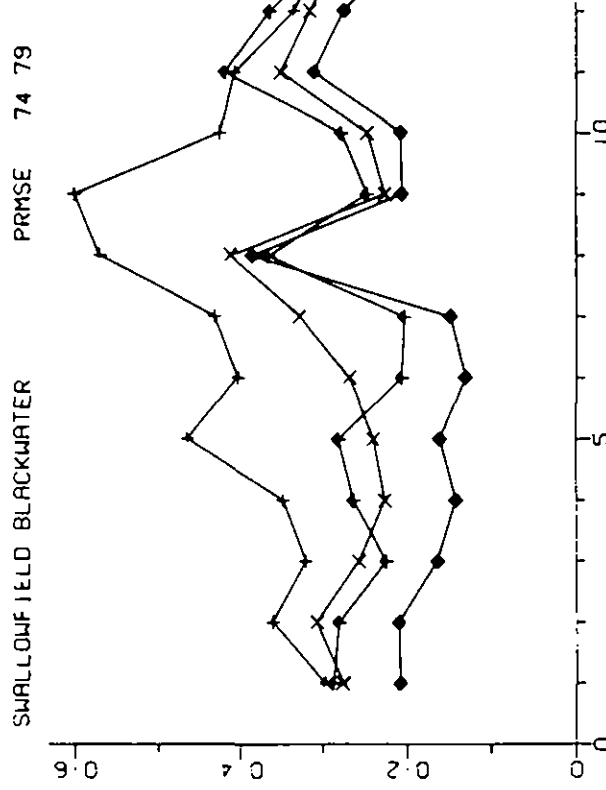
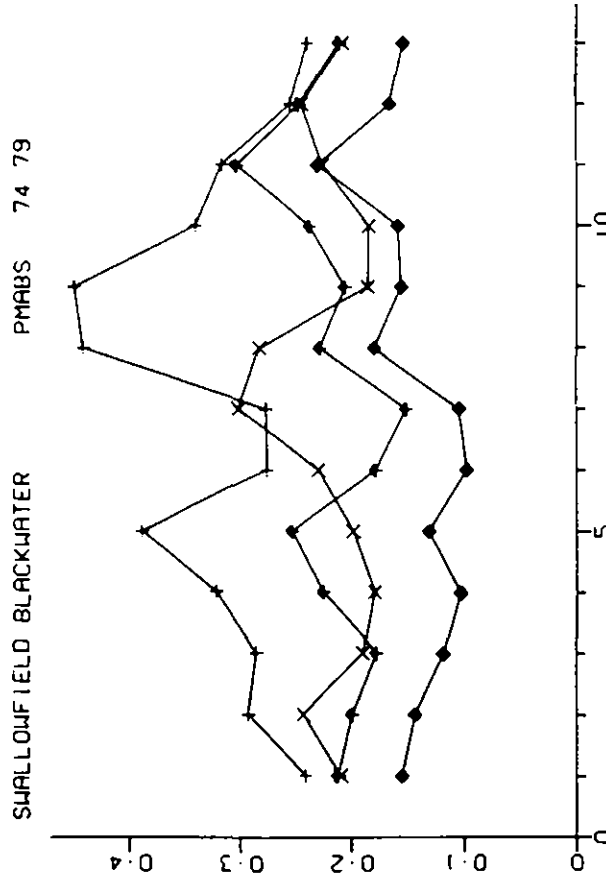
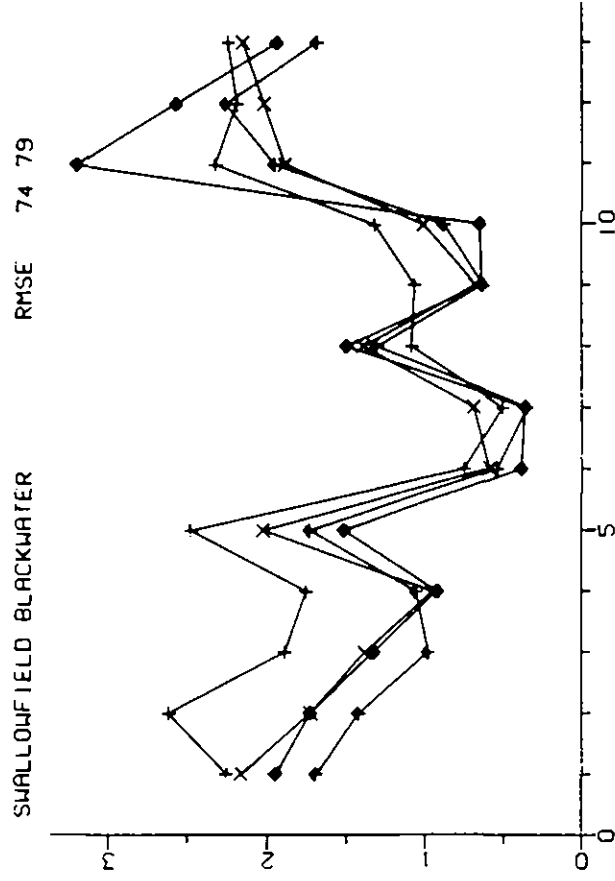
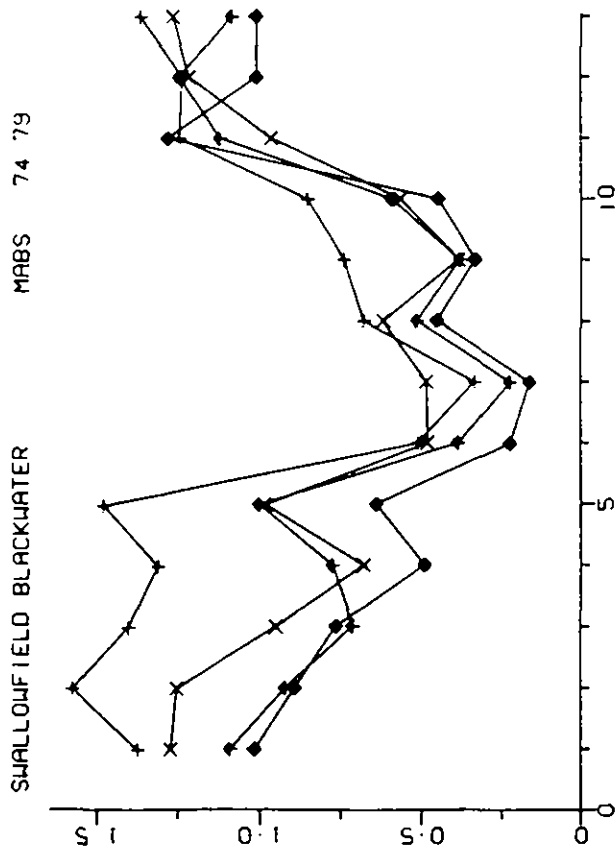
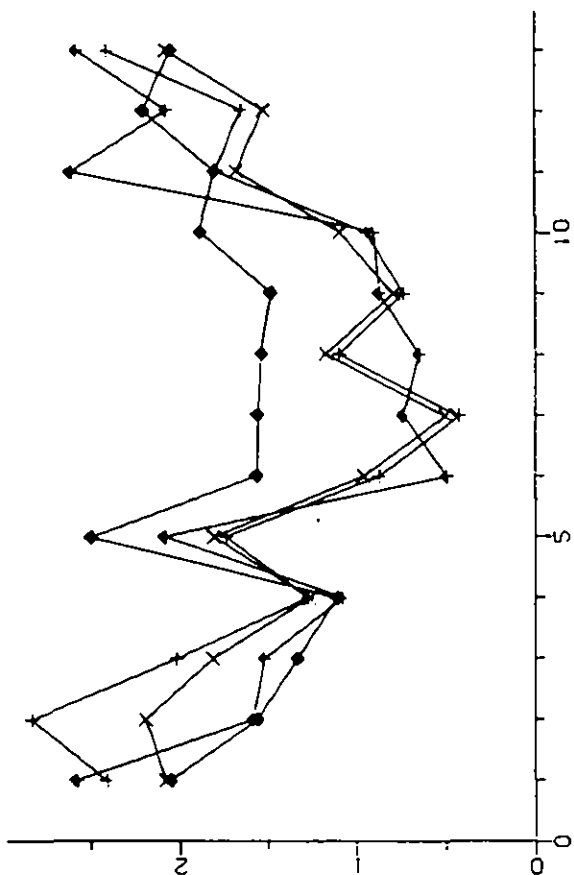
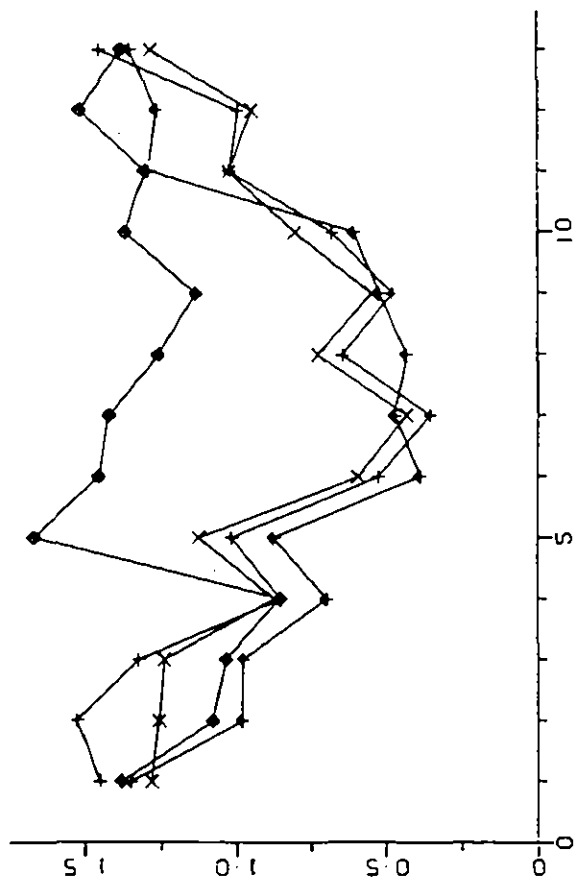


Figure 4.2.7(a). Error criteria for the Blackwater. Evaluation period October 1974 to September 1979.  
 Months: 1 and 13 = Jan, 2 = Feb, etc.  
 Models: + = PDMI, X = IHCM, ◆ = NWS1, ♣ = TWMI

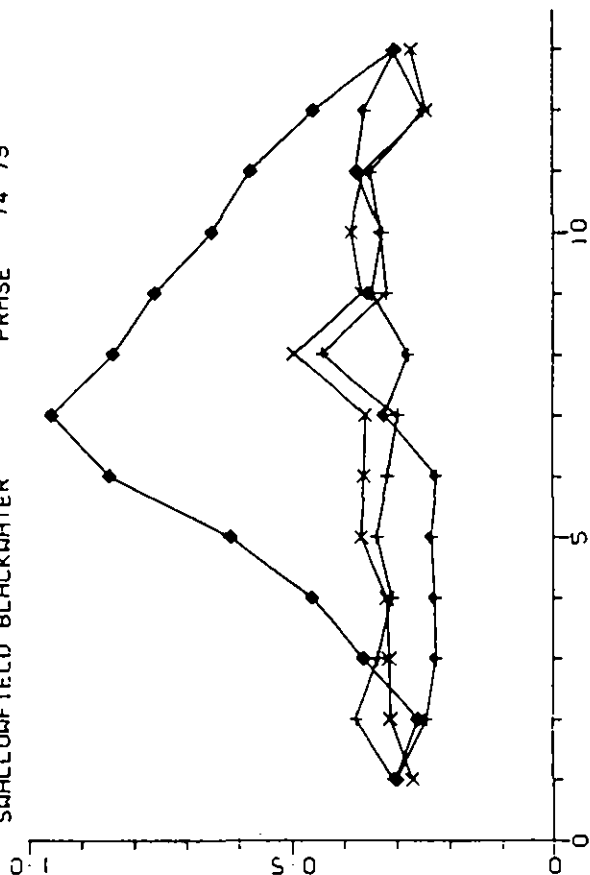
SWALLOWFIELD BLACKWATER RMSE 74 79



SWALLOWFIELD BLACKWATER MABS 74 79



SWALLOWFIELD BLACKWATER PRMSE 74 79



SWALLOWFIELD BLACKWATER PMABS 74 79

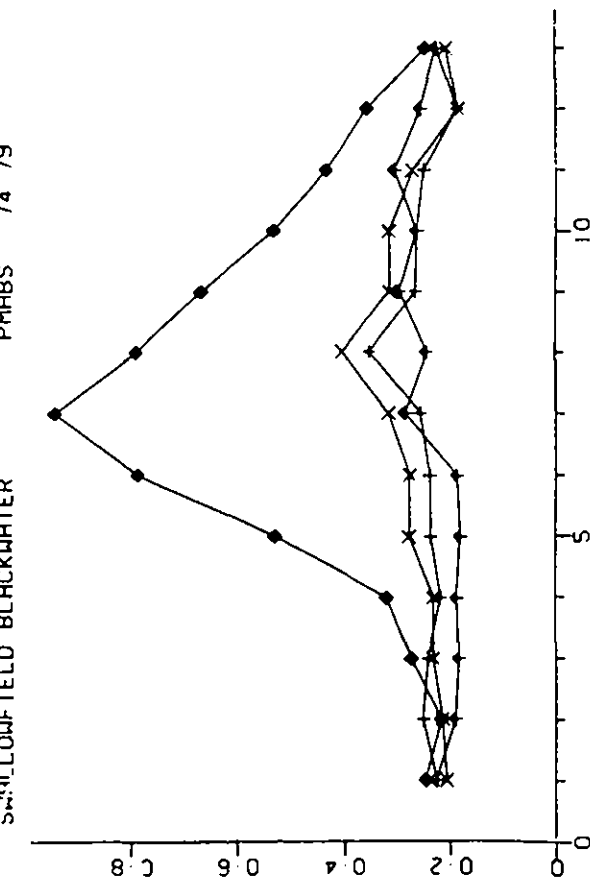


Figure 4.2.7(b). Error criteria for the Blackwater. Evaluation period October 1974 to September 1979.

Months: 1 and 13 = Jan, 2 = Feb, etc.

Models: + = CLS1, X = CLS2, ◆ = CLS3, ▲ = RECI

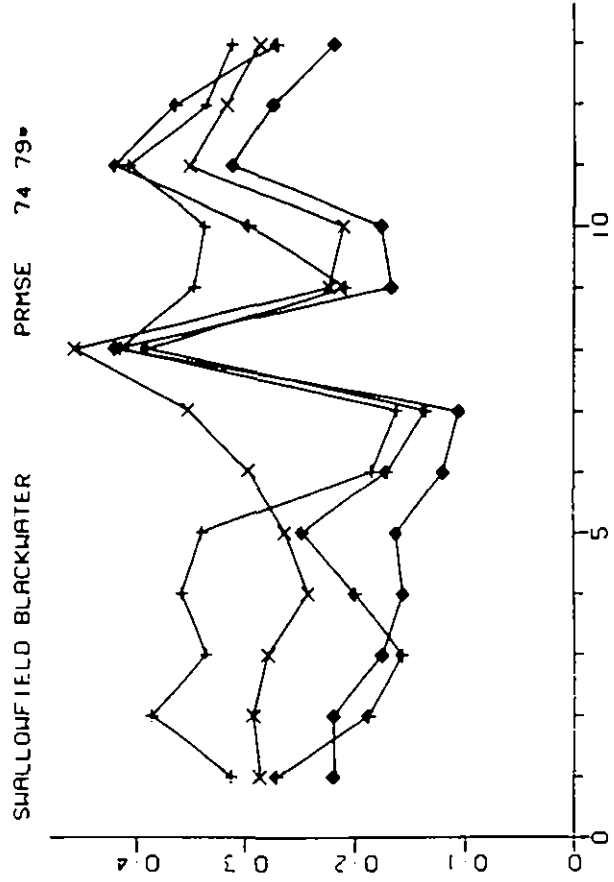
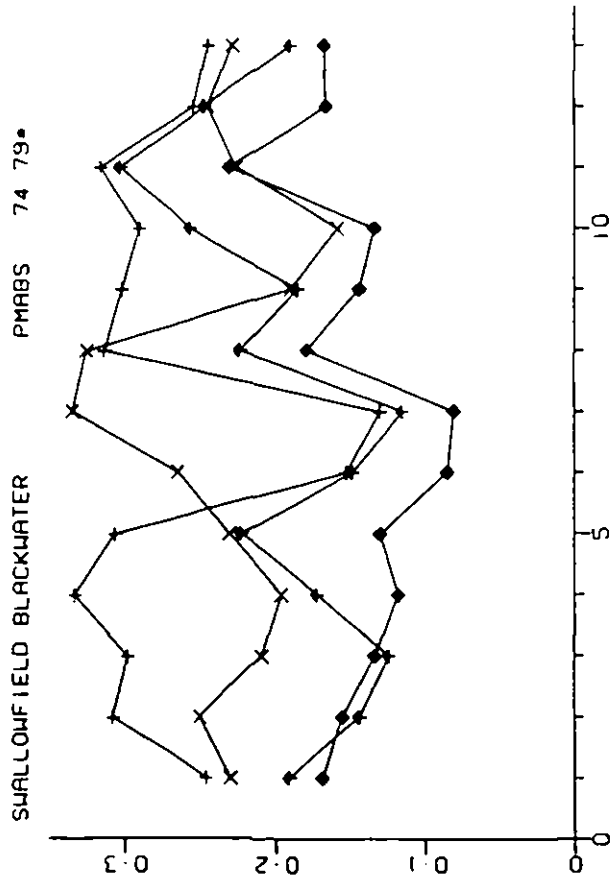
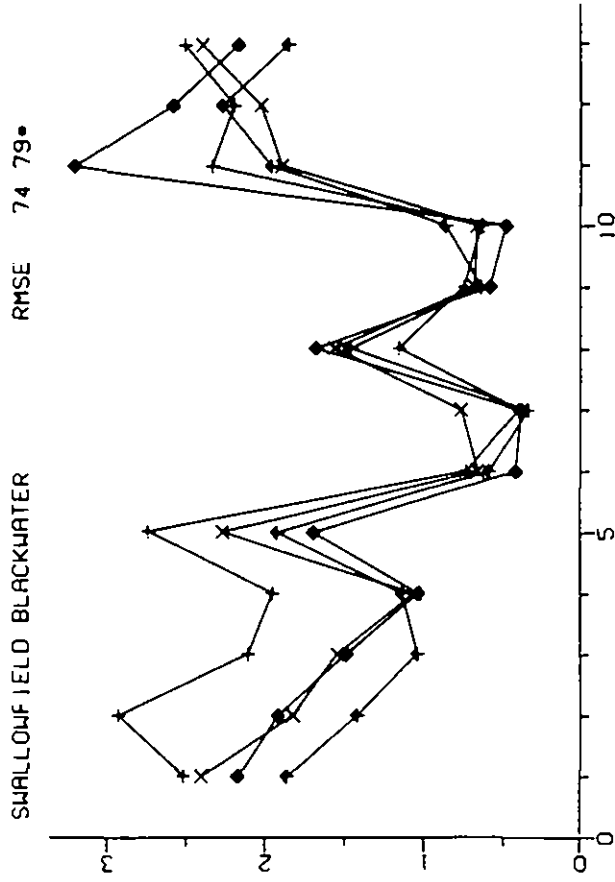
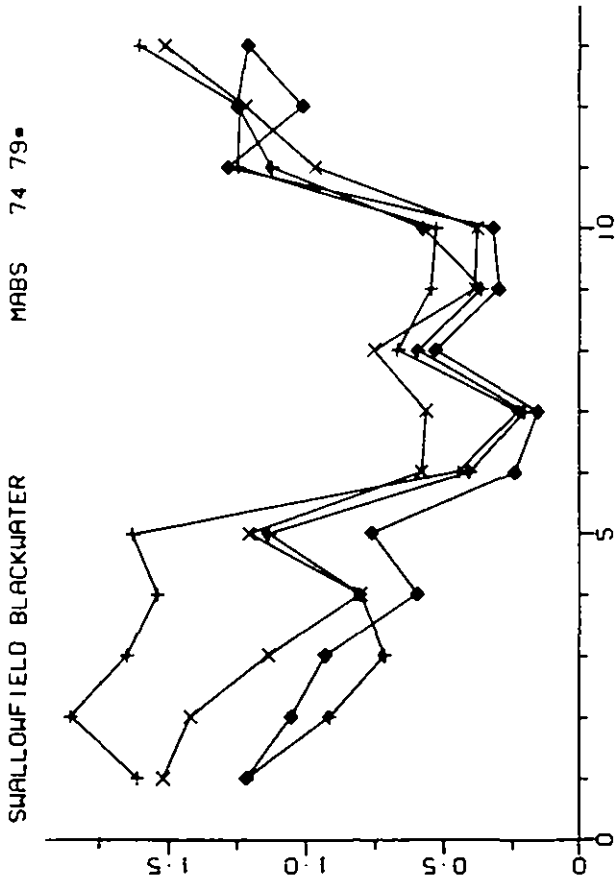


Figure 4.2.8(a). Error criteria for the Blackwater. Evaluation period October 1974 to September 1979, excluding Jan-Oct of 1976. Months: 1 and 13 = Jan, 2 = Feb, etc.

Models: + = PDM1, X = IHCM, ◆ = NMS1, † = TWM1

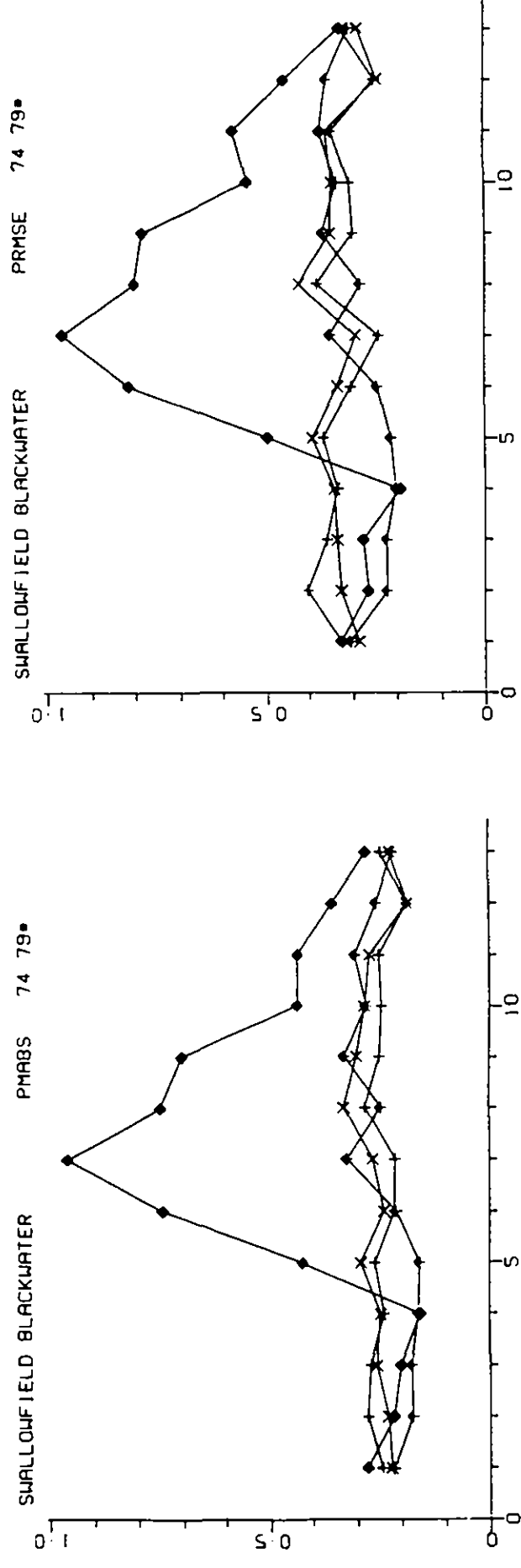
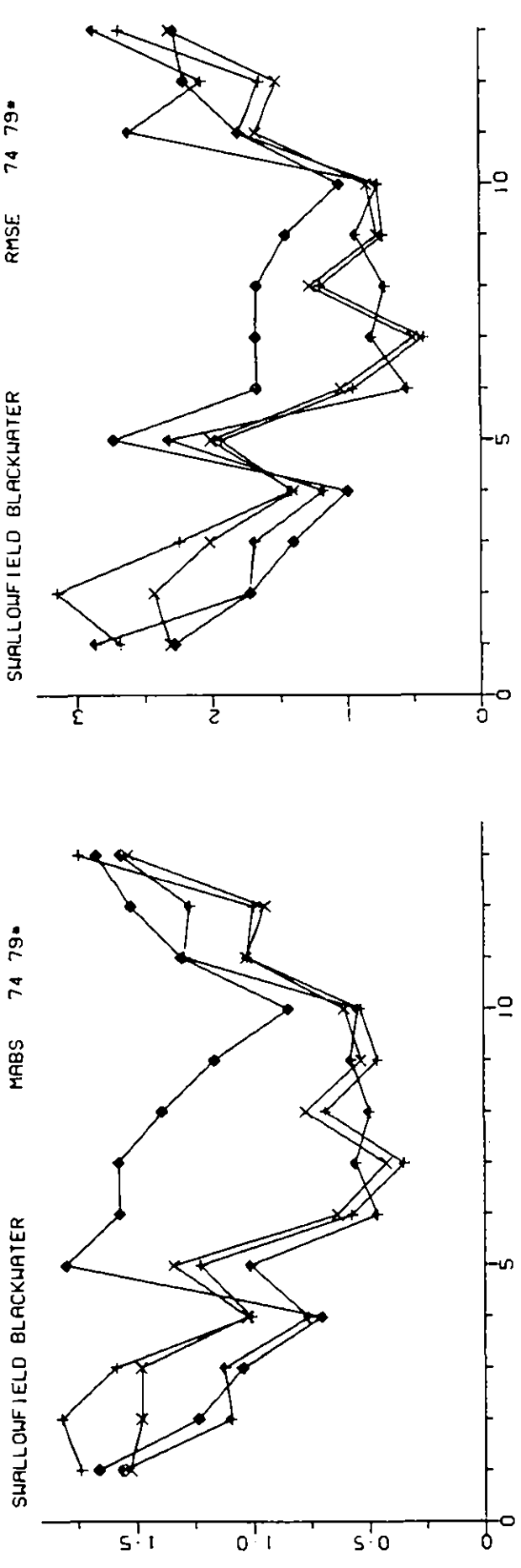


Figure 4.2.8(b). Error criteria for the Blackwater. Evaluation period October 1974 to September 1979, excluding Jan-Oct of 1976. Months: 1 and 13 = Jan, 2 = Feb, etc.  
 Models: + = CLS1, X = CLS2, ◆ = CLS3, † = RECI

FROM 1 / 1/69 TO 31 / 1/69  
 ENSLOW MILL CHERWELL

+ OBSERVED  
 x POM  
 • LH CATCHMENT MODEL  
 ◆ NWS MODEL  
 \* THAMES WATER MODEL

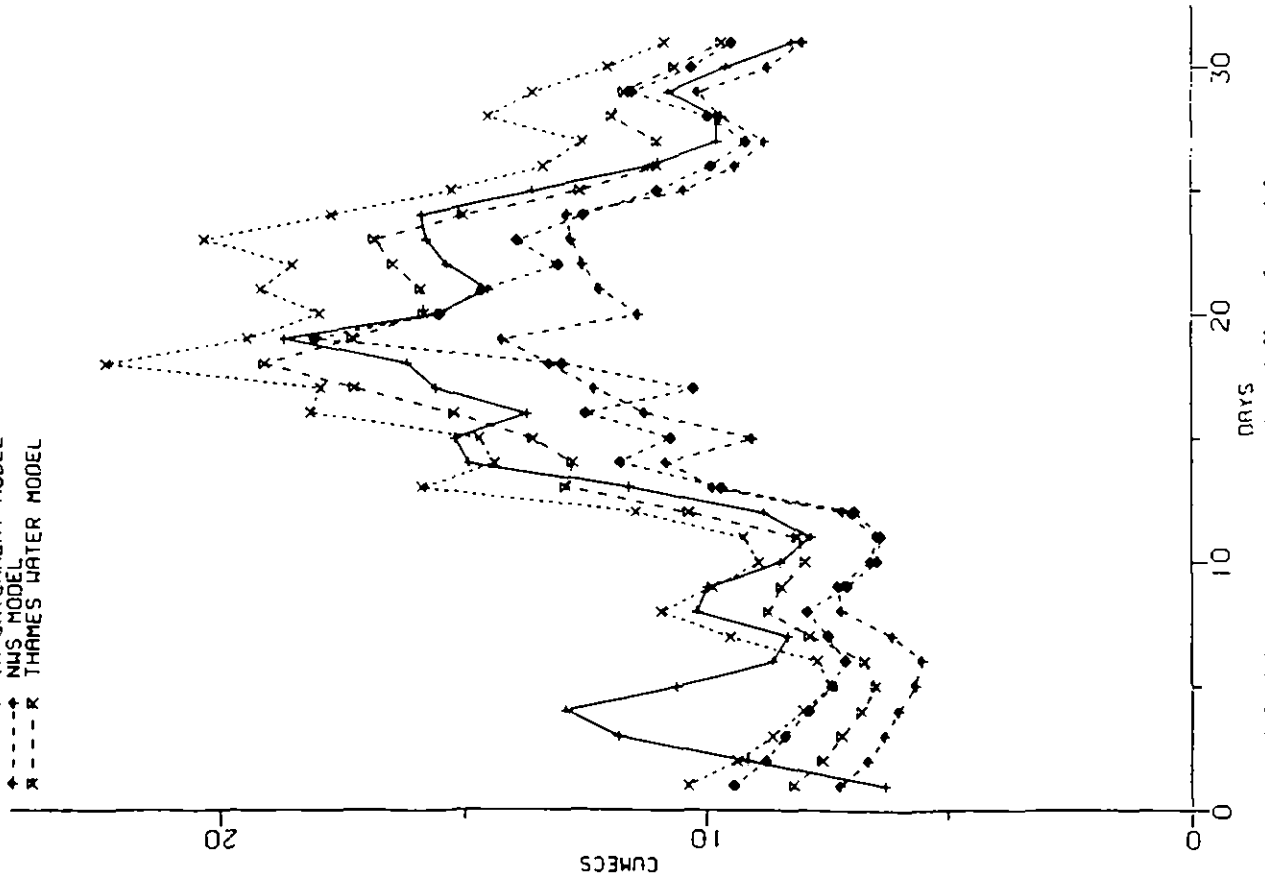


Figure 4.3.1(a) Observed and predicted flows for models POM1, IMCH, NWS1, TWR1

FROM 1 / 1/69 TO 31 / 1/69  
 ENSLOW MILL CHERWELL

+ OBSERVED  
 x CLS/EFH1 (CLS1)  
 • CLS/EFH2 (CLS2)  
 ◆ CLS/DPL (CLS3)  
 \* RECESSION MODEL

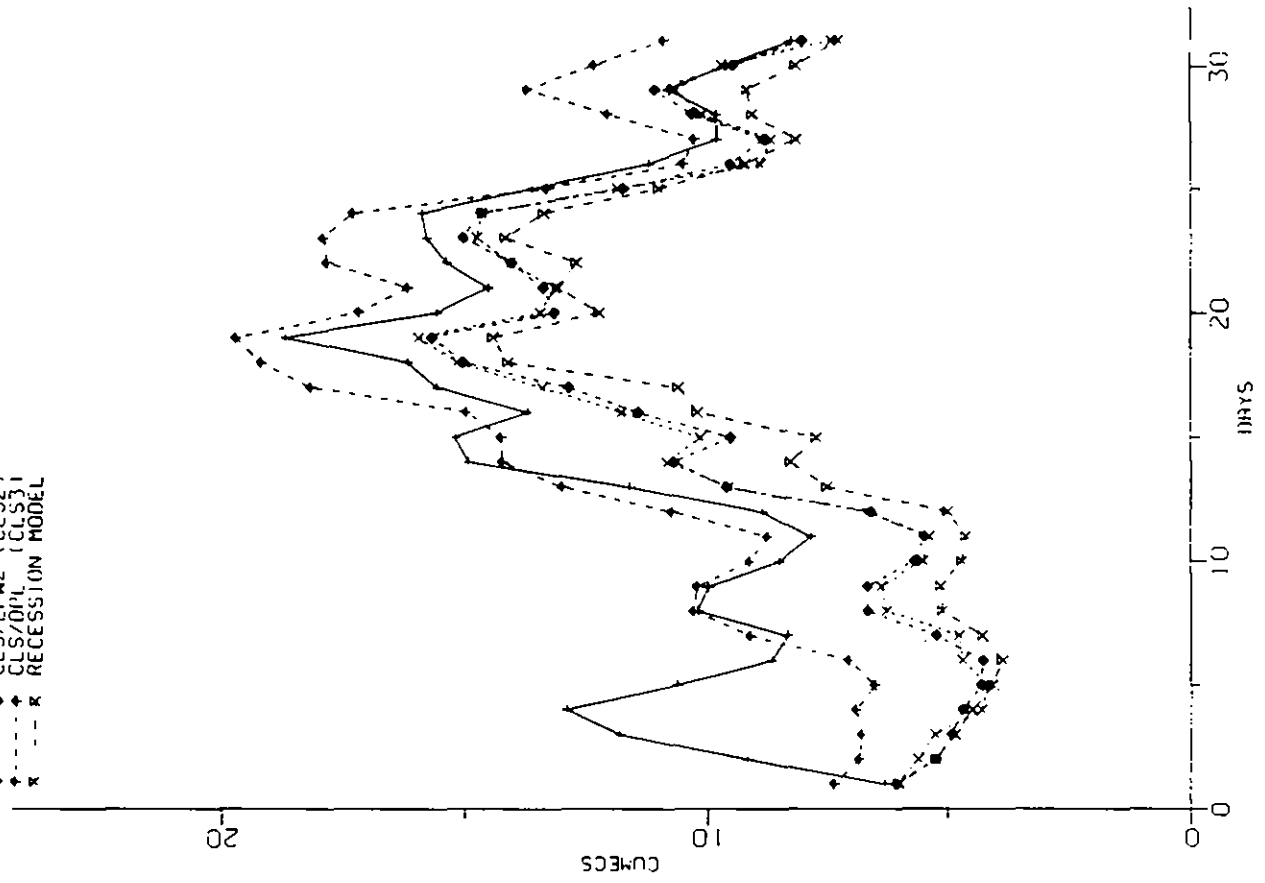


Figure 4.3.1(b) Observed and predicted flows for models CLS1, CLS2, CLS3, RECI

FROM 1 / 6 / 71 TO 1 / 7 / 71  
 ENSLOW MILL CHERWELL

OBSERVED  
 PDM  
 IH CATCHMENT MODEL  
 NWS MODEL  
 THAMES WATER MODEL

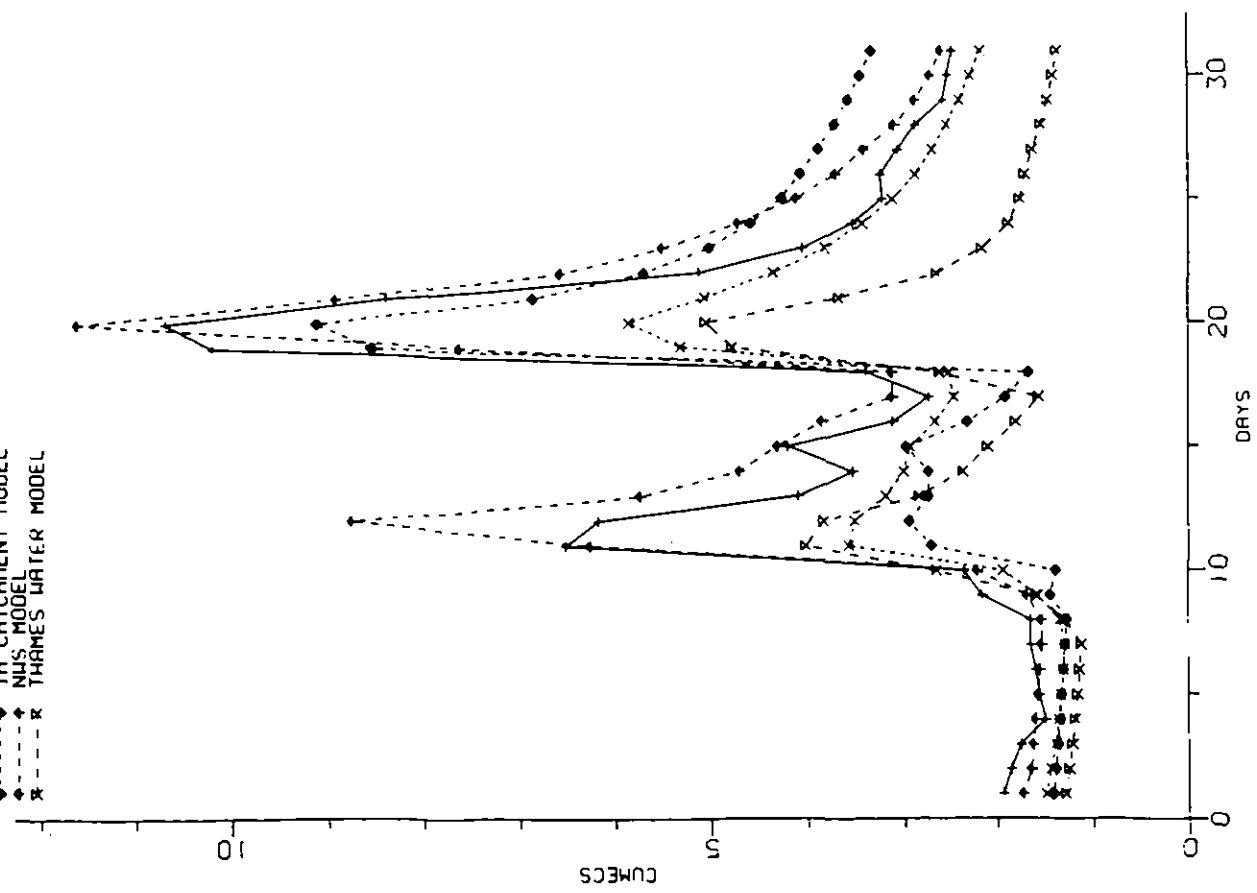


Figure 4.3.2(a) Observed and predicted flows for models PDM, IHCM, NWS1, TWT1

FROM 1 / 6 / 71 TO 1 / 7 / 71  
 ENSLOW MILL CHERWELL

OBSERVED  
 CLS/EFH1 (CLS1)  
 CLS/EFH2 (CLS2)  
 CLS/DPL (CLS3)  
 RECEPTION MODEL

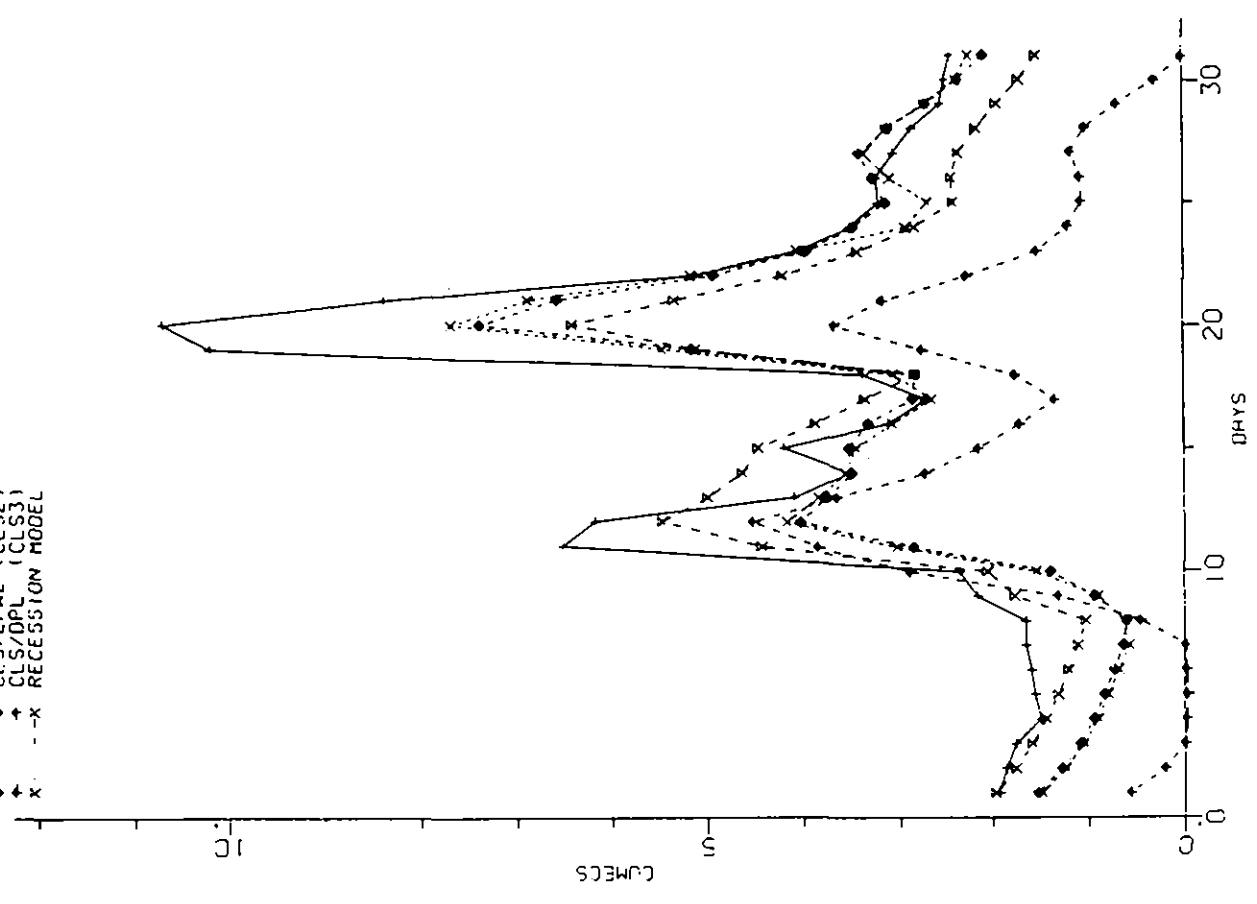


Figure 4.3.2(b) Observed and predicted flows for models CLS1, CLS2, CLS3, RECI

FROM 1/ 1/72 TO 31/ 1/72  
ENSLOW MILL CHERWELL

OBSERVED  
PDM  
IH CATCHMENT MODEL  
NWS MODEL  
THAMES WATER MODEL

— x  
- - - x  
- - - x  
- - - x  
- - - x

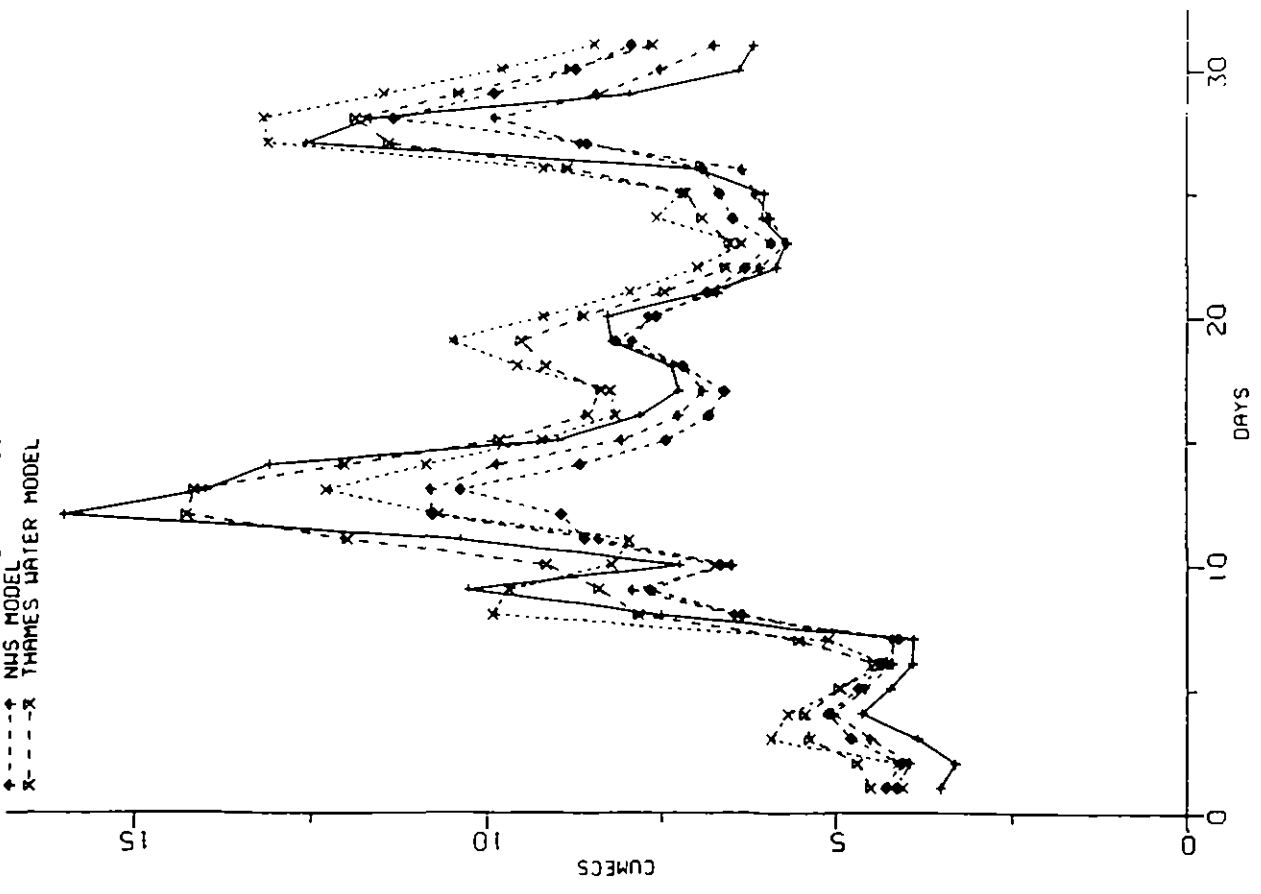


Figure 4.3.3(a) Observed and predicted flows for models PDM, IHCM, NWS, TWI

FROM 1/ 1/72 TO 31/ 1/72  
ENSLOW MILL CHERWELL

OBSERVED (CLS1)  
CLS/FFH1 (CLS1)  
CLS/FFH2 (CLS2)  
CLS/DFL (CLS3)  
RECESSION MODEL

— x  
- - - x  
- - - x  
- - - x  
- - - x

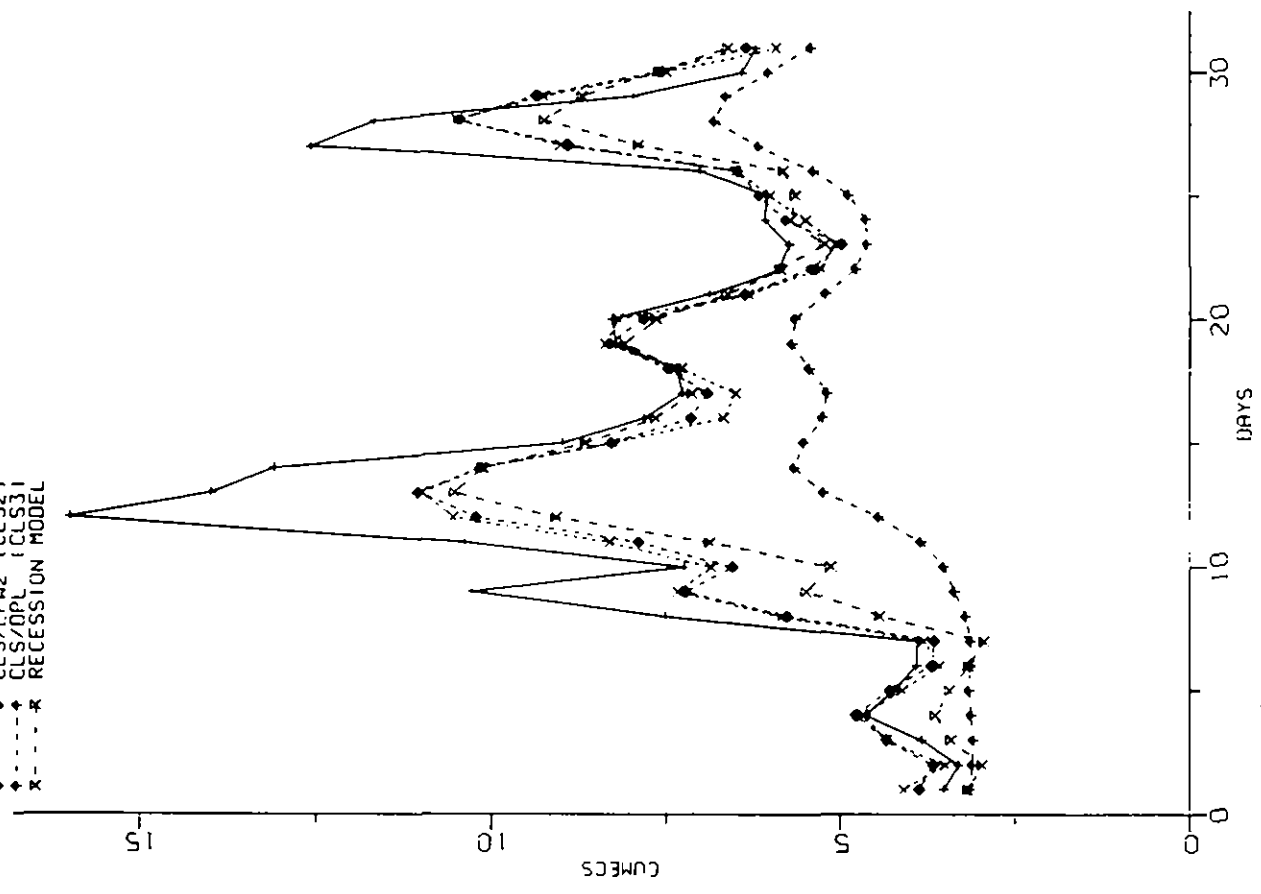


Figure 4.3.3(b) Observed and predicted flows for models CLS1, CLS2, CLS3, RECI

FROM 31/ 8/74 TO 30/ 9/74  
 ENSLOW MILL CHERWELL

OBSERVED  
 POM CATCHMENT MODEL  
 IH CATCHMENT MODEL  
 NWS MODEL  
 THAMES WATER MODEL

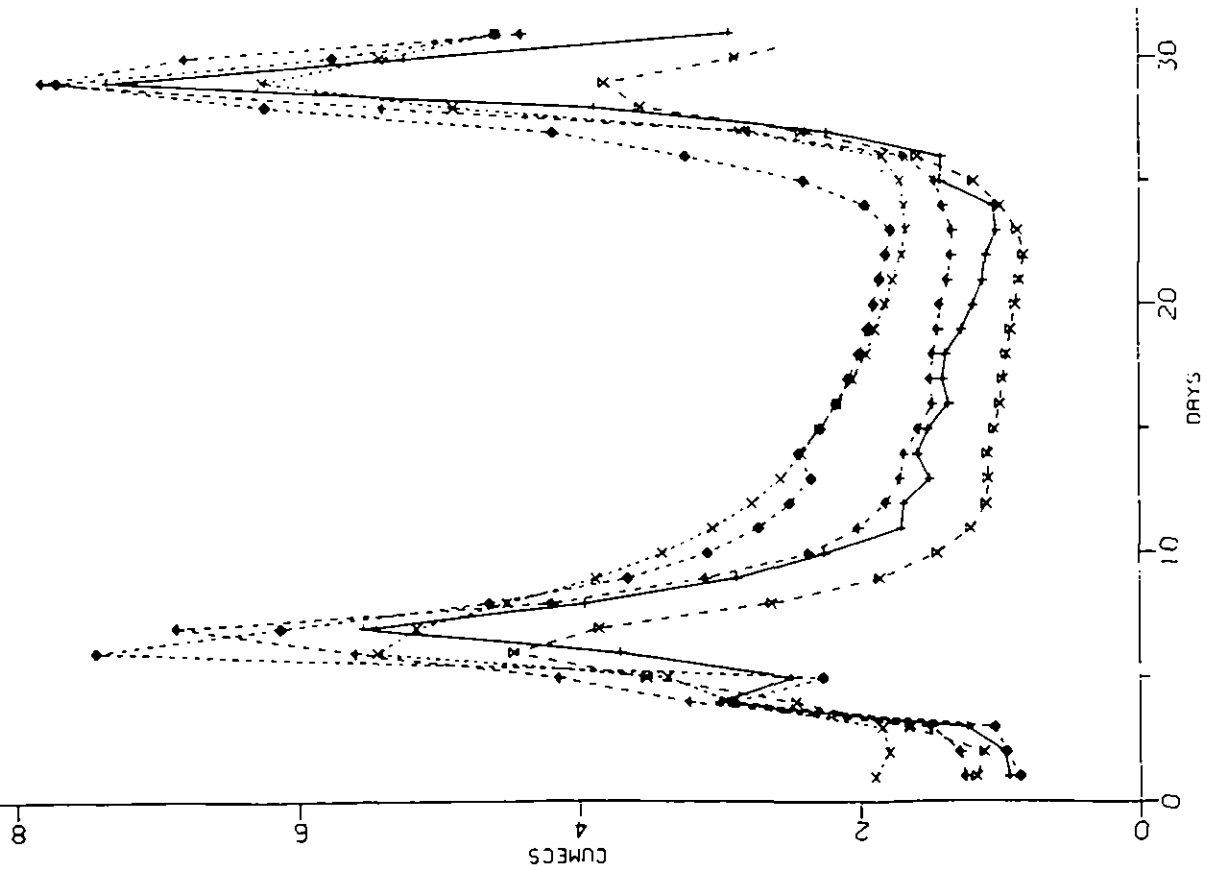


Figure 4.3.4(a) Observed and predicted flows for models  
 POM1, IHCH, NWS1, TWMI

FROM 31/ 8/74 TO 30/ 9/74  
 ENSLOW MILL CHERWELL

OBSERVED  
 CLS/EFH1 (CLS1)  
 CLS/EFH2 (CLS2)  
 CLS/DPL (CLS3)  
 RECESSION MODEL

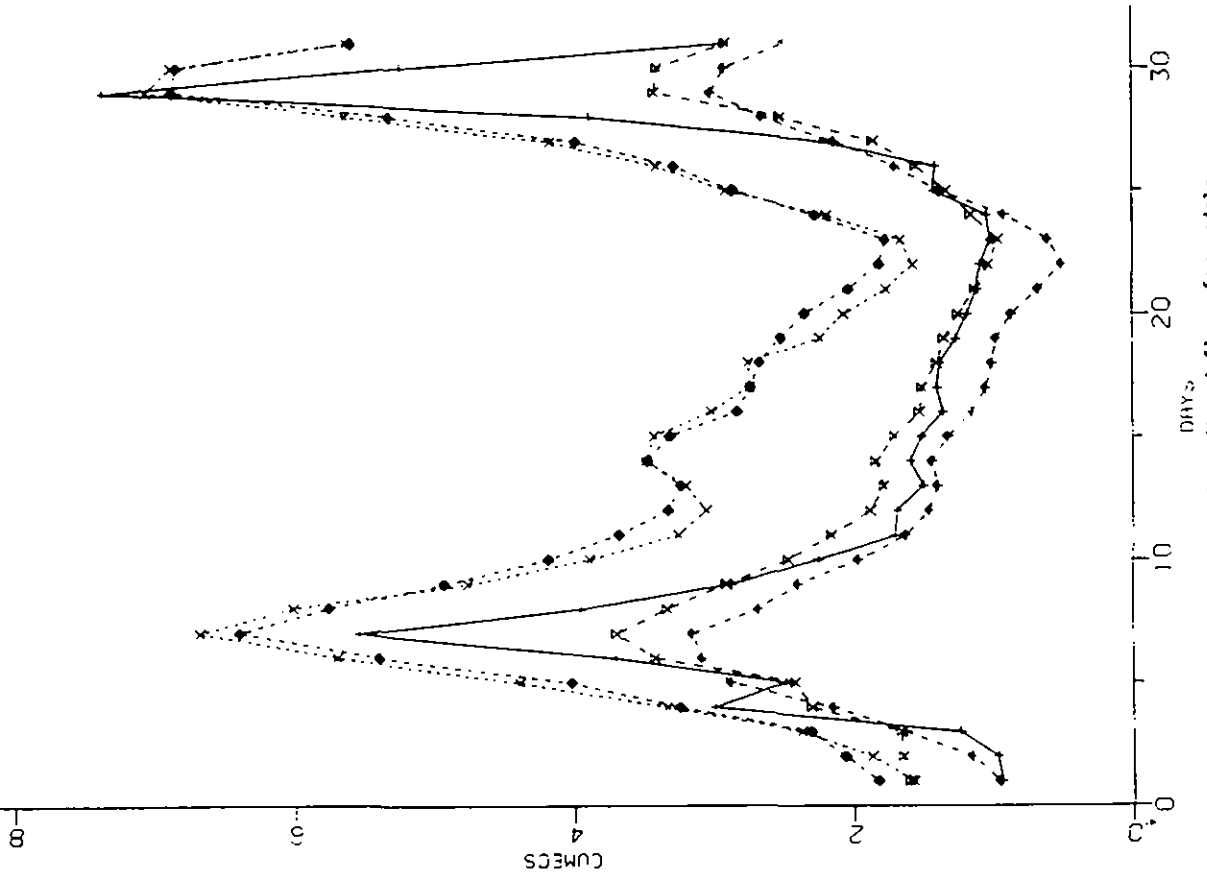


Figure 4.3.4(b) Observed and predicted flows for models  
 CLS1, CLS2, CLS3, RFC1

FROM 1 / 3 / 75 TO 31 / 3 / 75  
 ENSLOW MILL CHERWELL

OBSERVED  
 PDM  
 IH CATCHMENT MODEL  
 NUS MODEL  
 THAMES WATER MODEL

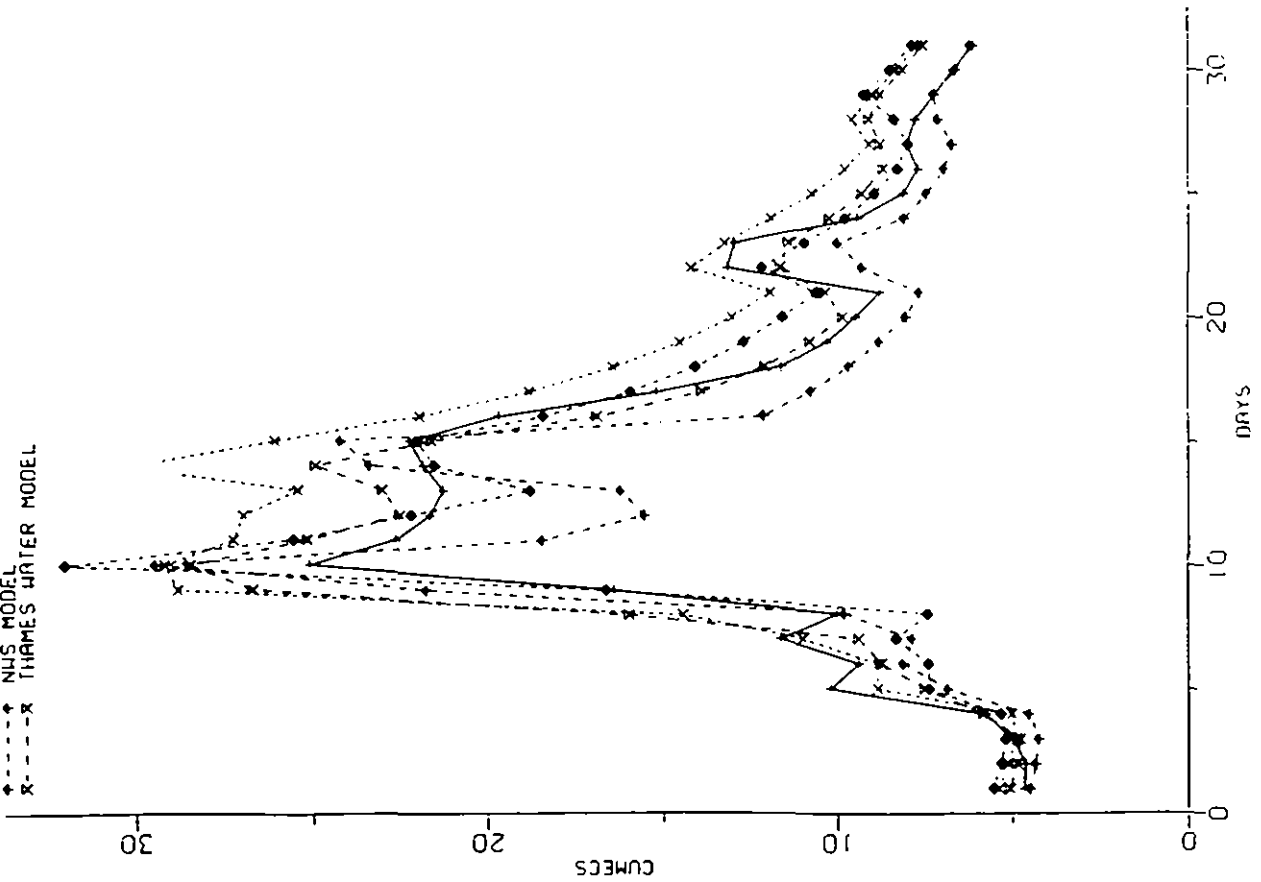


Figure 4.3.5(a) Observed and predicted flows for models PDM, IHCH, NUS1, TWMI

FROM 1 / 3 / 75 TO 31 / 3 / 75  
 ENSLOW MILL CHERWELL

OBSERVED  
 CLS/EFM1 (CLS1)  
 CLS/EFM2 (CLS2)  
 CLS/DPL (CLS3)  
 RECEPTION MODEL

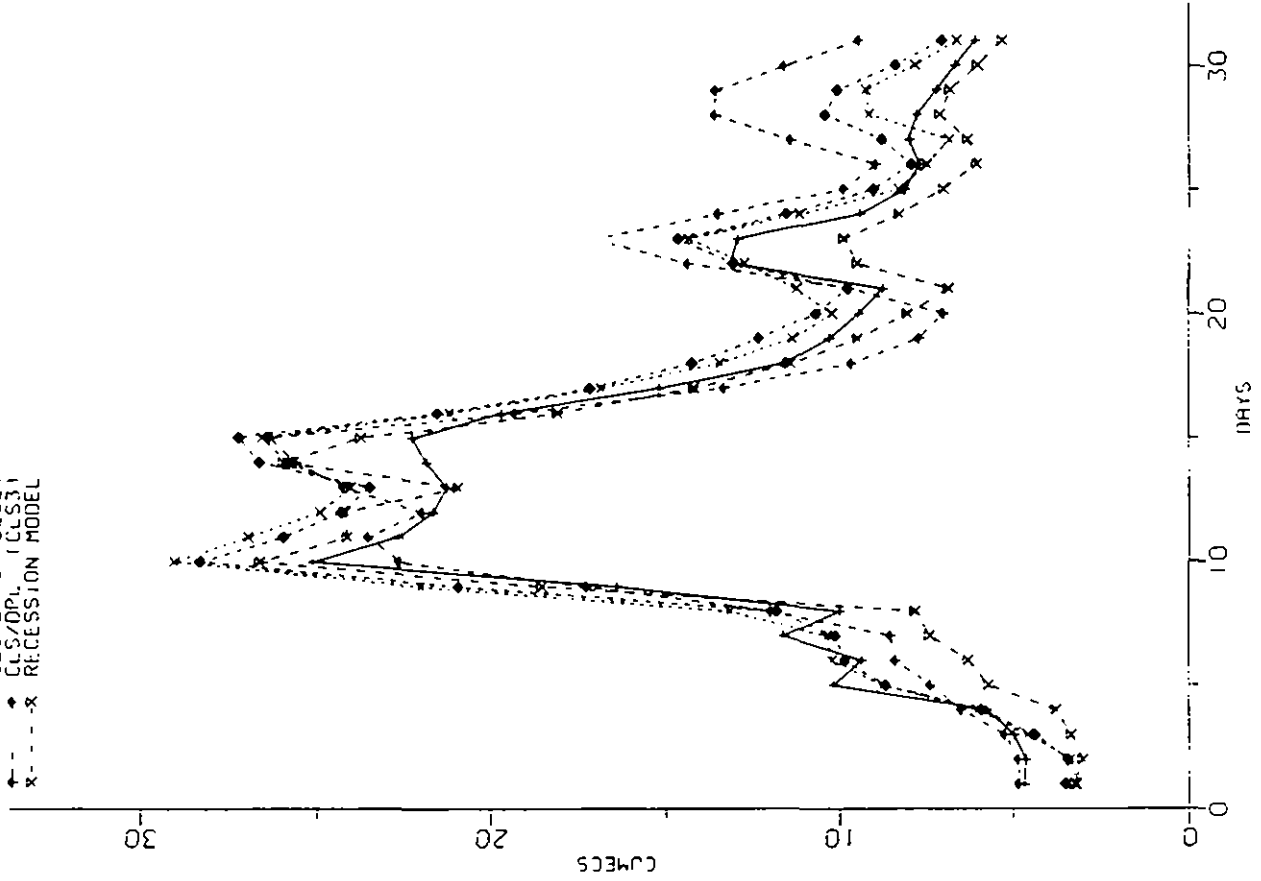


Figure 4.3.5(b) Observed and predicted flows for models CLS1, CLS2, CLS3, RECI

FROM 20/ 8/76 TO 19/ 9/76  
ENSLOW MILL CHERWELL

— OBSERVED  
x PDM CATCHMENT MODEL  
• IH CATCHMENT MODEL  
+ NWS MODEL  
x THAMES WATER MODEL

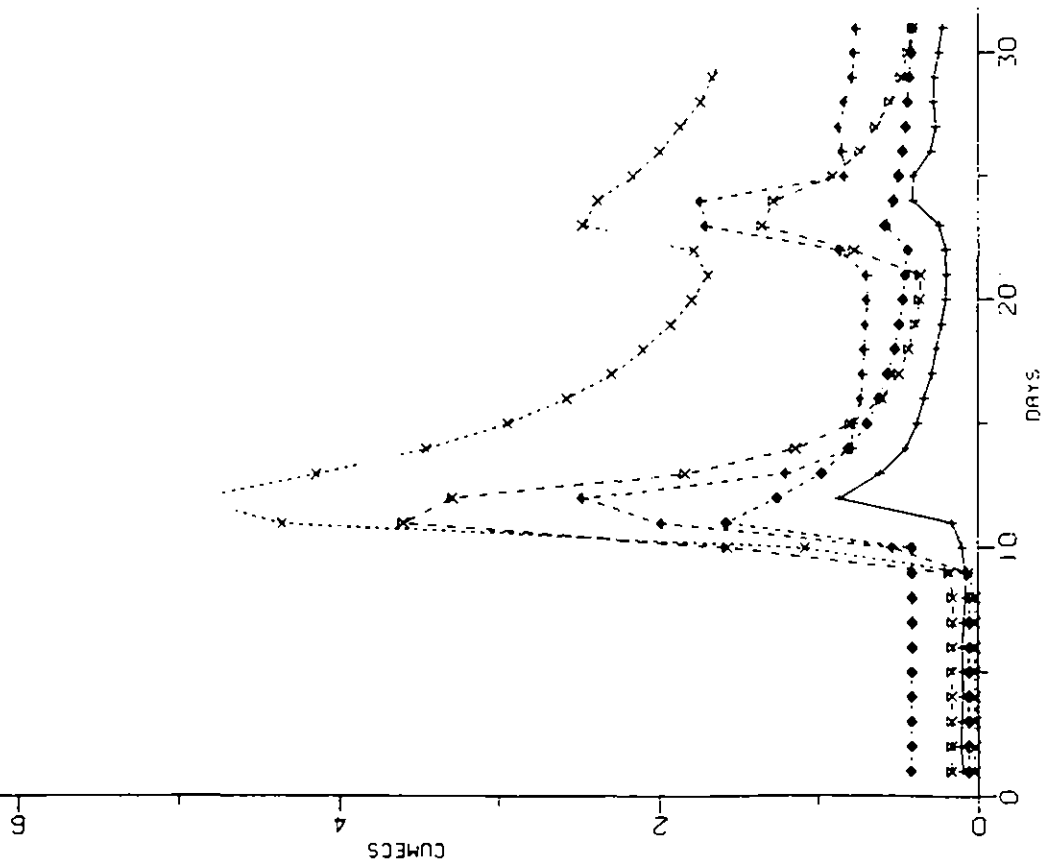


Figure 4.3.6(a) Observed and predicted flows for models PDM1, THOM, NWS1, TW1.

FROM 20/ 8/76 TO 19/ 9/76  
ENSLOW MILL CHERWELL

— OBSERVED  
x CLS/FFH1 (CLS1)  
• CLS/FFH2 (CLS2)  
+ CLS/DPL (CLS3)  
x REGRESSION MODEL

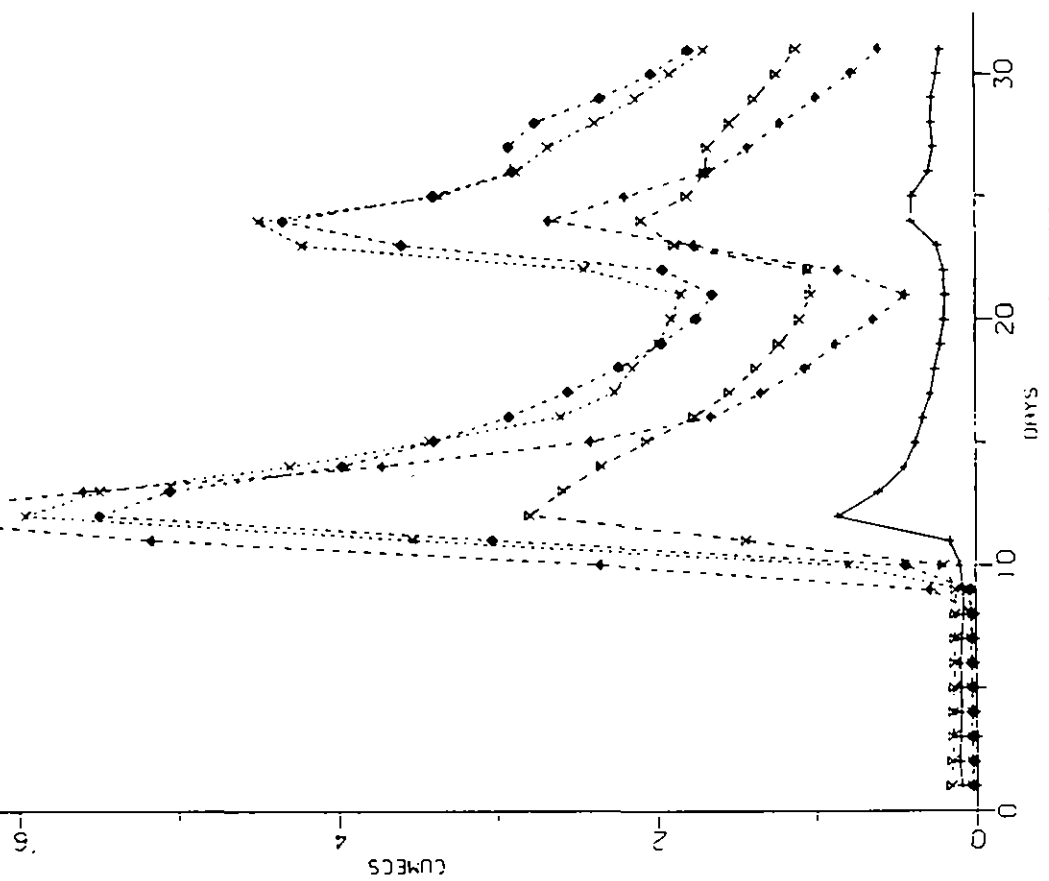


Figure 4.3.6(b) Observed and predicted flows for models CLS1, CLS2, CLS3, REG1.

FROM 1/12/77 TO 31/12/77  
ENSLOW MILL CHERWELL

OBSERVED  
 PDM  
 IH CATCHMENT MODEL  
 NJS MODEL  
 THAMES WATER MODEL

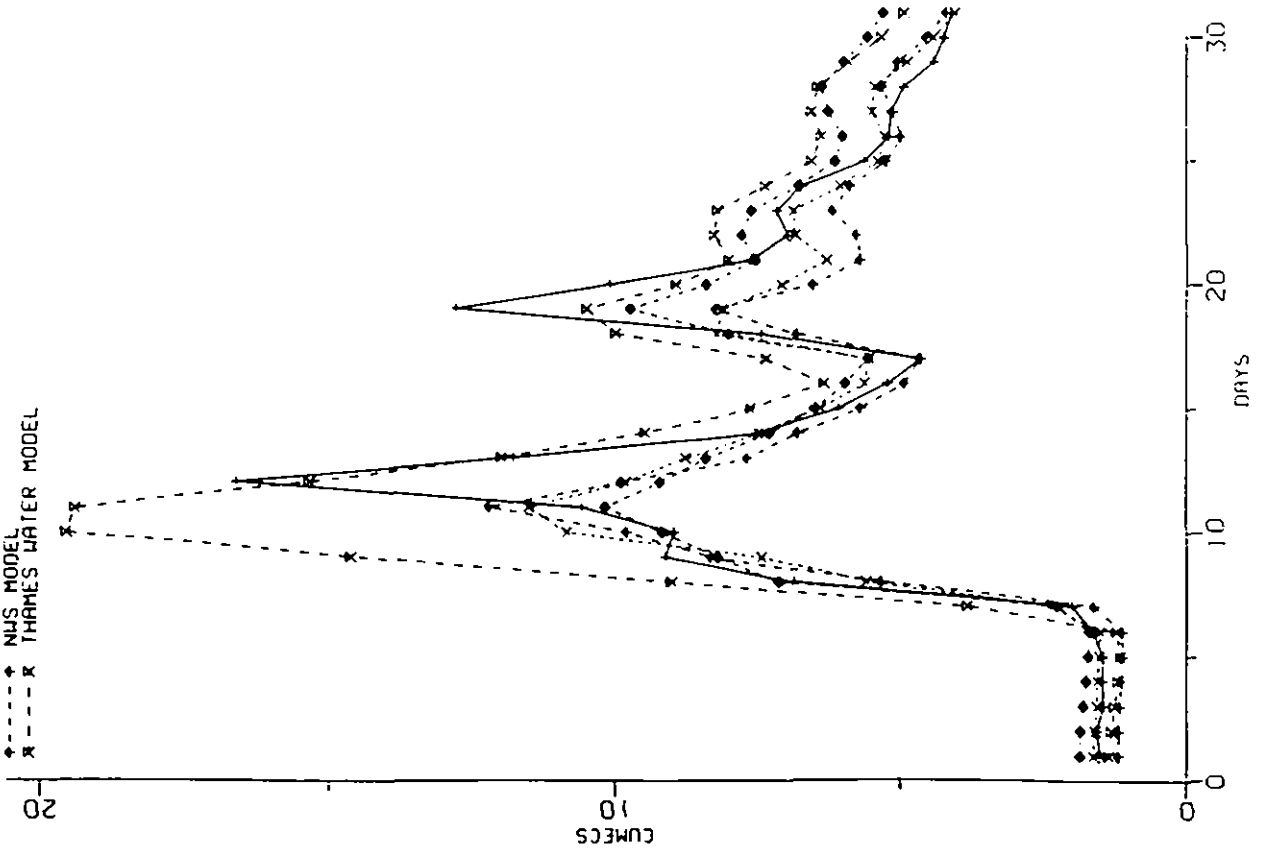


Figure 4.3.7(a) Observed and predicted flows for models PDM1, IHCH, MWS1, TWML.

FROM 1/12/77 TO 31/12/77  
ENSLOW MILL CHERWELL

OBSERVED  
 CLS/EFW1 (CLS11)  
 CLS/EFW2 (CLS2)  
 CLS/DPL (CLS3)  
 RECESSION MODEL

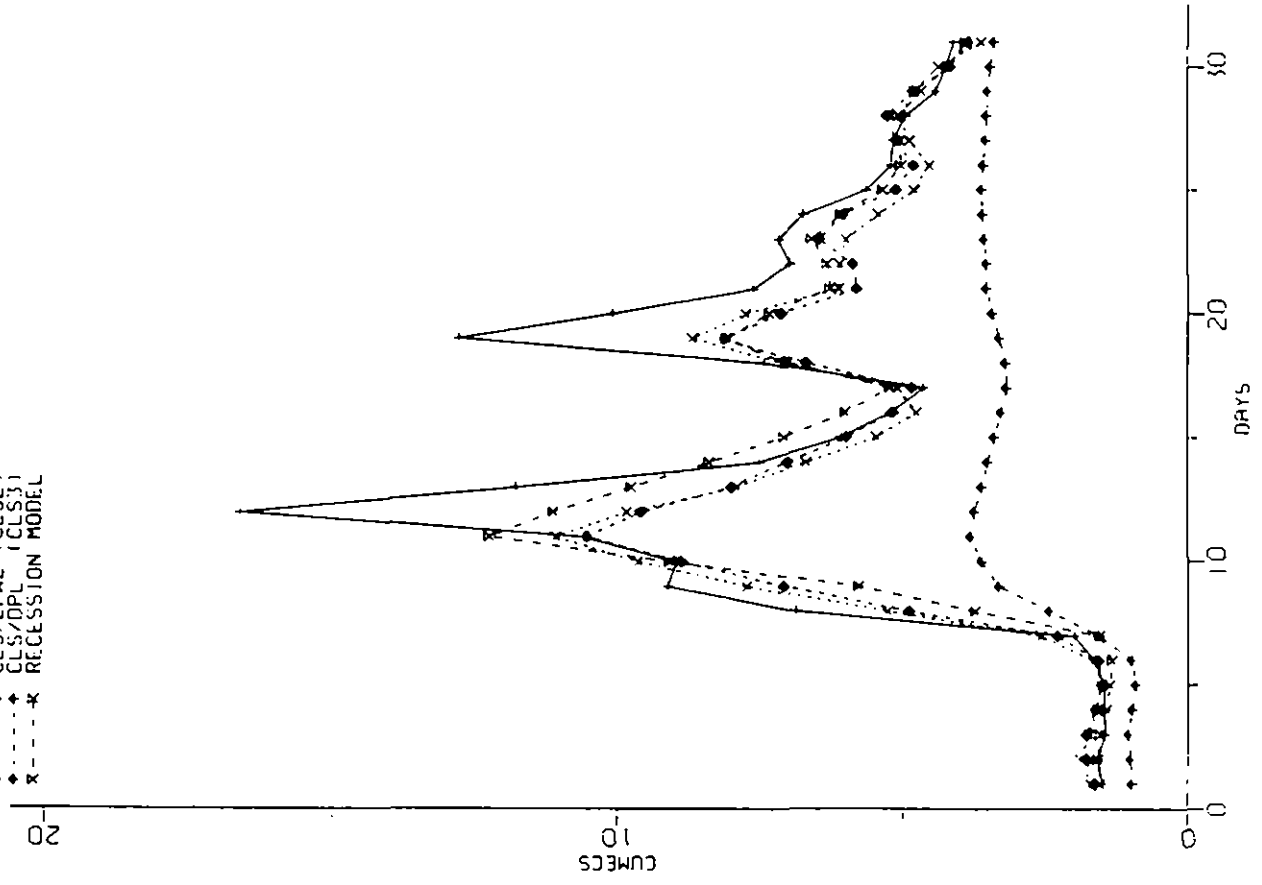


Figure 4.3.7(b) Observed and predicted flows for models CLS1, CLS2, CLS3, RECL.

FROM 1 / 5/73 TO 31 / 5/73  
CASTLE MILL MOLE

OBSERVED  
 PDM  
 ITH CAATCHMENT MODEL  
 NWS MODEL  
 THAMES WATER MODEL

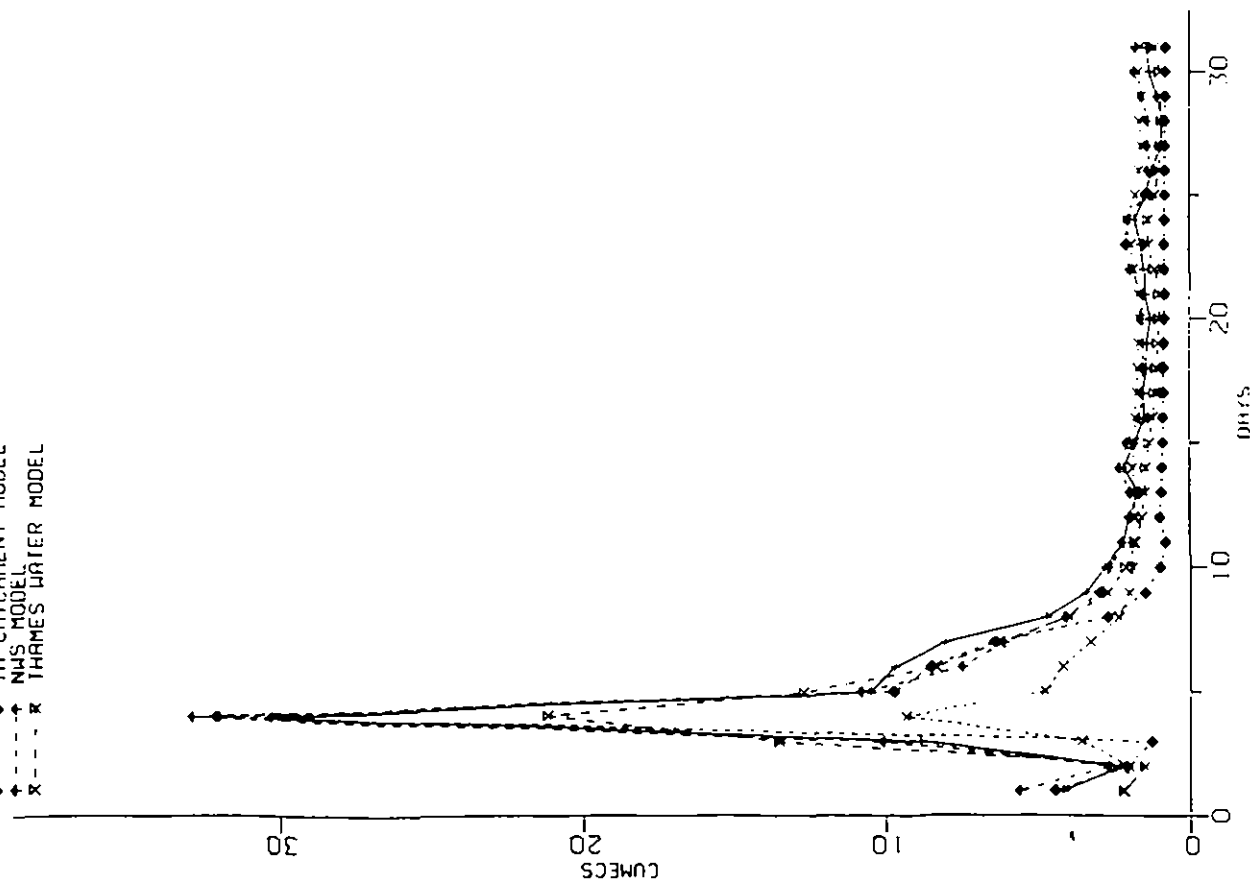


Figure 4.3.8(a) Observed and predicted flows for models PDM, ITH, NWS, TWMI.

FROM 1 / 5/73 TO 31 / 5/73  
CASTLE MILL MOLE

OBSERVED  
 CLS/EFM1 (CLS1)  
 CLS/EFM2 (CLS2)  
 CLS/OP1 (CLS3)  
 RECEPTION MODEL

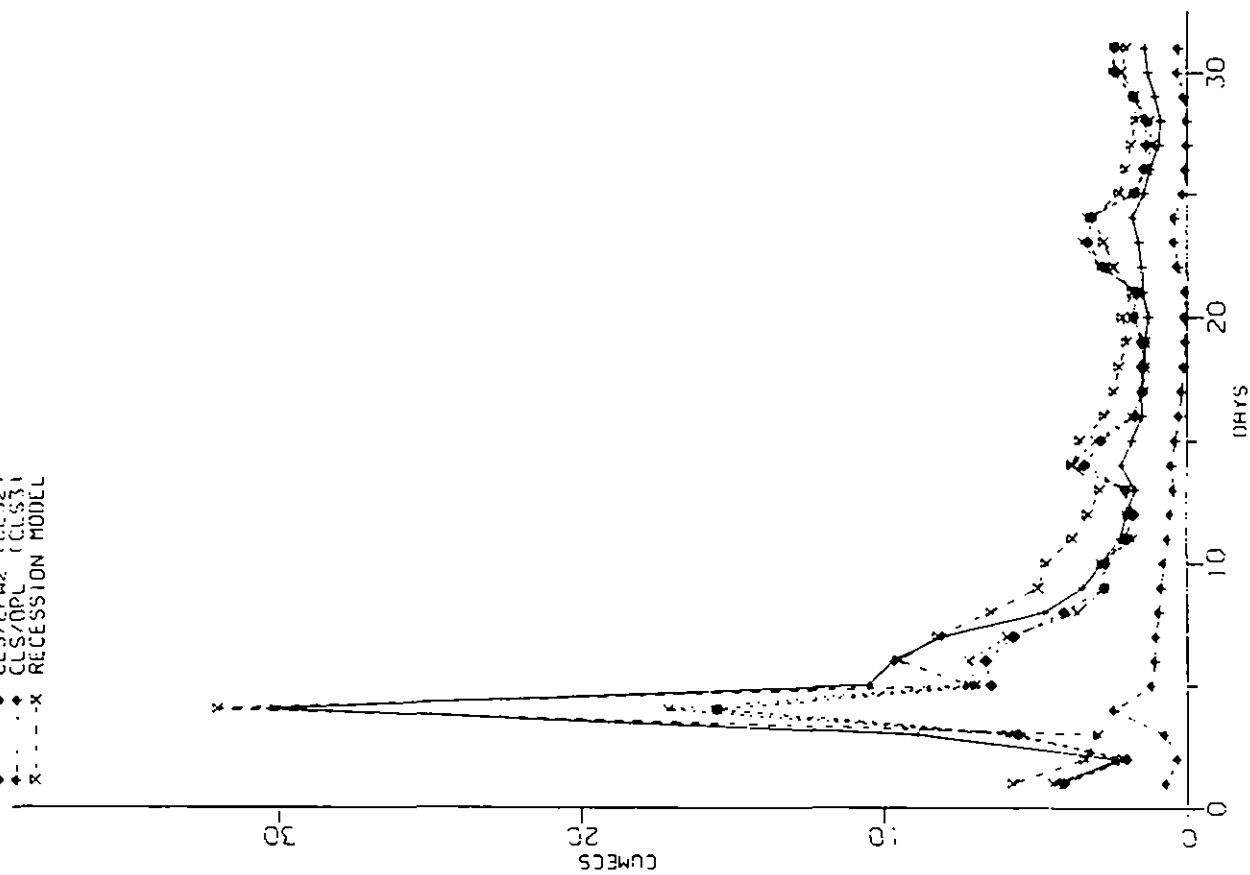


Figure 4.3.8(b) Observed and predicted flows for models CLS1, CLS2, CLS3, RECI.

FROM 31/ 8/74 TO 30/ 9/74  
CASTLE MILL MOLE

OBSERVED (x)  
 CLS/FFH1 (CL.S1)  
 CLS/FFH2 (CL.S2)  
 CLS/DFL (CL.S3)  
 RECEPTION MODEL (R)

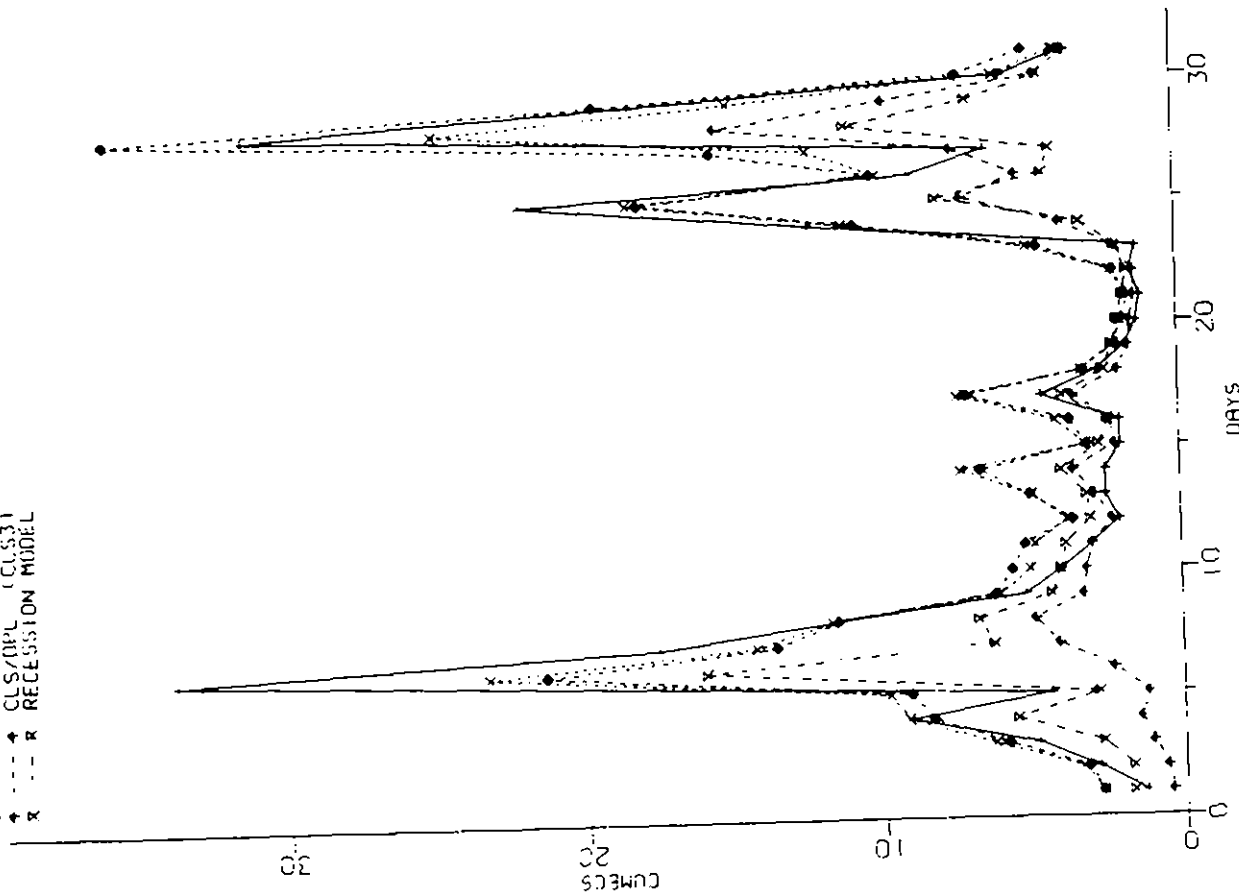


Figure 4.3.9(b) Observed and predicted flows for models CLS1, CLS2, CLS3, RECI

FROM 31/ 8/74 TO 30/ 9/74  
CASTLE MILL MOLE

OBSERVED (x)  
 PDM (x)  
 IH CATCHMENT MODEL (x)  
 NWS MODEL (x)  
 THAMES WATER MODEL (x)

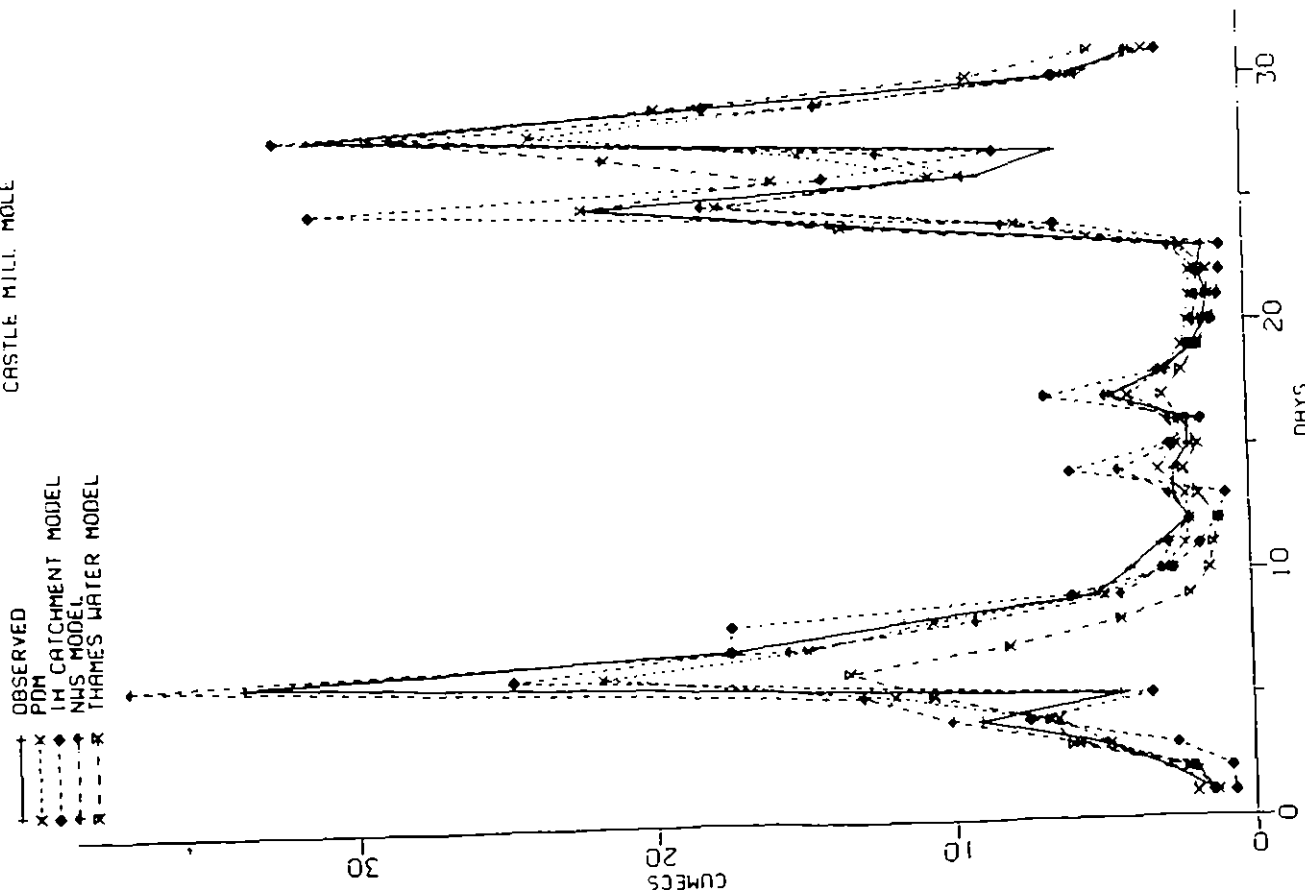


Figure 4.3.9(a) Observed and predicted flows for models PDM, IH, NWS, THAMES WATER

FROM 1/11/74 TO 1/12/74  
 CASILE MILL MOLE

+ OBSERVED  
 x PDM  
 . IH CATCHMENT MODEL  
 \* NUS MODEL  
 - THAMES WATER MODEL

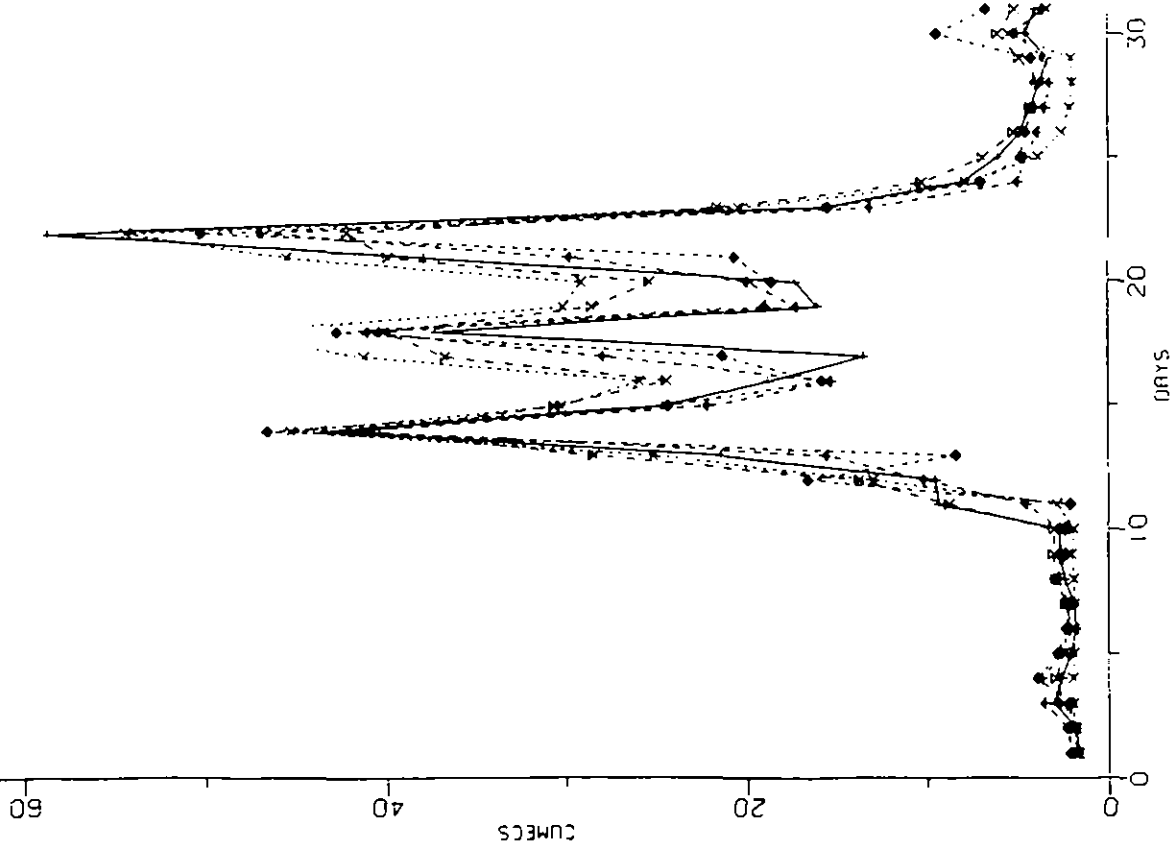


Figure 4.3.10(a) Observed and predicted flows for models PDM, IH, NUS, THAMES WATER MODEL

FROM 1/11/74 TO 1/12/74  
 CASILE MILL MOLE

+ OBSERVED  
 x CLS/EFM1 (CLS1)  
 . CLS/EFM2 (CLS2)  
 \* CLS/DPL (CLS3)  
 - RECESION MODEL

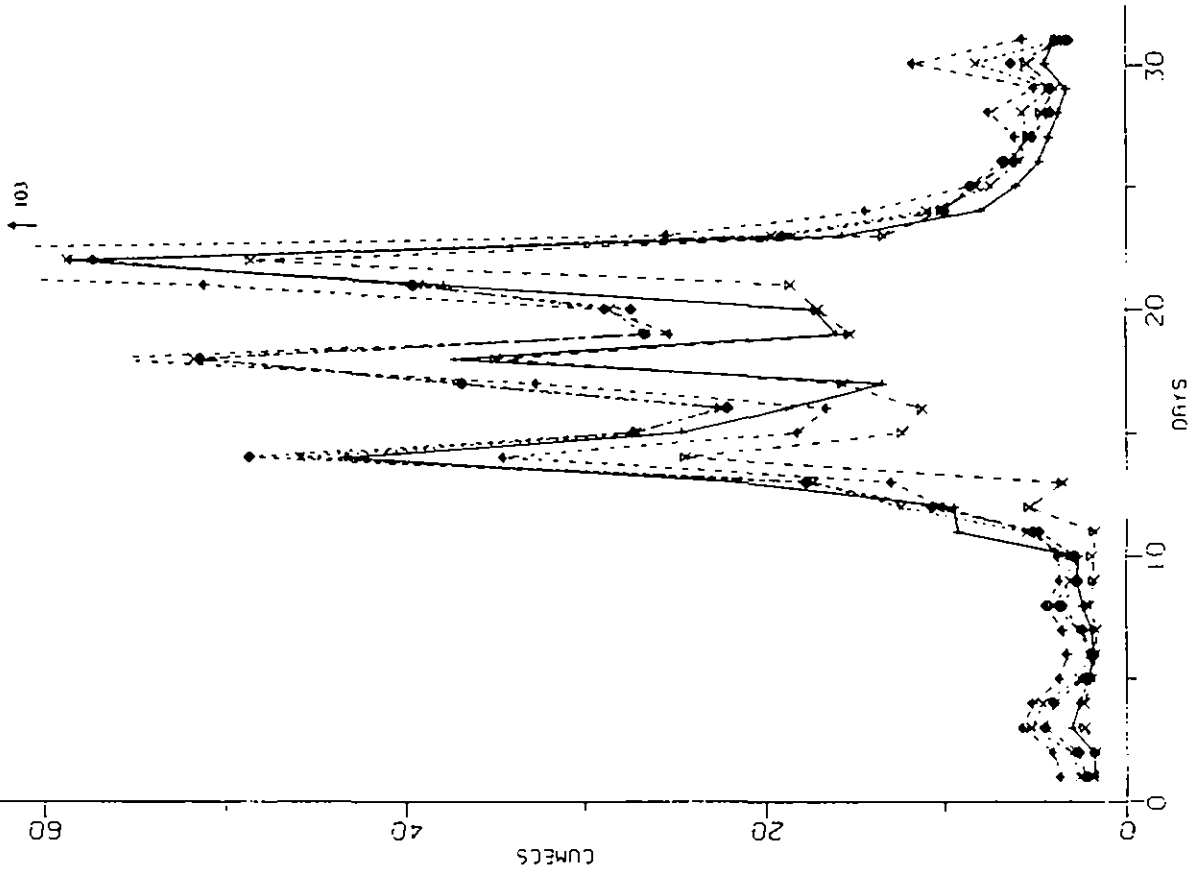


Figure 4.3.10(b) Observed and predicted flows for models CLS1, CLS2, CLS3, RECI

FROM 1 / 3/75 TO 31 / 3/75  
CASTLE MILL MOLE

- OBSERVED
- - - PDM
- ITH CATCHMENT MODEL
- ◆◆◆ NWS MODEL
- ◆◆◆ THAMES WATER MODEL

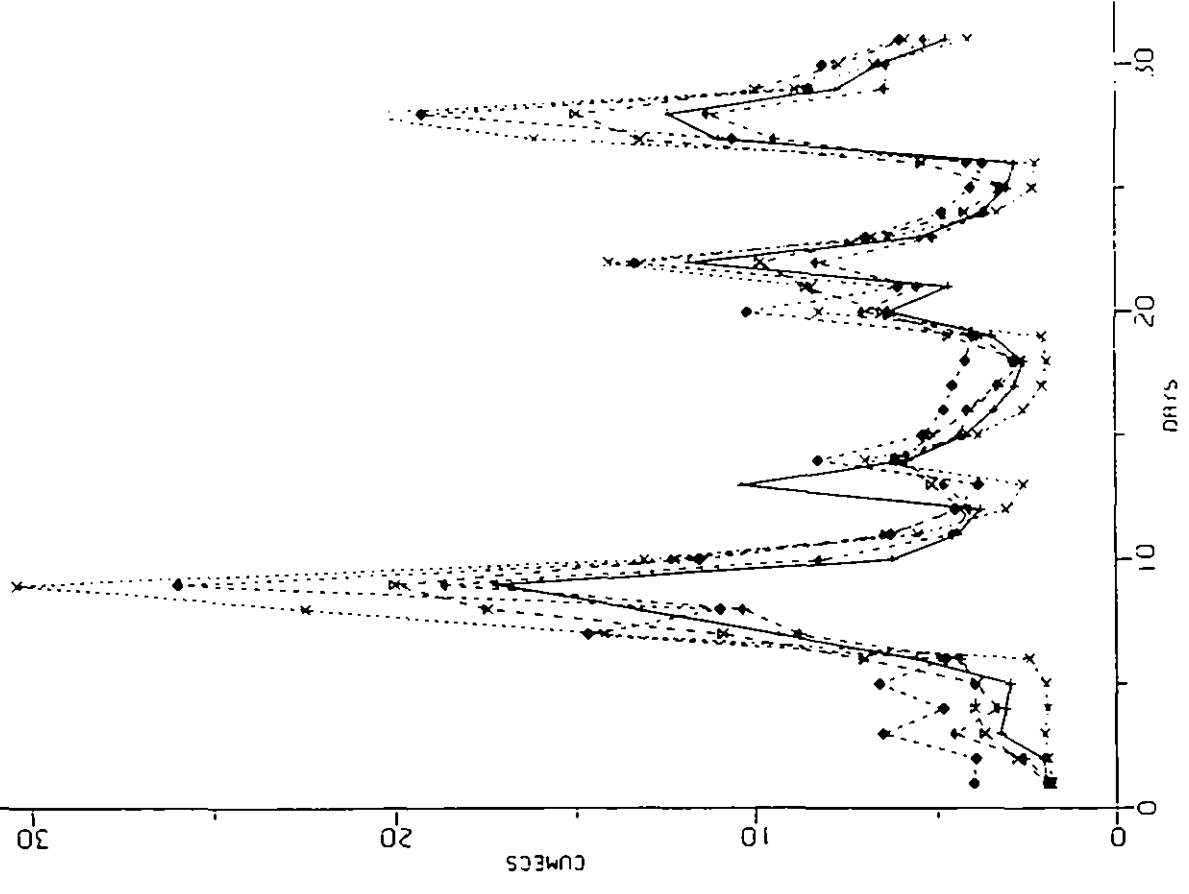


Figure 4.3.11(a) Observed and predicted flows for models PDM, ITH, NWS, TWRI

FROM 1 / 3/75 TO 31 / 3/75  
CASTLE MILL MOLE

- OBSERVED
- - - CLS1
- CLS/EFM1
- ◆◆◆ CLS/EFM2
- ◆◆◆ CLS/DPL
- ◆◆◆ RECEPTION MODEL

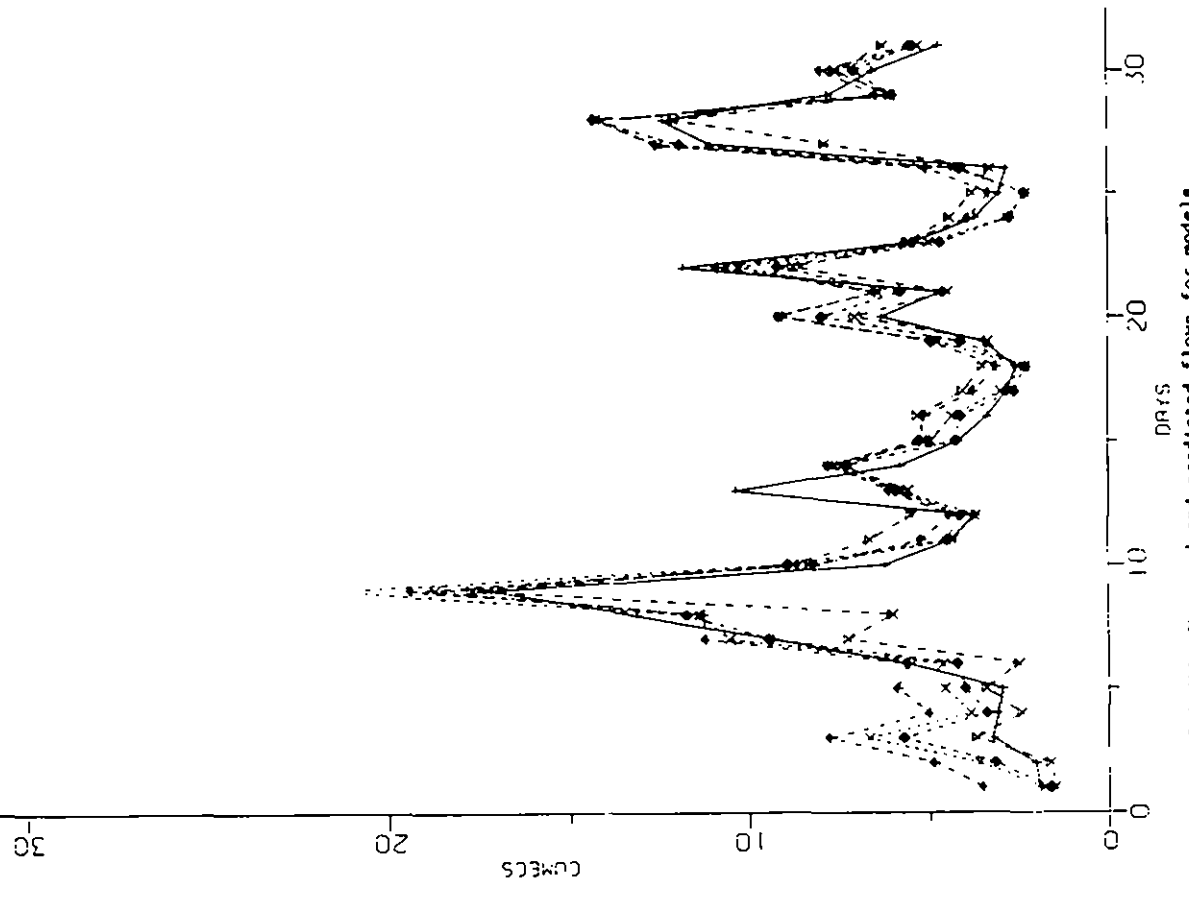


Figure 4.3.11(b) Observed and predicted flows for models CLS1, CLS2, CLS3, RECI

FROM 20/ 7/78 TO 19/ 8/78  
 CASTLE MILL MOLE

OBSERVED (x)  
 PDM CATCHMENT MODEL (.....)  
 IH CATCHMENT MODEL (.....)  
 NUS MODEL (.....)  
 THAMES WATER MODEL (x)

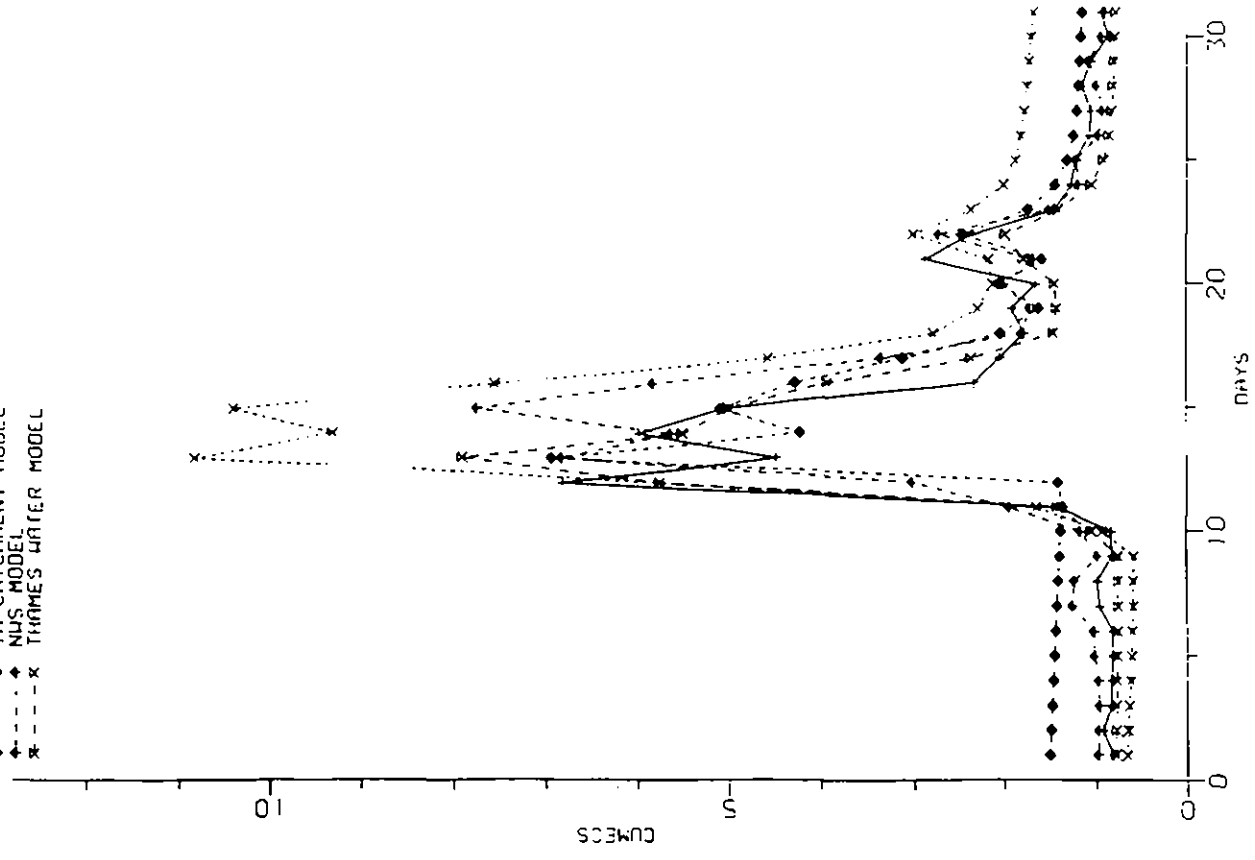


Figure 4.3.12(a) Observed and predicted flows for models PDM1, IHCM, NMS1, TW1

FROM 20/ 7/78 TO 19/ 8/78  
 CASTLE MILL MOLE

OBSERVED (x)  
 CLS/EFH1 (.....)  
 CLS/EFH2 (.....)  
 CLS/DPL (.....)  
 RECESSTON MODEL (x)

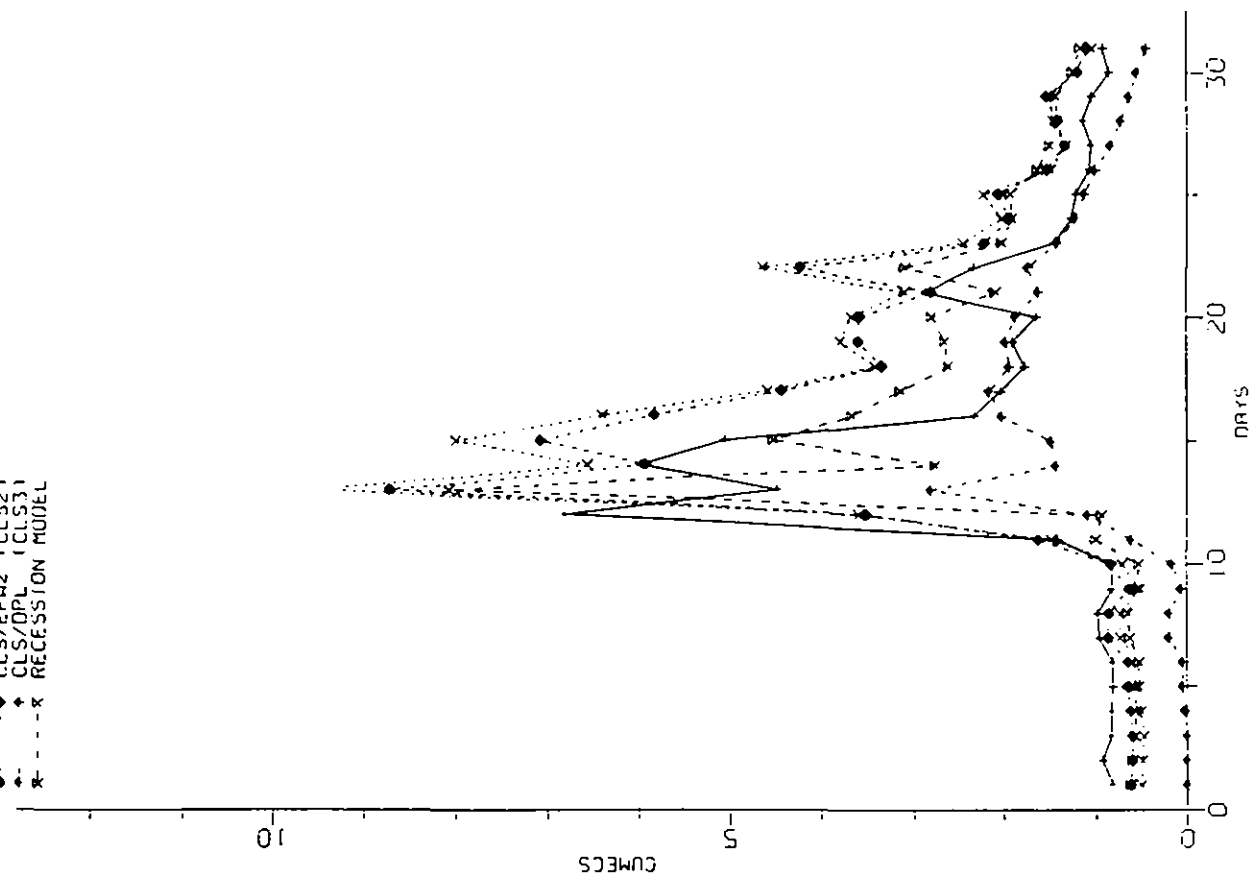


Figure 4.3.12(b) Observed and predicted flows for models CLS1, CLS2, CLS3, RECI

FROM 1/1/79 TO 31/1/79  
CASTLE MILL MOLE

+ OBSERVED  
 x PDM  
 \* LH CATCHMENT MODEL  
 o NWS MODEL  
 - THAMES WATER MODEL

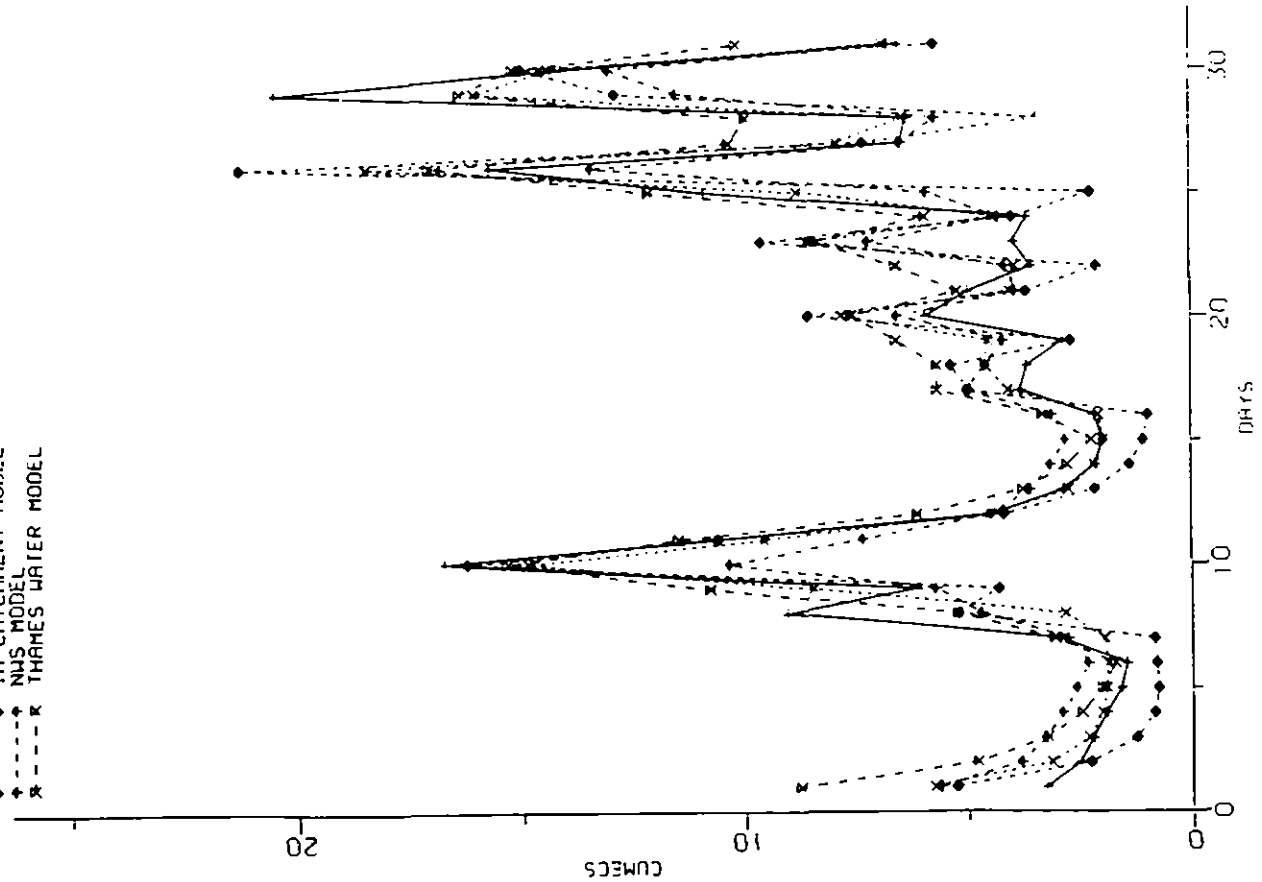


Figure 4.3.13(a) Observed and predicted flows for models PDM, LHCH, NWS1, TW1

FROM 1/1/79 TO 31/1/79  
CASTLE MILL MOLE

+ OBSERVED  
 x CLS/EFW1 (CLS1)  
 \* CLS/EFW2 (CLS2)  
 o CLS/DPL (CLS3)  
 - RECEPTION MODEL

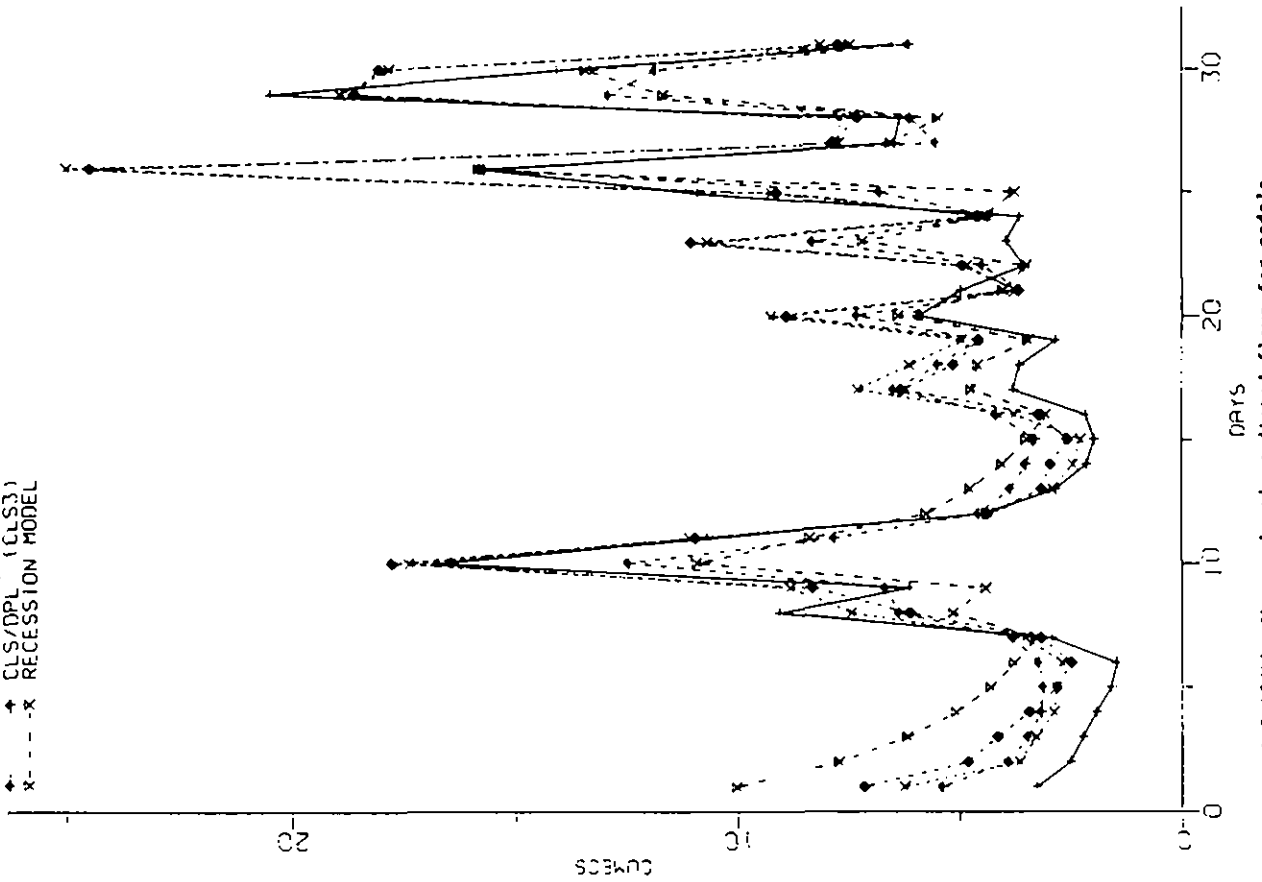


Figure 4.3.13(b) Observed and predicted flows for models CLS1, CLS2, CLS3, RECI

FROM 31/ 3/83 TO 30/ 4/83  
CASTLE MILL MOLF

+---+ OBSERVED  
 x---x PDM  
 \*---\* IFA CATCHMENT MODEL  
 ◆---◆ NWS MOOFI  
 \*---\* THAMES WATER MODEL

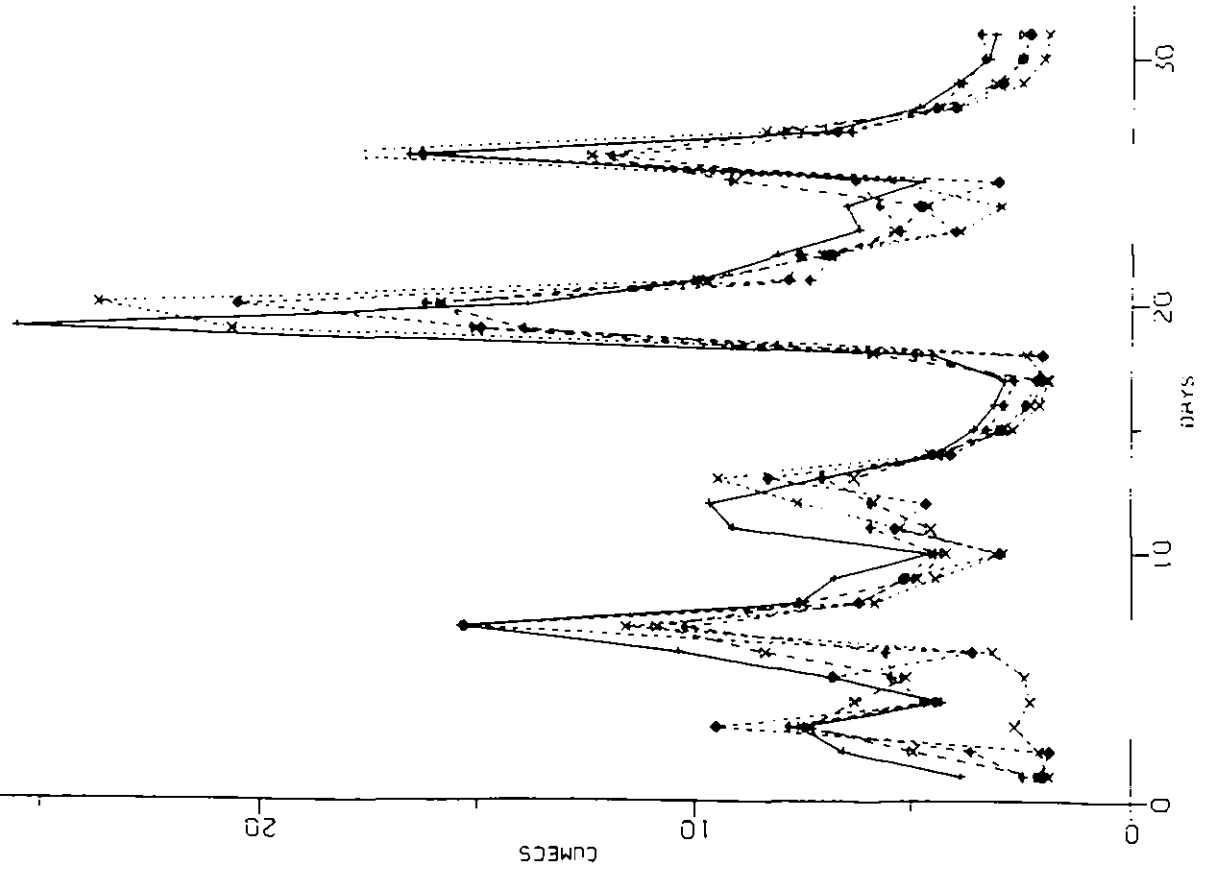


Figure 4.3.14(a) Observed and predicted flows for models PDM1, IFCM, NWS1, TWM1

FROM 31/ 3/83 TO 30/ 4/83  
CASTLE MILL MOLE

+---+ OBSERVED  
 x---x CLS/EFW1 (CLS1)  
 \*---\* CLS/EFW2 (CLS2)  
 ◆---◆ CLS/DPL (CLS3)  
 \*---\* RECUSSION MODEL

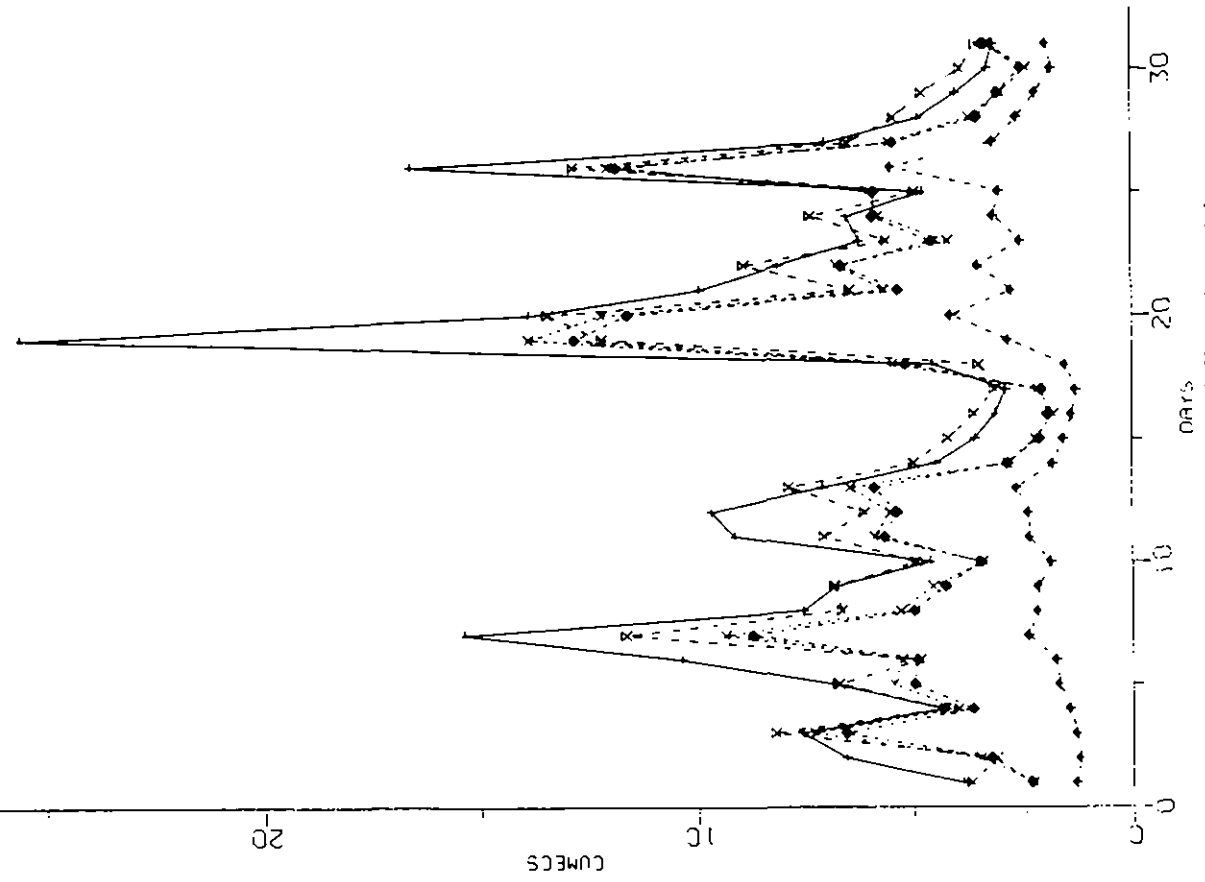


Figure 4.3.14(b) Observed and predicted flows for models CLS1, CLS2, CLS3, RECU

FROM 1/1/69 TO 31/1/69

SHALLOW FELD BLACKWATER

OBSERVED  
 PDM  
 IH CATCHMENT MODEL  
 NWS MODEL  
 THAMES WATER MODEL

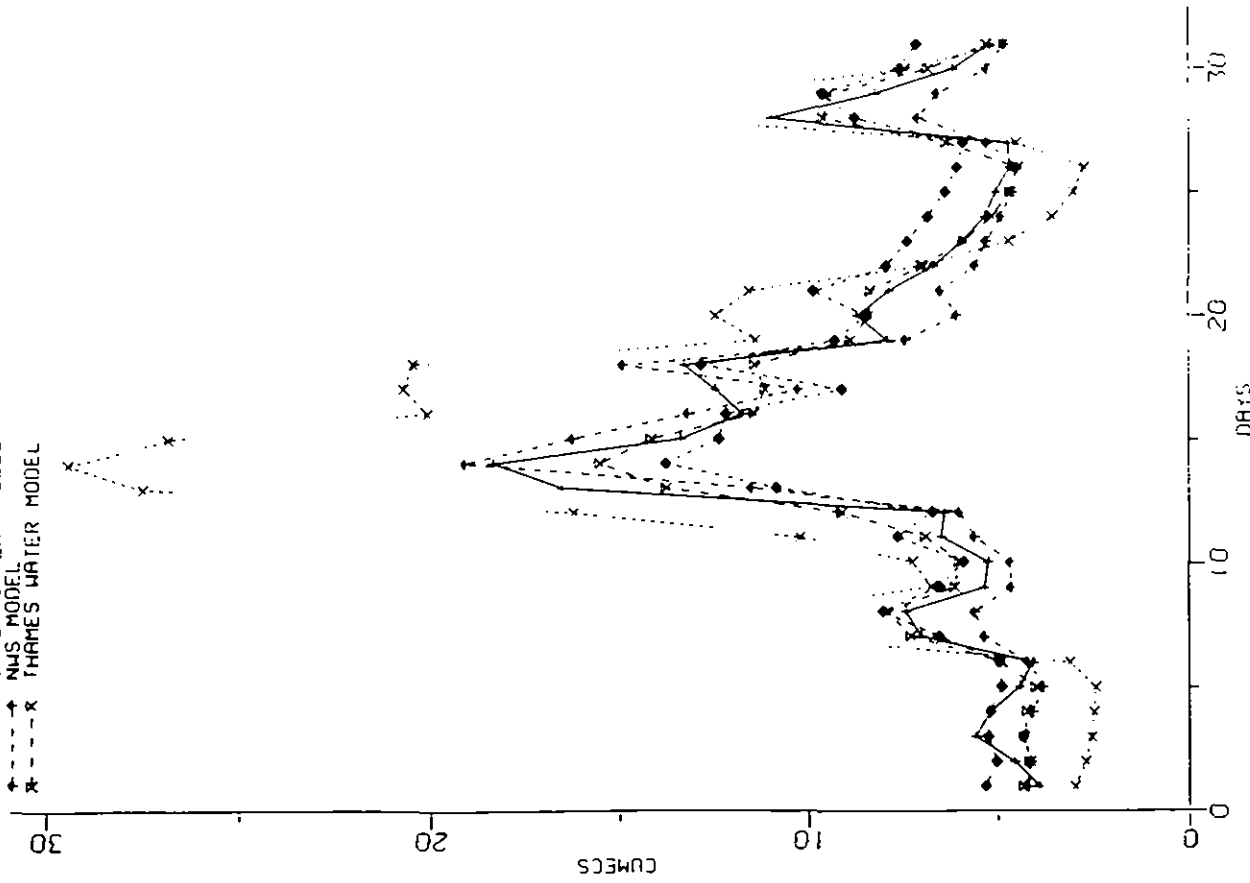


Figure 4.3.15(a) Observed and predicted flows for models PDM, IHCM, NWS1, TW1

FROM 1/1/69 TO 31/1/69

SHALLOW FELD BLACKWATER

OBSERVED  
 CLS/EFW1  
 CLS/EFW2  
 CLS/OP1 (CLS3)  
 RECEPTION MODEL

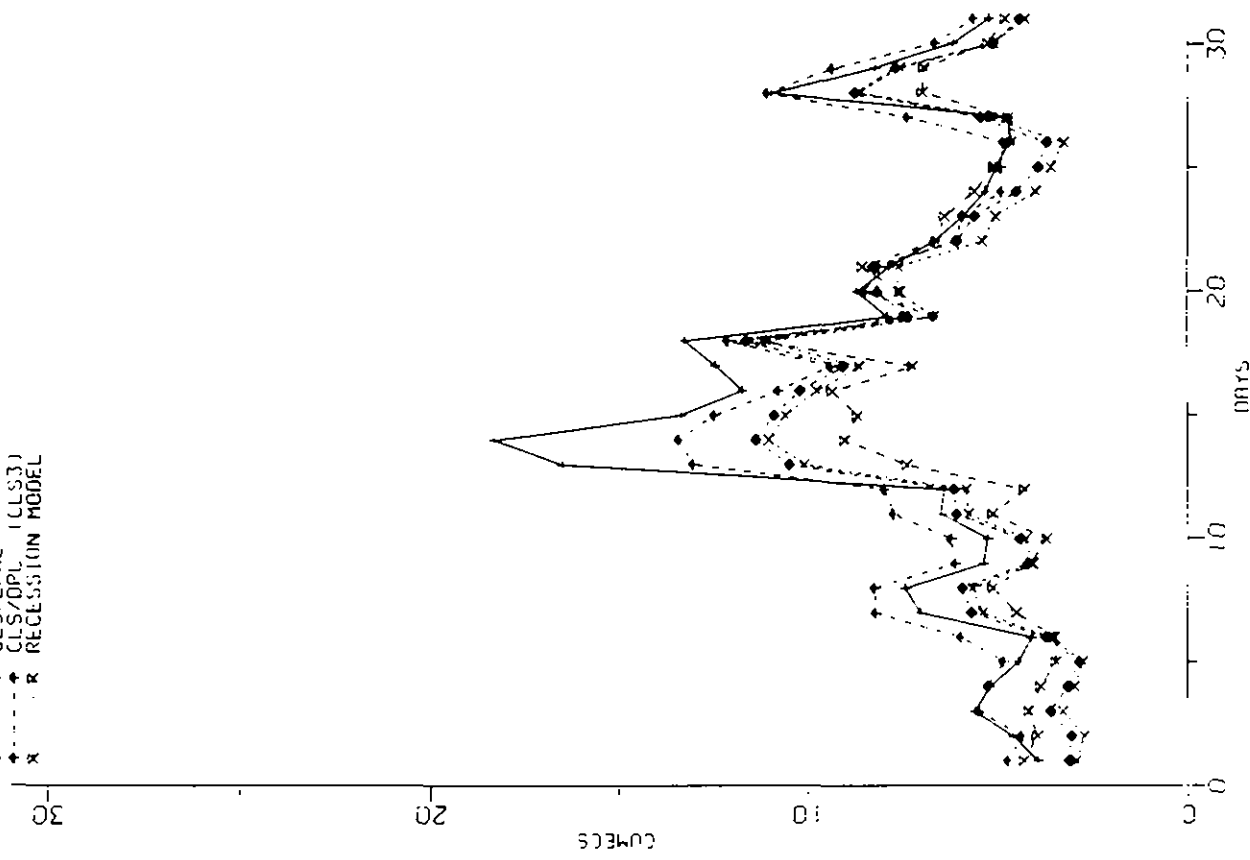


Figure 4.3.15(b) Observed and predicted flows for models CLS1, CLS2, CLS3, RECL.

FROM 1 / 6 / 71 TO 1 / 7 / 71  
SWALLOWFELD BLACKWATER

LEGEND:  
OBSERVED (x)  
PDM (x)  
IH CATCHMENT MODEL (x)  
NHS MODEL (x)  
THAMES WATER MODEL (x)

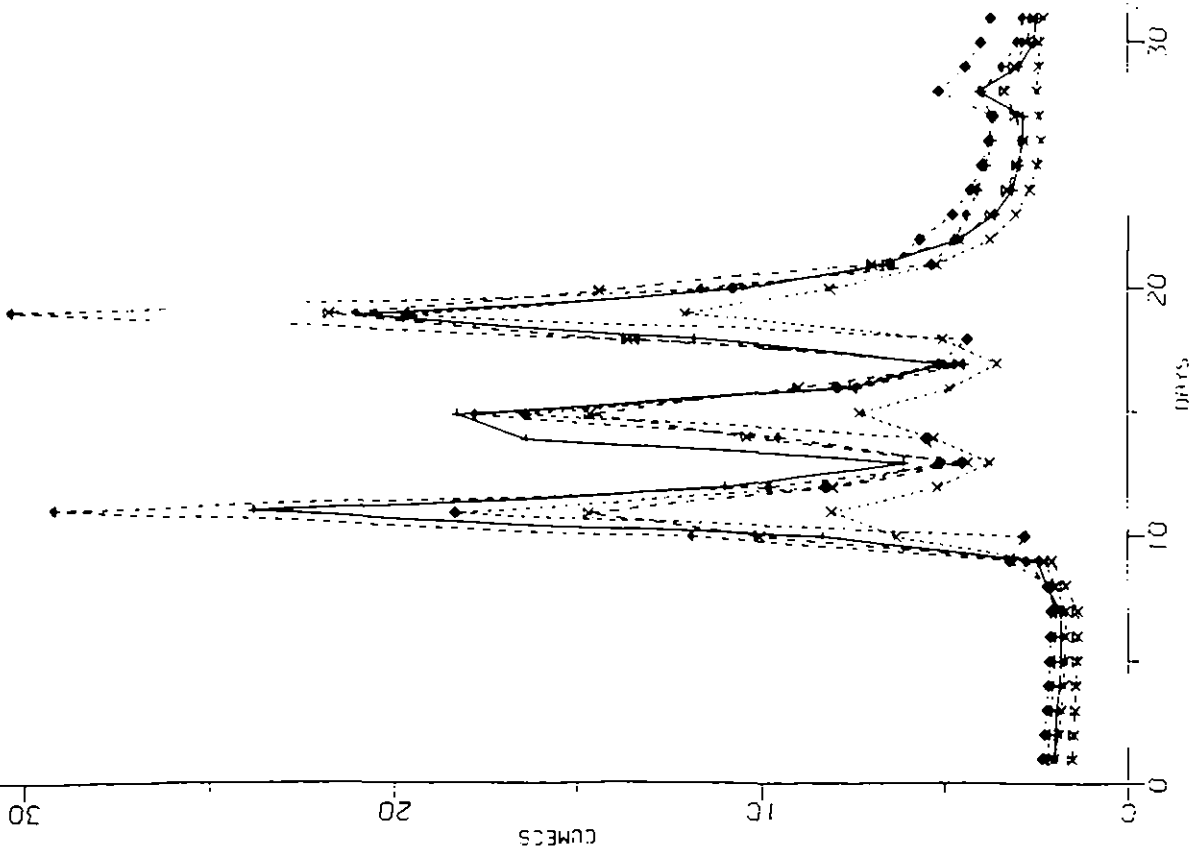


Figure 4.3.16(a) Observed and predicted flows for models PDM, IHCM, NHSI, TWM

FROM 1 / 6 / 71 TO 1 / 7 / 71  
SWALLOWFELD BLACKWATER

LEGEND:  
OBSERVED (x)  
CLS/EFM1 (x)  
CLS/EFM2 (x)  
CLS/DPT (CLS3) (x)  
REGRESSION MODEL (x)

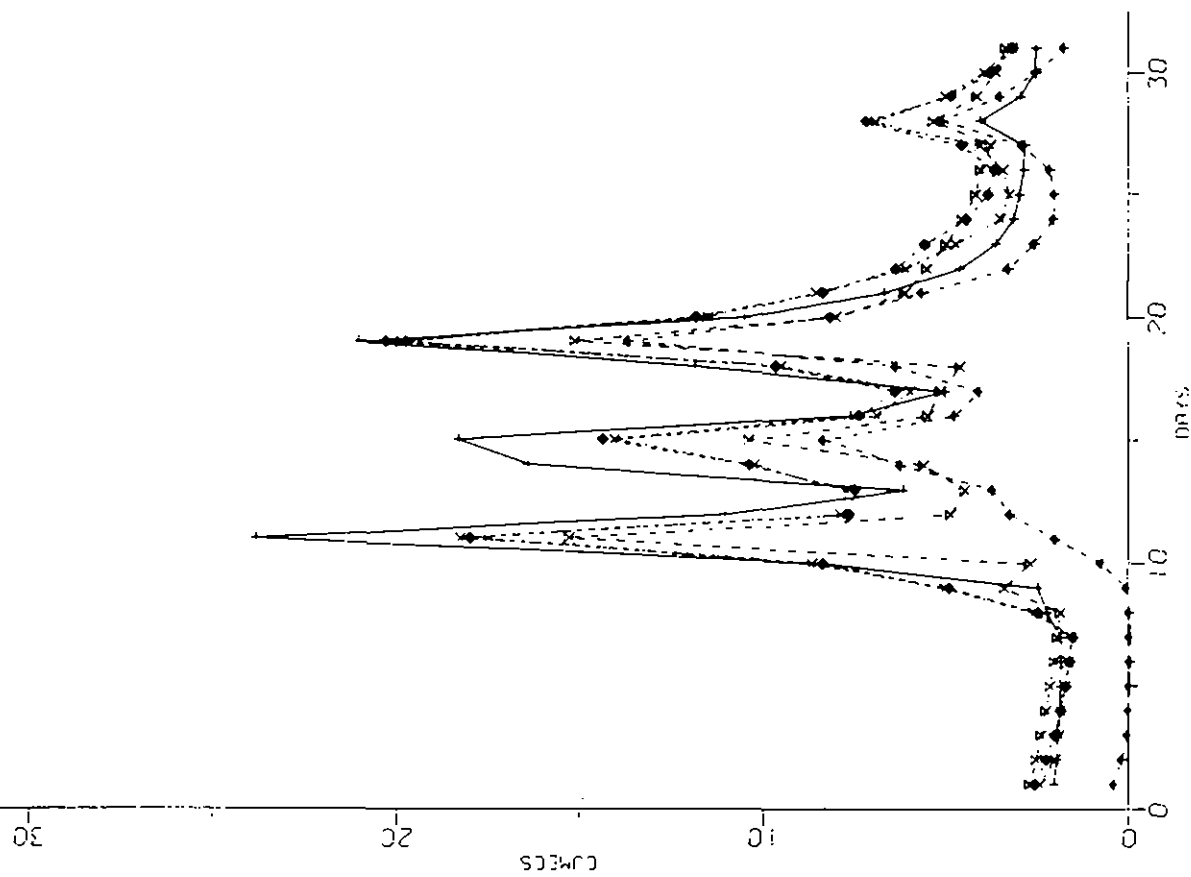


Figure 4.3.16(b) Observed and predicted flows for models CLS1, CLS2, CLS3, RECI.

FROM 31/ 8/74 TO 30/ 9/74  
SHALLOW FELD BLACKWATER

- OBSERVED
- x- PDM
- ..... IH CATCHMENT MODEL
- ◆ NWS MODEL
- x- THAMES WATER MODEL

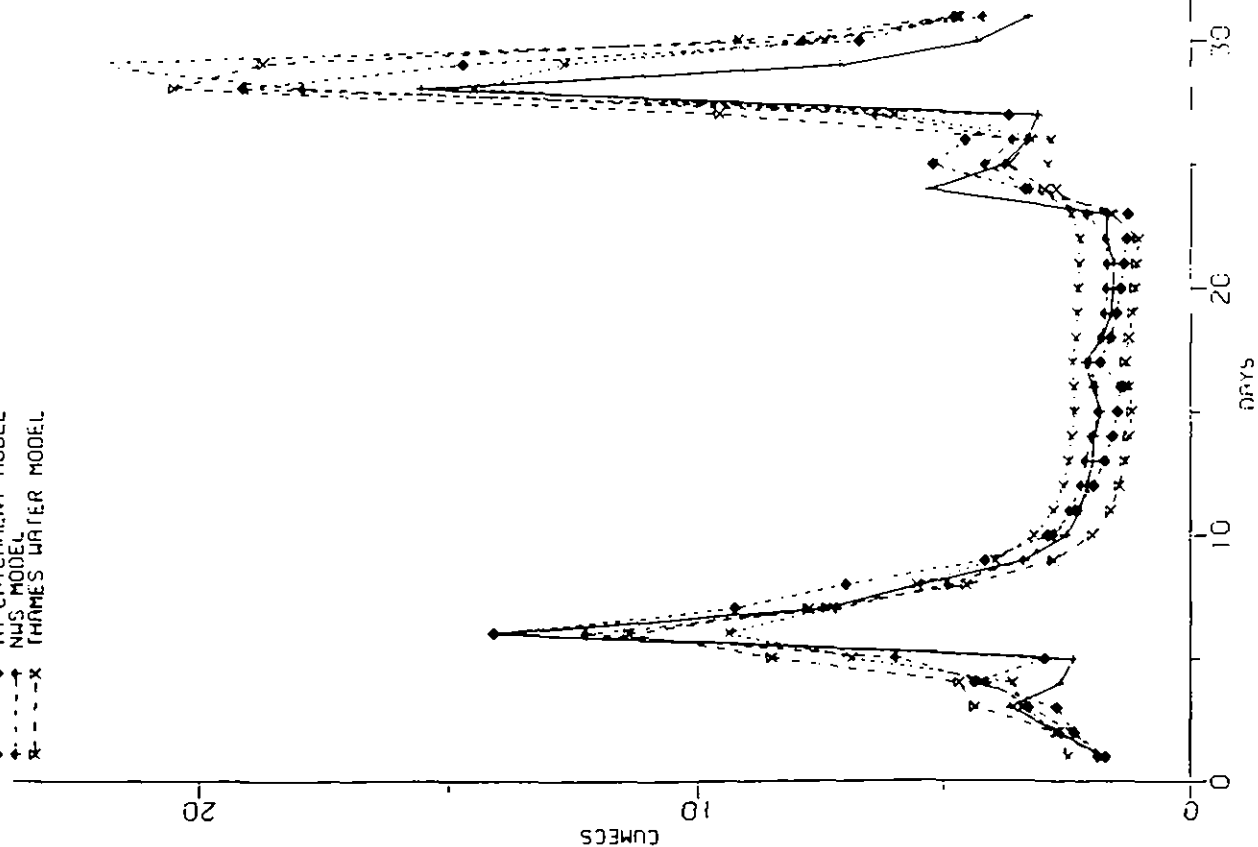


Figure 4.3.17(a) Observed and predicted flows for models PDM, IH, NWS, TWM

FROM 31/ 8/74 TO 30/ 9/74  
SHALLOW FELD BLACKWATER

- OBSERVED
- x- CLS/TFM
- ◆ CLS/EFM2
- x- CLS/OP1
- ..... CLS/3
- x- REPRESSION MODEL

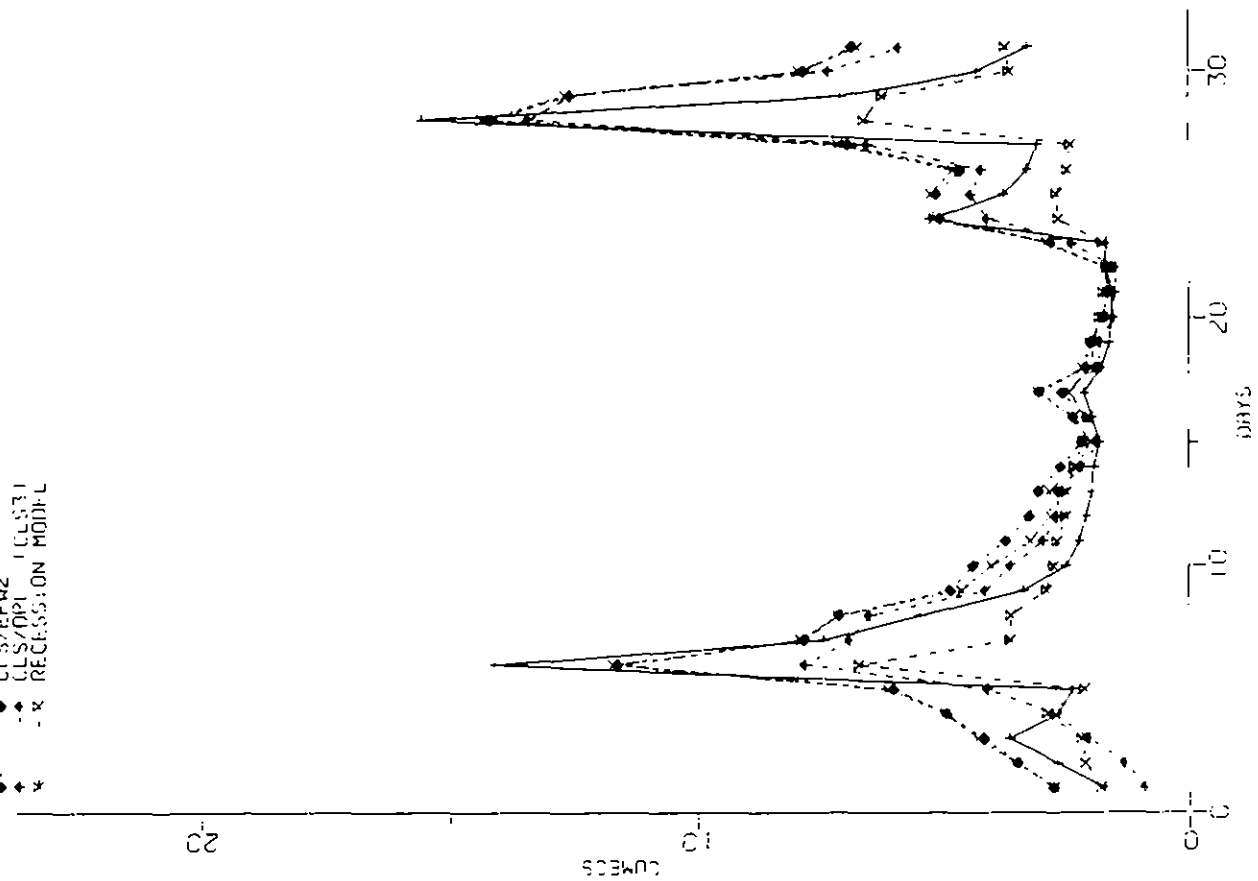


Figure 4.3.17(b) Observed and predicted flows for models CLS1, CLS2, CLS3, REC1

FROM 31/10/74 TO 30/11/74  
SHALLOWFIELD BLACKWATER

- OBSERVED
- CLS/EFH1
- CLS/EFH2
- CLS/DPL (CLS3)
- RECEPTION MODEL

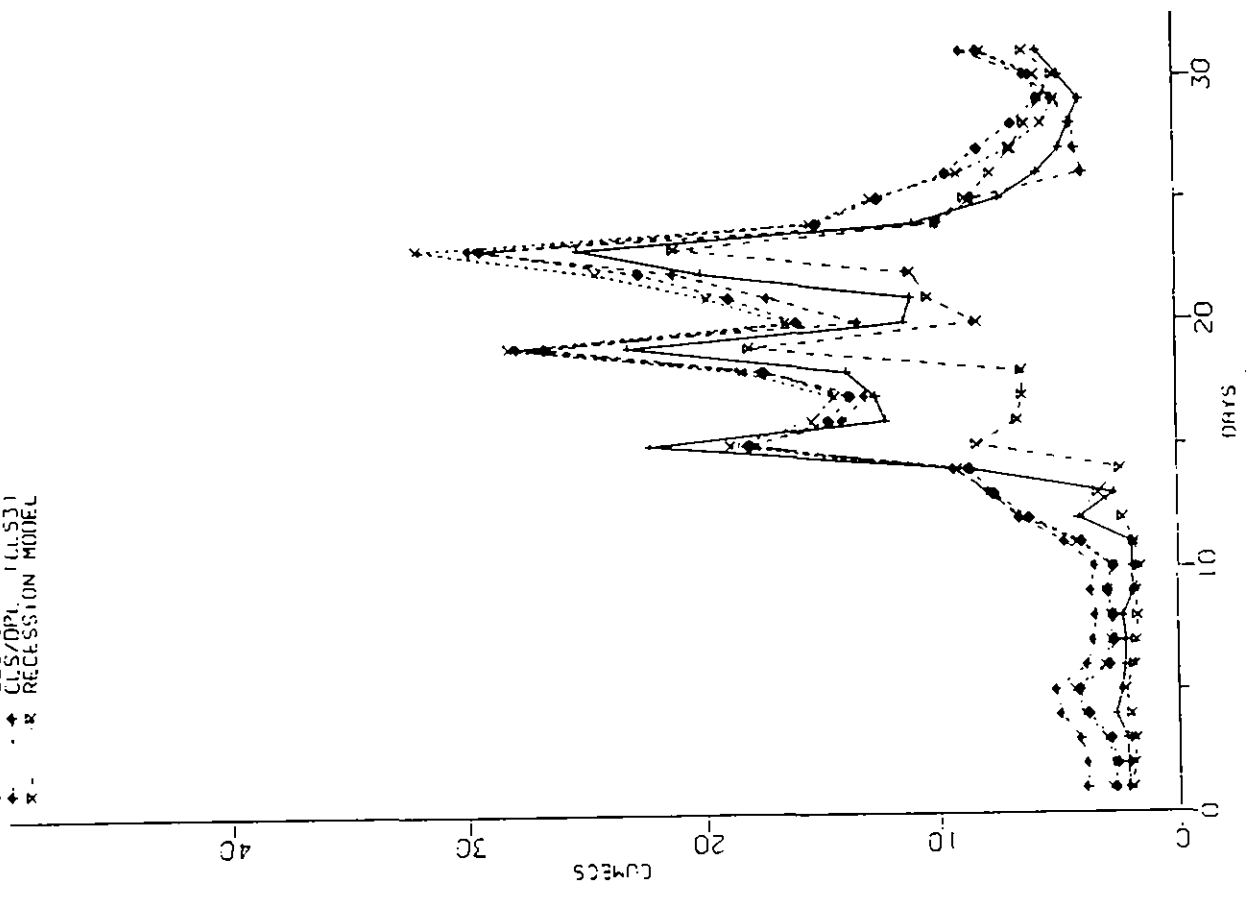


Figure 4.3.18(b) Observed and predicted flows for models  
CLS1, CLS2, CLS3, RECI

FROM 31/10/74 TO 30/11/74  
SHALLOWFIELD BLACKWATER

- OBSERVED
- PDM
- LH CRATCHMENT MODEL
- NWS MODEL
- THAMES WATER MODEL

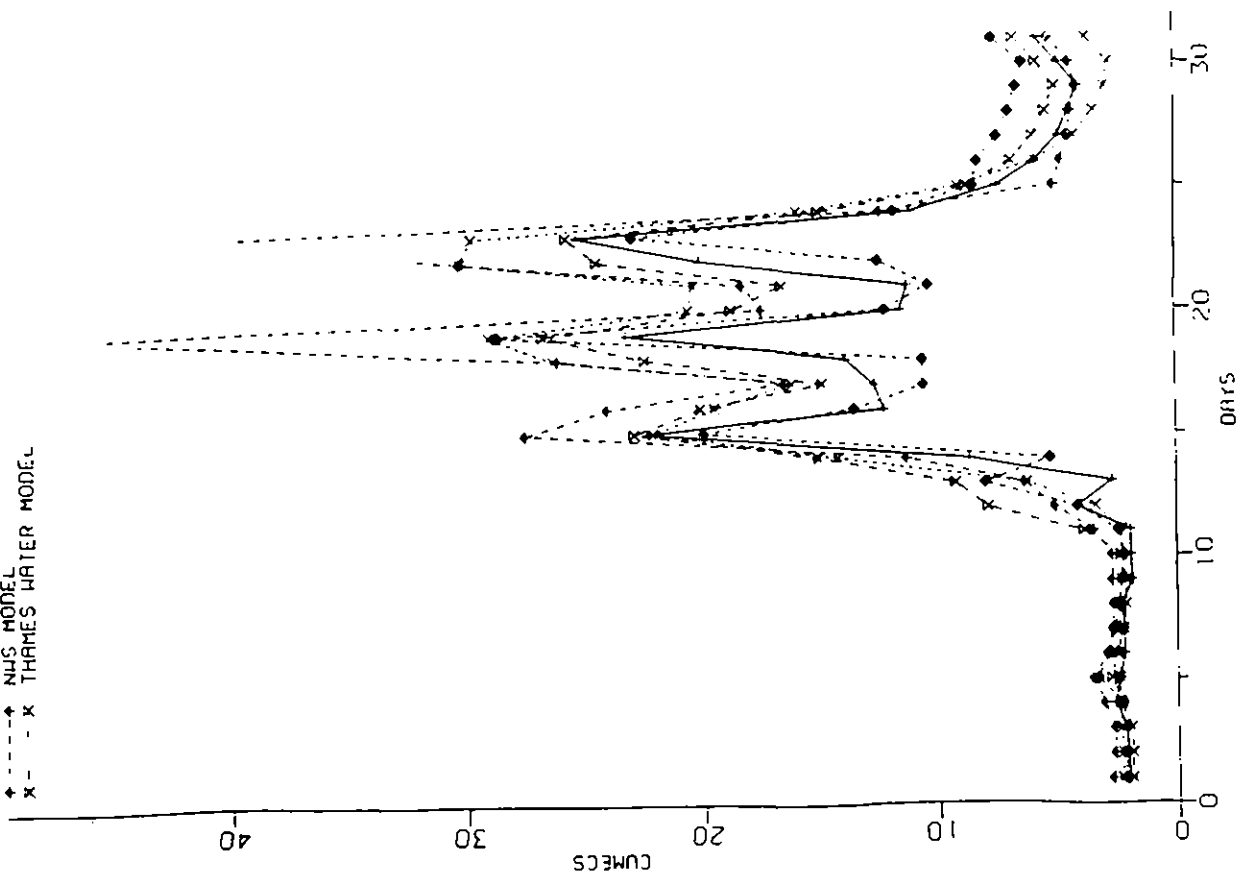


Figure 4.3.18(a) Observed and predicted flows for models  
PDM, LH, NWS, THM1

FROM 1 / 3 / 75 TO 31 / 3 / 75  
SHALLOW FIELD BLACKWATER

- OBSERVED
- x- PDM
- ♦- JH CATCHMENT MODEL
- NWS MODEL
- x- THAMES WATER MODEL

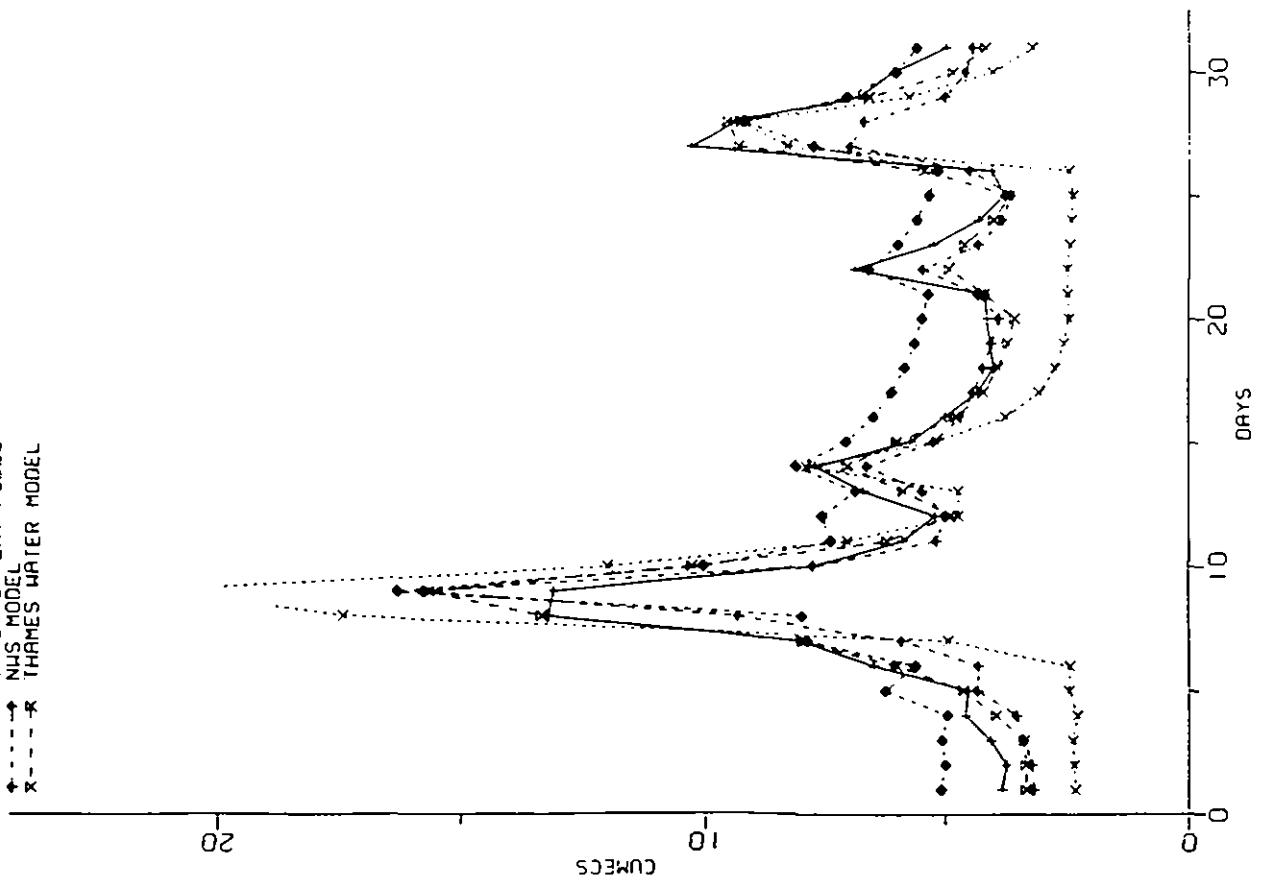


Figure 4.3.19(a) Observed and predicted flows for models PDM, JH, NWS, TW

FROM 1 / 3 / 75 TO 31 / 3 / 75  
SHALLOW FIELD BLACKWATER

- OBSERVED
- x- CLS/EFW1
- ♦- CLS/EFW2
- CLS/DPL (CLS3)
- x- RECEPTION MODEL

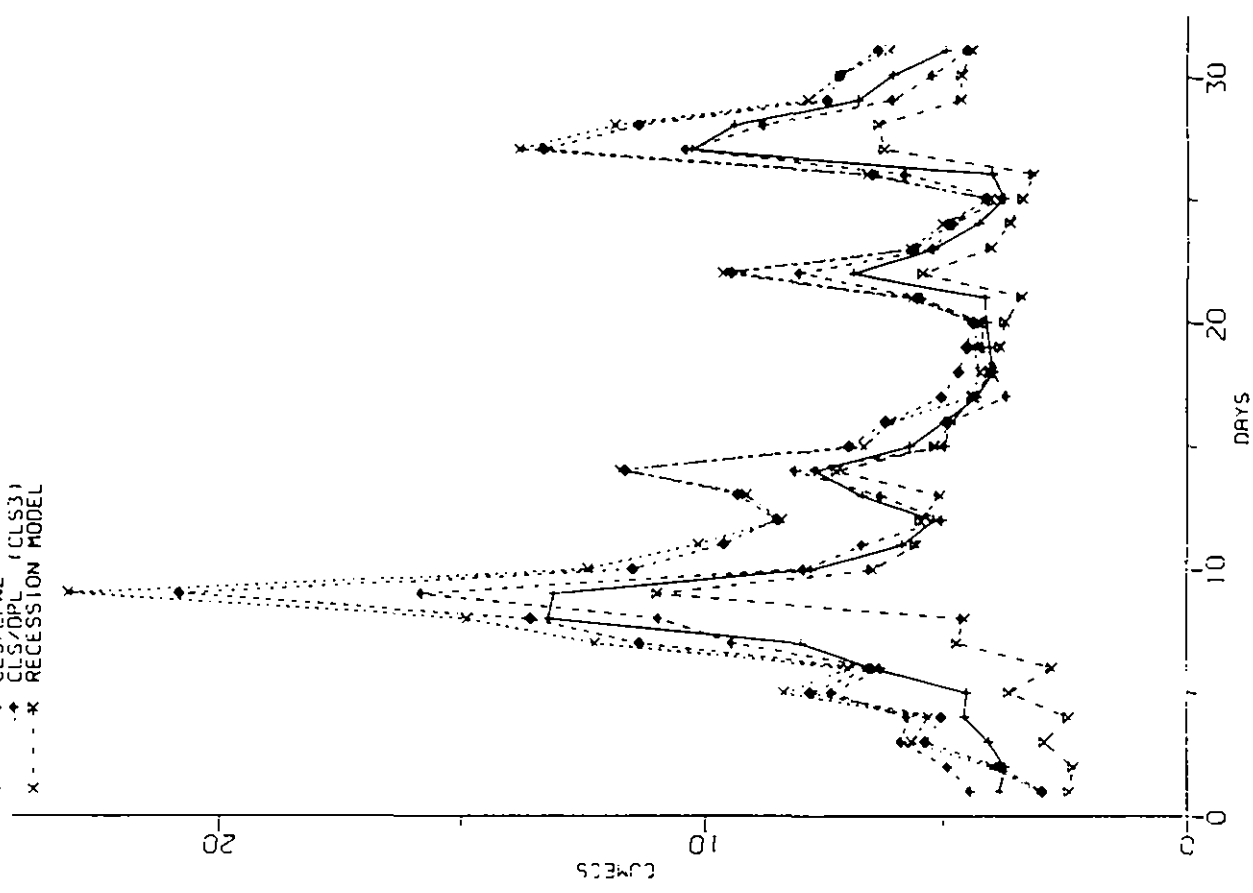


Figure 4.3.19(b) Observed and predicted flows for models CLS1, CLS2, CLS3, RECI

FROM 20/ 8/76 TO 19/ 9/76  
SHALLOW FELD BLACKWATER

+ OBSERVED  
 x PDM  
 - IH CATCHMENT MODEL  
 • NUS MODEL  
 x THAMES WATER MODEL

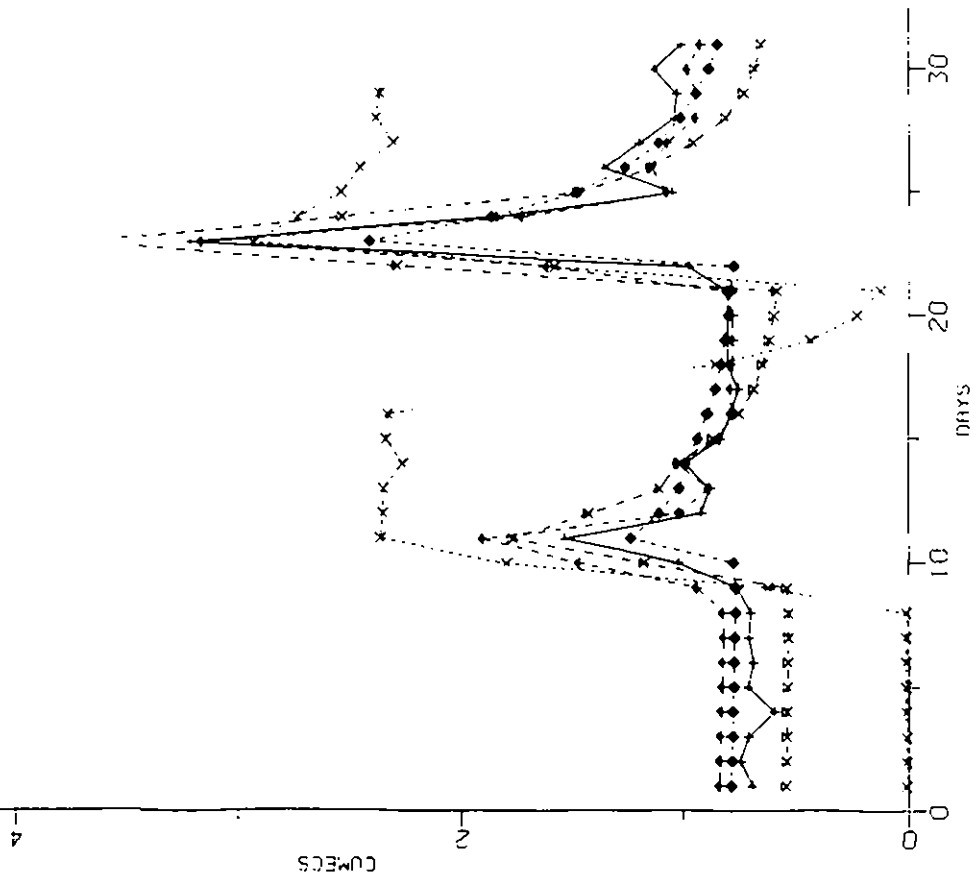


Figure 4.3.20(a) Observed and predicted flows for models PDM, IH, NUS, THAMES WATER MODEL

FROM 20/ 8/76 TO 19/ 9/76  
SHALLOW FELD BLACKWATER

+ OBSERVED  
 x CLS/EFM1  
 • CLS/EFM2  
 - CLS/DPL (CLS3)  
 x RECESSTION MODEL

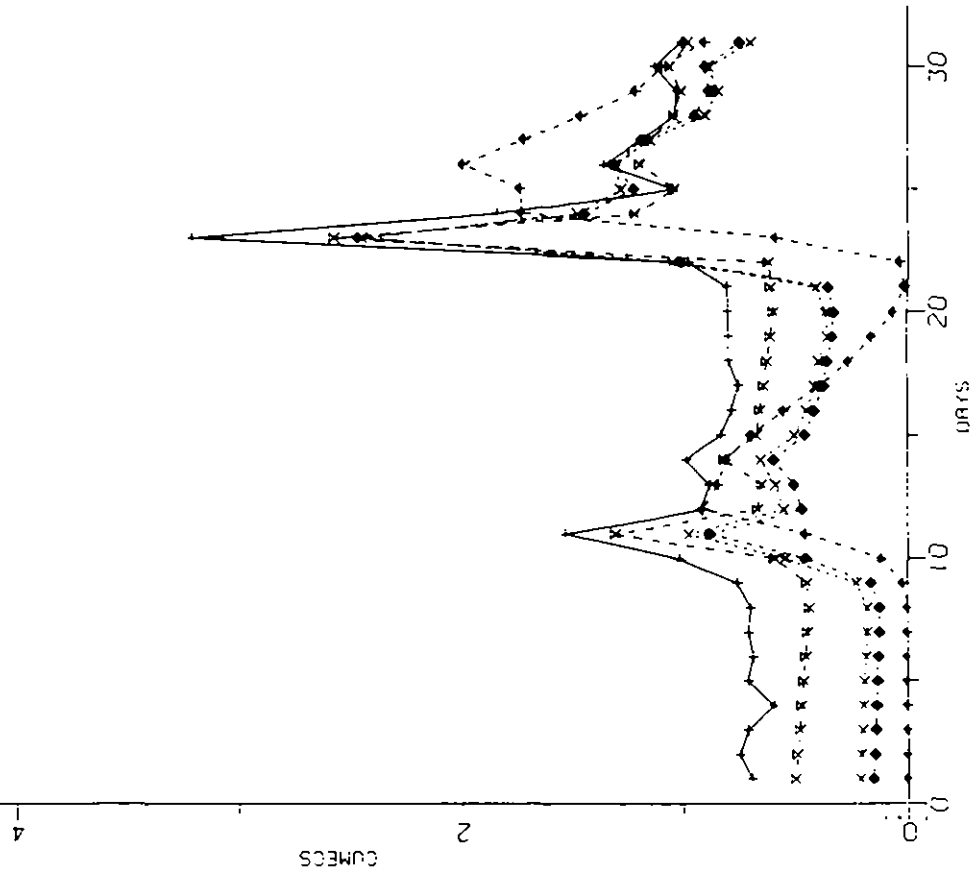


Figure 4.3.20(b) Observed and predicted flows for models CLS1, CLS2, CLS3, RECI

FROM 1/ 8/77 TO 31/ 8/77  
 SHALLOWF IELD BLACKWATER

- OBSERVED
- x- POM
- ♦- JH CATCHMENT MODEL
- ♦- NUS MODEL
- x- THAMES WATER MODEL

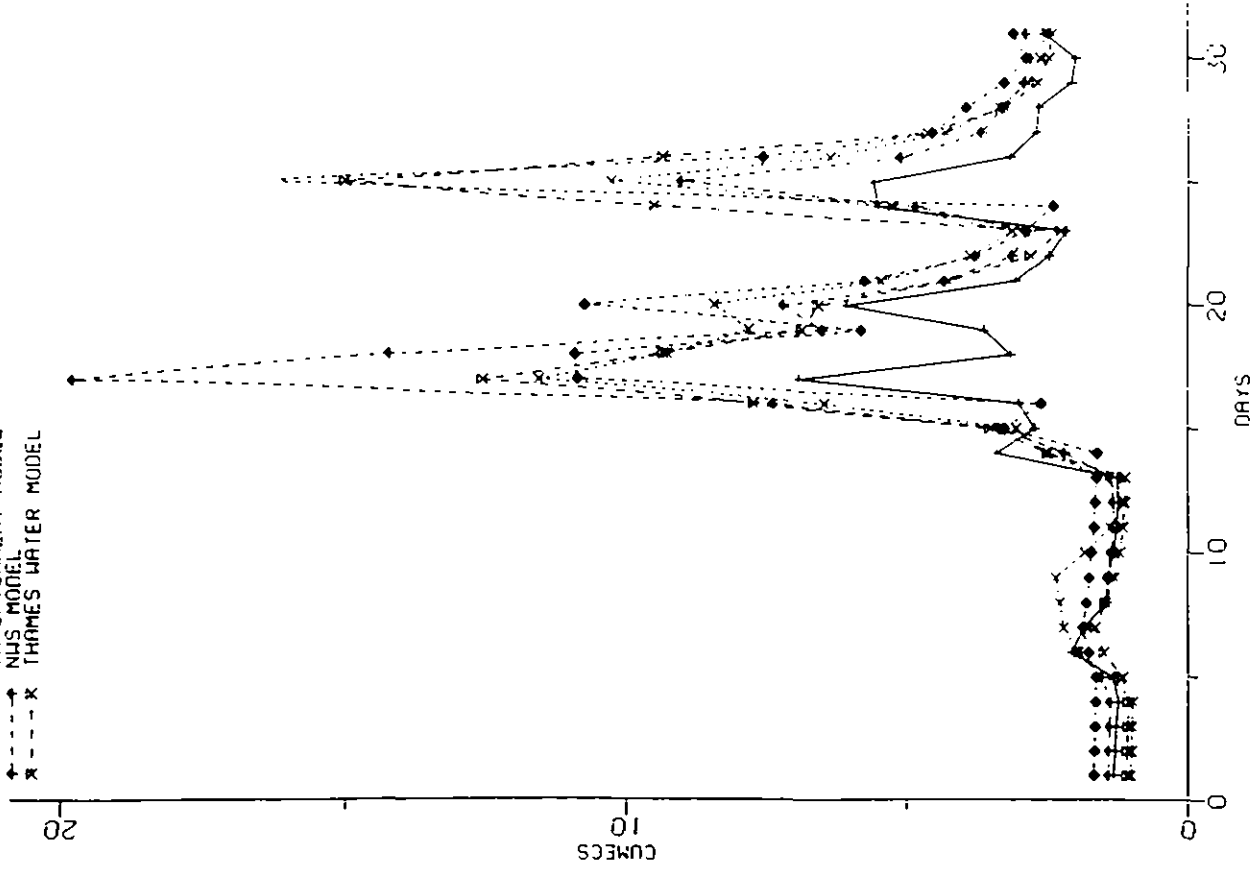


Figure 4.3.21(a) Observed and predicted flows for models  
 POM, JH, NUS, TW

FROM 1/ 8/77 TO 31/ 8/77  
 SHALLOWF IELD BLACKWATER

- OBSERVED
- x- CLS/EJ41
- ♦- CLS/EJ42
- ♦- CLS/DPL (CLS3)
- x- RECESSION MODEL

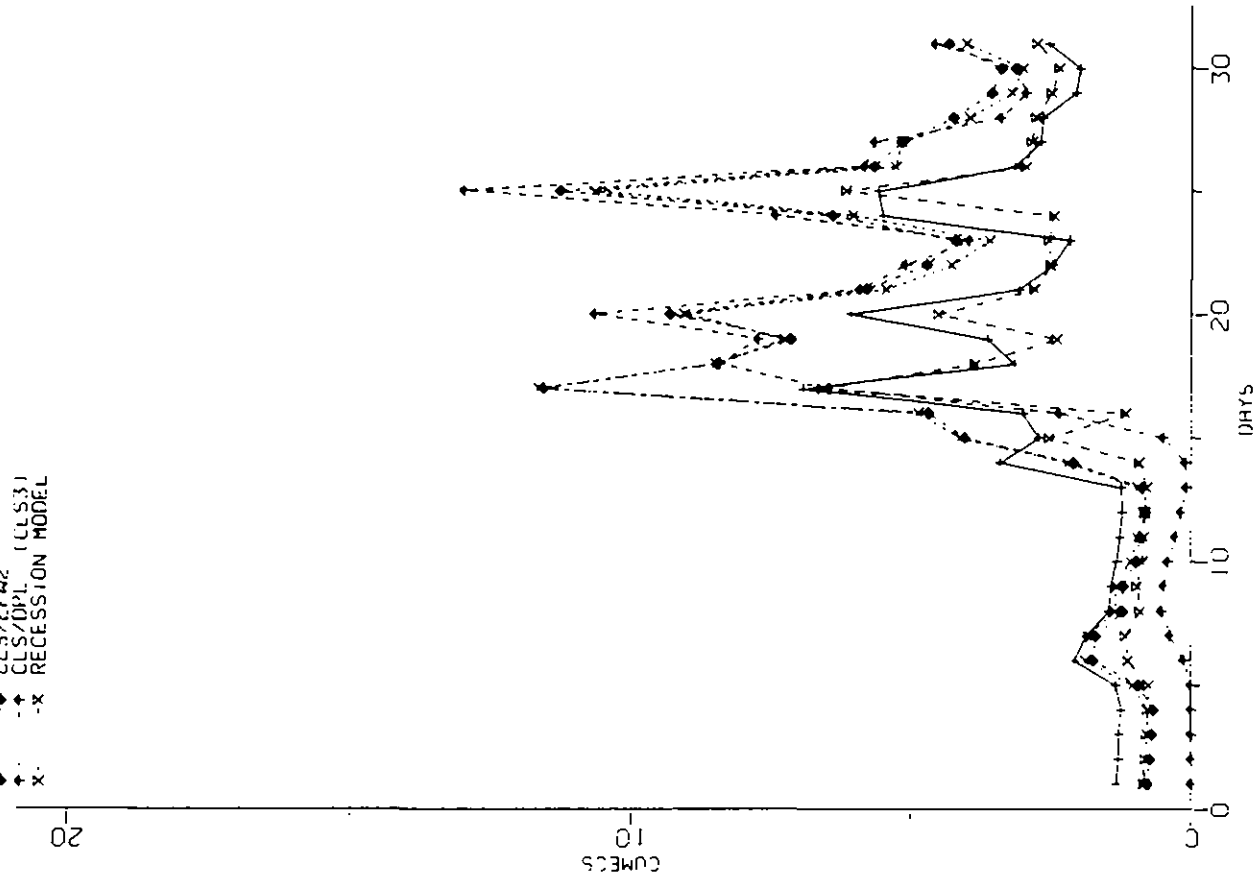


Figure 4.3.21(b) Observed and predicted flows for models  
 CLS1, CLS2, CLS3, RECI

FROM 1/12/77 TO 31/12/77  
SWALLOWFIELD BLACKWATER

- OBSERVED
- x- PDM
- o- IH CATCHMENT MODEL
- ♦- NWS MODEL
- x- THAMES WATER MODEL

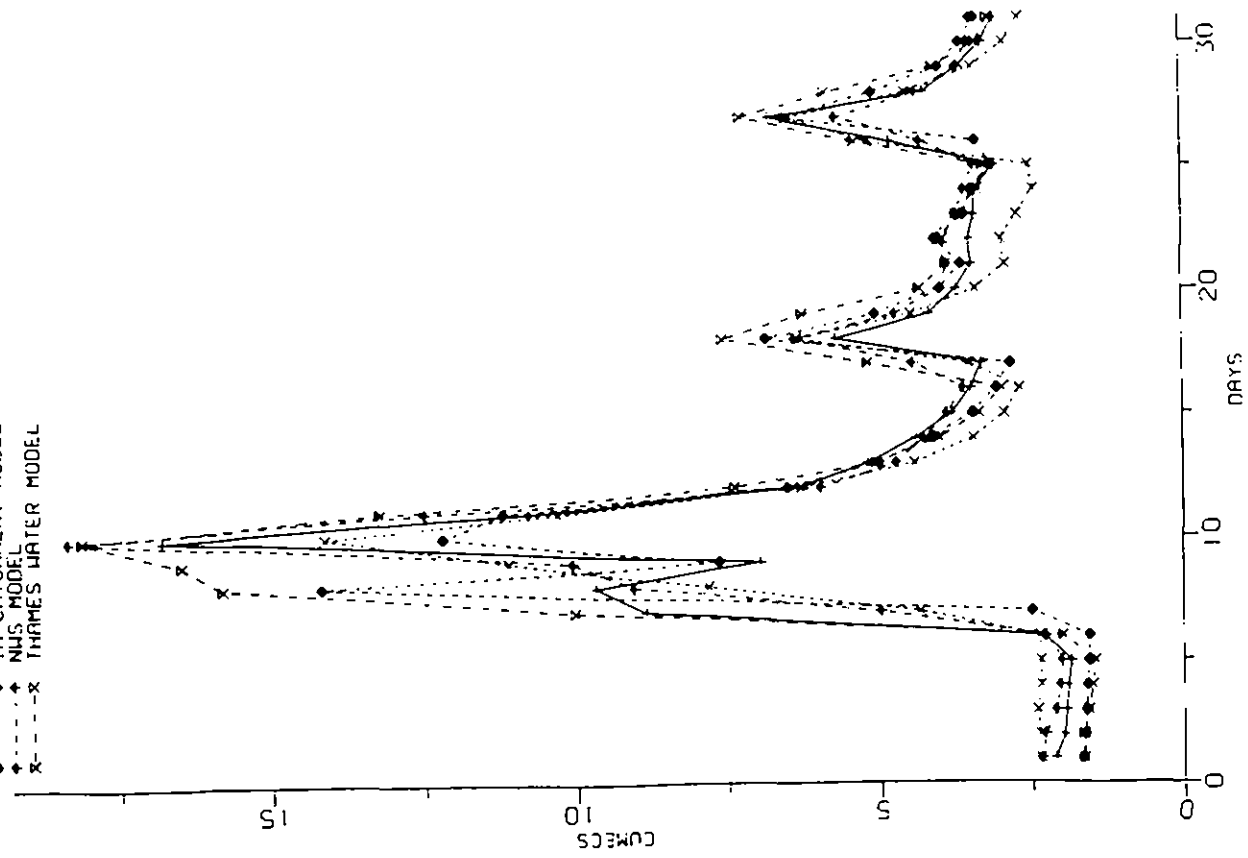


Figure 4.3.22(a) Observed and predicted flows for models PDM, IHCM, NWS1, TW1

FROM 1/12/77 TO 31/12/77  
SWALLOWFIELD BLACKWATER

- OBSERVED
- x- CLS/EFH1
- ♦- CLS/EFH2
- o- CLS/DPL
- x- RECEPTION MODEL

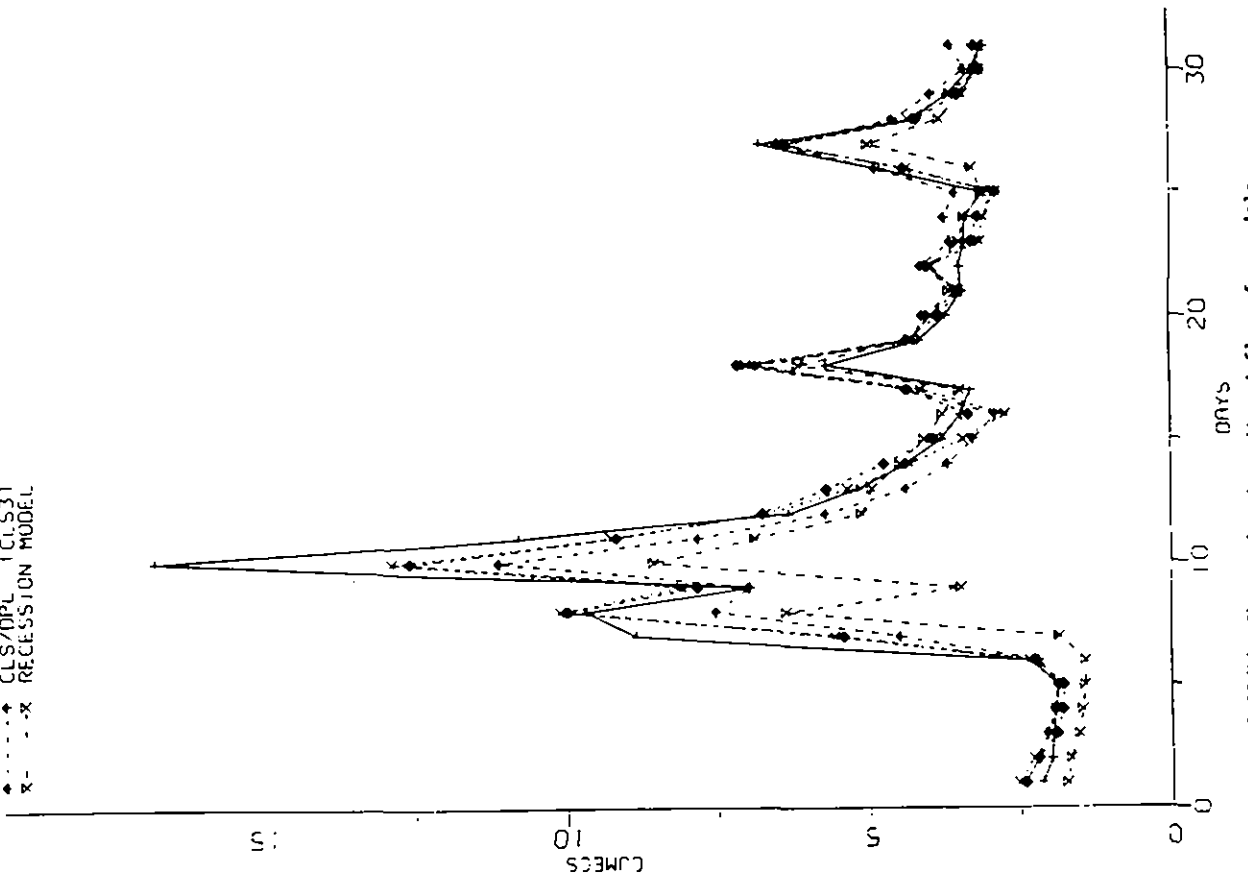


Figure 4.3.22(b) Observed and predicted flows for models CLS1, CLS2, CLS3, RECI

REFERENCES

- Anderson, E.A.,(1973), "National Weather Service river forecast system - snow accumulation and ablation model", NOAA Tech. Memo NWS HYDRO-17, U.S. Dept. of Commerce., Silver Spring, Md.
- Betson, R.P., (1969), "What is Watershed Runoff", J. Geophys. Res. 69(8), 1541-1552.
- Blackie, J.R., (1979), 'The use of conceptual models in catchment research', E. Afr. agric. For. J., 43, 36-42.
- Datta, B. and Lettenmaier, D., (1985), "A Non-linear Time-Variant Constrained model for Rainfall-Runoff", J. of Hydrology (forthcoming).
- Dickinson, W.T. and Douglas, J.R., (1972), "A conceptual runoff model for the Cam catchment", Inst. Hydrol. Report No. 17.
- Dooge, J.C.I., (1973), "Linear Theory of Hydrologic Systems", Tech. Bull. 1468, USDA, pp 327.
- Douglas, J.R., (1974), "Conceptual modelling in hydrology",Inst. Hydrol. Report No. 24.
- Dunne, T., and Black, R.D., (1970), "Partial Area Contributions to Storm Runoff in a Small New England Catchment", Wat. Resour. Res. 6(5), 1296 - 1311.
- Eeles, C.W.O., (1978), "A conceptual model for the estimation of historic flows", Inst. Hydrol. Report No. 55.
- Eeles, C.W.O., (1984), "Estimation of daily streamflow 1882-1951 for the River Thames catchment to Eynsham using a conceptual model", Inst. Hydrol. Report (in press).
- Folks, J.L and Chhikarak, R.S., (1978), "The inverse Gaussian distribution and its statistical application - a review", J.R. Statist. Soc. B, 40(3), 263-289.

- Fread, D.L., (1973), "A dynamic model of stage-discharge relations affected by changing discharge", NOAA Tech. Memo. NWS HYDRO-16.
- Gottschalk, L., (1977), "Correlation structure and time scale of simple hydrologic systems", Nordic Hydrology, 8(3), 129-140.
- Hyoms, C.M., (1980), "Development of a soil moisture model for the estimation of percolation", M. Phil. Thesis, City University.
- Johnston, N.L. and Kotz, S., (1970), "Distributions in Statistics: Continuous Univariate Distributions-1", 137-153, Wiley.
- Mandeville, A.N., O'Connell, P.E., Sutcliffe, J.V. and Nash, J.E., (1970), "River flow forecasting through conceptual models Pt.III - The Ray catchment at Grendon Underwood", J. Hydrol., 11, 109-128.
- Monro, J.C., (1971), "Direct search optimization in mathematical modelling and a watershed model application", NOAA Tech. Memo. NWS HYDRO-12.
- Moore, R.J., (1982), "Calibration of a basin soil moisture deficit and streamflow model using neutron probe measurements of soil moisture" (abstract), EOS Trans. AGU, 63(45), 921.
- Moore, R.J. and Clarke, R.T., (1981), "A distribution function approach to rainfall-runoff modelling", Water Resour. Res., 17(5), 1367-1382.
- Moore, R.J. and Clarke, R.T., (1983), "A distribution function approach to modelling basin sediment yield", J. of Hydrology, 65, 239-257.
- Morris, D.J. (1975), "The use of a multizone hydrologic model with distributed rainfall and distributed parameters in the National Weather Service River Forecast System" NOAA Tech. Memo. NWS HYDRO-25, 1975.
- Nash, J.E. and Sutcliffe, J.V., (1970), "River flow forecasting through conceptual models. Pt.I - A discussion of principles". J. Hydrol., 10, 282-290.

- Natale, L. and Todini, E., (1976), "A Stable Estimator for Linear Models", *Wat. Resour. Res.*, 12(4), 667-676.
- National Weather Service, (1972), "National Weather Service River Forecast System forecast procedures", NOAA Tech. Memo NWS HYDRO-14.
- Natural Environment Research Council, (1975), "Flood Studies Report", Vol.1, Chap.4.
- Nelder, J.A., and Mead, R., (1965), "A simplex method for function minimisation", *Computer J.*, 7, 308-313.
- O'Connell, P.E. and Jones, D.A., (1979), "Some experience with the development of models for the stochastic simulation of daily flows", in: *Inputs for Risk Analysis in Water Resources* (Ed: E.A.McBean, et.al.) Fort Collins, Colorado, Water Resources Publ., 287-314.
- Pandolfi, C., Gabos, A. and Todini, E., (1983) "Real-Time Flood Forecasting and Management for the Han River in China", IUGG Symposium, Hamburg.
- Peck, E.L., (1976), "Catchment modeling and initial parameter estimation for the National Weather Service River Forecast System", NOAA Tech. Memo NWS HYDRO-31.
- Penman, H.L., (1941), "Laboratory experiments on evaporation from fallow soil", *J. Agri. Sci.*, 31, 454-465.
- Penman, H.L., (1948), "Natural evaporation from open water, bare soil and grass", *Proc. Roy. Soc. A.* 193, 120-146.
- Penman, H.L., (1949), "The dependence of transpiration on weather and soil conditions", *J. Soil Sci.*, 1, 74-89.
- Ripple, C.D., Rubin, J., and van Hylkama, T.E.A., (1972), "Estimating Steady-state Evaporation Rates from Bare Soils under Conditions of High Water Tables", USGS Water Supp. Paper 2019-A.

Rosenbrock, H.H., (1960), "An automatic method of finding the greatest or least value of a function", *Comp. J.*,3, 175-184.

Tweedie, M.C.K., (1945), "Inverse statistical variates", *Nature*, 155, 453.

Venetis, C., (1968), "On the impulse response of an aquifer", *Bull. Int. Assoc. of Scientific Hydrology*, 13(3), 136-139.